Master's thesis

NTNU
Norwegian University of Science and Technology
Faculty of Natural Sciences
Department of Biotechnology and Food Science

Camilla Sende Grägg

A study of the polysaccharide Psl in *P. fluorescens* by controlling the amount of proteins (putatively) involved in Psl synthesis

Master's thesis in Biotechnology (MBIOT5)
Supervisor: Helga Ertesvåg
May 2023

NTNU
Norwegian University of
Science and Technology

Camilla Sende Grägg

A study of the polysaccharide Psl in *P. fluorescens* by controlling the amount of proteins (putatively) involved in Psl synthesis

Master's thesis in Biotechnology (MBIOT5)
Supervisor: Helga Ertesvåg
May 2023

Norwegian University of Science and Technology
Faculty of Natural Sciences
Department of Biotechnology and Food Science

NTNU
Norwegian University of
Science and Technology

Preface

This master's thesis was conducted at the Department of Biotechnology and Food Science at the Norwegian University of Science and Technology (NTNU) in Trondheim and marks the completion of MBIOT5, the five-year integrated Master's Degree Program in Biotechnology.

The thesis was written from January 2022 to June 2023, in collaboration with my supervisor Helga Ertesvåg, and her molecular genetics group. I would like to thank Helga Ertesvåg for teaching me experimental skills and giving me the tools needed to develop my critical thinking and theoretical approach to the project and for her guidance and support throughout the whole period. Thank you to all members of the molecular genetics research group for all help and valuable discussions, and for providing an enjoyable learning environment. I would also like to express my gratitude to Olav A. Aarstad for all the help and guidance with the monosaccharide analysis, and for teaching me experimental procedures.

Lastly, I would also like to thank all my family and friends for the intense and never-ending support I have received during the project period, and for never failing to brighten up the mood when needed.

Trondheim, May 2023

Camilla Sende Grägg

Abstract

Polysaccharide synthesis locus (Psl) is an exopolysaccharide found in *Pseudomonas aeruginosa*, and consists of mannose, rhamnose, and glucose. Psl is involved in biofilm formation and has been found to be important for biofilm maturation and cell attachment. Psl gene clusters have been found in several *non-aeruginosa Pseudomonas*, such as in *Pseudomonas fluorescens* SBW25. This study aimed to get insight into the possible production of Psl from *P. fluorescens* by characterising the genes in the Psl gene cluster and analysing the exopolysaccharide content. The gene analysis revealed that the Psl genes are most likely within the same operon, allowing for the insertion of an inducible promoter to control gene expression.

The PmG5 promoter can therefore be inserted in front of the Psl operon in different derivatives of SBW25*mucA* through homologous recombination. Different combinations of deletion and overexpressing AlgA/AlgC/AlgD and Psl in *P. fluorescens SW25mucA* strains were made, to further investigate the role of AlgA and AlgC on Psl synthesis. While monosaccharide analysis revealed that Psl from *P. fluorescens* likely consists of rhamnose, mannose, and glucose, the results also indicated that lack of either AlgA or AlgC seemed to slow down Psl production. In addition, some strains were found to have a high glucose content, possibly producing a polyglucose compound when Psl production is low.

The role of Psl, AlgC, and AlgA was investigated on *P. fluorescens* motility and phenotypical traits. The result showed that less Psl operon expression due to inactivation of the PmG5 promoter causes large colonies when the strain is lacking either AlgA or AlgC, potentially due to an imbalance in exopolysaccharide production affecting the colony size. Furthermore, overexpressing AlgC along with Psl with deletion or wild-type AlgA seems to yield the largest colonies grown on 0.5% agar, possibly indicating that Psl overproduction is dependent on AlgC overproduction. Psl-negative strains also showed that Psl is likely to be important for growth and biofilm formation, especially in cold temperatures.

Lastly, the phosphomannose isomerase (PMI) and phosphomannomutase (PMM) activity were attempted to be measured for the *P. fluorescens* mutant strains. PslB is thought to have PMM activity, similar to AlgA and WbpW in the synthesis of precursor molecules to alginate and lipopolysaccharides. To test PMI activity, a PMI assay was conducted, yielding few detectable results. Thus, the PMI assay would require further optimalisation for obtaining reliable measurements in *P. fluorescens*. AlgC has PMM activity and is thought to be required to produce the precursor molecules involved in Psl production in *P. fluorescens*. The PMM assay was conducted yielding reliable measurements, and the results indicated a loss of PMM activity when Psl genes were overexpressed. However, the low measured activity for AlgC, even when the PmG5 promoter was activated could indicate the need for optimalisation of the PMM assay as well for *P. fluorescens*.

Sammendrag

Polysaccharid synthesis locus (Psl) er et polysakkarid produsert av blant annet *Pseudomonas aeruginosa*, hvor det består av mannose, rhamnose og glukose. Psl er involvert i dannelsen av biofilm, og har vist seg å være viktig for modning av biofilm og cellefesting. Man har funnet Psl-genklynger i flere ikke-*aeruginosa Pseudomonas*-arter, deriblant i *Pseudomonas fluorescens* SBW25. Målet med denne studien var å få et innblikk i den mulige Psl-produksjonen i *P. fluorescens* ved å karakterisere genene i Psl-genklyngen og analysere innholdet i polysakkaridet som blir produsert.

Genanalysene viste at Psl-genene med stor sannsynlighet ligger i samme operon, noe som lar oss sette inn en induserbar promoter for å kunne kontrollere genuttrykket. PmG5-promotoren ble derfor satt inn foran Psl operonet i ulike SBW25*mucA*-stammer ved bruk av homolog rekombinering. Ulike kombinasjoner av fjerning og overuttrykk av AlgA/AlgC/AlgD og Psl i *P. fluorescens* SBW25*mucA*-stammer ble laget for å kunne undersøke rollene til AlgA og AlgC i Psl-syntesen. Monosakkaridanalysene viste at Psl fra *P. fluorescens* sannsynligvis består av rhamnose, mannose og glukose. I tillegg indikerte resultatene at mangel på enten AlgA eller AlgC kan føre til en saktere Psl-produksjon. Dessuten ble det funnet høye glukosemengder for noen av stammene, som dermed trolig kan produsere en polyglukoseforbindelse når Psl-produksjonen er lav.

Rollene til Psl, AlgC og AlgA ble undersøkt ved å se på forflytningsevnen til *P. fluorescens* og fenotypiske trekk. Det ble vist at mindre Psl operon-uttrykk på grunn av inaktivering av PmG5-promoteren gav kolonier med stor diameter når stammen manglet enten AlgA eller AlgC, sannsynligvis på grunn av en ubalanse i produksjonen av polysakkarider som dermed påvirker kolonistørrelsen. Videre ble det vist at overuttrykk av AlgC i kombinasjon med overuttrykk av Psl, dersom AlgA enten var villtype eller fjernet, gav de største koloniene i 0.5% agar, noe som kan indikere at for øke Psl-produksjonen må AlgC overuttrykkes i tillegg. Psl-negative stammer viste også at Psl produksjon trolig er viktig for vekst og biofilmdannelse, særlig ved kalde temperaturer.

Til slutt ble fosfomannose isomerase-aktivitet (PMI) og fosfomannomutase-aktiviteten (PMM) forsøkt målt for *P. fluorescens*-mutanter. PslB har trolig PMI-aktivitet, slik som AlgA og WbpW, som begge er involvert i syntesen av forløpermolekyler til alginat og lipopolysakkarider. For å teste PMI-aktivitet ble det forsøkt utført et PMI-assay, som gav få resultater. Assayet krever dermed optimalisering for å få troverdige målinger fra *P. fluorescens*. AlgC har fosfomannomutase (PMM)-aktivitet, og er trolig nødvendig i produksjonen for forløpermolekylene som er involvert i Psl-produksjon. PMM-assayet ble utført med målbare tall, og resultatene indikerte tap av PMM-aktivitet ved overuttrykk av Psl-gener. Likevel var de målte enzymatiske aktivitetene for AlgC lave selv når PmG5-promoteren var aktivert, som indikerer at PMM-assayet også bør forsøkes å optimaliseres ved videre bruk i *P. fluorescens*.

Contents

Abbreviations

Psl	Polysaccharide synthesis loci
EPS	Exopolysaccharide
LPS	Lipopolysaccharide
WS	Wrinkly spreaders
GMP	GDP-mannose phyrolase
PMI	Phosphomannose isomerase
F6P	Fructose-6-phosphate
M6P	Mannose-6-phosphate
M1P	Mannose-1-phosphate
G1P	Glucose-1-phosphate
G6P	Glucose-6-phosphate
HPLC	High-performance liquid chromatography
GS	Gas chromatography
HPEAC	High-performance anion exchange chromatography
PAD	Pulsed amperometric detection
NMR	Nuclear magnetic resonance
MQ	Milli-Q water
bp	base pairs
SLIC	Sequence and ligation-independent cloning
PMM	Phosphomannomutase
ZWF	Glucose-6-phosphate 1-dehydrogenase

1 Introduction

Polysaccharide synthesis loci (Psl) is an exopolysaccharide (EPS) involved in the formation of biofilm and is most studied in *Pseudomonas aeruginosa*, a much-used model organism due to its clinical importance [1]. Little research has been conducted on Psl and the Psl production in *P. fluorescens,* which have been found to contain Psl-like clusters in its genome [2]. This also means that few studies have investigated regulation and how AlgA and AlgC, two important enzymes in the production of other sugar nucleotides, affect Psl [3]. In this study, Psl production from *P. fluorescens* was therefore investigated aiming to determine the building blocks of the exopolysaccharide, as well as to see the effects of AlgA and AlgC on the Psl production.

This chapter will deal with the standard theory of *Pseudomonas fluorescens,* which is the main bacterium used in this study, as well as the structure and biosynthesis of the polysaccharides and sugar nucleotides examined. In addition to AlgC and AlgA, alginate will also be discussed as this is also an important part of many biofilms and could potentially affect Psl production. To create *P. fluorescens* mutants, homologous recombination was used, and this tool along with some key characteristics and genetic elements of the utilised plasmids in this study will also be explained.

1.1 Pseudomonas fluorescens

P. fluorescens is a gram-negative, non-pathogenic, and mobile bacterium found in a variety of environments, including soil, plant surfaces, and mammalian hosts [4]. The ability to grow in such a diverse range of environments could be explained by the extreme versatile metabolic capacities the bacterial strains possess [5]. The *P. fluorescens* bacterial group consists of more than 40 different strains, as well as some clinical isolates [6, 7]. Even if *P. fluorescens* is obligate aerobic during cellular respiration, nitrate can also be utilized as the final electron acceptor for some strains [4]. The bacterium gets its name from the pyoverdine molecules it produces, which is a siderophore that causes autofluorescence and makes the colonies appear yellow-green [8]. The absorbance spectrum for pyoverdine is between 270 – 450 nm, the emission peak is around 460 nm, and the absorbance peak depends on environmental factors such as pH and iron [8, 9].

Several Pseudomonas species have been investigated through their ability to form biofilms [10]. While *Pseudomonas aeruginosa* produces the extracellular polysaccharides alginate, pellicle loci (Pel), and Psl, which are all important parts of biofilm formation, *P. fluorescens* is thought to only produce alginate and Psl [3, 11]. Furthermore, cellulose, a compound composed of D-glucose with β-1,4-glycosidic linkages produced from the *wss* operon, and lipopolysaccharides (LPSs) which are compounds consisting of lipid A, core-polysaccharide, and an O-polysaccharide found in the outer membrane in gram-negative bacteria, are important for structure and matrix molecules in *P. fluorescens* biofilm [12, 13]. In addition, the capsular polysaccharide levan, composed of branched β-2,6 polyfructan, is found in a subset of *Pseudomonas* and is thought to be part of the biofilm as a nutrition storage [14]. Biofilm formation can also be influenced by biosurfactants such as rhamnolipids [15]. While cellulose,

LPS, and levan have been characterised, Psl has only been thoroughly investigated in *P. aeruginosa*. However, other Pseudomonas species have also been found to have Psl-like clusters in their genomes, such as *Pseudomonas syringae,* and *P. fluorescens* [2]. The synthesis and regulation of Psl in these *non-aeruginosa Pseudomonas* have not received much attention and therefore, much of the information we have about Psl comes from *P. aeruginosa,* where it is known to be a virulence factor [16].

Due to the opportunistic and pathogenic nature of *P. aeruginosa,* other *Pseudomonas* species such as *P. fluorescens* have been subject to investigation in the past years. *P. fluorescens* has proven to be an interesting organism to study in regard to alginate production. The bacteria can be engineered into becoming an effective alginate producer as well as the mutants have proven to be very stable and non-pathogenic [17]. In addition, *P. fluorescens* can be cultivated in high-density fermentations, an advantageous trait for industrial settings [17]. However, *P. fluorescens* wild-type strains do not produce alginate under laboratory conditions [10, 17]. One such wild-type strain is the SBW25 strain, which was first isolated in 1989 from a sugar beet plant and sequenced in 2009 at the Wellcome Sanger Institute and has since then become a much-used model organism [18]. From this strain, mutants such as the SBW25*mucA* strain have been made, which can produce alginate due to the deletion of the anti-sigma factor *mucA* [10] as described in more detail in section 1.3.2. The SBW25*mucA* mutant was therefore used to investigate Psl production and synthesis in this study, as well as the effect of alginate on the Psl and biofilm production.

1.1.1 A short introduction to biofilm in *P. fluorescens*

Biofilm is often characterised as a structured, surface-associated community of bacteria that can adhere to surfaces or adjacent bacteria [19]. However, non-associated surfaces are now also recognized as biofilm, such as viscous mucus found in the airways of individuals with cystic fibrosis [20]. The biofilm often consists of extracellular polysaccharides, which will promote attachment to surfaces as well as act as a scaffold and protect the bacterial cells [21-23]. In addition to polysaccharides, biofilm can also be composed of proteins, lipids, and extracellular DNA [2].

Biofilms are not only protecting the bacteria from outside factors such as shear stress, toxic compounds, and desiccation, it is also advantageous for nutrient acquisition and transport to the bacterial community [20]. One much-used model organism for studies of biofilm is the gram-negative *P. aeruginosa,* due to its clinical importance [3, 21]. The initial model for biofilm formation proposed a five-stage cyclic process based on investigations of *P. aeruginosa,* starting with reversible attachment, followed by irreversible attachment longitudinal, maturation in two stages, and dispersion [20]. However, it fails to describe the complexity of biofilm in the real world, and in industrial, natural, and clinical settings. The new updated model includes aggregation and attachment, growth and accumulation, and disaggregation and detachment, but is independent of surface attachment and can therefore consider different habitats, environments, and conditions [20].

The exact composition of biofilms can vary within each bacterial strain and also within the genus. For *P. aeruginosa*, the biofilm contains alginate, Psl, and Pel among other polysaccharides. While Psl and alginate are described in more detail in sections 1.2 and 1.3 respectively, Pel is a locus consisting of seven genes encoding for components involved in matrix formation [2]. For the *P. aeruginosa strain* PA14, at least one of the carbohydrate-rich components produced by Pel or Psl is found to be required for the formation of mature biofilm [24]. *P. fluorescens* SBW25 has been found to have *alg*, *wss*, and *psl*-clusters in its genome, encoding the main exopolysaccharides involved in biofilm formation [2]. The *alg* operon encodes for proteins involved in the formation of alginate, while the *wss* operon encodes for proteins involved in the synthesis of an acetylated cellulose-like polymer. The *psl*-cluster is thought to transcribe all genes necessary for Psl synthesis. While Psl is thought to play an important role in the biofilm of *P. aeruginosa,* its role in *P. fluorescens* has not been studied enough to conclude the same.

1.1.2 The wrinkled phenotype biofilm of SBW25

Overexpression of an acetylated form of cellulose, encoded for by genes in the *wss* operon, has been found in the biofilm of Wrinkly Spreaders (WS) along with attachment factors and LPS. This WS phenotype is characterised by having an air-liquid (AL) forming biofilm formed on the surface layer of static bodies where colonies are wrinklier and drier when plated out on agar than the wild-type [12, 25]. The resulting biofilm provides advantages such as access to nutrition from the liquid layer as well as oxygen from the air [25]. Experiments have shown that mutations in *wssFGHIJ* cause overproduction of the cellulose polymer, which causes expression of the wrinkly spreader characteristics [12]. Furthermore, WssGHI are homologous of AlgFIJ in *P. aeruginosa*, which are important for acetylating alginate and are thought to play a similar role in the cellulose synthesis pathway.

The cellulose expression in *P. fluorescens* can be upregulated by an increased transcription rate of the *wss* operon or increased c-di-GMP levels regulated by genes in a chemosensory signal-transduction operon [26]. For *P. aeruginosa,* elevated c-di-GMP levels will cause a higher production of the extracellular polysaccharides including Psl [19]. For *P. fluorescens*, little to no studies have been conducted on the relationship between Psl production and c-di-GMP.

1.1.3 Different exopolysaccharide synthesis strategies

Exopolysaccharides are important for all bacterial cells, and the synthesis of the polysaccharides can be divided into four categories depending on the composition of the monomers making up the polysaccharide [27]. When the polysaccharide is synthesised as a homopolymer, the cell utilises either the synthase pathway or extracellular enzymes, such as levansucrase in the production of levan. When the polysaccharides are assembled as heteropolysaccharides, stepwise transfers of the units occur, either through the ABC transporter pathway or the Wzx/Wzy pathway [27]. A schematic overview of the pathways is given in Figure 1 [27].

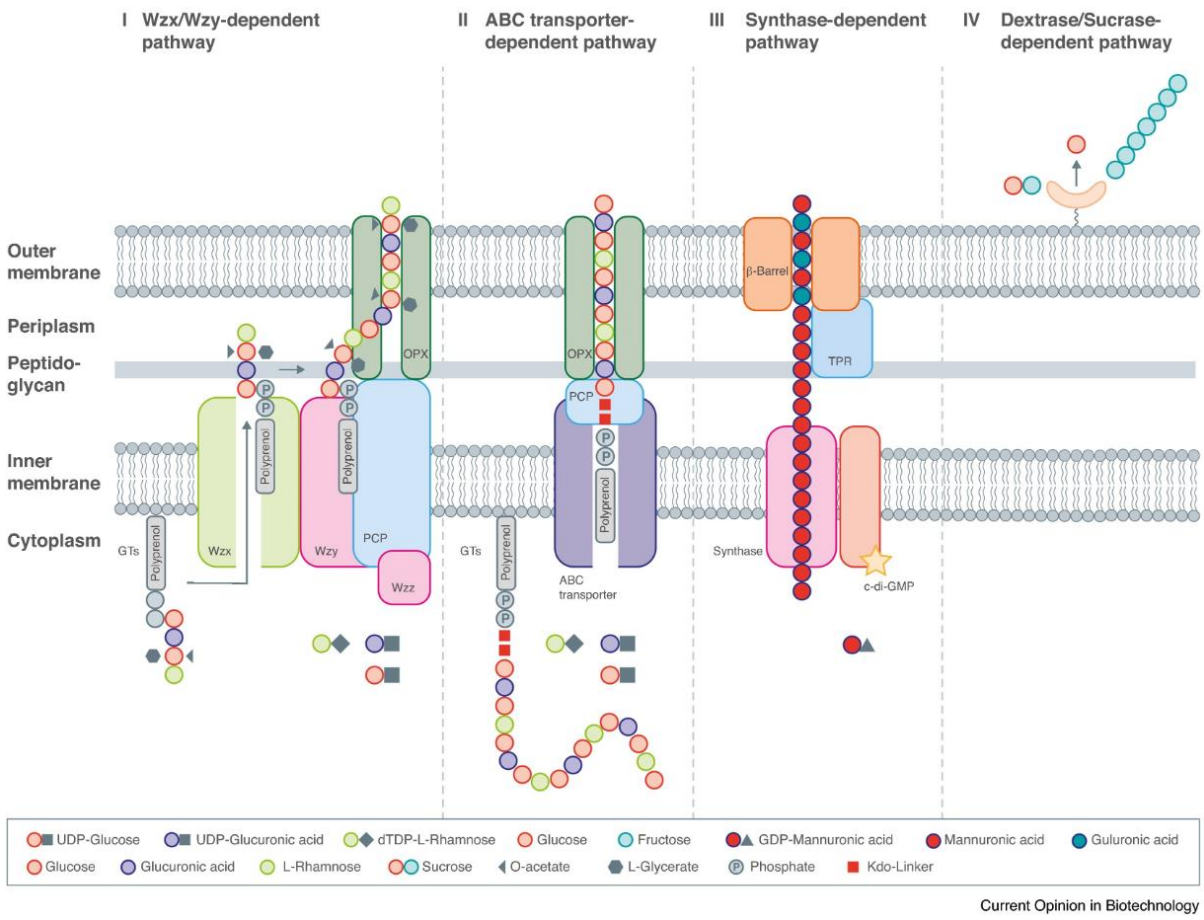

Figure 1: A schematic overview of the four categories of the synthesis of exopolysaccharides in microbes. *The first two pathways are used by heteropolymers, while the synthase-dependent and enzyme-dependent pathways are used by homopolymers. The Wzx/Wzy-dependent pathway synthesises the exopolysaccharides while the prolonged chain is being exported out. The ABC transporter-dependent pathway will export the chain after it has been assembled. The synthase-dependent pathway assembles the chain before exporting it out of the cell, while the enzyme-dependent pathway requires exocellular enzymes for the assembly of the exopolysaccharide. The figure is retrieved from Schmid et al. [27]*

For cellulose or alginate, biosynthesis is based on a synthase pathway. Cellulose is an EPS involved in biofilm formation, and the UDP-glucose monomers are assembled in the cellulose synthase complex, encoded by the Bcs operon genes [27, 28]. In SBW25, the *wss* operon encodes homologous genes of the *bcs* operon, and these gene products synthesise acetylated cellulose residues [28]. Alginate is synthesised as a homopolymer, beginning with the synthesis of the GDP-D-mannose precursor molecules which are polymerised into a chain. The chain is transported directly across the inner membrane by the synthase complex encoded by genes in the Alg operon, further described in section 1.3.2. Pel is thought to have a similar mechanism as alginate [11].

For heteropolymers, two different mechanisms are used [27]. Wzx/Wzy is a common heteropolymer biosynthesis mechanism, often involved in the synthesis of exopolysaccharides such as EPSs and Psl, and the capsular polysaccharides group (CPS) 1 in *Escherichia coli* [11, 27]. The precursor sugars that make up the repeating unit of the polysaccharide are recognized by a biosynthetic complex and loaded onto an isoprenoid lipid carrier where the monomers are assembled [11]. The nascent polysaccharide is transported through the periplasm and to the cell surface. The polymerase Wzy and the flippase Wzx, along with specific glycosyltransferases

will bind the polysaccharide to a lipid carrier, which will be flipped from the cytoplasmic leaflet of the inner membrane into the periplasmic leaflet by the flippase [21, 29]. For CPS1, the glycosyl transferase WbaP is involved in the initiation of the polysaccharide biosynthesis [30]. In addition, Wza, Wzb, and Wzc, being a lipoprotein, a phosphatase, and a tyrosin autokinase respectively, are involved in the polymerisation control and translocation to the cell surface [30].

The second mechanism is the ABC transporter system, commonly used by capsular polysaccharides linked to the cell envelope [27]. In this mechanism, monomers are assembled on the cytosolic membrane before ABC transporters, being Wza proteins, export the polysaccharide out of the cell [27]**.** The production of A-band LPS is conducted in such a way, and WbaP, a gene within the A-LPS gene cluster has been found to resemble AlgA, possessing GDP-mannose phyrolase (GMP) and phosphomannose isomerase (PMI) activity [31]. The WbaP is thus involved in the production of the active precursor molecules used for A-band LPS synthesis [3].

1.2 The polysaccharide synthesis locus operon and its genes synthesise a polysaccharide called Psl

The Psl cluster was first identified in *P. aeruginosa* by three independent research groups [24, 32, 33]. They all concluded with the Psl being important in biofilm formation, a role that was previously attributed to alginate. To this date, Psl has been described in various *P. aeruginosa* strains, and briefly in some plant-associated *Pseudomonas* strains, such as *P. syringae, P. fluorescens,* and *Pseudomonas chlororaphis* [2].

1.2.1 Structure and genes of Psl

In *P. aeruginosa*, Psl is a charge-neutral polysaccharide composed of D-mannose, L-rhamnose, and D-glucose, and is important in biofilm formation where it provides structural support [3, 34]. Different research groups have determined the structure of Psl, with somewhat different results regarding the quantification of each monomer. While some have found Psl to contain galactose, others have found no trace of galactose but with substantial amounts of mannose instead [3, 22, 24]. Figure 2 shows the residues making up the repeating pentamer polysaccharide Psl as found in *P. aeruginosa* by the use of NMR from Byrd et al. [3].

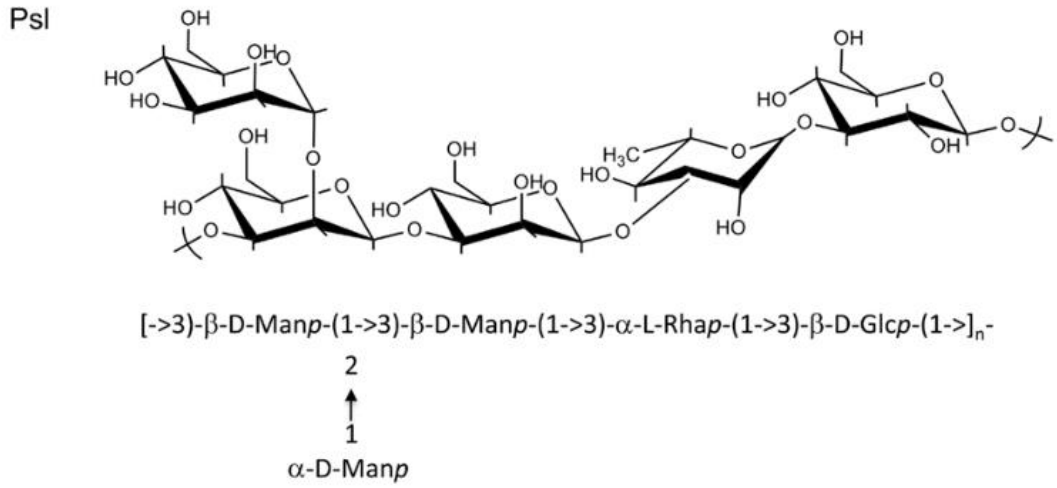

Figure 2: The structure of Psl from P. aeruginosa, containing D-mannose, L-rhamnose, and D-glucose*. The image is retrieved from Franklin et al. [11].*

Psl is thought to be involved in cell-cell attachment and cell-substrate attachment [35]. Most *P. aeruginosa* strains express Psl, and the polysaccharide has been found in both natural and clinical isolates [36]. The Psl operon in *P. aeruginosa* PAO1 consists of 15 genes, with different functions as indicated in the lower panel of Figure 3. Byrd et al. further concluded that there were 11 essential genes for the production of Psl, being *pslACDEFGHIJKL*. Deletion of each of these genes caused deficient Psl-production in the PAO1 strain [3]. Psl-like gene clusters have also been found in some environmental non-aeruginosa *Pseudomonas* species. Some of these also lack orthologues to pslMNO genes such as *P. fluorescens* SBW25, however, they have been found to be non-essential for Psl production in *P. aeruginosa* [2, 3].

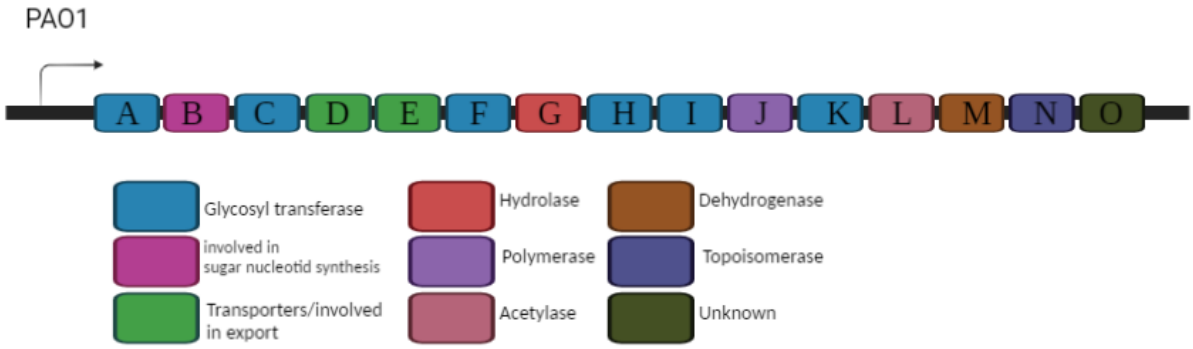

Figure 3: Characterisation of the studied genes in the Psl operon of P. aeruginosa PAO1*. The genes are colour coded with their predicted or determined function explained in the lower panel. The illustration is a modified version of Figure 1 made by Byrd et al. [3].*

1.2.2 Psl biosynthesis

The proteins involved in the biosynthesis of Psl in *P. aeruginosa* have several predicted structural similarities to proteins involved in the synthesis of capsular polysaccharides group 1 in *E. coli* [11]. Therefore, the synthesis of Psl is thought to resemble this process, shown in Figure 1 (part I), which requires an isoprenoid lipid carrier where the repeating oligosaccharide structure will be built prior to assembling and export of the nascent chain into the extracellular matrix [11], as outlined in Figure 4. This assumption is further supported by structural similarities between Psl proteins and proteins in the Wzy-dependent pathway [3, 11, 30].

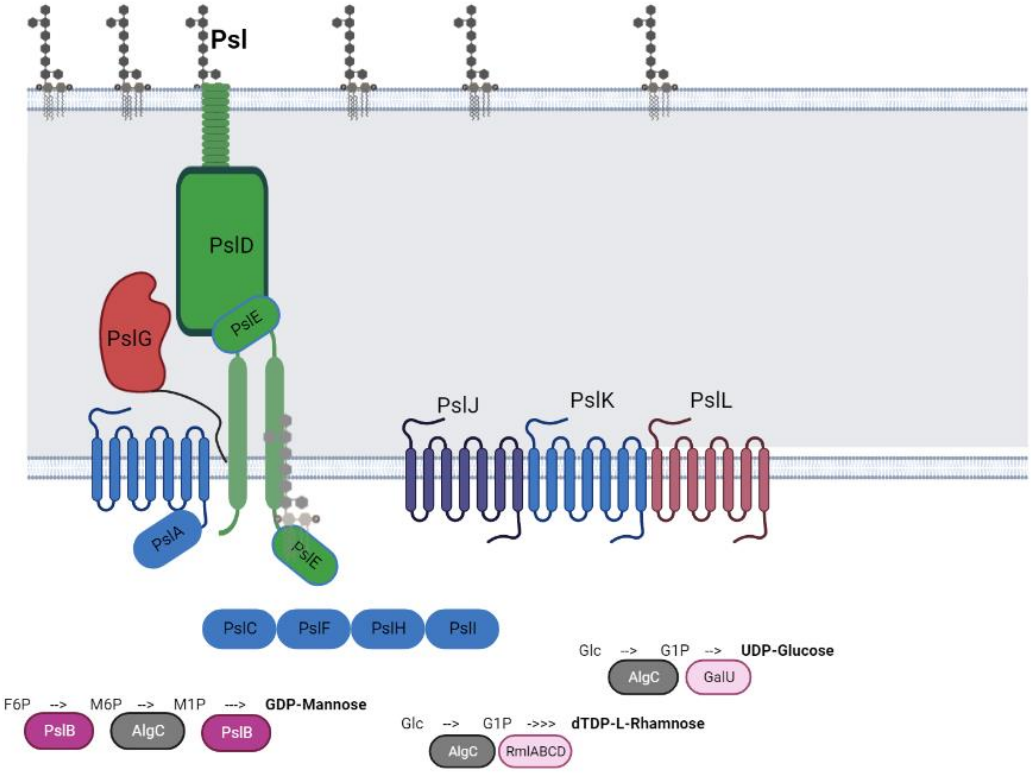

Figure 4: An overview of Psl synthesis in P. aeruginosa. *PslCFHI are thought to transport the precursor sugars to the membrane complex, consisting of PslAEJKL. PslG and PslD are thought to play a role in the export of Psl. The proteins are coloured according to their predicted function, as explained in* ***Figure 3****. The image is based on figures from Wu [21, 37] and Franklin et al. [11]. Abbreviations: F6P = fructose-6-phosphate, M6P = mannose-6-phosphate, M1P = mannose-1-phosphate, Glc = glucose, G1P = glucose-1-phosphate.*

For the Psl biosynthesis to take place, the required precursors must be synthesised. Psl requires the precursor nucleotides GDP-D-mannose, UDP-D-glucose, and dTDP-L-Rhamnose, which later are converted to D-mannose, D-glucose, and L-rhamnose, respectively [11]. PslB is the only protein in the Psl operon thought to be involved in the production of the precursors, which in addition requires the enzymes AlgC, RmlABCD, and GalU which functions as shown in Figure 4 [3]. Furthermore, PslB and WbpW from the A-band LPS synthesis pathway have overlapping functions, and like AlgA, they both possess GMP and PMI activities required for the GDP-D-mannose synthesis [3, 31]. Since a double deletion mutant of *pslB*/*wbpW* but not a single deletion mutant in the non-alginate producing *P. aeruginosa* PAO1 caused loss of Psl-production, the two PMI/GMPs are thought to be interchangeable for production of the precursor nucleotide [11]. *pslB* is therefore thought not to be essential for Psl production.

After the formation of precursor nucleotides, polymerisation will take place. PslC, PslF, PslH, and PslI are thought to transfer precursor sugars from nucleotide donors aiding the formation of repeating units of Psl by catalysing glycosyl transfers [11]. The polymerisation phase involves several Psl proteins, with PslAEJKL being likely to make up the Psl polymerisation complex, shown as proteins with membrane-spanning domains in Figure 4 [11]. PslA is thought to be encoding a UDP-glucose carrier protein, showing similarity to WbaP described in section 1.1.3 [11, 38]. PslJ, PslK, and PslL are all inner membrane proteins, and it is thought that PslJ might function as Wzy, with PslK as the flippase [11]. Both PslE and PslA show structural similarities to proteins in the Wzy-pathway, and it has been found that PslE has the

characteristic domains of a Wzc-homolog [21]. It is therefore thought to act as a polysaccharide co-polymerase as its homolog in the Wzy-pathway, also being able to affect the chain length of the polysaccharide. PslE is also thought to interact with PslD, helping it localize the outer membrane [21].

PslD and PslG are involved in the translocation and export phase of Psl [11, 21]. PslG has glycoside hydrolytic activity and is thought to resemble AlgL and PelA from the alginate and Pel synthesis, respectively [11, 21]. While a study found PslG to not be essential for Psl production [39], Wu et al. found that PslG is essential in the degradation of Psl when the enzyme is located in the periplasm [21]. Thus, PslG seems to be important, but not necessary for Psl production. PslD has been found to be critical for PslG localization, and a *P. aeruginosa PAO1* mutant lacking PslD was found not able to produce the complex biofilm associated with this strain [40]. In addition, PslA and PslE are important for PslG placement, and PslE will also help PslD localize the outer membrane [21].

The last genes located within the Psl operon, PslM, PslN, and PslO, are not essential in the Psl biosynthesis pathway and it is therefore thought that their gene product can have regulatory functions, or that they in some other way will modify Psl without changing its properties [3].

1.2.3 Psl regulation

While the regulation of alginate has been the subject of investigation for a long time, little is known about the regulation of Psl expression and biosynthesis, especially in *non-aeruginosa Pseudomonas* [41]. For *P. aeruginosa*, Psl expression has been found to induce an increase of the secondary messenger c-di-GMP through the two diguanylate cyclases SiaD and SadC, causing an increase in the expression of several other biofilm-associated genes [42]. The increase of c-di-GMP will then further increase the Psl synthesis, along with other biofilm components [42]. For *P. fluorescens*, an increase in c-di-GMP levels causes increased biofilm formation [19], but the connection to Psl has not been investigated yet.

AmrZ (alginate and motility regulator) is an AlgU-responsive transcription factor within *P. aeruginosa*, which has been found to activate the expression of the alginate operon and repress the expression of the Psl operon [43]. AmrZ thus functions as a regulator of the production of the two exopolysaccharides [43]. Exogenous iron supply has also been found to inhibit AmrZ expression, causing a higher synthesis of Psl. In addition, Psl was found to be able to bind to iron and function like an iron pool for the stimulation of biofilm formation [44]. For *P. fluorescens*, AmrZ has been found to be part of both iron homeostasis and c-di-GMP production [45]. Thus, AmrZ might be involved in Psl regulation in *P. fluorescens*.

There is also some internal regulation within the Psl operon, with the hydrolase PslG being able to prevent the formation and assembling of the biofilm when supplied exogenously [44]. In addition, PslG is important for the morphology of the bacteria, as loss of PslG caused phenotypically long chains of cells not seen when PslG was present in *P. aeruginosa* [46]. Exactly how PslG might regulate Psl production is not known, especially considering how it is not necessary for Psl production.

1.3 Alginate and its biosynthesis

1.3.1 Alginate structure

Alginate is an anionic polymer composed of β-D-mannuronic acid (M) and its C5 epimer α-L-guluronic acid (G), linked together by 1-4 glycosidic linkages [17, 47]. The epimerase mannuronan-C5-epimerase will convert M-residues into G-residues [48]. The structure is shown in Figure 5, and the residues can be arranged in M-blocks, G-blocks, or alternating MG-blocks of various lengths. While most alginate used in the industry comes from brown sea algae, several bacterial species such as some *Pseudomonas* and all *Azotobacter* are naturally alginate-producing bacteria [49]. These alginates differ from algae alginate by often being O-acetylated on some M-residues [50]. The acetyl groups are thought to have a protective function hindering both epimerisation of M-residues into G-residues and alginate lyases from accessing the polymer [51]. Alginate from *Pseudomonas* has not been found to contain G-blocks [17].

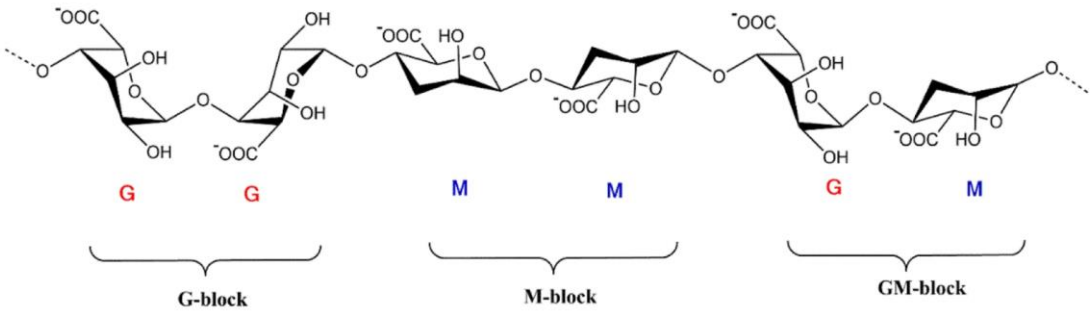

Figure 5: The alginate structure. *Alginate consists of β-D-mannuronic acid (M) and its C5 epimer α-L-guluronic acid (G), and the order and amount of each residue vary in different alginate producers. The figure is adapted from Abasalizadeh et al. [52].*

Alginate is an important polysaccharide due to its many characteristics and properties. Industrially, alginate is often used as thickeners and stabilisers due to its viscous nature [17]. In the medical field, alginate is much used in drug delivery, tablet formulations, and in tissue engineering [52, 53]. G-blocks are especially important, as these can bind to adjacent G-blocks via most covalent ions, such as Ca^{2+}[53]. The amount of G-blocks correlates well with the gel strength, with the longest G-blocks giving the strongest gels [54]. By using different alginate types, the gel properties such as viscosity, porosity, and stiffness can also be controlled [17]. Since alginate is an anionic polyelectrolyte, it can make neutral complexes with cations, such as Na^+ and K^+. When alginate is in its acid form it is insoluble in water. This is exploited in the production of industrial alginate, where alginic acid can be separated from co-ions such as Mg^{2+} and Ca^{2+} before it is washed, filtrated, and neutralised, often with Na^+ [55].

1.3.2 Alginate biosynthesis

In alginate-producing *Pseudomonas spp*, all but one of the proteins involved in the biosynthesis are expressed from one operon, being controlled by the *algD* promoter [56]. Alg8 and Alg44 are involved in the polymerisation step, while *algK*, *algE*, *algG*, *algX*, *algI*, *algJ*, and *algF* encodes for proteins that are important for modification and translocation of alginate to the periplasm [11, 17]. AlgD, AlgA, and AlgC, where the latter has its gene located outside of the operon and with its own internal promoter, are involved in the conversion of fructose-6-

phosphate (F6P) into GDP-mannuronic acid [17]. The genes within the alginate operon and their functions are shown in Figure 6.

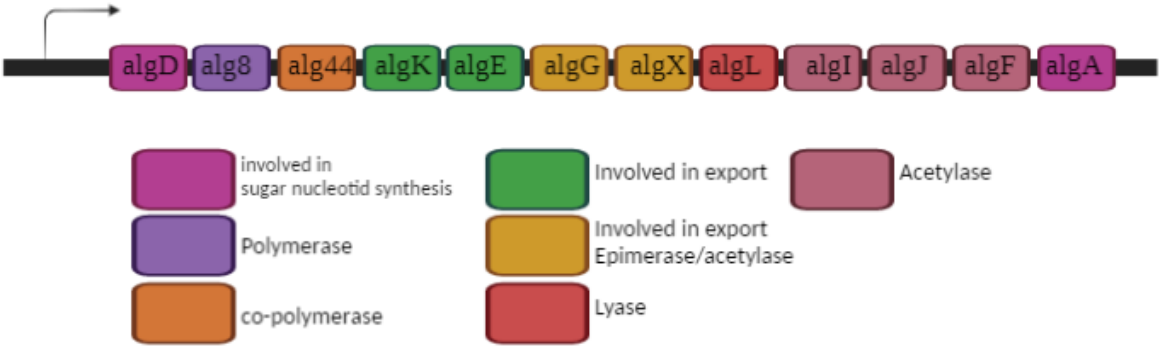

Figure 6: Characterisation of the genes within the alginate operon*. The genes are colour coded based on their main function. The image is modified from Franklin et al. [11] and inspired by Maleki et al. [17].*

When grown on glucose, fructose, or glycerol, the carbon sources will be mainly metabolised through the Entner-Doudoroff and pentose phosphate (PP) pathway, rather than through glycolysis [57, 58]. F6P will be produced, either from glucose-6-phosphate (G6P) or from 6-phosphogluconate by the more preferred PP pathway [59]. The rate of alginate biosynthesis has also been found to be dependent on the amount of available F6P [57]. From F6P, the alginate precursor GDP-mannuronic acid will be made, involving AlgA, AlgC, and AlgD [17]. AlgA is a phosphomannose isomerase/GDP-mannose phyrolase (PMI/GMP) catalysing F6P into mannose-6-phosphate (M6P) [11, 17]. AlgC, being a phosphomannomutase, will convert the M6P into mannose-1-phosphate (M1P). AlgA will then convert the M1P into GDP-mannose, before AlgD, being a GDP-mannose dehydrogenase, converts the GDP-mannose into GDP-mannuronic acid [11, 17].

Alg8 is a glycosyl transferase, assisted by the co-polymerase Alg44 [17]. They are in a six-protein membrane complex along with AlgX, AlgG, AlgK, and AlgE [37]. These proteins are all necessary for the polymerisation and secretion of alginate [11]. AlgXGK will guide the alginate through the periplasm and also protect the chain from AlgL [37]. AlgL will function as a “clean-up” protein, removing alginate originating from defect export complexes [60].

In the periplasm, it is thought that O-acetylation will be the first modification to alginate [37]. AlgFIJ makes up the O-acetylation complex, and they will transport acetyl to AlgX, which is an O-acetyltransferase [37]. AlgX will then transfer the acetyl groups to M-residues [17]. AlgG is able to catalyse the epimerization of M-residues to G-residues, creating G-blocks that are important for properties such as gel formation and thickening [37]. Lastly, AlgE will be responsible for the secretion of the mature alginate, guided to the outer membrane porin by AlgK, where the latter has a TPR domain important for protein-protein interactions [11, 37, 61].

Regulation of alginate synthesis can happen on several different levels. The sigma factor AlgU promotes transcription of the *algD* promoter, as well as having a positive regulatory effect on its own operon and other genes such as AlgC [62]. AlgU can be inhibited by the anti-sigma factors MucA and MucB, that when not inactivated will bind and disrupt AlgU. By disturbing the MucA factor, it will no longer be able to disrupt the sigma factor AlgU. In SBW25*mucA*

the bacteria produces high amounts of alginate due to the MucA inactivation [10]. In comparison, the SWB25 wild-type strain will hardly express the *alg* operon under laboratory conditions. Post-translational regulations include O-acetylation, which protects M-residues from epimerisation [37], and regulation by MucR, which can produce c-di-GMP that binds allosterically to Alg44 and activates the co-polymerase [17]. AlgC is also thought to be involved in alginate regulation through its PMM and PGM activity, as it is involved in the synthesis of other precursor molecules used for the synthesis of Psl, rhamnolipids, and LPS exopolysaccharides, which can compete for the same substrates and precursor nucleotides as alginate [3].

1.4 Sugar nucleotides involved in *P. fluorescens* biofilm are sharing common precursors

Alginate and Psl are thought to both be part of the *P. fluorescens* biofilm, and the synthesis of the exopolysaccharides involves several common precursor molecules or enzymes which are also needed for other biofilm components and LPS synthesis [63]. UDP-D-glucose and dTDP-L-rhamnose are also used to synthesise the LPS core, while GDP-D-mannose synthesised by AlgC and WbpW is used to create the A-band LPS [63]. Alginate requires GDP-D-mannose, while cellulose (not shown) is composed of glucose, and rhamnolipids consist of rhamnose units [2, 11, 64]. *P.* aeruginosa Psl require GDP-D-mannose, UDP-D-glucose, and dTDP-L-rhamnose [3]. An overview of the precursor and enzymes involved in the conversion of each molecule is given in Figure 7.

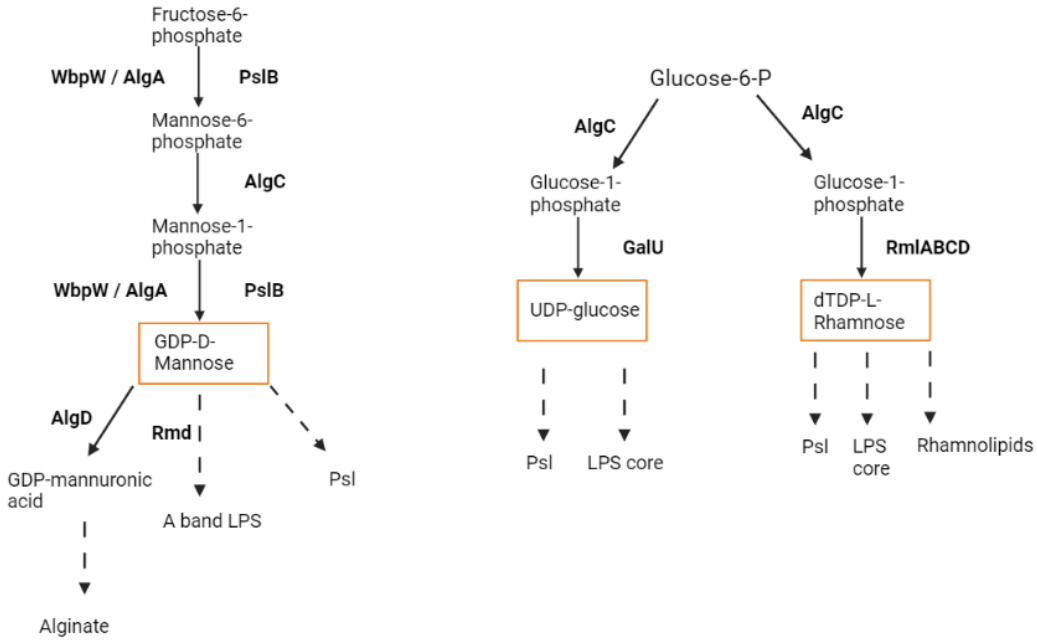

Figure 7: Production of the precursors involved in alginate, LPS, rhamnolipid, and Psl production. *Alginate, LPS, and Psl share GDP-D-mannose as a precursor molecule. While AlgC is thought to participate in all three pathways, Psl uses PslB, alginate uses AlgA, and LPS uses WbpW in the remaining steps. In addition, Psl requires UDP-Glucose and dTDP-L-rhamnose, with steps catalysed by AlgC, GalU, and RmlABCD. dTDP-L-rhamnose made in this pathway is also a precursor for rhamnolipids. For details about the biosynthesis of Psl from the precursor sugars see section 1.2.2. LPS also uses UDP-glucose and dTDP-L-rhamnose as precursors for the LPS core, as well as GDP-D-mannose as a precursor for the A band LPS but with different enzymes not shown. Image is inspired by figure 5 from Byrd et al. [3].*

Both alginate and *P. aeruginosa* produced Psl require GDP-D-mannose as a precursor molecule [3, 11]. For alginate, this conversion of F6P consists of three steps, with AlgA catalysing the first and third steps, and AlgC catalysing the second step [49]. For Psl, PslB is thought to resemble AlgA, having similar activity. This is also the case for A-band LPS synthesis, using WbpW instead of AlgA. In addition, AlgC is thought to be required for the catalysation of M6P into M1P [3]. For Psl, GDP-D-mannose is then converted to D-mannose making up parts of the Psl polysaccharide. For alginate, AlgD will further convert GDP-D-mannose into GDP-mannuronic acid, which is the M-residue in alginate [17].

Psl from *P. aeruginosa* further requires two more precursor molecules. AlgC is also likely involved in producing the substrate for GalU, which will convert glucose-1-phosphate into the UDP-glucose precursor [64]. LPS also utilises UDP-glucose, as does cellulose (not shown) [28]. The last sugar residue found in Psl is L-rhamnose. This is produced in the Rml pathway, involving RmlC [3]. A study found that deletion of *rmlC* caused defective Psl production [65]. When the precursor sugars for Psl are synthesised, they will be polymerised, translocated, and exported to the periplasm by the proteins in the Psl operon [3, 11].

dTDP-L-rhamnose is also a precursor for the biosurfactant rhamnolipid, along with Psl from *P. aeruginosa*, and LPS. Rhamnolipid is most often found in the form of a dimer of fatty acid and either one or two rhamnose molecules [66]. Just as for Psl and LPS, G6P is converted into G1P by AlgC, and then to L-rhamnose by RmlABCD in several steps [66]. Thus, AlgC is used to create precursors for several exopolysaccharides and lipids, having the compounds competing for the same resources. One study in *P. aeruginosa* also found that rhamnolipid-negative strains produced more Psl, indicating that there is some sort of balance between the production of the two compounds [67].

1.5 Monosaccharide analysis

One of the main goals of this thesis was to investigate the monosaccharide composition of the Psl polysaccharide. For this analysis, there are several suitable methods. Different methods will have different strengths and weaknesses, and it is important to find a reliable method that is giving an accurate output without being too expensive or too demanding to perform. Monosaccharide analysis can be complex and difficult because the complexity of carbohydrates can make it hard to liberate monosaccharides without destroying them prior to analysis. The free monomers must then be separated before analysis, which is done differently for each method. The liberation of free monosaccharides is usually completed using acid hydrolysis, where the glycosidic linkages between the monomers are cleaved [68]. The use of concentrated sulfuric acid is characterised by a high conversion rate. However, not all compounds are suitable for this, as it can also be associated with a lot of unwanted side reactions [68]. The Saeman hydrolysis is a two-stepped procedure where concentrated sulfuric acid is added to swell the sample while incubated at room temperature before the temperature is elevated and water is added to dilute the acid. The first step will cause the release of carbohydrates from within the sample, with swelling of crystalline polysaccharides such as cellulose and chitin making them available for degradation. The liberated polysaccharides will then be hydrolysed in the second step [69].

After the monomers have been liberated, they must be separated and analysed. The most common analysis method for such carbohydrate analysis includes gas chromatography (GS), high-performance liquid chromatography (HPLC), high-performance anion exchange chromatography with pulsed amperometric detection (HPAE-PAD), and nuclear magnetic resonance (NMR), and each method can be connected to several other methods for more specific analysis as well [70]. HPLC uses a mobile phase containing the sample, which is passed onto the stationary phase where compounds bind to the column based on parameters such ah pH, size, and viscometry [71]. Then, a detector will recognize the analytes based on their elution time and convert the signals into a chromatogram [72]. Gas chromatography includes chromatographic techniques where the compounds are in the gas phase. Firstly, the compounds to be analysed must be vaporised into a gas before it is sent into a stationary phase which could be a solid or a liquid [73]. If the stationary phase is a liquid, the technique is termed gas-liquid chromatography [73]. After the separation, a detector will measure the compound. NMR, or proton-NMR, is a widely used technique for determining the molecular structure of a sample and is able to detect one isotope at a time, based on different characteristic behaviour [74]. This technique allows for the detection of detailed information about structures, bindings, and conformation of each compound.

1.5.1 HPAEC-PAD

HPAEC-PAD is a method where carbohydrates will be separated by anion exchange. When the monosaccharides are exposed to high pH, the OH groups will ionize into oxyanions [75]. By sending in a buffer solution containing OH-groups, the hydroxyl groups will bind to the functional groups in the column, which are quaternary amines [76]. When the mobile phase is added to the column, the OH^- groups in the carbohydrates will start competing for the binding sites. Different monosaccharides will have different pKa, which is the basis of the separation. Carbohydrates having low pKa will bind stronger to the column and be eluted later than carbohydrates with high pKa. Neutral or cationic components will not interfere with the carbohydrates of interest, as they elute in the void volume of the column.

After separation, the monosaccharides will be oxidised on a gold-surfaced electrode, creating an electrical current that can be measured [71, 76]. After the measurement, the gold surface must be cleaned, which happens by first racing the potential so that the gold surface can be oxidised so that the carbohydrate oxidation products fall off. Then, the electric potential is lowered enough for the gold surface to reduce back to gold, and a new measurement can be done. A total of three potentials are thus created.

When conducting the analysis, reference compounds must be included. By creating standards of typical monosaccharides with known concentrations, the content of the sample can be determined by comparing the tops in the chromatogram. A chromatogram showing the retention time for a series of common monosaccharides is shown in Figure 8.

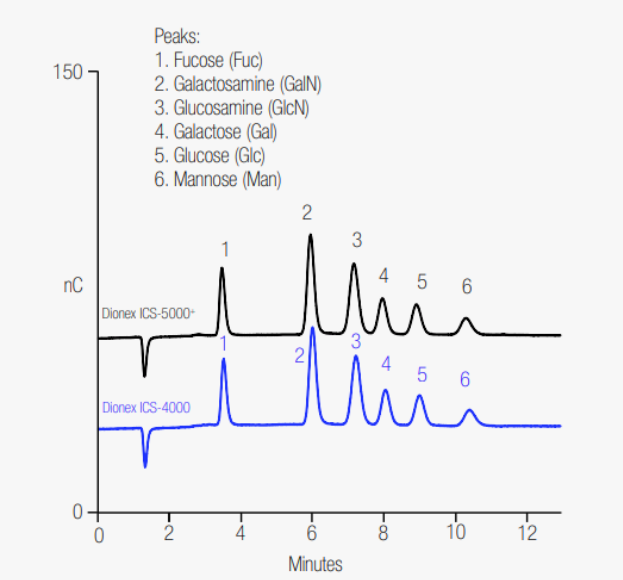

Figure 8: The chromatogram from six common monosaccharide sugars with known concentration being analysed with HPAEC-PAD. *The analysis is conducted on two different Dionex columns by the manufacturer. The picture is taken from a brochure by Thermo Scientific [77].*

1.6 Genetic engineering

1.6.1 DNA can be transferred to other organisms through plasmids

E. coli is a much-used organism for cloning plasmids. Even if the target organism is another species, *E. coli* is still the organism of choice for the construction of plasmids for a variety of reasons [78]. It is not only easy to grow and have a short replication time, but laboratory strains are considered safe, and plasmid DNAs can be engineered to carry foreign DNA fragments and still replicate within the bacteria. In 1970 the first successful experiments with E. coli taking up naked DNA from bacteriophages when treated with $CaCl_2$ were conducted [78].

Foreign DNA must be able to replicate within the host cell to not be lost during cell division. The DNA of interest is therefore often transported through plasmids [78]. A plasmid is a circular double-stranded DNA molecule that exists in addition to the chromosomal DNA and often contains accessory genes which are genes that are not necessary for survival but give the organism advantages such as antibiotic resistance [78]. A plasmid must contain several elements to be able to replicate within the host cell. The origin of replication (ORI) is essential for the replication of the plasmid making the plasmid able to replicate independently of the host cell chromosome, while the genes of interest within the plasmid must have promoters to have their gene product expressed [79]. A plasmid will also often contain a multiple cloning site, being a short DNA segment with multiple restriction sites where foreign DNA can be inserted through restriction cutting and ligation [78].

XylS/PmG5

The XylS/Pm regulator/promoter system is much used for regulating the expression of genes in different bacteria such as *E. coli* and *Pseudomonas* [80, 81]. The Pm promoter is originating from the *Pseudomonas putida* TOL plasmid pWWO [80]. Its regulator XylS can be induced by binding of an effector, such as m-toluate or other benzoic acid derivatives [81]. The activated XylS will then bind as a dimer to a σ^{32}-dependent RNA polymerase in early stationary phase, or a σ^{38}-dependent RNA polymerase in late exponential phase [82]. When XylS is bound in the

activator seat, the RNA polymerase will bind to the Pm promoter and initiate the transcription of the genes the promoter controls.

The Pm promoter can be activated at different levels by changing the concentration of the inducer [83]. Separate elements of the XylS/Pm system can also be modified to improve its use and effect in specific bacteria or to control specific genes. One of the mutated XylS/Pm derivatives is the PmG5 promoter. The PmG5/XylS system is weaker than the Pm promoter [60], but the derivative PmG5 is thought to be better at ensuring low background expression of the genes it controls. This is an advantage compared to the Pm promoter, which has been reported to create high background levels of the genes it controls in *P. fluorescens* [80].

1.6.2 Homologous recombination

Homologous recombination is based on two DNA molecules having extended, nearly identical sequences, allowing for the exchange of genetic material [84]. When the exchange of DNA only occurs at a particular DNA sequence with short homologous regions, the process is referred to as site-specific recombination [85].

Homologous recombination is often involved in repairing double-stranded breaks in the DNA. The DNA repair machinery will then use a DNA sequence with homologous regions as a template and synthesise a new strand [85]. Homologous recombination can also occur by bacterial conjugation, where the bacteria will transfer chromosomal DNA into another bacteria [85]. Homologous recombination is widely used by bacterial scientists, allowing the exchange of DNA between two bacteria [84]. It is especially useful for moving mutations in or out of the bacterial chromosome.

For homologous recombination to occur, the insert molecule and the host molecule must contain two almost identical sequences, allowing exchange of DNA [85]. In the insert DNA molecule, the desired sequence that should be integrated into the host chromosome is flanked by regions identical to regions on the host chromosome. The exact sequence does not matter as long as it is nearly identical to regions in the vector DNA [85].

In *E. coli*, the cells use the recombinase RecA along with the endonucleases RecBCD or RecF to complete homologous recombination [84]. The RecF pathway is slower, and also requires more proteins than the RecBCD pathway, but is often utilized in the case of defective replication forks [84]. RecBCD will bind to DNA and create ssDNA overhangs. RecB will move in the 3’5’ direction, while RecD moves in the 5’3’ direction at the other strand [85]. When encountering a chi sequence, 5’-GCTGGTGG-3’, RecC will bind, and this causes decreased degradation of the 5’ strand and increased degradation of the 3’ strand [85]. The resulting ssDNA with a 3’ end will then be bound to by RecA, which binds to ssDNA and forms DNA-protein filaments. These filaments will search for other DNA molecules with homolog regions. The RecA filaments will pair and assist in exchanging strands between the two homologous segments [84]. The exchange can either happen by single-strand annealing or by a strand invasion mechanism [84]. In the case of single-strand annealing, the two homologous DNA sequences will have a dsDNA break at different points, where 3’ overhangs will be made, and when the complementary sequence is exposed, the two strands will be annealed. In the case of the more common strand invasion, RecA will be bound to 3’ ssDNA, find homologous unbroken DNA, and invade this duplex, creating a branched DNA structure.

The DNA exchange promoted by RecA can cause gaps in the DNA strand, and the recombination intermediates are called Holliday structures. These can be resolved by branch migration mediated by the protein complex RuvAB and cleavage by the nuclease RuvC [85]. Lastly, the resulting nicks in the DNA will be sealed by a DNA ligase.

Site-specific integration includes only short stretches of homology and will therefore target a specific DNA sequence rather than occurring throughout the genome with homologous sequences with the exogenous DNA [85]. Thus, site-specific recombination is useful for inserting a new gene or DNA fragment at a specific location in the host cell chromosome. Site-specific recombination involves DNA with homologous regions, as well as a recombinase [86]. The recombinase will promote the formation of a Holiday junction with the two DNA fragments, and then either insertion, excision or inversion will occur. In case of insertion, the recombinase mediates cleavage, strand exchange, and ligation of the cleavage. This causes the left side of the homologous region of the inserted DNA to be joined with the right side of the homologous region on the host chromosome, as seen in the first recombination event in Figure 9 showing the recombination of the Psl operon in *P. fluorescens* and the pCSG4 plasmid having homologous regions flanking the PmG5 promoter that is to be inserted into the chromosome. In the case of excision or inversion, the recombinase will bind the recombination sites that is found on the same DNA segment, and mediate cleavage and exchange, causing the DNA sequence between the restriction sites to be inverted or excised.

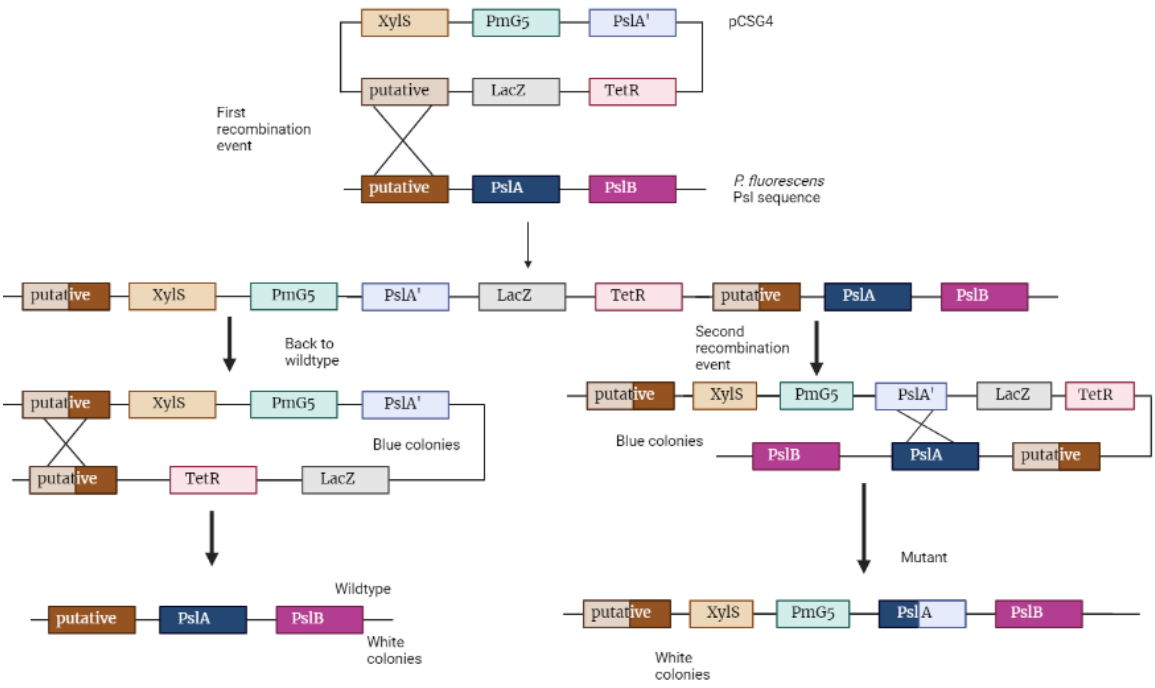

Figure 9: An overview of the homologous recombination process, and the two possible outcomes when using a plasmid containing the LacZ gene and an antibiotic selection marker. *For both, the first recombination event will happen which will be shown by colonies turning blue due to the disruption of the lacZ gene. By cultivating the bacteria in LA media, the second recombination event is allowed to occur, as shown to the right. Signs of the second recombination event are that colonies are no longer turning blue, as well as they have lost their antibiotic resistance. However, colonies that have gone back to wild-type, as shown to the left, no longer have the lacZ gene nor the tetracycline resistance gene, requiring testing with PCR to be certain whether the colony is a mutant or has reverted into the wild-type.*

2 Aims

While alginate is well studied in *P. fluorescens* engineered strains, Psl is barely investigated. Most information about Psl comes from *P. aeruginosa*, where it consists of L-rhamnose, D-glucose, and D-mannose, and is involved in biofilm formation, surface adhesion, and biofilm architecture [2]. Therefore, it is interesting to investigate the Psl molecule in *P. fluorescens*, to see if it is similar to Psl in *P. aeruginosa*, where it is known to be a virulence factor. The main goal was to determine the composition of Psl, and then to see if alginate and the enzymes AlgC and AlgA affect the production of Psl. The objectives can be divided into four different parts:

1. How similar are the genes within the Psl operon?
2. Is the composition of the Psl polysaccharide from *P. fluorescens* similar to Psl from *P. aeruginosa*?
3. Will increased Psl production affect phenotypical traits such as growth and biofilm formation?
4. Is the Psl production affected by AlgA and/or AlgC? And will increased Psl expression interfere with alginate production?

The Psl gene cluster identified in *P. fluorescens* SBW25 was investigated and compared to the known genes in *P. aeruginosa* using a variety of different biochemical tools. Arguments as to why the Psl genes are within the same operon were also provided from the analytical results.

The second objective was to investigate the compound of the Psl and to see if *P. fluorescens* was able to produce the exopolysaccharide. The monosaccharide analysis of different mutants created with a PmG5 promoter in front of the Psl operon, overexpressing the Psl genes was investigated using a Psl extraction protocol by Byrd et al. [3] and analysed using HPAEC-PAD. The results were compared to try to determine the amounts and composition of Psl.

As Psl is known to affect biofilm and biofilm structure in *P. aeruginosa*, this was also to be investigated in *P. fluorescens*. By conducting a motility assay, the difference in motility for Psl operon overproducing strains was compared, to try to see if the motility was affected by increased Psl genes expression, as it was for *P. syringae*, where Psl overexpression caused less swarming than in wild-type mutants [87]. In addition, Psl in *P. syringae* is thought to be promoted by cold temperatures, leading to the testing growth and colony shapes of *P. fluorescens* Psl operon overproducing mutants when grown at 8 ℃ and 30 ℃. The phenotype of mutant overexpressing Psl genes and wild-type strains were also compared, with the expectation that Psl would stimulate growth and form more rigid-formed colonies in *P. fluorescens* based on its role in biofilm architecture in *P. aeruginosa* [34].

Lastly, the effect of PMM and PMI activity was attempted measured, using a protocol developed for PMM and PMI activity in *P. aeruginosa* [88]. The protocol had to be adapted for *P. fluorescens*, using knowledge and experience to find suitable conditions for detecting high enough levels of each enzyme. The aim was to use the measurements to determine the role and importance of AlgA and AlgC in relation to Psl production.

3 Materials and Methods

In this chapter, the recipes for the media used will be provided, as well as an explanation of all protocols and techniques used in this study. In addition to the methods used in the lab, such as making media, cultivation of bacteria, plasmid isolation, and PCR, software and web tools will also be explained.

3.1 Solutions

3.1.1 Psi-medium

- 5 g/L yeast extract
- 20 g/L tryptone
- 5 g/L $MgSO_4$

pH was adjusted to 7.6 using KOH and autoclaved.

3.1.2 Transformation buffer I (TBF1)

- 30 mM $C_4H_6CaO_4$
- 100 mM RbCl
- 10 mM $CaCl_2$ x $2H_2O$
- 50 mM $MnCl_2$ x $4H_2O$
- 15% v/w glycerol

pH was adjusted to 5.8 with dilute acetic acid, and distilled water was added to a total volume of 200 ml. The mixture was sterilized by filtration.

3.1.3 Transformation buffer 2 (TBF2)

- 10 mM Morpholinepropanesulfonic acid (MOPS)
- 10 mM RbCl
- 75 mM $CaCl_2$ x $2H_2O$
- 15% v/w glycerol

pH was adjusted to 6.5 with a dilute NaOH, and distilled water was added to a total volume of 100 ml. The mixture was sterilized by filtration.

3.1.4 Super Optimal Broth (SOC)

- 20 g/L tryptone
- 5 g/L yeast extract
- 0.5 g/L NaCl
- 2.5 mM KCl
- 3.6 g/L glucose
- 5.08 g/L $MgCl_2$

Distilled water was added for a total volume of 50 mL. The mixture was sterilised using filtration and stored at -20 ℃.

3.1.5 Luria Broth (LB)

- 10 g/L tryptone
- 5 g/L yeast extract
- 5 g/L NaCl

The mixture was autoclaved. When making LA plates, 15 g/L agar was added prior to autoclaving. When adding antibiotics to the plates, the mixture was cooled down to around 50 ℃ before adding the appropriate antibiotics and mixing well before pouring the plates.

3.1.6 Pseudomonas Isolation Agar (PIA)

- 45 g/L Difco PIA
- 20 mg/L glycerol

Water was added before the mixture was autoclaved and poured into agar plates. When adding antibiotics, the solution was cooled down to 50 ℃ and the solution was mixed thoroughly using a magnet stirrer before pouring it into the plates.

3.1.7 DEF3 minimal medium

- 0.39 g/L yeast extract
- 0.65 g/L KH_2PO_4
- 2.73g/L $(NH_4)_2HPO_4$
- 0,9 g/l citric acid·H_2O
- 0.001 g/L H_3BO_3
- 0.005 g/L $MnCl_2·4H_2O$
- 0.0039 g/L EDTA·$2H_2O$
- 0.0005 g/L $CuCl_2·2H_2O$
- 0.0008 g/L $Na_2Mo_4O_4·2H_2O$
- 0.0008 g/L $CoCl_2·6H_2O$
- 0.0027 g/L $Zn(CH_3COO)_2·2H_2O$
- 1,56 g/l NaCl2
- 5 g/L MOPS
- 20 g/L Fructose
- 0.57 g/l $MgSO_4·7H_2O$

Everything until and including MOPS was added in the exact order and dissolved in 900 µL RO-water. When suitable, compounds were added as trace elements from a stock solution. pH was adjusted to 7.00 using 10M NaOH, and the mixture was autoclaved. Fructose was dissolved in 100 µL RO water and autoclaved, while $MgSO_4$ was sterile filtered. All components were mixed, and the appropriate antibiotic was added prior to cultivation.

3.1.8 Kings Broth

- 20 g/L peptone
- 10 mL/L glycerol
- 1.5 g/L $MgSO_4$
- 1.5 g/L $KHPO_4$
- 15 g/L agar

Everything but $MgSO_4$ was mixed with distilled water. The pH was adjusted to 7.2 before adding $MgSO_4$. The mixture was autoclaved, and antibiotics or m-toluate were added just before pouring the plates.

3.2 Cultivation and storage of bacteria

When bacteria were cultivated from frozen culture or solid culture on agar plates, a toothpick was used to scrape some of the bacteria and transfer it to liquid media or agar plates with the appropriate antibiotics. In the case of *E. coli*, the liquid LB culture was cultivated at 37 ℃ in the shaking incubator (225 rpm), containing the appropriate antibiotics to preserve the inserted plasmids. When plating out *E. coli* on agar, LA with the appropriate antibiotic was used, and the plates were cultivated at 37 ℃. For *P. fluorescens*, the bacteria were cultivated in liquid media at 30 ℃ in the shaking incubator (225 rpm). When plating out *P. fluorescens* on agar, PIA or LA were used, along with the appropriate antibiotics, and incubated at 30 ℃ for 1-2 days.

To identify the growth state of the bacteria, OD_{600} is often measured. The bacterial growth curve consists of an initial lag phase, characterised by no growth and no change in OD [19]. The following exponential phase is characterised by exponential growth, and it is in this phase the cells are the healthiest. The stationary phase is characterised by no change in OD, as the number of cells that dies and the multiplication rate is in balance [19]. When the measured OD is declining after reaching the stationary phase, cell death is happening faster than cell growth. To prevent cell death, the growth can be slowed down by lowering the temperature. In this study, colonies on agar plates were kept in the fridge (-4℃) for up to 4 weeks before they were thrown away. The liquid culture was spun down and the pellet was put in the -20 ℃ fridge for short-term storage, and for long-time storage 900 µL of the culture was added in cryotubes along with 300 µL 60% glycerol and placed in the -80 ℃ freezer.

3.2.1 Antibiotics

Table 1 gives an overview of the kind of antibiotics used as well as the stock solution, and the concentration used for the different strains.

Table 1: An overview of the antibiotics and the concentration used in this study.

Antibiotics	**Stock concentration (µg/mL)**	**Concentration (µg/mL) used for *P. fluorescens***	**Concentration (µg/mL) used for *E. coli***
Ampicillin (Amp)	200	-	200
Tetracycline (Tet)	10	10	12.5
Apramycin (Apr)	25/50	25	50
Triclosan (TCA)	1000	0.0025	-

3.3 Plasmid isolation

Isolation of plasmids was done using the ZymoPURE^{TM}Plasmid Miniprep Kit by Zymo Research [89]. Plasmid isolation is a method for separating plasmid DNA from chromosomal DNA and other cell components in the bacteria, giving only the plasmid DNA. The Zymo Miniprep Kit is a modified version of the method developed by Birnboin & Doly and exploits the fact that plasmid DNA and chromosomal DNA have different characteristics, such as size, denaturation, and renaturation at different pH levels [89, 90].

Protocol

All centrifugations happened at 13 300g at room temperature. 1.5 ml culture of bacteria (2 parallels in case of plasmids with low copy numbers) was centrifuged for 2 minutes, and the supernatant was discarded. 200 µL P1 buffer was added to the tube, and the pellet was resuspended. In the case of plasmids with low copy numbers, the liquid with the suspended pellet was transferred to the second Eppendorf tube, and the second pellet was resuspended. 200 µL P2 buffer was added to the tube and mixed by inverting the tube 2-4 times. P2 buffer contains NaOH and SDS, which will lysate the cells through a modified alkali lysis method. The sample was then incubated at room temperature for 2 minutes and when turning clear, purple, and viscous, 400 µL of P3 buffer was added. P3 contains RNase, which will degrade all ssRNA molecules in the sample. In addition, P3 buffer contains potassium dodecyl phosphate, causing neutralisation of the sample and precipitation of chromosomal DNA and denatured proteins. The sample was mixed gently until it turned yellow and then incubated at room temperature for 4-5 minutes. The sample was then centrifuged for 5 minutes to remove debris. The resulting supernatant was added to a collection tube, placed inside a Zymo-Spin^{TM} IIN column, and centrifuged for 1 minute. Any flow-through was discarded, and 200 µL Endo-Wash Buffer was added to the column and centrifuged for 1 minute, causing DNA to bind to the column and flowthrough of waste products such as proteins. 400 µL Plasmid Wash buffer was then added, and the column was centrifuged for 2 min to get rid of lipopolysaccharides and proteins. The column was lastly transferred to an Eppendorf tube, and 50 µL DNA elution buffer was added to the column. The sample was incubated for 1 min at room temperature, before being centrifuged for 1 minute to elute the DNA. The amount of DNA was then measured using the NanoDrop as described in section 3.4 and stored at -20 ℃.

3.4 Measure DNA and protein concentration

Using UV absorbance to measure the DNA concentration is a common technique, based on the conjugated double bonds in purine and pyrimidine rings in DNA and RNA [85]. These residues have an absorption peek at 260 nm which can be measured, and the value will be proportional to the concentration of the measured nucleic acid [91].

The NanoDrop uses a modification of the Beer-Lambert equation to calculate the concentration of the sample.

$$c = A * \frac{1}{\varepsilon * b} \quad \text{(I)}$$

A is the absorbance, e is the wavelength-dependent molar extinction coefficient (ng-cm/μL), b is the sample path length (cm), and c is the concentration in ng/μL. The equation can also be simplified to c = A * f, where f is called a factor (ng-cm/μL). For dsDNA, the factor is set at 50 ng-cm/μL [92]. The instrument can also give information about the purity of the sample, by showing purity ratios. For DNA, A260/A280 ~ 1.8 is accepted as a pure ratio, while A260/A230 between 1.8 and 2.2 is considered pure for DNA and RNA [92]

The protein concentration was measured using the Protein A280 application, measuring the concentration at 280 nm. 1 Abs = 1 mg/mL was chosen because the extinction coefficient was not known, and the rough estimate of the protein concentration was sufficient. If needed, the extinction coefficient would have been calculated or determined empirically [92]. The purity ratio for proteins is shown as the A260/A80 value, with 0.57 being accepted as pure [92].

Protocol

The NanoDrop Spectrophotometer was first cleaned with 2 μL MQ-water for 30 seconds on the lower pedestal and the arm was lowered, before using a laboratory wipe to remove the water. After choosing the type of molecule to measure, 2 μL of the blank (elution buffer for DNA and sonication buffer for proteins) was used to remove background noise from the sample. The sample was removed with a laboratory wipe. 2 μL of the sample was then added to the instrument. The screen showed the concentration of each sample, as well as the purity rate. The concentrations were noted, and the instrument was lastly cleaned using 2 μL of MQ-water for 30 seconds, for a total of three times.

3.5 Restriction cutting

A restriction enzyme is a protein that is able to recognize restriction sites in DNA sequences [78]. When the enzyme encounters such sites, it will cut the DNA. The discovery of such enzymes was awarded a Nobel prize in 1978, and more than 900 enzymes have been isolated so far [78]. The use of restriction enzymes to get DNA fragments with predictable lengths in gel electrophoresis is thus an easy, important, and much-used technique in the laboratory [93]. However, cutting DNA is not necessarily good if the DNA is not supposed to be cut. To avoid having its own DNA degraded by restriction enzymes produced by the bacteria, the organism will also produce methylases that will methylate the binding sites in its own genome, rendering it unavailable by the restriction enzyme [78].

The recognition sites for the enzymes are often 4, 6, or 8 nucleotides long, and inverted repeats are also common [79]. When the enzyme cuts, it will break the DNA backbone by cutting phosphodiester bonds between the sugar residues, creating a 3’ hydroxyl and a 5’ phosphate [78]. Group I enzymes will cut DNA several base pairs away from the restriction site, involving DNA looping and requiring ATP-hydrolysis [94]. Type II will, on the other hand, cut the DNA fragment in the recognition site, and is generally more used in laboratory settings [78].

Two kinds of ends can be created with restriction enzymes, being blunt or sticky ends [79]. Blunt ends are when both DNA strands are cut at the same time and place, giving no overhangs. Sticky ends are when the enzyme cut the two strands at different places and will give overhanging ends. Such sticky ends are much easier to ligate together because blunt ends will

most of the time drift apart, while sticky ends can bind to complementary sticky ends from another DNA fragment, and then be ligated together [79]. In this study, restriction enzymes have been used to create new plasmids and check DNA fragments using gel electrophoresis. An overview of all restriction enzymes used in this study is provided in Appendix A.

Protocol

2 µL buffer, between 3 and 17 µL of DNA, and 0.5 µL of each enzyme were mixed, together with distilled water for a total volume of 20 µL. The mixture was spun down and placed in a water bath at 37 ℃, for a minimum of one hour and a maximum of one day. When needing to convert sticky ends to blunt ends, 0.5 µL Klenow polymerase and 0.5 µL dNTPs were added and the sample was incubated at 15 minutes at 37 ℃. If necessary, the restriction mixture was stored at -20 ℃.

3.6 Ligation

DNA ligase was discovered in 1967 and soon became a much-used biotechnological tool [78]. Two DNA fragments can be ligated together, yielding a new, longer DNA fragment. If two DNA molecules are cut with the same restriction enzymes, giving the same ends, the two fragments can be joined together by the ligase enzyme. Ligase will create a new, covalent phosphodiester binding between 5' phosphate and the 3' OH group in each fragment, yielding a new, longer DNA fragment from the two previous fragments [79]. The role of DNA ligase outside the laboratories is to seal nicks in double-stranded DNA after replication and is necessary for DNA synthesis and DNA repair. The most common ligase in the laboratory setting is T4 originating from bacteriophage T4 [79].

Protocol

The DNA to be joined together was first purified and then added into an Eppendorf tube. A molar ratio of 3:1 (insert, vector) was used to obtain successive ligation. 2 µL 10x ligase buffer (T4 buffer) and 1 µL ligase (T4) was added to the mixture. Distilled water was added to a total volume of 20 µL. The mixture was then placed between 4 – 14 ℃ and ligated overnight. For ligation at 4 ℃, the sample was allowed to ligate for a maximum of 2 days.

3.7 Gel electrophoresis

Gel electrophoresis is a common method for separating DNA or RNA fragments based on their size [95]. DNA is negatively charged due to its phosphate groups and will be attracted to positive charges [79]. Gel electrophoresis is performed using an agarose gel. Agarose is purified agar, a substance isolated from seaweeds and red algae, which is a polysaccharide consisting of β-D-galactose and 3,6-anhydro-α-L-galactose, and is soluble in boiling water above the melting point of agarose [79]. When cooled below the melting point, agarose will form a porous gel, allowing molecules to move through the gel. When applying a negative charge at one end and a positive charge at the other end of the gel, charged molecules can be drawn through the gel. Small molecules will move faster through the gel than larger molecules, and the agar concentration of the gel will also affect the movement of the molecules [79].

Agarose is dissolved in Tris-Acetate-EDTA buffer (TAE) to keep the pH of the solution at the desired level, as well as provide the solution with ions to lead electricity that will move the DNA towards the positive charges [79, 95]. After the agarose mixture has cooled down, the gel will be placed in TAE buffer and the DNA samples are loaded into the wells. For visualisation of the samples, GelRed is mostly used as this is more sensitive than GelGreen. When cutting DNA from the gel, GelGreen is often used as it is compatible with blue light transilluminators. This is to avoid exposure to UV radiation, which could be very damaging to DNA. Gel electrophoresis can also be used with ethidium bromide staining to quantify the amount of nucleic acid on the gel, as it will give higher intensity with a higher amount of DNA [96]. Loading Dye must also be added to the DNA samples to be able to visualise the DNA fragments in the gel, as well as making the DNA solution a bit heavier to ease the load into the wells.

Protocol

0.8% agarose gel with either GelRed or GelGreen was used, depending on the purpose of the gel electrophoresis. The samples were run at 100V for the appropriate amount of time before visualising the gel using the BioRadChemiDoc XRS+ along with ImageLab software.

A gel chamber was placed in a mold, along with a well-forming. About a third of the gel tray was filled with agarose gel and let solidify for 15 minutes. In the meantime, the samples were prepared. 2 µL Gel Loading Dye Purple (6x) was mixed with between 1 and 17 µL DNA and nuclease-free H_20 giving a total volume of 20 µL. DNA standards (λDNA cut with PstI and λDNA cut with HindIII, see Appendix E) were made using 5 ng DNA, 2 µL of loading dye, and water. The samples were put in the wells, and the gel was run at 100V and 400 mA using BioRad PowerPac Basic Power Supply for 35-50 minutes, based on the size of the desired fragments. The resulting gel was put in the ChemiDoc and ImageLab to visualize the DNA bands, also allowing to change the colours and the colour intensity if needed.

When cutting out fragments from the gel, the gel was put on a blue screen protection plate, and a shield and UV glasses were used to see the bands and protect us from UV light. The fragment was cut from the gel using either a scalpel or a plastic tool and then put the gel piece in an Eppendorf tube. The sample was then purified, as described in section 3.8.

3.8 Gel extraction and purification of liquid DNA

3.8.1 Extraction of DNA from gel

After cutting out DNA fragments on agarose gel, the sample should be purified before it is used further. In this study, Monarch ® DNA Gel Extraction Kit of New England Biolabs was used for gel extraction and purification [97]. Gel purification of DNA fragments is based on solid-phase extraction of DNA, a method first proposed in 1989 [98]. The method is based on adding chaotropic agents to help the binding of DNA to a solid phase, such as silica. They will interfere with the three-dimensional macromolecular structure of the DNA, causing it to bind to the silica matrix [99]. The chaotropic agents will also help lyse cells and inactivate deoxyribonucleases.

Protocol

For the gel extraction, all centrifuging was done using 13 300 rpm. The desired DNA fragment was cut from the 0.8% agarose gel containing GelGreen under UV light and put into an Eppendorf tube. The gel slice was then weighed, and 4 volumes of Gel Dissolving Buffer were added to the tube to dilute and dissolve the gel. The sample was incubated at 50 ℃ until the gel was dissolved, taking about 10 minutes. Every 4-5 minutes, the sample was vortexed. For DNA bands larger than 8 kb, 1.5 volume of RO-H_2O was added to the dissolved sample to improve the binding of the DNA to the column. The sample was then loaded into the column in the collection tube and centrifuged for 1 minute at room temperature. After discarding flow through, 200 μL of DNA Wash Buffer containing ethanol was added, and the sample was recentrifuged for 2 minutes. This was repeated twice to get rid of proteins, short primers, and other cell debris with low molecular weight. The column was then transferred to an Eppendorf tube, and 15 μL DNA Elution Buffer was added to the column. The sample was first incubated at room temperature for 1 min, and then centrifuged for 1 minute. In case of larger DNA sequences, the Elution Buffer was pre-heated to 50 μL before use.

3.8.2 Extraction of DNA from solution

Purification of DNA from solution is sometimes necessary to get access to enough DNA, and boiling cells to disrupt the cell wall might not be sufficient. DNA can therefore be extracted using a commercial kit, such as the EPICENTRE MasterPure™ Complete DNA and RNA Purification Kit [100]. In this kit, cells are lysed by adding Cell Lysis Solution along with Proteinkinase K for increased efficiency of the lysis and to get rid of any contaminating proteins in the cell pellet [100]. RNAse can also be added to remove RNA by breaking down the molecules. Then, the MPC Protein Precipitation Reagent is added for removal of cell debris and proteins. The mixture is washed with isopropanol to precipitate DNA, and the resulting pellet is washed with ethanol to remove co-precipitated salts and residual isopropanol, as ethanol is more volatile and can easier be removed before redissolving the DNA in an elution buffer.

Protocol

For DNA extraction and purification from solutions, all centrifugation was conducted at 13 300 rpm for 10 minutes at 4 ℃. 1μL of Proteinase K was added to 300 μL of Tissue and Cell Lysis Solution for each sample, while the cells were harvested by centrifuging. The supernatant was discarded, leaving approximately 25 μL of liquid. The pellet was resuspended in the Lysis solution containing Proteinase K and incubated at 65 ℃ for 15 minutes. Every 5 minutes, the sample was vortexed. Then, the sample was placed on ice for 5 minutes, before adding 1 μL RNAse and allowing the sample to incubate at 37 ℃ for 30 minutes. 150 μL of MPC Protein Precipitation Reagent was added to each sample and vortexed for 10 seconds. The sample was centrifuged, and the supernatant was recovered. 500 μL isopropanol was added to the sample and the tube was inverted 40 times. The sample was centrifuged, and the isopropanol was removed without dislodging the pellet. The pellet was washed with 500 μL 70% ethanol twice and put sideways with the lid off for 30 minutes to remove all ethanol. Lastly, the pellet was resuspended in 100 μL 10 mM Tris and left shaking at 37 ℃ for a minimum of one hour.

3.9 PCR

Poly chain reaction (PCR) is a simple way of amplifying specific DNA fragments. It involves primers, which are short single-stranded nucleotide sequences, complementary to the ends of the DNA fragment to be amplified [79]. In addition to primers, all four deoxynucleotides (dNTPs), DNA polymerase, a buffer making it favourable for the DNA polymerase to function, and the DNA to amplify must be added to the reaction mixture. For GC-rich organisms such as *Pseudomonas*, CG-enhancer should also be added as well. In this study, Q5 Polymerase made from protein engineering was used. Q5 has almost 280 times higher fidelity amplification than Taq, the most common polymerase in PCR, causing extremely low error rates [101].

The PCR consists of three stages, denaturation, annealing, and extension. During denaturation, the temperature is raised high enough for the two strands to denature and become single-stranded, often using 90-95 ℃ [79]. Then, the temperature is lowered to around 3 ℃ lower than the lowest melting point of the primers, allowing the primers to bind to the specific sequences [78]. The higher the temperature is in this step, the lower chance for primer binding to almost-complementary sequences, but too high a temperature will cause no binding at all [79]. In the extension stage, the temperature is elevated to the optimum temperature of the DNA polymerase, often 72 ℃. During this stage, the DNA polymerase will get to work, and use the bound primers to elongate the DNA strands. During the following elevation of temperature in the denaturation stage, the primers will fall off, and the newly created double-stranded DNA will become single-stranded again [78]. The PCR is normally allowed to go for 25-35 cycles, depending on how much DNA is needed to amplify [79]. In theory, the amount of DNA will amplify for each cycle. For the first strands, elongation will only stop when the temperature is elevated, creating much longer ssDNA strands than desired. However, as the cycles go on, the newly created DNA strands will also function as templates, eventually creating double strands with the desired length, which will outnumber the initial strands [78].

Protocol

50 µL mixture

- 0.5 µL DNA
- 1,25 µL (20mM) forward primer
- 1,25 µL (20 mM) reverse primer
- 1 µL dNTPs (10 mM)
- 10 µL 5X High GC enhancer
- 10 µL 5X Q5 reaction buffer
- 0.5 µL Q5 High-Fidelity DNA polymerase
- Nuclease-free water up to 50 µL

For colony PCR, a small amount of the colony was scraped of and used as PCR substrate directly. When needed, the colony was resuspended in 25 µL distilled water and boiled at 98℃ for 15 minutes before using it as PCR substrate.

PCR programme

1.	Initial denaturation	98 ℃ for 30 seconds
2.	Denaturation	98 ℃ for 10 seconds
3.	Annealing	Lowest T_m of the primers – 3℃ for 30 seconds
4.	Elongation	72 ℃ with 30 seconds per 1 kb in the desired fragment
5.	Repeat	step 2-4 were repeated for 35 cycles.
6.	Final elongation	72 ℃ for 2 minutes
7.	Hold	4℃

The PCR contents were added in PCR tubes on ice, with the enzyme being added last. All samples were spun down before placing them in the thermocycler. The lid should reach 72℃ before adding the samples. For samples longer than 4 kb, 1 minute per 1 kb were used as the total elongation time. The primers used in this study are shown in Appendix B.

3.9.1 PCR cleanup

To remove polymerases, primers, dNTPs, and other non-DNA products from the PCR sample, Monarch PCR & DNA Cleanup Kit was used [102]. The principle resembles the one already explained in section 3.8 for gel extraction.

Protocol

DNA Clean-up Binding Buffer was added according to the manufacturer's protocol, mixing well. The sample was then loaded onto the column and centrifuged for 1 minute. The supernatant was discarded, and 200 µL DNA wash buffer was added, before centrifuging the sample for 2 minutes. This was done twice. The column was then transferred to a clean Eppendorf tube, before adding 15 µL of DNA elution buffer. The mixture was incubated at room temperature for one minute, before centrifuging at 13 300 rpm for one minute.

3.10 Transfer of plasmids to bacteria

Horizontal gene transfer is a mechanism bacteria use to spread genetic material between organisms [103]. The concept is extremely useful for spreading acquired genes giving the bacteria an advantage, such as antibiotic-resistant genes. Horizontal gene transfer can occur either by transformation, conjugation, or transduction [78]. During transformation, bacteria will take up exogenous DNA from the environment, while conjugation is the transfer of genetic material between bacteria. Transduction is when bacterial viruses are moving genes between bacteria [104]. Horizontal gene transfer is a key role in bacterial evolution and can also be utilized in the lab to create plasmids and transfer them to our desired bacteria. In this study, horizontal gene transfer was utilized to introduce plasmid DNA into competent *E. coli* cells, for later transferring the plasmids into *P. fluorescens* by homologous recombination.

3.10.1 Preparation of competent cells

To enhance the likelihood of bacteria taking up exogenous DNA such as plasmids, they can be made competent. DNA is negatively charged and will therefore not easily cross the cell membrane by itself. Cells must be in a competent state for uptake to happen, which can happen either naturally, or be induced chemically [105], even if the former is rather rare. There are several ways to make cells competent, all of which will aim to increase the number of pores in the cell membrane to aid DNA uptake. Electroporation will by applying an electric field to the bacteria create more pores in the cell membrane, while chemical treatments use salts and ions to achieve the same [78]. There are also several chemical ways to make cells competent, but studies have shown that using divalent cations such as Ca^{2+} is the most efficient chemical method [78, 105]. The competent cells must have deficiencies in restriction systems to avoid degradation of the foreign DNA [78]. In the process of making the cells competent in this study, they will be washed using a cold solution containing a variety of salts, such as RbCl and $MnCl_2$. When made competent, the cells can be exposed to heat shock to aid the uptake of the exogenous DNA.

Protocol

A pre-culture was made with competent *E. coli* S.17 cells and cultivated in 10 mL Psi medium at 37 °C overnight. 1% from the pre-culture was then inoculated in new 10 mL Psi medium and inoculated at 37 °C until the cells reached OD_{600} = 0.4. The cells were then placed on ice for 15 minutes before they were centrifuged at 4000 rpm for 5 minutes and resuspended in 40 mL cold TBF1. The cells were then incubated on ice for 5 minutes before they were centrifuged at 4000 rpm for 5 minutes and resuspended in 3 mL cold TBF2. 100 µL of the mixture was added into an Eppendorf tube, and the cells were frozen in liquid nitrogen for 10 seconds, before storage at -80 °C.

3.10.2 SLIC-cloning

To clone something simply means to produce several replicas of an organism, cells, or DNA fragments. The perhaps simplest way to clone something is to create a plasmid with the DNA fragment one wants to amplify and introduce it to a bacterium. The bacteria can then take up the plasmid and copy it while it replicates itself [78].

Another way to clone is by using the SLIC method. SLIC cloning uses T4 DNA polymerase and utilizes its 3'-5' exonuclease activity to combine two DNA fragments into one. The T4 endonuclease will create overhangs on the single-stranded vector and insert, which will then be used to mimic the homologous recombination that can happen *in vivo* in *E. coli*. Homologous recombination, rather than site-specific recombination, does not rely on specific sequences, but rather on homologous regions [106]. By creating a recombinant intermediate DNA using T4 DNA polymerase to create 5' overhangs for joining the DNA segments together and introducing it to bacteria, the bacterial DNA repair mechanism will repair any gaps and get double-stranded plasmids. The only requirement for SLIC is that the vector and the inserts contain 15 base pairs or longer end sequences that will give stable annealing [106]. The vector must first be linearised, with the inserts having 15 bp homologous regions to the end of the vector [107].

Protocol

The SLIC cloning was performed as a slightly modified version of the SLIC method by Jeong et al. [107]. Before starting SLIC cloning, the DNA fragments were prepared. First, the vector molecule was digested with an appropriate restriction enzyme overnight before it was visualised and cut from a gel containing GelGreen. The gel slice was purified according to the protocol described in section 3.8 up and until the elution step. The DNA was eluted using an Elution Buffer containing Tris (and lacking TE). The vector DNA concentration was then measured using the NanoDrop. Secondly, the inserted gene was amplified using PCR, using primers with more than 15 bp homology to the DNA vector sequence. After visualising the PCR product on the gel, the PCR product was purified according to the protocol described in section 3.9 and eluted with DNA elution buffer containing 10 mM Tris before the concentration was measured using the NanoDrop.

The linearized vector and the insert were mixed, with a molar ratio of 1:2. Then, 2 μL10X NEB buffer 2.1 was added to the mixture, as well as water to get a total volume of 10 μL. 0.2 μL of T4 DNA polymerase was added to the mixture, before incubation at room temperature for 2.5 minutes. The mixture was then put on ice, and incubated for 10 minutes, before following the heat-shock transformation protocol as described in section 3.10.3.

3.10.3 Heat-shock transformation of competent cells

In addition to chemical transformation, electroporation, and gene guns are all methods for the transformation of DNA into competent cells [78]. While electroporation reversibly creates pores in the membrane for DNA to enter, the gene gun will fire DNA that is coated onto microscopic beads into the cells [78]. Both gene guns and electroporation can easily irreversibly damage the cells, and therefore, the chemical method is more widely used.

In the chemical method, divalent cations such as $CaCl_2$ are used to induce pores before the cells are mixed with the exogenous DNA that is to be taken up in the cell [108]. The exact mechanism of DNA entry into the cell is still unknown. However, we do know that the divalent cations will bind to both the cell and the DNA, causing a neutralisation of the charges hindering DNA to enter by itself [109]. The calcium that is bound to the DNA will also help the DNA to be absorbed into the competent cell [109]. The protocol also involves a lot of steps on ice, which is due to the fluidity of the membrane that will be restricted in low temperatures, and this is thought to strengthen calcium-cell interaction [109]. After allowing the cells and DNA to mix and be incubated on ice, the cells will be exposed to heat for a short amount of time. When exposing the cells to heat shock, the temperature will be in imbalance, and DNA molecules will be more likely to be pushed into the cells. Then, medium will be added to allow the cells to grow for a single generation, allowing genes such as antibiotic resistance to be expressed. When plating out the cells on plates containing antibiotics or other selection markers, only cells with the correct DNA incorporated will survive.

Protocol

Competent *E. coli* S17.1 cells were thawed on ice, and while melting, 10 µL DNA was added to the Eppendorf tube with the competent cells. For positive control, 1 µL of plasmid DNA was added, and for the negative control, 10 µL of H_2O was added. The DNA and the cells were mixed gently before they were incubated on ice for 30-60 minutes. Then, the mixture was put in a 37 ℃ water bath for two minutes, before being incubated on ice for two minutes. 900 µL of pre-warmed SOC medium was added to the mixture and incubated at 37 ℃ in the shaking incubator for 1-2 hours. The mixture was then plated out on LA containing the appropriate antibiotics and incubated at 37 ℃ overnight.

3.11 Sequencing

DNA sequencing is a useful tool for determining the exact order of nucleic acid in a DNA sample [79]. Over the years, DNA sequencing has developed in line with the development of technologies, becoming faster, cheaper, and more accurate. DNA sequencing is thus a very much used approach to accurately determining the DNA sequence of the sample. The first-generation DNA sequencing was based on determining the nucleic acid one at a time with the use of radioactive nucleotides and a polymerase, incorporating these [79].

Today, third-generation DNA sequencing is mostly used, as it is less time-consuming, easier to analyse, and can sequence several samples at the same time [79]. In this study, all samples are sequenced by Eurofins using the LightRun Tube Sequencing service. They utilise an automated Sanger sequencing process. Here, primers, DNA polymerase, the single-stranded DNA template, and deoxynucleotides are mixed, and the DNA polymerase will make copies of the template. The synthesis will be stopped at each base pair, yielding molecules that differ in size. Nucleotides lacking the 3'-hydroxyl group (ddNTPs) in the mixture will be incorporated into a molecule, causing no addition of new nucleotides to the chain. The DNA polymerase will therefore start synthesising new strands from the 3' end of the primer and stops whenever a ddNTP is added [110]. This causes DNA fragments with different lengths to be made, ranging from 1 to the total length of the molecule. By capillary electrophoresis, the different molecules will be separated by length, and as all four ddNTPs are coloured in a different colour, the fluorescent label can be measured, and the sequence can be determined [110]. The resulting chromatogram can be viewed using a software.

Protocol

Firstly, a bar code was added on an Eppendorf tube that was to be sent for sequencing. The amount of purified DNA was added according to the manufacturer's protocol (5-10 ng/µL for plasmids between 300 bp and 3000 bp). The DNA was mixed with 0.75 µL DMSO and 1,25 µL 10 pmol/µL sequencing primers. For each sample, only one primer was added to be able to distinguish the results. Distilled water was added for a total volume of 15 µL. The sample was flicked and spun down several times, before sending them to Eurofins Genomic GATC for automated Sanger sequencing.

3.12 Homologous recombination

Bacterial conjugation

Bacterial conjugation is a process where genetic material is transferred from one bacterium to another through contact between the bacteria [78]. The process will happen by creating a protein filament that will bind to the recipient and draw the cells together. Then, a conjugation bridge will be formed, allowing the DNA to travel through a channel and to the recipient [19]. One of the strands will open up, moving through the conjugation bridge. The incoming strand will then be used as a template for creating a new complementary DNA strand in the recipient cell. This will also make sure that the donor cell will not lose the plasmid [19].

Selection marker

By using selection markers, such as genes encoding for antibiotic resistance, we can distinguish between cells that have undergone recombinant events and those that have not [78]. It also allows us to distinguish cells that have undergone a single or double recombination event. Such selection markers are often genes encoding antibiotic resistance, and cells grown on plates containing the antibiotics must have taken up the plasmid to survive. In addition, blue-white screening is an easy method for distinguishing bacteria that have taken up the plasmid and those that have not [79]. When using blue-white screening, *lacZ* is inserted into the plasmid [78]. This gene encodes the alpha fragment of β-galactosidase. When the whole plasmid is first integrated into the *P. fluorescens* chromosome, the LacZ gene will remain intact, and when exposed to XGal (5-bromo-4-chloro-3-indolyl-β-D-galactoside), the alpha fragment will be able to cleave the Xgal into galactosidase and 5-bromo-4-chloro-3-hydroxyindole, causing the cells to turn blue when the latter product is oxidized [79].

In this study, all constructed plasmids incorporated into the genome of *P. fluorescence* contained genes providing antibiotic resistance toward tetracycline, being a negative selection marker for the first cross-over event, and a positive selection marker for the second recombination event. In addition, the plasmids also contained the LacZ gene, causing them to turn blue when exposed to Xgal with the plasmid inserted, being a positive selection marker.

Protocol

Firstly, pre-cultures with *P. fluorescence* and *E. coli* containing the desired plasmid were made. *P. fluorescens* was inoculated in 10 ml LB and incubated at 30 ℃ overnight. *E. coli* was inoculated in 10 ml LB containing the appropriate antibiotics to limit plasmid loss and inoculated at 37 ℃ overnight. The following day, 1% culture of both cultures was transferred to 10 mL LB and incubated under the same conditions as the pre-cultures, until they reached exponential growth (OD_{600} between 0.4 and 1). *E. coli* was incubated for approximately 2 hours, while *P. fluorescence* needed double the amount of time. When the cell density of the two cultures looked similar (or if the OD_{600} was the same), the same volume of each culture was used. If the density was non-similar, the volume of the cultures was adjusted. 3 mL of each culture (or the appropriate volume) was added to a sterile 13 mL tube, centrifuged for 5 minutes at 5000 rpm at room temperature, and the supernatant was discarded, leaving about 0,1 mL of fluid. The pellet was resuspended in the remaining supernatant and placed on an LA plate at 30℃ overnight. The suspension was scraped off the next day and transferred to 1 mL LB. A dilution series with undiluted culture, 10^{-2}, 10^{-4}, and 10^{-6}, was made, and 100 µL of each dilution

was plated out on PIA containing tetracycline and any other appropriate antibiotics to ensure only *P. fluorescens* containing the plasmid grew up. 30 minutes before plating out the colonies, the plates were prepared by plating out 60 µL XGal (20 mg/mL DMSO). The plates were then incubated at 30℃ for around 2 days, or until most of the colonies had gotten blue to further ensure that the colonies had incorporated the plasmid correctly into its chromosome.

Then, two or three blue colonies were picked, restreaked on PIA with antibiotics and XGal, and incubated at 30 ℃ for 2 days. In the case of strains that proved difficult to make, blue colonies were replica plated over on PIA with antibiotics and tested with PCR to find the rarest integration type to cultivate further. From the PCR results, three blue colonies were selected to restreaked on PIA with antibiotics and XGal and incubated at 30 ℃ for two days in the dark. Two to three colonies from the restreaked plates were picked and inoculated in separate flasks with 10 ml LB at 30 ℃ overnight to allow the second recombination event to happen. These cultures were denoted K1. For 2-4 days, 10 µL of the old culture was inoculated in 10 mL new LB, each time being denoted with a new K. After around four days, 100 µL of dilution series (undiluted, 10^{-2}, 10^{-4}, and 10^{-6}) of the culture was plated out on LA with XGal. The plates were incubated at 20℃ for two days. In addition, new K was made, by diluting 10 µL of the old culture in new 10mL LB. This was repeated until the number of white colonies on the plates was satisfying, indicating that the unwanted parts of the plasmid, containing LacZ and Tet^r were no longer present. 50 white cultures from the plates were then replica plated over on replica plates, being LA without and LA with antibiotics. Colonies that grew on LA, but not on LA with antibiotics were further checked with PCR. Correct mutants were stored at -80℃.

3.13 PMM/PMI assay

The phosphomannomutase/phosphomannose isomerase (PMM/PMI) assay was based on a protocol by Sá-Correia et al. [88]. The assay is an enzyme-coupled assay, measuring the activity of PMM and PMI through the reduction of NADP and oxidation of 6-phosphoglucoacetone.

PMI catalyses the reversible isomerisation of fructose-6-phosphate into mannose-6-phosphate. Then, M6P is converted into mannose-1-phosphate by PMM, as shown in equation II. AlgA is a protein with PMI activity. In alginate production, it will catalyse the first and third steps in the conversion of the precursor molecule. The same precursor molecule is used to produce Psl, but this reaction will be catalysed by PslB, which also possesses PMI/GMP activity [3]. The enzymatic pathways for Psl, alginate, LPS, and rhamnolipids are shown in Figure 7.

PMM is responsible for catalysing several reactions in the production of polysaccharides, and most notably in the second step of the creation of GDP-D-mannose where M6P is converted into M1P as seen in reaction III. In addition, AlgC with its PMM activity is involved in the conversion of glucose-6-phosphate into glucose-1-phosphate, which can be further used to create both D-glucose and L-rhamnose for Psl synthesis.

$$F6P \xrightarrow{PMI} M6P \xrightarrow{PMM} M1P \qquad \text{(II)}$$

$$M1P \xrightarrow{PMM} GDP - D - mannose \quad \text{(III)}$$

The assay measures the increase in NADPH, having an optimal density at 340 nm. PMI activity is measured by measuring the increase in NADPH. PMI catalyses the formation of F6P from the substrate added, being M6P. By adding a phosphoglucoisomerase (PGI), F6P is catalysed into G6P, which is further oxidated to 6-phosphoglucoacetone, coupled with the reduction of NADP into NADPH, a reaction catalysed by glucose-6-phosphate dehydrogenase (ZWF) [111].

PMM activity is measured with the same principles. Glucose 1,6-diphosphate is an intermediate in the interconversion between G1P and G6P. By adding this, PMM will catalyse the formation of G6P from G1P, which is then catalysed to F6P by PMI. PGI will then catalyse the formation of F6P into G6P, with ZWF catalysing the oxidation into 6-phosphoglucoacetone coupled with NADP reduction [112, 113].

The OD_{340} measurements were conducted on the TECAN-InfiniTE M200-Microplate reader. A total of 150 µL liquid was added to each well, with three parallels for each replica. To find the path length, 150 µL of a coloured liquid was added to a well, first measuring the OD_{340} as normal, before selecting to correct for the path check. By dividing the former absorbance value by the latter, the path length in the well was found and could be used when calculating the concentration using Beer Lamber's law, described in section 3.4.

The path length was found to be $\frac{OD_{340\ pathcheck} = 0.578}{OD_{340\ no\ pathcheck} = 1.540} = 0.38$ cm.

The increase in optical density due to the reduction of NAD was measured using the microplate reader, measuring the absorbance at 340 nm. The enzyme activity was calculated using the absorbance coefficient of NADH/NADPH, 6.22 L/mmol/cm [114], and the protein concentration in the samples.

Protocol

A 30 mL LB overnight culture containing the appropriate antibiotics was made for all mutant strains. 10 mL of these was used to inoculate 200 mL LB in 500 mL baffled flasks. M-toluate was added after 1.5 hours, and the colonies were grown for 16 hours at 30 °C. For all cultures, 2 x 1.5 mL were harvested for B-PER extraction, while the remaining cells were used for sonication. For B-PER, cells were harvested by centrifugation at 5000 x g for 10 minutes, and 5 mL B-PER Complete Reagent/g biomass was warmed to room temperature and added to the cell pellet. The suspension was made homogenous and rocket gentle at room temperature for 15 minutes. The sample was then centrifuged at 16 000 x g for 20 minutes to get rid of the insoluble proteins. The remaining culture was centrifuged at 10 000 x g for 10 minutes at 4 °C, and the pellet was washed with 0.9% NaCl. If not used immediately, cell pellets were frozen at -80 °C. Thawed cell pellets were then resuspended in 3 mL sonication buffer (10 mM MOPS, 2 mM DTT, pH 7.0) and sonicated in an oscillator. The samples were then centrifuged at 27 000 x g for 40 minutes at 4 °C, and the supernatant was used further. Prior to conducting the assay, the protein content in each supernatant was measured using NanoDrop.

PMI: 1 mL of the reaction mixture contained 0.05 TRIS hydrochloride buffer (pH 7.5), 10 µmol $MgCl_2$, 0.5 U phosphoglucoisomerase, 0.5 U glucose-6-phosphate dehydrogenase (ZWF), and 1 µmol NADP, and was initiated with 200 µL freshly prepared crude extract and 3 µmol D-mannose-6-phosphate.

PMM: 1 mL of the reaction mixture contained 0.05 TRIS hydrochloride buffer (pH 7.5), 10 µmol $MgCl_2$, 0.25 µmol α-D-glucose-1,6-diphosphate, 0.5 U PGI, 0.5 U ZWF, 0.5 U phosphoisomerase (PMI), and 1 µmol NADP, and was initiated with 100 µL freshly prepared crude extract and 1 µmol α-D-mannose-1-phosphate.

Calculations: The increase was calculated in a linear area for each parallel. After finding the average increase for each mutant, the average increase for initial linear rates of NADP reduction was subtracted, being the cells lacking substrate. From this, the concentration was found using Beer Lambert's law and the extinction coefficient for NADPH. Protein concentration was measured using NanoDrop. One U is defined as the enzyme required to reduce 1 µmol NADP per min under the specified assay conditions.

3.14 Psl extraction and monosaccharide analysis

Monosaccharide analysis is an important chemical analysis for determining the sugar content in complex carbohydrates [115]. The methods for such analysis are diverse and have different strengths and drawbacks, but commonly they can either quantify or qualify the monosaccharide content in pre-prepared samples quite accurately. Conventional monosaccharide analysis methods include gas chromatography, HPAEC-PAD, HPLC, and NMR among others. Different methods can be coupled to different detectors, such as mass spectrometry or refraction index detectors, measuring different characteristics of the sample content [115].

In this study, there are several challenges to overcome before the analysis. Firstly, the most suitable method for analysing the monosaccharide content in the sample must be found. Several of the mutants can produce alginate, which also must be taken into account. The analysis of Psl in *P. aeruginosa* gives some clues as to how the Psl in *P. fluorescens* might look like, but this does not mean that Psl produced by *P. fluorescens* is identical. The monosaccharide analysis chosen in this study is based on HPEAC-PAD and is able to show if the sample contains any of the sugars in the standard sugar mixture, being either mannitol, fucose, rhamnose, arabinose, glucose, galactose, mannose, or xylose. The method also allows for the quantification of the detected sugars. HPAEC-PAD is described in more detail in section 1.5.1.

By using other methods, such as NMR, more details could have been found, such as if the sugars were in alpha- or beta configuration, but as the main goal of this study is to find the components of the Psl polysaccharide, the standards used should be sufficient to determine the identity of the monomers in the polysaccharide. The second challenge is to find a suitable method for isolating Psl. Most of the protocols for *P. aeruginosa* include either extraction with an anti-Psl antiserum or utilises methods and equipment not available in the lab used for this study. The extraction of the extracellular proteins and polysaccharides was therefore done according to a protocol by Byrd et al [3], which was modified to suit *P. fluorescens* as well as the lab equipment available. As the method chosen for monosaccharide analysis was selective for the

monosaccharides, this was also taken into consideration when modifying the protocol for extraction.

Protocol

The mutants were grown in 100 mL DEF3 with the addition of 2% fructose from an overnight culture. 0.15 mL/L of Alkalase 2.4L and Neutrase 0.8 were added to all samples producing alginate. 0.25 mM m-toluate was added to the samples after 1.5 hours. The first set of mutants was grown for 24 hours, while the second set was grown for 48 hours. The biomass was collected by centrifugation at 7500 g for 20 minutes at 4 ℃ before the pellet was resuspended in 0.9% NaCl. The resuspended pellet was re-centrifuged. 25% ethanol and 0.1M $CaCl_2$ were added to the supernatant to remove extracellular DNA before the supernatant was dialysed using a 6-8 kDA cut-off membrane for a minimum of 24 hours. The samples were then lyophilized before they were acid hydrolysed and analysed. The lyophilization, acid hydrolysis, and monosaccharide analysis were mainly conducted by Olav A. Aarstad.

For the acid hydrolysis, the exact weight of each sample was noted. Since no sample was above the 10 mg ideal minimum weight for the protocol, only one parallel from each sample was weighted out. For the samples having almost no solid material, the two parallels when the strains were grown in 2x50 mL DEF3 were combined with MQ water and lyophilized again prior to acid hydrolysis. For the Saeman hydrolysis, 0.5 mL 12 M sulfuric acid was added to the samples before they were incubated at room temperature at 30 ℃. 2.5 mL MQ-water was added to the sample before hydrolysation at 100 ℃ for four hours. 6 mL MQ-water was added to the room-tempered sample before 180 uL of the solution was pipetted out and NaOH was added so that each sample had a pH between 4 and 7. The samples were then further diluted with MQ-water. The samples were analysed on a ICS5000+ system (Thermo Scientific) using a 4 x250 mm CarboPac SA10 column. For qualification, standard sugar mixtures with known concentrations (0.1-10 mg/L) were analysed before and after the unknown samples. The resulting chromatogram was then used to determine if the sample contains any of the known sugars in the standard monosaccharide mixture.

3.15 Motility assay

Swarming motility and biofilm formation are often co-regulated [87]. For *P. aeruginosa*, high motility is correlating with low expression of Psl and a high rhamnolipid production [87]. Swarming is a flagella-dependent movement over surfaces and requires the production of biosurfactants for many strains [87]. The swarming pattern often consists of dendritic patterns on the agar surface [87, 116]. Swimming motility is dependent on a flagella and describes the movement on liquid on agar, and shows halo-like circles [116]. The last motility movement found and described in *Pseudomonades* is twitching, dependent on pili contraction [116]. To test the swarming motility for *P. fluorescens* with increased Psl operon expression and deletion or overexpression of AlgA and AlgC, a similar motility assay was conducted, measuring the motility of the strains on the soft agar surface.

Protocol

Small agar plates containing KB medium diluted 20-fold in distilled water (salts were not diluted due to maintaining the correct osmotic pressure of the cells) and with 0.5% agar were made. Mutant strains from LA plates were stab inoculated on the centre of the plates. Three replicas for each mutant were made, as well as one plate with liquid culture to see if it created different swarming patterns. For mutants containing the PmG5 promoter, additional 3 replicas were made with plates containing m-toluate. The plates were incubated for 48 hours at 30 ℃ before the diameter was measured.

3.16 Software

Psl operon analysis

The Psl operon was analysed using the Pfam database [117]. Pfam is a database containing large amounts of protein families and domains. The database uses hidden Markov models, a statistical model used to capture hidden information from nucleotidic sequences and other observable sequential symbols. The predicted functions of the Psl genes were found using Pseudomonas Genomic Database, a well-known community-based annotation database containing high-quality *Pseudomonas* (*P. aeruginosa* PAO1) genome annotation [118]. The subcellular location of each gene was attempted analysed using pSORTb v.3.0 but only yielded inconclusive results for most of the proteins.

Benchling

Benchling (https://benchling.com) is an online, free biotechnological tool used to visualise DNA sequences, align sequences, assemble new DNA sequences through virtual cloning, restriction cutting, and ligating, predict restriction digests, design primers, and analyse PCR reactions based on the created primers and sequences.

BioRender

Biorender (https://biorender.com) is an online visualisation tool used to create figures, design workflows, and visualise concepts based on a library containing icons, figures, and schematic elements.

Phyre2

Phyre2 [119] is a web portal containing tools to predict protein structure and build models based on known protein structures with homology to the sequence in question. These models are then used to predict the protein function and analysing it.

OperonMapper

Operon-mapper [120] is a web server with tools to predict the operon of a bacterial genome, based on the intergenic distance between adjacent genes, and the functional relationship between the proteins encoded for by the genes.

3.17 Plasmids and strains

In this section, a short description of all plasmids made and used in this study are given, as well as all strains used. The strains are described in Table 2, and the plasmids in Table 3. The source of each strain and plasmids is also included. A plasmid chart of all created plasmid in this study is provided in Appendix D.

Table 2: An overview and short description of all strains used and created in this study.

Strains	Description	Source
E. coli S17-1	recA pro (RP4-2Tet:: Mu Kan::Tn7)	[121]
SBW25*mucA*	SBW25-derivative where a stop codon has been inserted in front of MucA. Can produce alginate	[10]
SBW25*mucA*HE230	SBW25*mucA*-mutant with PmG5 in front of AlgC	Ertesvåg, unpublished
SBW25*mucA*HE230pAlgD$^-$	SBW25*mucA*-mutant with PmG5 in front of AlgC and deletion of AlgA	Ertesvåg, unpublished
SBW25*mucA*Δ*algC*	SBW25*mucA* mutant with deletion of AlgC	[10]
SBW25*mucA*-CSG4	Mutant with PmG5 and XylS in front of Psl operon	This study
SBW25*mucA*-CSG2	Mutant with PmG5 in front of Psl operon, lacking XylS in the genome	This study
SBW25*mucA*HE230-CSG8	Mutant with PmG5 in front of Psl operon and AlgC. Apr^r	This study
SBW25*mucA*HE230pAlgD$^-$-CSG8	Mutant with PmG5 in front of Psl operon. *algD*$^-$. Apr^r	This study
SBW25*mucA*Δ*algC*-CSG6	Mutant with PmG5and XylS in front of Psl operon. Apr^r. Δ*algC*	This study
SBW25*mucA*-CSG10	Mutant with deletion of PslA. Apr^r	This study

Table 3: Overview of all plasmids used and created in this study.

Plasmid	Description	Source
pHNB4	Derivative of pIO100 and pMG48, Tet^r, Amp^r. LacZ.	Burud, unpublished
pHNB5	Derivative of pHM4 and pHNB1. AlgA cloned by PCR inserted into pHM4. PmG5 promoter controlling AlgA. Amp^r	Burud, unpublished
pHNB7	Derivative of pHNB3 and pHNB6. PslA controlled by PmG5. Amp^r	Burud, unpublished
pAT75	Plasmid containing the regulator and promoter XylS and PmG5. Amp^r, Kan^r	Tøndervik, unpublished
pIO100	Derivative of pEC-K18(mob) [122] containing an Apr^r gene from pYQ1[123]	Onsager, unpublished
pCSG1	Derivative of pHNB4 and pHNB5. TC^r, Amp^r. LacZ for blue-white screening. *algA* controlled by PmG5-promoter.	This study
pCSG2	Derivative of pHNB4 and pHNB7. Tet^r, Amp^r. LacZ for blue-white screening. Psl operon controlled by PmG5-promoter.	This study
pCSG3	XylS from pAT75 into Sblf-cut pHNB7, to get XylS in front of PmG5 and pslA in pHNB7. Amp^r	This study
pCSG4	Derivative of pCSG3 and pHNB4 cut with NotI. pCSG3 cut with NotI and SpeI into pHNB4 cut with NotI and XbaI. XylS in front of PmG5 and *pslA*. Tet^r, Amp^r. LacZ for blue-white screening.	This study
pCSG5	Derivative of pCSG2 cut with MfeI, to remove part of *pslA* and upstream region. Psl-negative mutant. Tet^r, Amp^r. LacZ for blue-white screening.	This study
pCSG6	Derivative of AvrII-Spe-cut pCSG4 and SpeI-cut pIO100. Apr gene placed between rrnBT1B2 and XylS. AvrII-site close to PmG5. Apr^r, Tet^r, Amp^r. LacZ for blue-white screening.	This study
pCSG7	Derivative of AvrII-Spe-cut pCSG4 and SpeI-cut pIO100. Apr gene placed between rrnBT1B2 and XylS. AvrII-site close to XylS. Apr^r, Tet^r, Amp^r. LacZ for blue-white screening.	This study
pCSG8	Derivative of BglII-AvrII-cut pCSG7. XylS removed. Apr^r, Tet^r, Amp^r. LacZ for blue-white screening.	This study
pCSG9	StuI-cut pCSG1 and SpeI-cut pIO100 for placement of Apr-gene into the plasmid. Apr^r, Tet^r, Amp^r. LacZ for blue-white screening. *algA* controlled by PmG5-promoter.	This study
pCSG10	pCSG8-Δ*pslA*, removing the 276 first bases of PslA. Created by cutting pCSG8 with XbaI and StuI. Apr^r, Tet^r, Amp^r, LacZ for blue-white screening	This study

4 Results

4.1 The Psl genes are within the same operon

The genes in the Psl operon for *P. fluorescens SBW25* have been investigated using the Pseudomonas Genome Database, Blastp, and Pfam to find the predicted function and the motifs for the proteins. Based on these results, the functions of the proteins were determined, as shown in Table 4. More details, such as the predicted domains are shown in Appendix C. The Psl segment from *P. fluorescens* SBW25 was also investigated using the Operon finder software Operon Mapper, which identified one operon containing all *pslABCDEFGHIJKL* genes. The software compared pairwise genes and found the probability for them to be within the same operon, which was 97-98% for all twelve Psl genes. The similarity to *P. aeruginosa* PAO1 reference strain in Pseudomonas Genomic Database for each protein is also included. The biosynthesis of Psl as described for *P. aeruginosa* is shown in Figure 4.

Table 4: The genes within the Psl operon along with their predicted function in P. fluorescens SBW25. The predicted domains are further explained in Appendix C

Protein	**Predicted function**	**No. of predicted domains**	**Similarity to protein from *P. aeruginosa* [%]**	**Possible substrate/mode of function**
PslA	Glycosyl transferase	2	77.7	Assembly of monomers
PslB	Nucleotidyl transferase/PMI/PMM	4	79.1	Synthesis of precursors
PslC	Glycosyl transferase	3	78.3	Mannose
PslD	Polysaccharide exported-related	2	75.9	Chain export
PslE	Exopolysaccharide export/Chain length determining	2	80.3	Chain export
PslF	Glycosyl transferase	2	78.8	Glucose
PslG	Glycosyl hydrolase/ β-xylosidase	2	73.0	Chain export
PslH	Glycosyl transferase	4	78.4	Unknown
PslI	Glycosyl transferase	4	77.9	Unknown
PslJ	Putative membrane protein/o-antigen ligase	1	79.9	Chain assembly
PslK	Flippase/ Membrane protein/glycosyl transferase	3	79.0	Flippase
PslL	Acyltransferase/membrane protein	1	74.4	Modification

PslB analysed with Phyre2 showed the highest similarity (coverage 68%, id: 36%) with a mannose-1-phosphate guanylyltransferase from *Thermotoga maritima* (PDB ID: 2X5S). In addition, the Phyre2 analysis showed 37% identity with a mannose-6-phosphate isomerase from *Helicobacter pylori*, indicating PMI activity (PDB ID: 2QH5). These results are in line with the

PslB function in *P. aeruginosa*, resembling AlgA with both GMP and PMI activity, needed for the conversion of the precursor sugar nucleotides [11].

The Phyre2 analysis of the proteins PslC, PslF, PslH, and PslI indicate that they all have glycosyl transferase domains, indicating that they use the precursor molecules and convert them into the sugar nucleotides making up the monomers in Psl. PslC has motifs belonging to a glycosyl transferase-2 family, involved in the transfer of nucleotide-activated sugars including rhamnose, mannose, and glucose [11]. The analysis showed 83% coverage and 20% identity with a mannosyltransferase from *Pyrobaculum calidifontis* (PDB ID: 6YV8), indicating that mannose is one of the sugars making up Psl. PslF was found to have similarities with GlgM, a maltose-1-phosphate synthase from *Mycobacterium smegmatis* (92% coverage, 18% identity, PDB ID: 6TVP), indicating that PslF could be involved in incorporating activated sugar subunits into Psl, as predicted for *P. aeruginosa.* GlgM uses UDP-glucose as a donor, with G1P as the acceptor [124], which could indicate that PslF recognises glucose. PslI is structurally similar (95% coverage, 22% identity) to an inositol-3-phosphate glycosyltransferase from *M. hassiacum* (PDB ID: 7QSG), while PslH is similar to a phosphatidylinositol mannosyltransferase (PimA, PDB ID: 2GEJ) from *M. smegmatis* (87% coverage, 21% identity). The identity of each sugar is too low to determine which sugar they use as a substrate but can be used to indicate the function of the gene products.

PslA analysis showed that there were several domains covering the *pslA* gene, with the highest similarity to the membrane protein n,n' diacetylbacilliosaminyl-1-phosphatase transferase (PDB ID: 5W7L) from *Campylobacter concisus* (39% coverage, 38% identity). The transferase is involved in the first step of the assembly of glycoconjugates, indicating that PslA is involved in the first membrane-associated step of Psl assembly as well. In addition, a NAD(P)-binding Rossmann-fold-like domain came up as a strong result, further strengthening this hypothesis.

PslE is a protein with the suggested function as an export-related protein involved in chain length determination, having predicted domains suggesting involvement in the export of the polysaccharide and determination of the chain length [11]. PslE showed a high resemblance (80% coverage, 19% identity) with the putative transmembrane protein Wzc (PNB ID: 7NHR) as for the *P. aeruginosa* PslE, with an expected function of phosphorylating tyrosine during the export.

PslJ has an o-antigen ligase-domain, similar to those found in polymerases. Phyre2 analysis reviled a 74% coverage with the putative cell surface polysaccharide polymerase/ligase (PDB ID: 7TPG). The predicted function could therefore be to link sugars together into the polysaccharide chain. PslK was found to be similar to (99% coverage, 24% identity) the flippase Murj from *E. coli* (PDB ID: 6CC4), and it is possible that PslJ acts as a polymerase and PslK acts as a flippase, resembling the Wzx/Wzy pathway. PslL analysis indicated that it is a membrane protein, but no search result was higher than 49% certainty.

PslD is thought to have export-related domains, and a Phyre2 analysis showed that PslD has a high similarity (73% coverage, 26% identity) to the outer membrane lipoprotein Wza from *E. coli* (PDB ID: 2J58). PslG was found to have 73% identity (94% coverage) with PslG from *P. aeruginosa*, being a hydrolase. Thus, the function of PslG in *P. fluorescens* is therefore highly

likely to resemble the function in *P. aeruginosa*, being involved in the export of Psl and acting as a fail-safe for defective Psl molecules.

The results show that the proteins in *P. fluorescens* and *P. aeruginosa* PAO1 are not identical but contain similar domains and therefore also have similar functions. The biosynthesis of *P. fluorescens* Psl is therefore thought to resemble the process described in Figure 4, even if the gene analysis does not give a clear answer as to what sugar monomers are involved.

4.2 Construction of SWB25*mucA* derivatives to test Psl production

The gene analysis showed that the 12 Psl genes are likely to be part of the same operon, making it possible to regulate the gene expression by exchanging the Psl promoter with an inducible promoter. In this study, four different SBW25*mucA* derivatives was therefore used to mutate either the Psl operon or the Alg operon to test Psl production in *P. fluorescens*. To control Psl and sugar nucleotide production, the inducible promoter PmG5 was chosen together with the XylS regulator, as it has been found to be a well-functioning promoter to control the expression of genes in *P. fluorescens* [80, 83]. AlgC is needed for alginate synthesis and is predicted to be involved in the synthesis of the precursor sugar nucleotides for Psl production as well, possibly being the limiting factor for precursor production and thus possibly also Psl production. PslB is predicted to have a similar activity as AlgA. By creating different combinations of Psl/*algA/algC* mutants, the effect of each gene on Psl production and Psl genes overexpression can be examined. The mutants and their abbreviation used throughout the study is shown in Table 5. In the first mutant (ACP^+), AlgA and AlgC are present, and their enzymatic activity can be measured when Psl genes are overexpressed. By deleting AlgC but keeping AlgA and overexpressing Psl genes (AC^-P^+), and by overexpressing AlgC and Psl but with normal AlgA expression (AC^+P^+), the effect of AlgC can be measured. Similarly with AlgA, an AlgA deficient strain overexpressing the Psl operon and AlgC ($A^-C^+P^+$) can be made and compared against the ACP^+ strain and a strain overexpressing AlgA, AlgC, and Psl ($A^+C^+P^+$). A Psl-negative strain (ACP^-) containing AlgA and AlgC is made as a control. The effect of alginate on Psl production can also be attempted assessed by comparing the alginate producers with the non-alginate producers, and by comparing ACP^+ with ACP^+X^-, lacking XylS.

As mentioned in section 1.1, wild-type *P. fluorescens* strains do not produce alginate in laboratory settings. While the SBW25 strain hardly expresses the *alg* operon, the SWB25*mucA* mutant can produce alginate in high amounts due to the disruption of the anti-sigma factor *mucA* [10, 17]. MucA is thought to not be necessary for Psl production, and thus this strain is very useful when also looking at alginate production and how this affects Psl production [10]. In addition, a variety of *algC* and *algD* deficient mutant derivatives from SBW25*mucA* already exists and are easily available in the lab.

The overview of all created strains in this study is given in Table 5. PmG5 indicates that a PmG5-promoter has been placed in front of the gene or operon. The abbreviation *A* refers to AlgA, with plus or minus indicating deletion or controlled by PmG5. *C* refers to AlgC, while *P* refers to Psl. X^- means the strain is lacking XylS in the genome.

Table 5: An overview of the mutated strains created in this study with a focus on their Psl operon, AlgC gene, AlgA gene, and ability to produce alginate.

Strain	Alginate	*algA*	*algC*	Psl	Abbreviation
SBW25*mucA*-CSG4	+	+	+	PmG5	ACP^+
SBW25*mucA*-CSG2	+	+	+	PmG5	ACP^+X^-
SBW25*mucA*-CSG10	+	+	+	-	ACP^-
SBW25*mucA*Δ*algC*-CSG6	-	+	-	PmG5	AC^-P^+
SBW25*mucA*HE230-CSG8	+	+	PmG5	PmG5	AC^+P^+
SBW25*mucA*HE230pAlgD$^-$-CSG8	-	-	PmG5	PmG5	$A^-C^+P^+$
SBW25*mucA*HE230-CSG8+1	-	PmG5	PmG5	PmG5	$A^+C^+P^+$

4.3 Construction of an SBW25*mucA* derivative where the Psl operon is controlled by the PmG5-promoter (ACP^+)

The aim of inserting the pCSG4-plasmid into the SBW25*mucA* strain was to insert the regulator/promoter system XylS/PmG5 in front of the Psl operon. This would allow us to control the transcription of the Psl operon genes, and indirectly try to control the Psl production.

4.3.1 Creation of the pCSG3 and pCSG4 plasmids

The cloning steps to create plasmids pCSG3 and pCSG4 are shown in Figure 10. pCSG3 had incorporated the inducible regulator/promoter XylS/Pm in front of the Psl operon, while pCSG4 was used in the homologous recombination to get the desired DNA sequence into *P. fluorescens*.

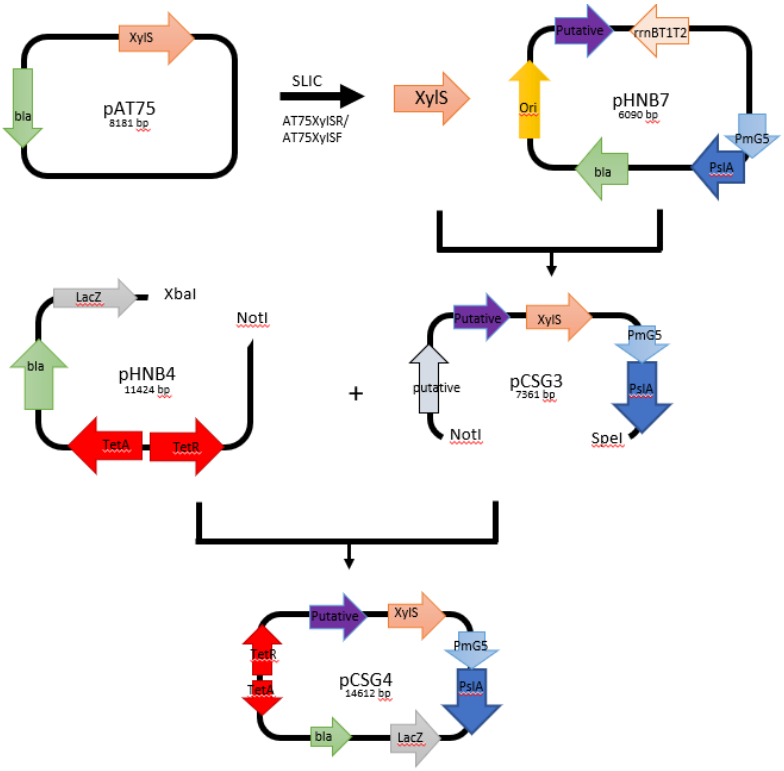

Figure 10: The cloning steps for the construction of pCSG3 and pCSG4. *XylS was amplified from pAT75 with PCR and then inserted into pHNB7 by SLIC cloning, creating pCSG3. NotI-SpeI-cut pCSG3 and XbaI-NotI-cut pHNB4 were ligated together, creating pCSG4. The restriction enzymes and their cutting sites are shown in the figure.*

To make pCSG3, the *xylS* gene from pAT75 was inserted into pHNB7. This was done by first cloning XylS using PCR with the AT75XylSF/AT75XylSR primer pair. The PCR product and the XbaI-NotI-cut pHNB7 vector are shown in Figure 11.

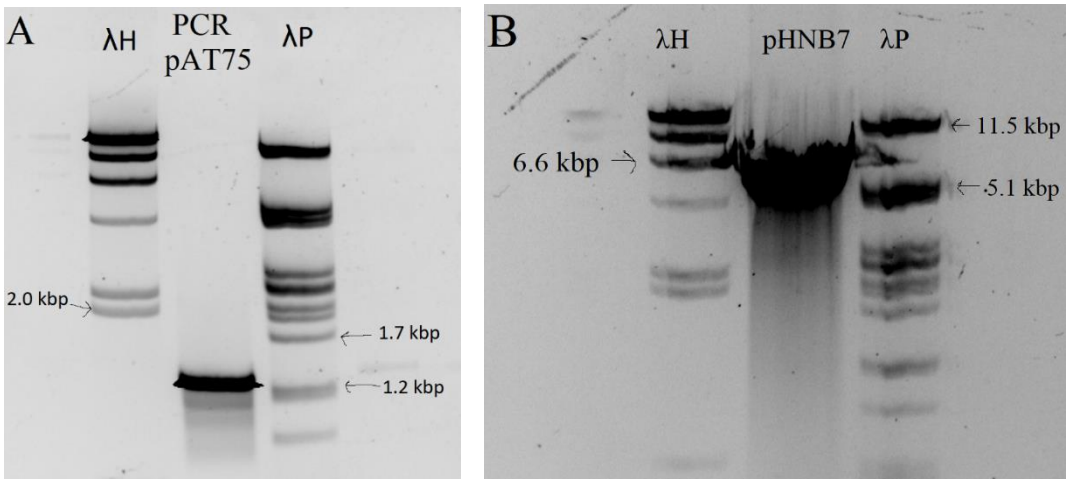

Figure 11: Cloning of pCSG3 *A) The PCR product XylS from pAT75 with an expected length of 1.3 kb. B) pHNB4 cut with Sbf1, having an expected length of 6.1 kb.*

After separation of the DNA fragments on a gel, the 1.3 kb fragment from the XylS insert and the pHNB7-vector backbone on 6.1 kb were cut and purified, followed by SLIC cloning. After transforming the new plasmid into *E. coli* S17.1, the plasmid was isolated, purified, and checked with AvrII as seen in Figure 12. The expected bands for pCSG3 were 2.4 and 5.0 kb, while the parental plasmid pHNB4 and pAT75 would have given one band each of 6.1 kb and 8.2 kb, respectively.

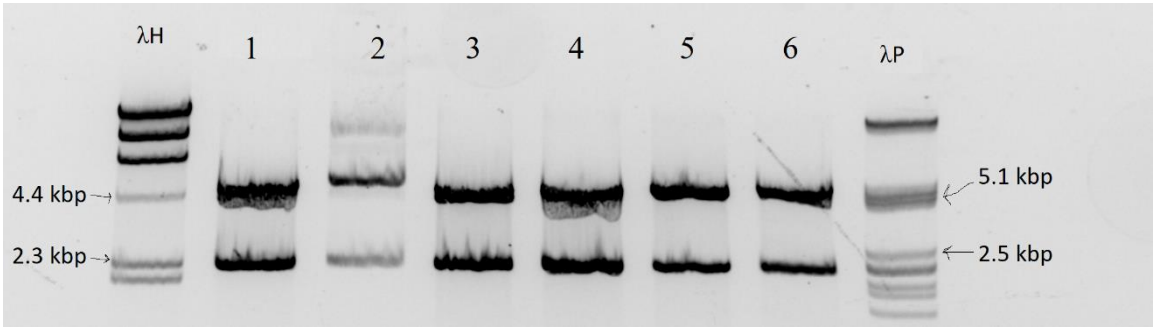

Figure 12: Verification of pCSG3*. pCSG3 cut with AvrII to check if the plasmid contained the XylS-insert in the pHNB4 vector after SLIC cloning. The expected lengths for pCSG3 are 5.0 and 2.4 kb, which can be seen in lanes 1, 3, 4, 5, and 6.*

The gel shows two bands for all samples with the expected lengths being 2.4 and 5.0 kb long. For sample 2, an additional band is visible, being around 8.0 kb. This is most likely due to partial restriction cutting. Colonies from sample 3 were annotated pCSG3 and used to create pCSG4.

Before starting homologous recombination, pCSG3 had to be inserted into pHNB4 as the backbone plasmid pHNB7 does not contain Tet^r and LacZ which is needed to confirm both recombination cross-over events when inserting the plasmid into the *P. fluorescens* chromosome. Therefore, pHNB4 was cut with NotI, XbaI, and XhoI to create a NotI-XbaI-cut fragment, with XhoI cutting outside this fragment to ensure that the unwanted part was properly cut and destroyed. pCSG3 was cut with NotI and SpeI, creating a 4.6 kb insert. After separating

the DNA fragments on a gel, the desired fragments were cut out and isolated. As seen in Figure 13, the 10kb band for pHNB4 was very weak so another sample was run on another gel, tripling the amount of cut DNA on the gel.

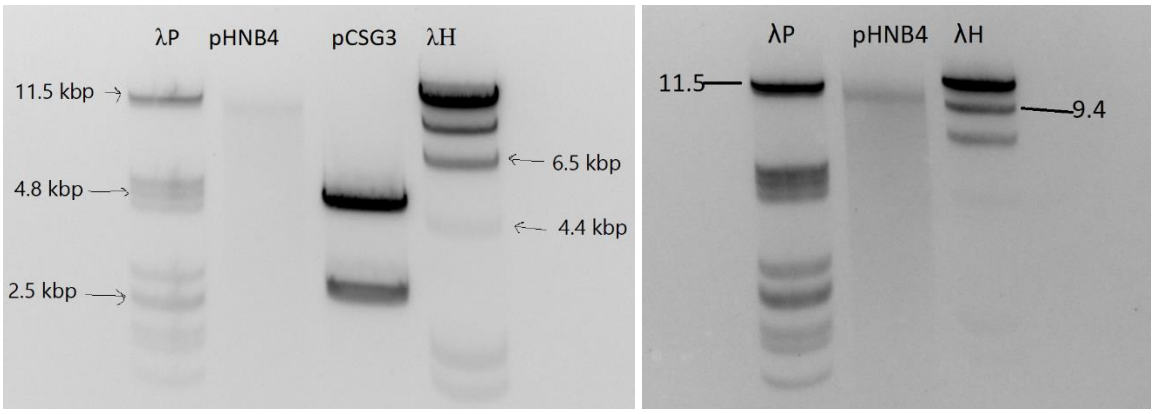

Figure 13: Creation of pCSG4. *A) The vector backbone pHNB4 and pCSG3 digested with NotI and XbaI. Expected lengths for the insert were 4.6 and 2.8 kb, and 10 kb for the vector plasmid pHNB4. B) NotI-XbaI digested pHNB4 using more DNA on the gel to create a stronger DNA band.*

The vector and the insert were ligated, transformed into *E. coli* S17.1 cells, and plated out on LA with Tet. To check the ligated DNA, the samples were cut with the restriction enzyme DraIII, which would give fragments of 5.9 kb and 8.7 kb for pCSG4, or 1.8 kb and 5.6 kb for pCSG3, and 11.4 kb for the vector plasmid pHNB4. As shown in Figure 14, two bands emerged for all samples indicating that the DNA was indeed pCSG4. Colony number 3 was used further and is now denoted pCSG4.

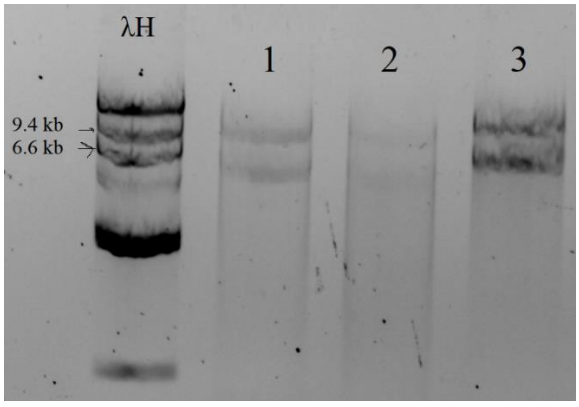

Figure 14: Verification of pCSG4. *DNA fragments from the separation of pCSG4 digested with DraIII. The expected bands were 8.7 and 5.9 kb, as seen in the gel. Colony 3 is now denoted pCSG4.*

4.3.2 Transferring pCSG4 into SBW25*mucA*

The genes flanked by the homologous parts with *P. fluorescens* in pCSG4 were to be inserted into the chromosome of *P. fluorescens*. This placed the promoter regulator XylS in front of PmG5, which is the promotor that would be controlling the Psl operon, as shown in Figure 15.

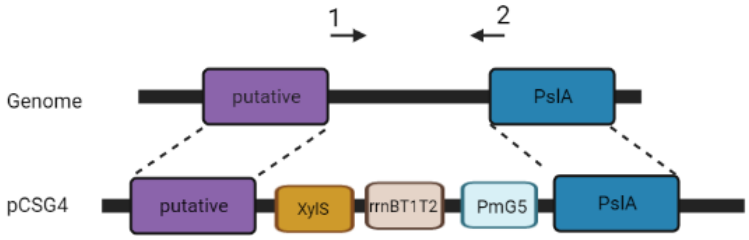

Figure 15: A schematic overview of the DNA fragment with XylS, rrnBT1T2, and PmG5 from the pCSG4 plasmid integrated into the P. fluorescens chromosome. *The arrows denote the primer binding seats for PslSjekkF (1) and PslSjekkR (2).*

pCSG4 was inserted in *P. fluorescens* SBW25*mucA* by using homologous recombination. After plating out samples from the third and fourth transfer to new LB medium, the number of white colonies on each plate was sufficient to begin testing them on LA and LA with Tet. The colonies growing on LA, but not on LA with tetracycline, had lost the Tet^r from pCSG4, which meant that either the second recombination event happened successfully, or the whole pCSG4 plasmid had been rejected and the colony had gone back to being wild-type. About 50 colonies were transferred from the LA with Xgal to LA plates with and without Tet. From these, some promising colonies were tested using PCR. Colony PCR proved not to be successful, so DNA had to be extracted from the colonies, as described in section 3.8.2. In addition, a different primer pairs were tested as the initial primer pair gave zero results for any of the colonies. The PCR using isolated DNA was successfully conducted with the PslSjekkA/R-primer pair, giving 2.5 kb for the correct mutant, and 0.5 kb for the wild-type. The resulting PCR product was separated on a gel as shown in Figure 16 and shows two correct mutants and two strains reverted to wild-type.

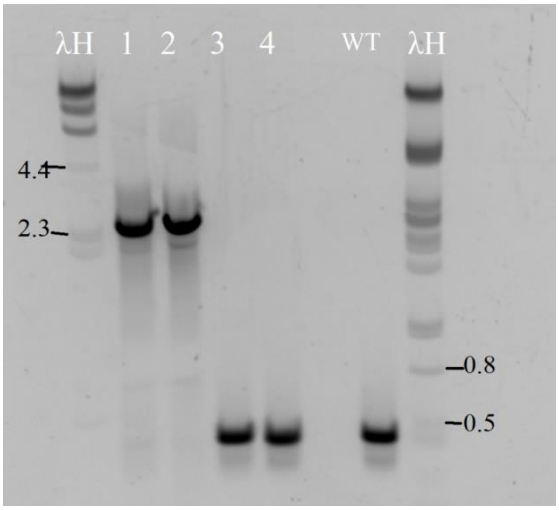

Figure 16: Verification of PCR product of SBWmucA-CSG4 mutant using PslSjekk primers. *The wild-type would give a band of 0.5, while the correct mutant was 2.5 kb long. As seen in the figure, sample 1 and 2 seems to be correct, while sample 3 and 4 are similar to the wild type, and thus have most likely thrown out the plasmid, going back to being wild-type.*

The strongest band for both samples 1 and 2 is the mutant band of 2.5 kb. Thus, samples 1 and 2 were concluded to have the correct insert and are therefore the correct mutant. They are now denoted SBW25*mucA*-CSG4A and B. Both mutant strains were stored at -80°C.

4.4 Construction of SBW25*mucA* derivative with PmG5-promoter controlling the Psl operon and lacking XylS (ACP^{+}X^{-})

To test the effect PmG5 and XylS have on the Psl operon, the XylS-deficient SBW25*mucA*-CSG2 strain was made. This strain was to be used to see if the promoter/regulator PmG5 and XylS had the desired effect on the production of alginate and/or Psl by activating the PmG5 promoter, or if high background expression happened even when lacking XylS.

4.4.1 Creation of the pCSG1 and pCSG2 plasmids

pCSG2 was to be integrated into the SBW25*mucA*HE230 chromosome, before pCSG1 was to be inserted into the same strain afterward to remove most genes in the alginate operon, rendering the mutant unable to produce alginate. Both plasmids were therefore created simultaneously as explained in this section. Both pCSG1 and pCSG2 used pHNB4 as the vector backbone but with pNB5 and pHNB7 as inserts, respectively, as shown in Figure 17.

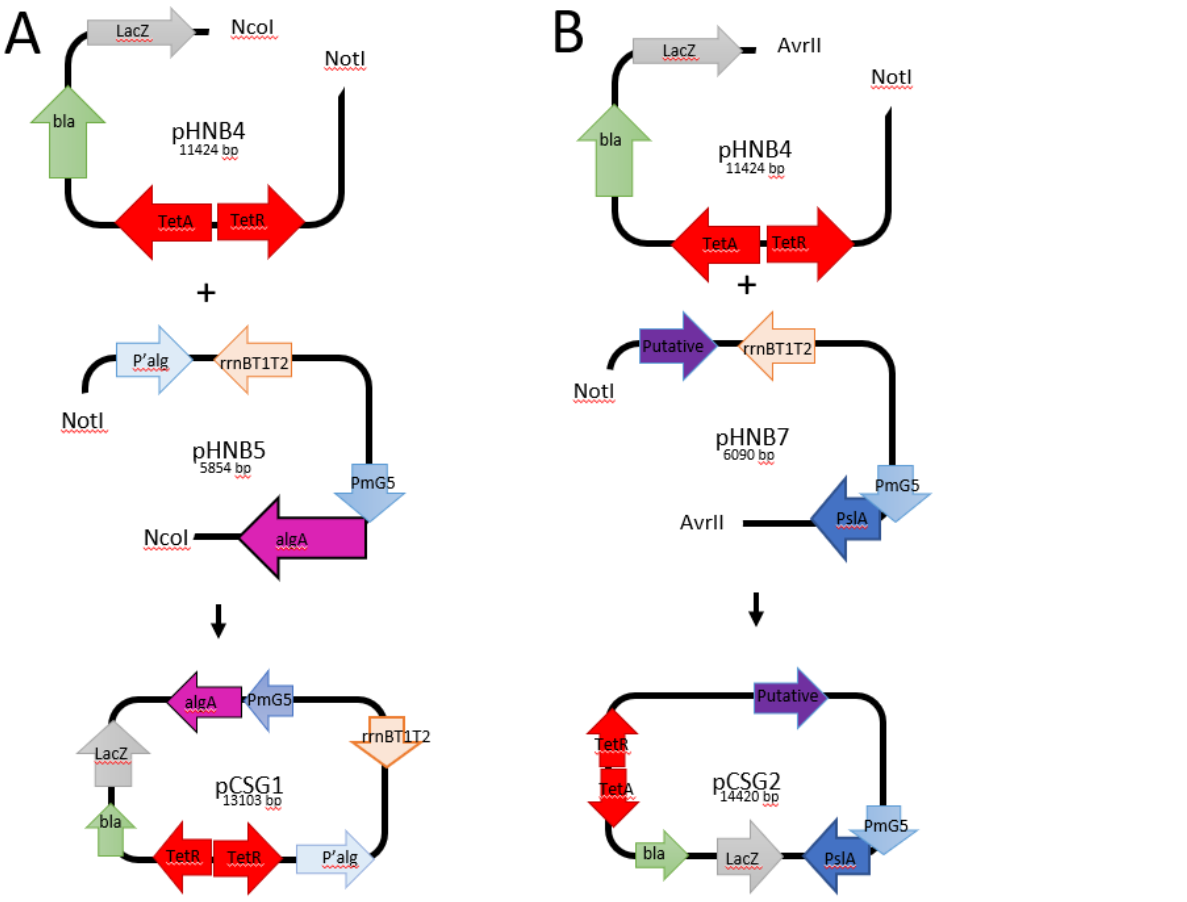

Figure 17: The cloning steps for the construction of pCSG1 and pCSG2. The restriction sites and enzymes used in each step are shown in the figure. A) pCSG1 is made by inserting pHNB7 into pHNB4. B) pCSG2 is made by inserting pHNB7 into pHNB4

To make pCSG1, pHNB5 and pHNB4 were both cut with NcoI and NotI. This yielded a pHNB5 DNA fragment of 3.1 kb that was inserted into the 10 kb long pHNB4 vector backbone. To make pCSG2, pHNB7 and pHNB4 were cut with NotI and AvrII, giving a 3.4 kb long DNA fragment from pHNB7 that was inserted into the 10 kb long vector backbone from pHNB4. The DNA outside of all fragment targets was simultaneously digested with an additional restriction enzyme each to ensure proper destruction of the non-desired fragment. The separation of the DNA fragments on a gel is shown in Figure 18A. After ligating the vector and inserts together, transformants were plated out on LA with ampicillin. To check if the transformants had taken up the correct plasmids, cells were harvested, and plasmids were isolated and cut with the restriction enzyme EcoRI, yielding bands with the sizes 6.7 kb, 3.7 kb, 2.4 kb, and 0.3 kb for pCSG1, and sizes 5.9 kb, 3.8 kb, 3.3 kb, 0.3 kb, and 0.2 kb for pCSG2. The same enzyme would have given bands of 5.9 kb, 3.8 kb, 1.1 kb, and 0.3 kb for pHNB4, 3.6 kb and 2.3 kb for pHNB5, and 2.8 kb and 3.3 kb for pHNB7.

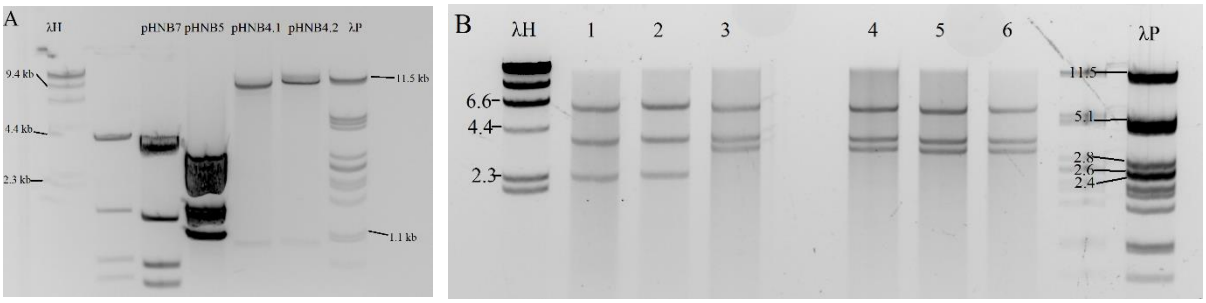

Figure 18: Separation of digested pHNB4 vector backbone and pHNB7 and pHNB5 inserts, and verification of pCSG1 and pCSG2*. A) The pHNB5 insert of 3.1 kb and pHNB4 (denoted pHNB4.1) backbone on 10 kb were both created by digestion with NcoI and NotI, while the pHNB7 insert on 3.4 kb and the vector pHNB4 (denoted pHNB4.2) of 10 kb digested with NotI and AvrII were separated on the same gel. B) Sample 1 and 2 shows the three biggest fragments expected for pCSG1 while samples 3-6 show the three biggest fragments expected for pCSG2.*

As seen in Figure 18B, all plasmids have the correct sizes, with only the three biggest bands being visible. For pHNB5 inserted into pHNB4, sample number 2 was used further used and denoted pCGS1, while for pHNB7 into pHNB7, sample number 3 is now denoted pCSG2.

4.4.2 Transferring pCSG2 into SBW25*mucA*

The integration of pCSG2 into the SBW25*mucA* strain was conducted using homologous recombination, with a similar strategy as the one used to create SBW25*mucA*-CSG4. The insertion of pCSG2 into the host chromosome is shown in Figure 19.

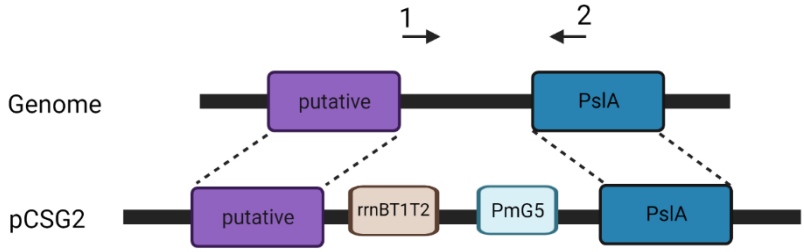

Figure 19: A schematic overview of the DNA fragment rrnBT1T2 and PmG5 from the pCSG2 plasmid integrated into the P. fluorescens chromosome. *The arrows denote the primer binding seats for PslSjekkF (1) and PslSjekkR (2).*

When the amount of white colonies on the LB agar plates with Xgal was sufficiently high, 50 white colonies from each plate were replica plated on LA with and without tetracycline. Promising colonies were then tested using colony PCR with the PslSjekk primer pair, expected to yield a band of 1.3 kb for the correct mutant, and 0.5 kb for the wild-type band. As scraping off small bits of a colony proved to be a poor PCR substrate and the extraction of DNA gave a too high workload given the many samples that should be tested, parts of the colonies were scraped off, mixed with distilled water, and heated at 98°C for 15 minutes instead. The PslSjekk primer pair was used, yielding only wild-type bands of 0.5 kb for all tested colonies. Thus, new blue colonies from the initial recombination plate were inoculated in LB for a few days, plated out on LA with Xgal, and tested. Some of the most interesting results are shown in Figure 20, showing one promising colony that have both the mutant band and the wild-type band.

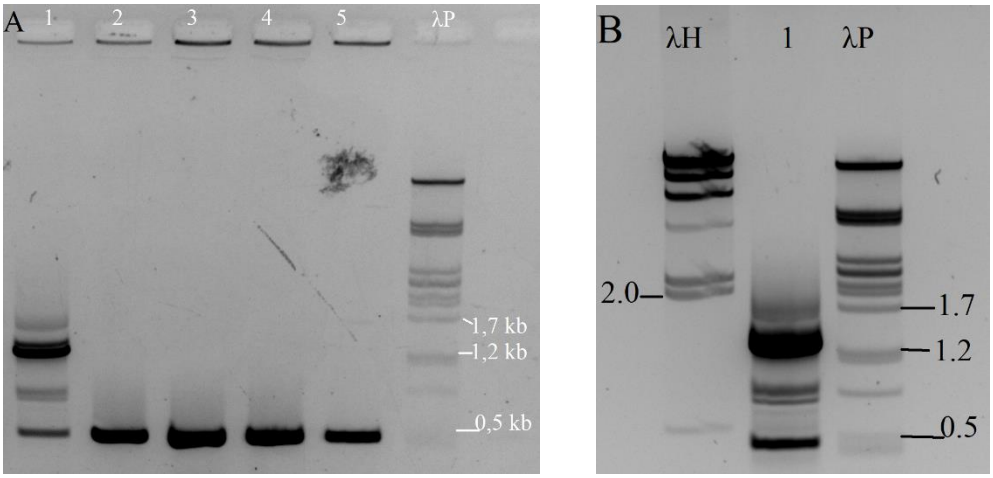

***Figure 20: Testing of SBW25mucA with pCSG2 using PCR**. A) PCR with PslSjekk gave the wild-type band for most samples except number 1, which have their most intense band being the mutant band of 1.2 kb. B) Colony number 1 was put on the gel by itself in case the mutant band was caused by one of its neighbouring samples. The gel shows that the strongest band is the mutant band of 1.2 kb, but several unspecified bands, including the wild-type band is also present, indicating that it is not a clean homologous recombination product.*

After several attempts in creating this mutant strain, mostly the wild-type band of 0.5 kb was found, as well as some samples having bands that were hard to explain. During the first initial recombination event, two possible outcomes could happen, with either a putative segment (type A) or the PslA sequence (type B), as seen in Figure 21. The thought was that the rarest event would give the desired recombination, as most recombinational events seemed to give back the wild type. To be able to distinguish between these, a new primer pair was created called CSG2blåA. The primers would bind and give bands of 1.2 kb for integration type A, and no bands would be visible for integration type B. In addition, the primer pair would give a band of 1.2 kb for the correct mutant.

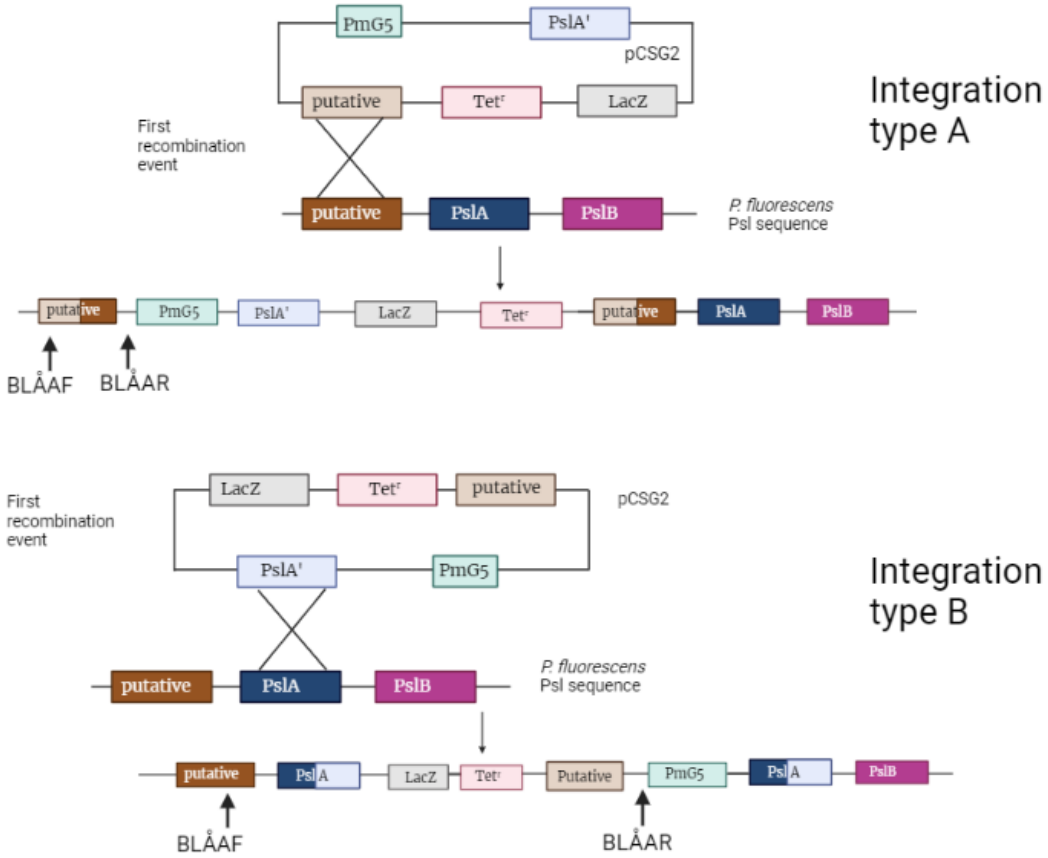

Figure 21: A schematic overview of the two possible outcomes after the initial recombination event has occurred with pCSG2. *In integration type A, the recombination happened in the putative segment, while for integration type B, the recombination happened at PslA. Ideally, both events would yield the same outcome, with the second recombination event happening at the opposite homologous region in the plasmid, but since such a large number of white colonies gave the wild-type band back, the thought is that one of the events is favoured over the other. The two outcomes can be detected using a primer pair where one is binding within the plasmid DNA, and the other binding to the genomic DNA. Primers are shown with arrows.*

Before conjugating SWB25*mucA* with pCSG2 again, seven blue and four white colonies from the selection plates were tested with the primer pair to see if it could tell which of the recombinant events had occurred for the blue colonies that still had LacZ in the chromosome. As seen in Figure 22A, 11 colonies from the initial recombination event were checked using the CSG2blåA primer pair, with ten of the same colonies being tested using PslSjekk as seen in Figure 22B. CSG2blåA primer pair gave a band of 1.2 for samples 2, 3, 4, 5, 7, and 11, indicating the plasmid is most likely inserted as integration type A. Samples 7-9 had a strong band of around 2.8, which was not expected for any of the integration types. In addition, several samples gave more bands than expected. Nevertheless, the results could indicate that integration type A is more common than integration type B. As some of the colonies checked were white, they were all checked with PslSjekk to see if they had the correct mutant band. This yielded one colony (number 8) with a strong mutant band in addition to some larger unspecific bands.

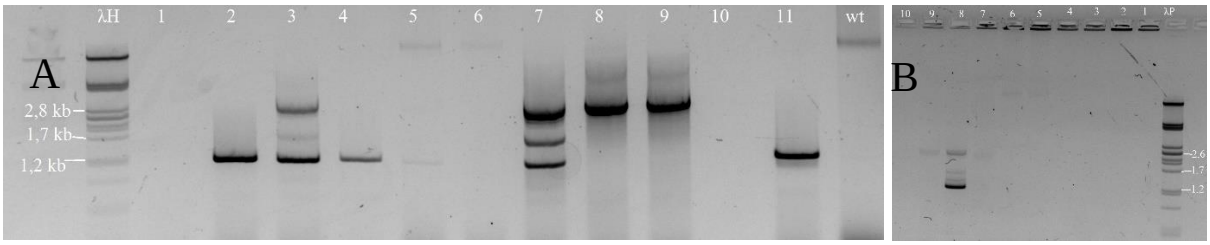

Figure 22: Verification of PCR fragments of SWB25mucA with pCSG2 integrated *A) 11 samples with the lacZ gene in the chromosome (as they were still blue) were tested using CSG2blåA primer pair, indicating that most samples have a variant of the integration type A integration B) The same colonies were tested using PslSjekk primer pairs, giving one promising sample, having a strong mutant band of 1.3 kb, as well as several unwanted and unspecific bands.*

As most colonies yielded no bands at all for the PslSjekk primer pair, more white colonies from the same plate were tested using the CSG2blåA primer pair and PslSjekk as shown in Figure 23. Three strains were tested using two parallels, with strain 2 yielding a band of 1.2 kb for CSG2blåA twice. When tested using PslSjekk, the correct mutant band appeared for both mutant 2 and 3, being 1.3 kb as seen in Figure 23B. Thus, the mutant strain number 2 was frozen at -80 ℃ and is now denoted SBW25*mucA*-CSG2.

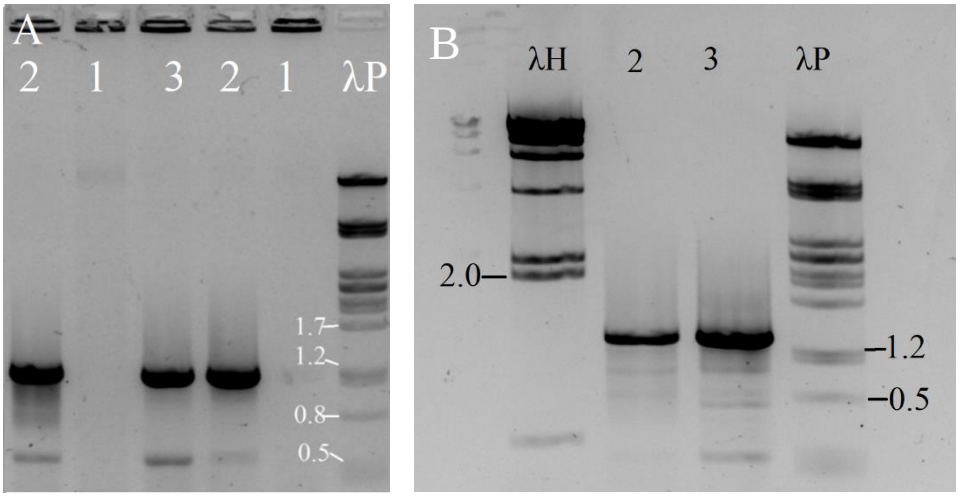

Figure 23: Validation of PCR products of SBW25mucA + pCSG2 mutants checked using CSG2blåA and PslSjekk. A) *Three samples, 1 -3, were tested using CSG2blåA primer pair to see the integration type. From the resulting bands, sample 2 and 3 seems to be either the correct mutant or have integration type A. B) Sample 2 and 3 were tested using PslSjekk, giving a strong mutant band of around 1.3 kb.*

4.5 Construction of SBW25*mucA*Δ*algC* derivative with Psl operon controlled by PmG5-promoter ($AC^{-}P^{+}$).

SWB25*mucA*Δ*algC* is a derivative of SBW25*mucA* where *algC* has been deleted, rendering a mutant that is unable to produce AlgC. Due to the *algC* deletion, the mutant is no longer able to produce alginate, as well as some other EPSs [64]. For this study, the PmG5 promoter and XylS regulator were inserted into the *P. fluorescens* host genome, allowing control of the Psl operon transcription. With this mutant, we could use the *algC* deletion to investigate if AlgC plays an important role in the production of Psl.

Initially, pCSG4 was used to be used to create the mutant, as with the SBW25*mucA*-CSG4 derivative. However, after several attempts with testing colonies and only getting the wild-type band back, a new plasmid was created to help select for the correct mutants. This new plasmid

is a pCSG4 derivative, containing an apramycin gene in front of XylS. By inserting such a marker gene into the *P. fluorescens* chromosome, they could be cultivated using apramycin, ensuring that no wild-type colonies were to grow up. The creation of this plasmid, which can have the apramycin gene in two different orientations, is shown in Figure 24.

4.5.1 Creation of the pCSG6 and pCSG7 plasmid

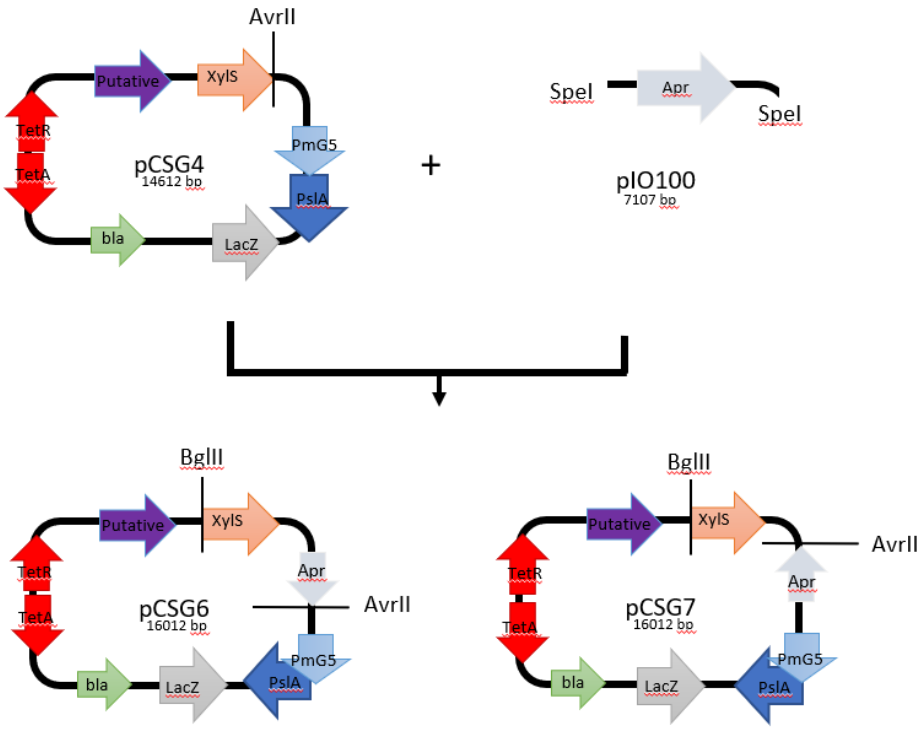

Figure 24: The creation of pCSG6 and pCSG7. *AvrII-cut pCG4 worked as the backbone for inserting the apramycin gene from SpeI-cut pIO100. After ligating the fragment into the vector, the Apr gene can take two orientations, with its AvrII site close to PmG5 (pCSG6) or close to XylS (pCSG7). The cutting sites for the used restriction enzymes are shown in the figure.*

pIO100 was cut with SpeI, yielding a fragment of 1.4 kb and 5.7 kb, with the smallest fragment containing the Apr gene. The vector backbone pCSG4 was cut with AvrII, yielding one big fragment of 14 kb as seen in Figure 25. After cutting both fragments out of the gel, they were purified, ligated together, and transformed into *E. coli* S17.1 cells.

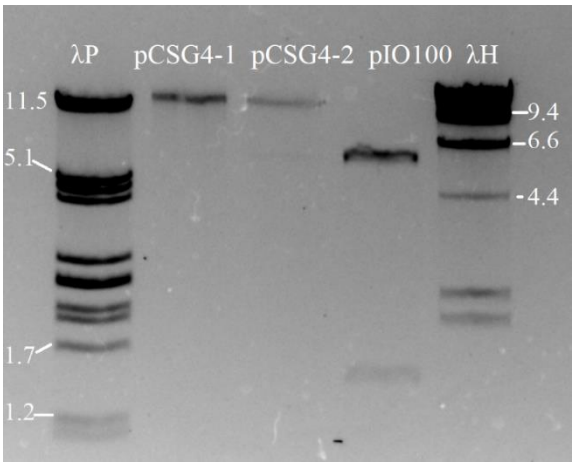

Figure 25: Digestion of pCSG4 and pIO100 with AvrII and SpeI, respectively. *AvrII-cut pCSG4 gave a band of 14,0 kb, while the apramycin gene was cut out of pIO100 with SpeI, yielding the desired fragment of 1.4 kb, and a bigger fragment of 5.7 kb.*

When inserting the DNA segment gene into pCSG4, it can have its AvrII restriction site laying either close to PmG5 (pCSG6) or close to XylS (pCSG7) as shown in the figure. For the creation of the SBW25*mucA*Δ*algC* mutant, the orientation did not matter, as long as the gene was inserted into the correct position. To create a new plasmid equivalent to pCSG2, pCSG4 with the Apr gene could be used by removing XylS from the plasmid, but this then required that the AvrII site from the apramycin fragment was located close to XylS. Both the insertion and the orientation of the Apr gene were therefore checked using restriction enzymes.

Initially, the transformants were cut with XbaI and XhoI, yielding three bands of 14.9 kb, 0.7 kb, and 0.4 kb for the plasmid with Apr laying the "wrong" way, three bands of 13.0 kb, 1.7 kb, and 0.4 kb for apramycin laying the desired way, and only one band of 14.6 kb for the parental pCSG4 plasmid. As seen in Figure 26A, samples 2, 3, and 4 have the 0.7 kb band, indicating that they have Apr with AvrII close to PmG5, while sample 1 is similar to pCSG4. Sample 2 was therefore cultivated in LB to start the conjugation. Simultaneously, more transformants as well as a different restriction enzyme were used to confirm the new plasmid and the orientation of the apramycin gene. AvrII and XbaI were expected to yield 15.2 kb and 0.7 kb bands for pCSG4 with AvrII close to PmG5, 13.9 kb and 2.1 kb for pCSG4 with apramycin inserted the desired way, and 13.9 and 0.7 for pCSG4. As seen in Figure 26b, samples 2, 3, and 7 gave bands corresponding to pCSG4 with AvrII close to PmG5, while sample 5 corresponds with pCSG4 with apramycin inserted the desired way.

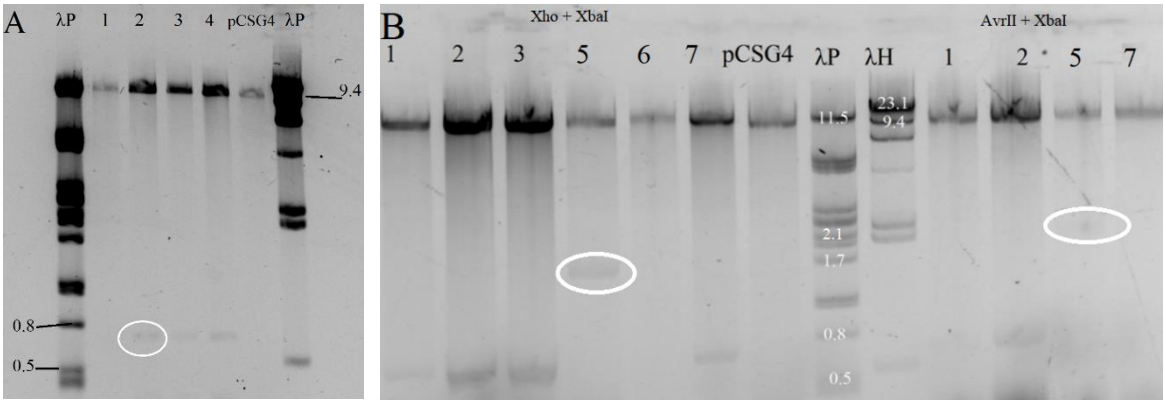

Figure 26: Verification of pCSG6 and pCSG7*. A) Transformants were cut with XbaI and XhoI, yielding bands of 14.9 and 0.7 kb for pCSG6 with AvrII close to PmG5 gene as seen for samples 2, 3, and 4, and 14.6 kb for the parental plasmid pCSG4. B) More transformants were cut with XhoI and XbaI to the left of the ladders, showing one transformant (sample 5) with AvrlII close to XylS giving visible bands of 13.0 and 1.7kb (circled) on the gel. This is further confirmed by the 13.1 kb and 2.1 kb (circled) bands on the right. Sample 2 is now denoted pCSG6, while sample 5 is denoted pCSG7.*

As the orientation of the Apr gene did not matter for this mutant, sample 2 was therefore used further in creating the SBW25*mucA*Δ*algC*-CSG6 mutant. Sample 2 was denoted pCSG6, and sample 5 was denoted pCSG7, further described in section 4.6 ($A^-C^+P^+$).

4.5.2 Transferring pCSG6 into SBW25*mucA*Δ*algC*

Before starting to work with the SBW25*mucA*Δ*algC* strain, it was verified using PCR with the algCR+F primer pair. As seen in Figure 27, the wild type with the intact *algC* sequence gave a band of 1.2 kb, while SBW25*mucA*Δ*algC* gave a band of 0.8 kb, as expected.

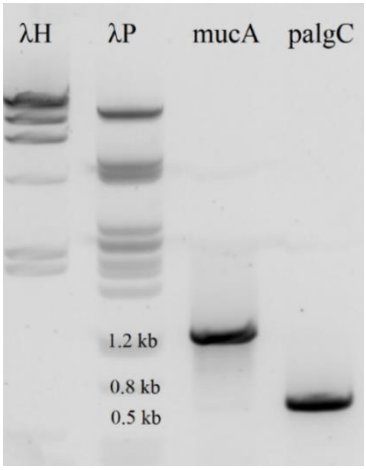

Figure 27: Verification of the algC deficient strain used to create SBW25mucAΔalgC-CSG6. *Mutants with the correct mutations in the AlgC sequence gave a band of 0.8 kb, while the P. fluorescens wild type gives a band of 1.2 kb using the algCF+R primer pair.*

Even with the new pCSG6 plasmid, the creation of SBW25*mucA*Δ*algC*-CSG6 proved to be very difficult, as most colonies still gave the wild-type band when testing with PCR. In addition to creating a new primer pair to see the mutant, termed PslWT, two additional new primer pairs termed 3AMF+R and 5AMF+R were made. These latter pairs allowed us to see which parts of the plasmid were still integrated into the chromosome, as all colonies grew on plates containing apramycin and had lost their tetracycline gene and the blue colour from having LacZ. The first recombination event will give two possible outcomes, based on if it is the putative segment (type A) or PslA (type B) that initiates the recombination, as shown in Figure 28.

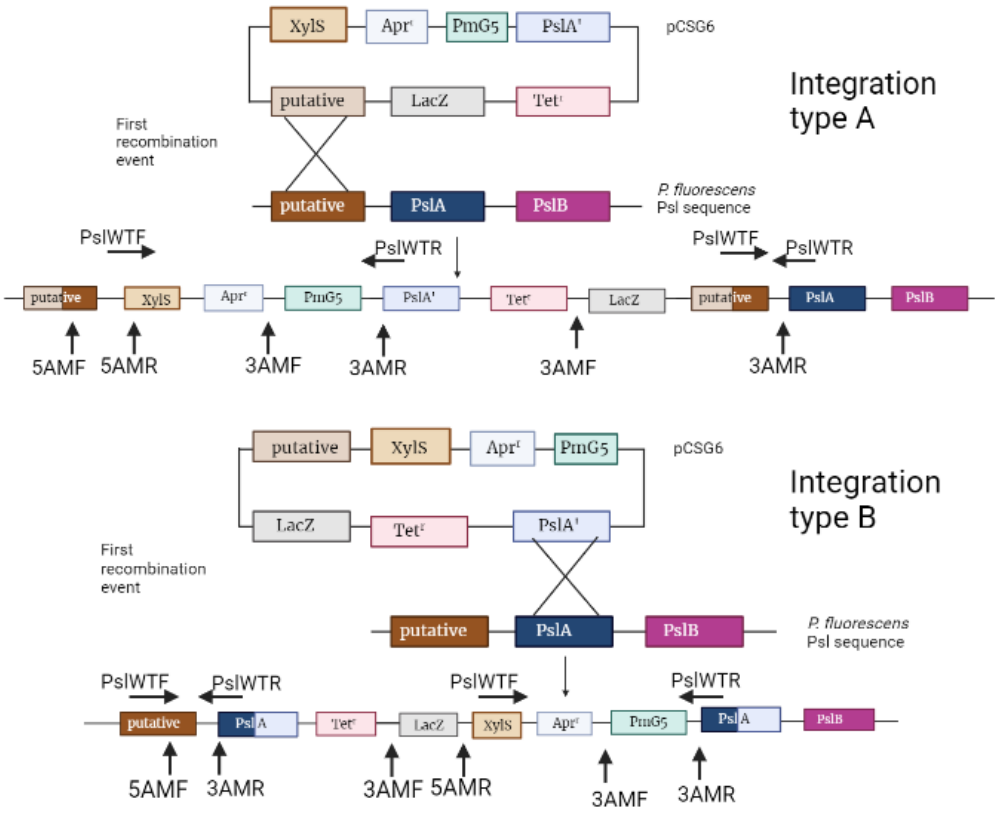

Figure 28: A schematic overview of the initial recombination event of the homolog recombination of pCSG6 and SBW25mucAΔalgC. *As seen in the figure, two different outcomes are possible, based on where the first recombinational event takes place. The arrows denote primer pair binding sites, with the PslWT primer pair displayed as vertical arrows.*

PslAM3R and PslAM5F will bind to the genomic DNA, and its partner will bind to the plasmid sequence. In addition, a new Psl mutant primer was made, PslWT. By combining these three primer pairs, we can then say something about which parts of the plasmid were still integrated in the host chromosome, and the direction of the plasmid. The thought is still that the rarest orientation will result in the mutant, as it seems like the bacteria most often ends up spitting out the whole plasmid, resulting in the wild-type band after PCR. Figure 29 shows four blue colonies after the initial recombination event tested with PslAM3F+R (A), PslAM5F + PslwtR (B), and PslAM5F+R (C).

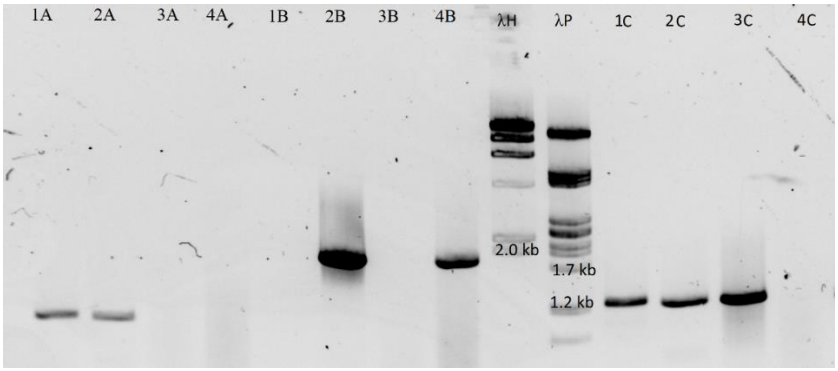

Figure 29: White colonies tested with a combination of 5AM, 3AM, and PslWT primer pairs. *Most colonies seem to have integration type A, yielding a 1.2 kb band for PslAM3R+F primer pair (A), and 1.2 kb for PslAM5F+R primer pair (C).*

PslAM3R+F would give a band of 1.2 kb for both integration types and the correct mutant, and no bands for integration type B. PslAM5F+PslWTR would give a band of 5.1 kb for integration type A, 1.7 kb for integration type B and the wild-type. PslAM5F+R would give a band of 1.2 for integration type A or the correct mutant, and no bands for integration type B. Based on the results, sample 1 was most likely integration type A, while sample 4 was most likely integration type B. As all mutants were blue, none were the correct mutant. Samples 2 and 3 were most likely also integration A, as they both had a band using PslAM5F+R primer pairs. Integration type A thus seems to be the most common type. An overview of the fragments, their lengths, and what they mean for the four colony samples is given in Table 6.

Table 6: An overview of the bands and integration of the plasmid for the four colonies tested with three different primer pairs

Primer pair / sample	**AM3R+F (A)**	**PslAM5F+PslWTR (B)**	**PslAM5F+R (C)**
1	1.2 (WT or Int A)	-- (IntA)	1.2 (IntA)
2	1.2 (WT or Int A)	1.7 (mutant or IntB)	1.2 (mutant or IntA)
3	-- (IntB)	-- (IntA)	1.2 (mutant or IntA)
4	-- (IntB)	1.7 (mutant or IntB)	-- (IntB)

After inoculating two colonies with integration type B and one with integration type A, samples were plated out on LA with Apr and m-toluate (0.25 mM) before being transferred into new LB. When enough colonies were white on the plates, colonies were replica plated on LA with and without Tet, and tetracycline-sensitive mutants were tested using PCR and the PslWT primer pair. Initial testing gave back some colonies having the correct mutant band, but a subsequent PCR with the same primer gave back the wild-type band. Thus, five new tetracycline-sensitive colonies from the replica plate were inoculated in LB and frozen at -80°C

directly, while simultaneously using the liquid culture as PCR substrate with the PslWT primer pair. As seen in Figure 30, sample 1 had the correct mutant band of around 4.6 kb, while sample 3 had both mutant and wild-type bands. The colony was also tested using the algCR+F primer pair (not shown), confirming that the mutant was *Pseudomonas.* The mutant strain number 1 was then denoted SBW25*mucA*Δ*algC*-CSG6.

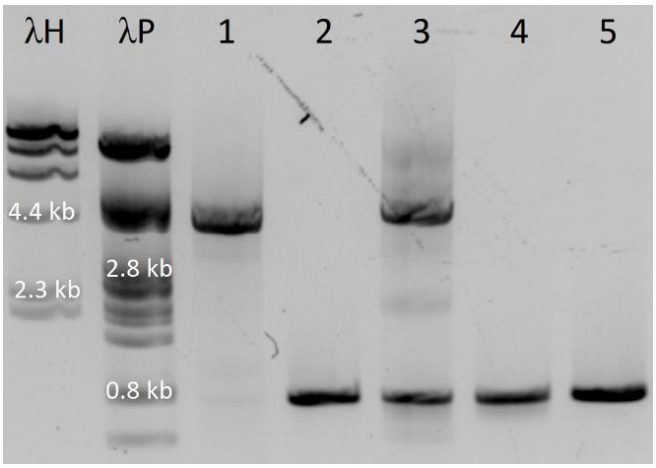

Figure 30: Verification of SBW25mucAΔalgC-CSG6 mutants with PslWT primers. *The testing of tetracycline-sensitive colonies with PCR and the PslWT primer paid yielded the correct mutant band of around 4.6 kb for sample 1. Liquid culture served as PCR substrate which was frozen at -80℃ prior to PCR testing.*

4.6 Construction of a SBW25*mucA*HE230pAlgD$^-$ derivative with Psl operon controlled by PmG5 promoter (A$^-$C$^+$P$^+$)

SBW25*mucA*HE230pAlgD$^-$ is a derivative of SBW25*mucA*HE230, where in addition to *algC* being controlled by a PmG5 promoter, *algD* is deleted, rendering the mutant unable to produce alginate. Since this AlgD$^-$ mutant already has a XylS regulator in its chromosome, a plasmid containing PmG5 flanked by homologous regions in the Psl sequence lacking XylS was used.

4.6.1 Creation of the SBW25*mucA*HE230pAlgD$^-$-CSG8 mutant (A$^-$C$^+$P$^+$)

The insertion of pCSG8 was conducted by using homologous recombination, and the insertion of pCSG8 into the host chromosome is shown in Figure 31**.**

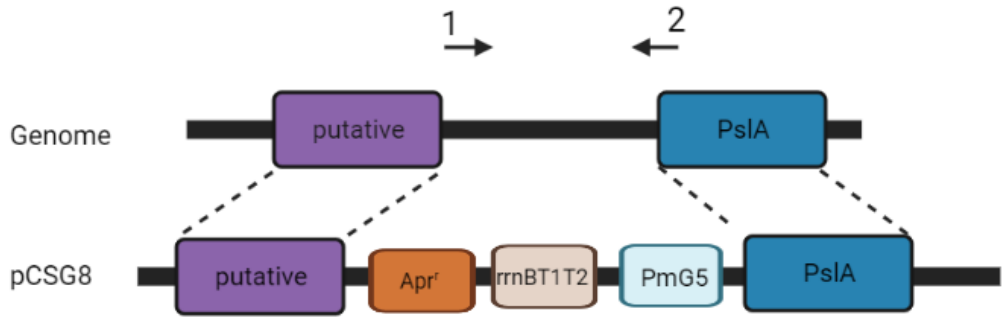

Figure 31: A schematic overview of the DNA fragment with apramycin, rrnBT1T2, and PmG5 from the pCSG8 plasmid integrated into the P. fluorescens SBW25mucAHE230 chromosome. *The arrows denote the primer binding seats for PslSjekkF (1) and PslSjekkR (2).*

Before conjugating pCSG8 into the SBW25*mucA*HE230pAlgD$^-$ strain, the strain was tested using PCR to confirm the deletion of the *algD* fragment. As the construction of this mutation was not completely known, the fragment was also sent to sequencing to confirm the sequence.

By using the pAlgD primer pair, the wild type would have yielded a band of 1.2 kb, while the correct mutant would have given a band of between 0.7kb and 1.0 kb. As seen in Figure 32A, the fragments were a little below 0.8 kb, and the correct sequence was further determined by the sequencing results (added in Appendix F). SBW25*mucA* wild-type can be seen to have the wild-type band of 1.2 kb.

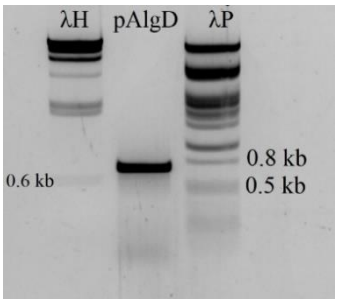

Figure 32: Confirmation of the deletion of the algD sequence in P. fluorescens. *The AlgD⁻ mutant was tested using PCR with pAlgD primer pair and later sent to sequencing.*

To create SBW25*mucA*HE230pAlgD⁻-CSG8, the initial strategy was to use the CSG2blåA primer pair to determine the rarest recombination event and cultivate mutants with the rarest integration type, as described for the creation of SBW25*mucA*-CSG2. The CSG2BlåA primer pair would give a band of 1.2 if the plasmid had integrated as type A, and nothing if integration type B happened. 24 blue colonies from the initial PIA-plate with tetracycline and XGal were tested using the primer pair, with the results shown in Figure 33. As one can see, they were a bit hard to interpret as we did not see the single band that was expected. However, we saw that samples 18 and 20 stood a bit out, and these were selected for initiating the second recombinant event. Nonetheless, this did only result in getting the wild-type band back, thus another strategy needed to be made to create the mutant.

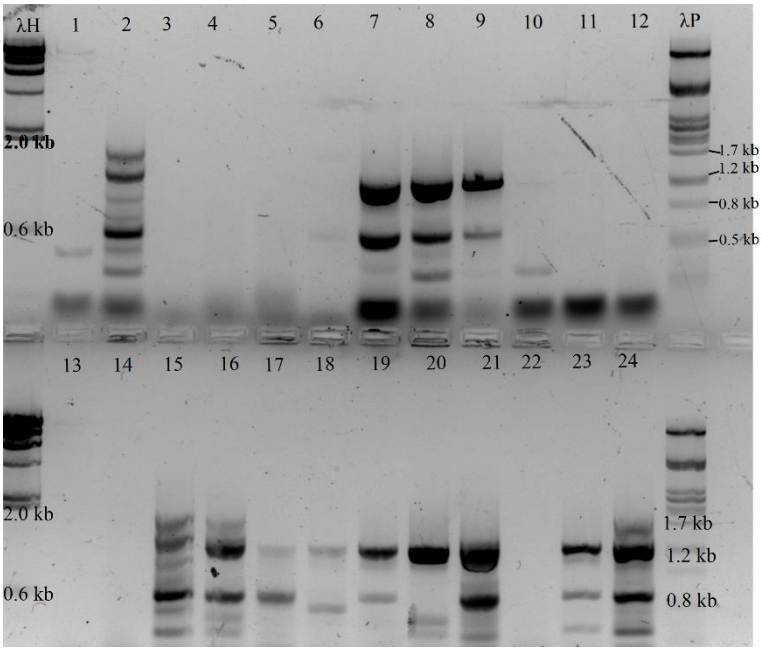

Figure 33: Testing blue SBW25mucAHE230pAlgD⁻-CSG8 colonies with CSGBlåA primer pair. *None of the samples gave the single band expected for integration type A. It is also difficult to determine if the samples yielding no bands are integration type B, or if there was an error when preparing the PCR substrate. Samples 18 and 20 were selected for further cultivation as these stood a bit out from the others.*

4.6.2 Construction of the pCSG7 and pCSG8 plasmids

As for the previous mutants, another strategy for selecting colonies with the plasmid inserted correctly had to be made. Therefore, the apramycin gene was inserted into the plasmid to select for colonies with apramycin resistance. Since pCSG7 was already made, having an AvrII and a BglII recognition site on each side of the XylS fragment, the XylS could be cut out with these restriction enzymes, giving a plasmid with the PmG5 promoter flanked by homologous regions to the *P. fluorescens* genome, and having the apramycin gene. A schematic overview of the creation of pCSG8 is given in Figure 34.

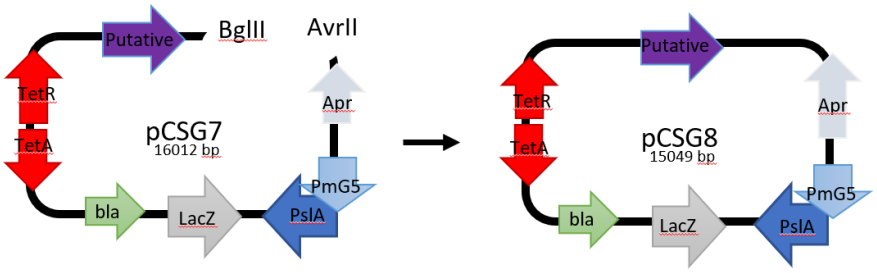

Figure 34: The creation of pCSG8. *pCSG7 was cut with BglII and AvrII to remove the XylS fragment. The restriction enzymes and their cutting sites are shown in the figure.*

Further testing and confirmation of sample 5, denoted pCSG7 from section 4.5 ($A^-C^+P^+$), is shown in Figure 35. The plasmid was cut with EcoRI, yielding the unique bands of 2.5 kb and 2.3 kb as expected for pCSG7. The samples were denoted pCSG7-1 and pCSG7-2, and frozen.

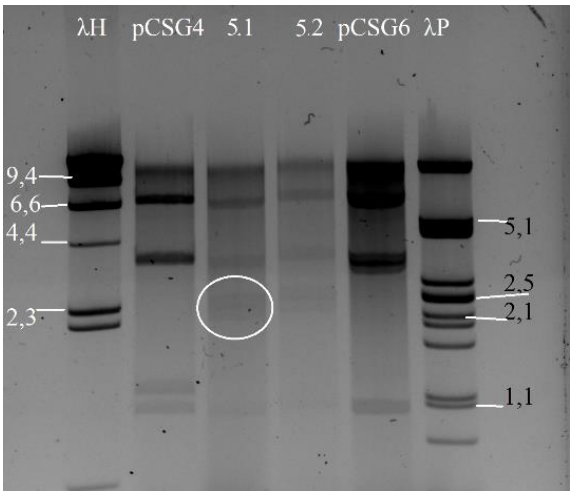

Figure 35: Confirmation of pCGS7. *To further ensure that sample 5 has the correct insert, more plasmid DNA was extracted from the same colony, purified, and cut with EcoRI, yielding unique bands of 2.3 and 2.5 kb for the desired plasmid.*

pCSG7(-1) was digested with BglII and AvrII, yielding bands of 15.0 and 1.0 kb. The larger 15kb band was cut from the gel as shown in Figure 36A to get rid of the XylS fragment before ligating the plasmid together, to avoid having two XylS fragments in the SBW25*mucA*HE230pAlgD$^-$ chromosome. Testing of the transformants was done by isolating the plasmids and cutting them with SphI and NotI, yielding 1.7 kb, 3.6 kb, and 10.0 kb bands for pCSG7, and 4.7 kb and 10.0 kb bands for the new pCSG8 plasmid. As seen in Figure 36B, all samples had the correct bands, and sample 4 was frozen for later use. This sample is now denoted pCSG8.

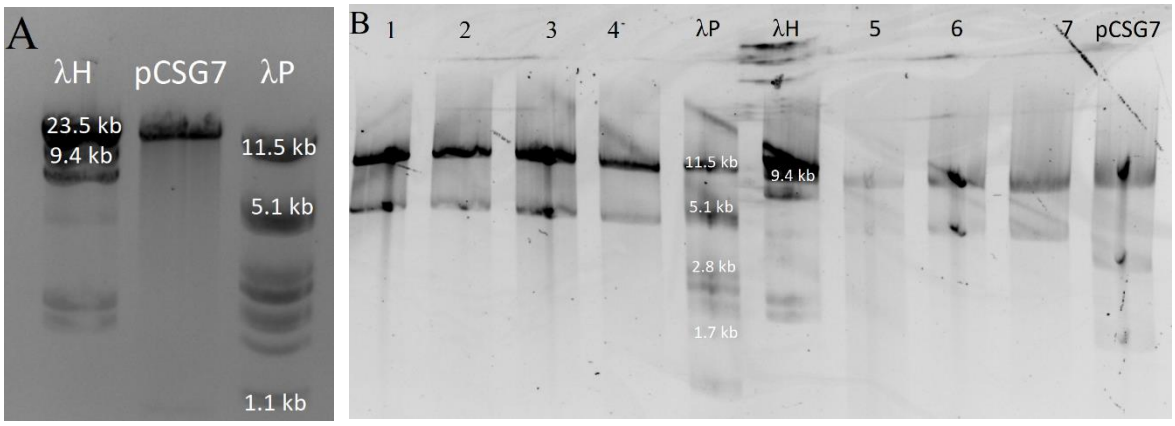

Figure 36: Separation of digested pCSG7 fragments, and verification of the new pCSG8 plasmid. *A) pCSG7 was cut with BglII and AvrII to yield a 15.0 kb fragment which was separated and cut from the gel. B) After ligation, new transformants were tested by isolating the plasmid and digesting it with SphI and NotI, yielding 4.7 kb and 10.0 kb bands for all samples but pCSG7.*

4.6.3 Transferring pCSG8 into SBW25*mucA*HE230pAlgD$^-$

Even with the new pCSG8 plasmid, the initial strategy of choosing the colonies with the rarest integration of the plasmid could be conducted using CSG2blåA primer pair. For integration type A (recombination at the putative element), a 2.6 kb band was expected, whereas for integration type B (PslA) zero bands would be visible.

Several blue colonies from after the initial recombination event were tested using the CSG2BlåA primer pair, as seen in Figure 37. The two strong bands for samples 1 and 3 can be interpreted as a type A integration band, while the lack of bands for the other samples could indicate integration type B. Thus, integration type A is determined to be the rarest event. Colonies 1, 2, and 3 were therefore cultivated further.

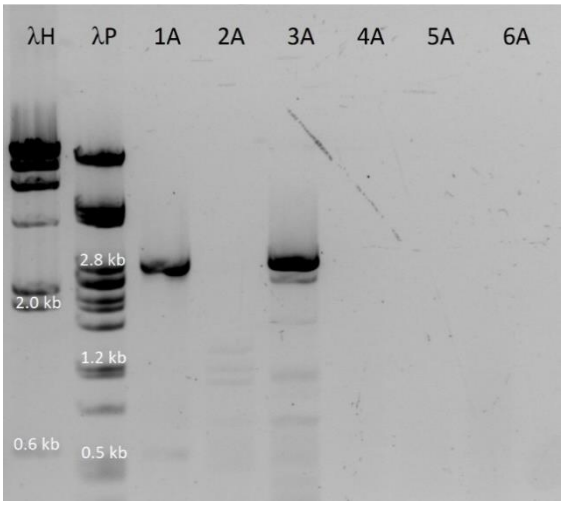

Figure 37: Testing of six blue SBW25mucAHE230pAlgD—CSG8 mutants with CSG2BlåA primer pair. *Integration type A was expected to yield bands of 2.6 kb, while integration type B was expected to yield zero bands.*

Initially, two promising colonies were discovered after dotting over colonies on LA with and without Tet, where one had a stronger wild-type band than the mutant band (sample 5), but it had a very different morphology, being whiter and showing increased motility compared to the rest of the colonies. Colony 4 from the same plate that initially had a correct mutant band later proved to not be *P. fluorescens* at all when testing with pAlgD- primers, as shown in Figure 38.

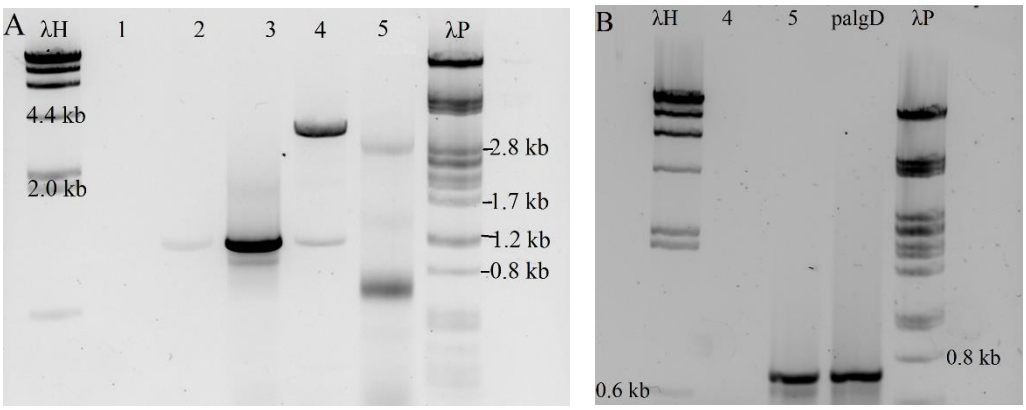

Figure 38: Testing of SBW25mucAHE230pAlgD-CSG8 mutants with PslWT primers and pAlgD primers. *A) Testing of five tetracycline-sensitive colonies using PslWT primer pairs, yielding sample number 4 with the correct mutant band of 4.1 kb, and a weird-looking colony number 5 with a strong band of around 0.7 kb and 2.8 kb. B) samples 4 and 5 were tested using pAlgD primer pairs along with the AlgD- wild type, yielding bands of around 0.7 kb for all but sample 4, indicating that sample 4 is not Pseudomonas.*

Several white colonies after transfers 7-10 into fresh LB media were then plated on PIA and LA with tetracycline, before testing tetracycline-sensitive colonies with PCR and PslWT-primer pair as shown in Figure 39. The PCR showed colonies 1 and 2 with the correct mutant band of 4.6 kb, as well as several colonies with the wild-type band of 1.2 kb. Later testing of the mutant with pAlgD$^-$ primer pair gave back the expected 0.7 kb mutant band (not shown). The mutant strain number 1 was denoted SBW25*mucA*HE230pAlgD$^-$-CSG8 and stored at -80°C.

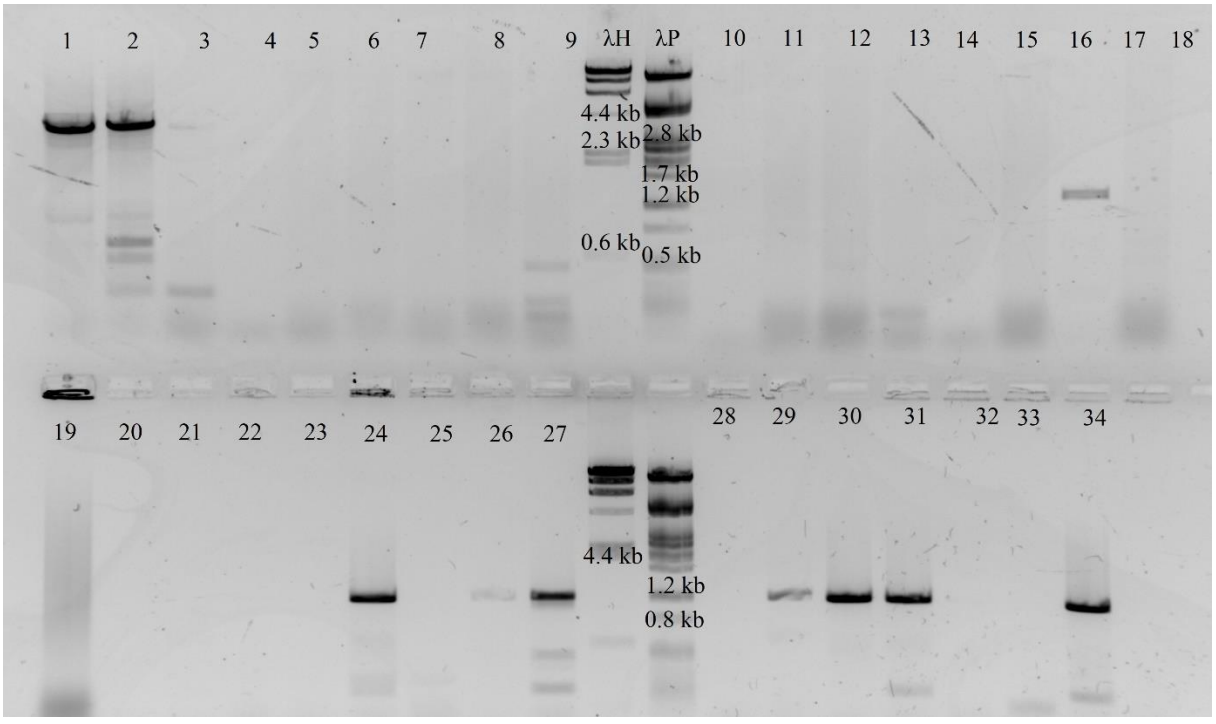

Figure 39: Verification of SBW25mucAHE230pAlgD-CSG8 mutants with PslWT primers. *The tested colonies with tetracycline sensitivity using PCR and the PslWT primer paid yielded the correct mutant band of around 4.6 kb for samples 1 and 2.*

To compare the phenotypic traits for colonies showing tetracycline sensitivity and mutants with the whole plasmid still integrated into the chromosome with the Tet^r gene, colonies were replica

plated out on PIA and LA with tetracycline. Figure 40 shows some promising mutant colonies, with what later proved to be the correct mutant circled in blue. The shape of these mutants was oval-like, and the diameter was quite small. The colony marked in red gave back the wild-type band, and both shape and size are similar to the correct mutant. The mutants marked with purple on the left are tetracycline-resistant and have a slightly larger diameter than the tetracycline-sensitive colonies that gave off either mutant or wild-type bands during PCR.

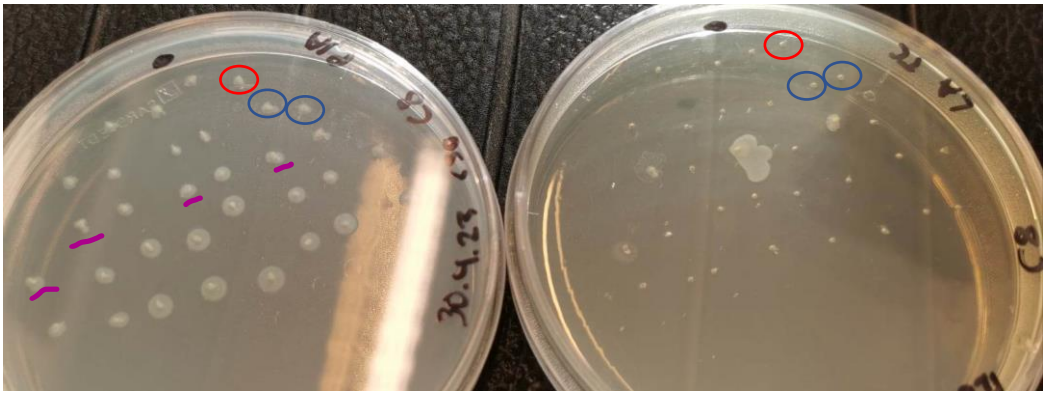

Figure 40: ***Mutant colonies of SBW25mucApAlgD⁻-CSG8 replica plated over on PIA and LA with tetracycline****. As seen for the last row on both plates, the tetracycline-sensitive colonies tend to be bigger and rounder than the tetracycline-resistant colonies.*

4.7 Construction of SBW25*mucA*HE230 derivative with PmG5-promoter controlling the Psl operon (AC⁺P⁺)

SBW*mucA*HE230 is a derivative of the SBW25*mucA* strain, having the PmG5 promoter and the XylS regulator in front of AlgC. This allows for control of the expression of AlgC by adding m-toluate, which will activate the PmG5 promoter through binding to the activator XylS. XylS works in trans and can therefore induce PmG5 promoters laying further away as well so that only one copy of XylS is needed in the chromosome. By inserting the pCSG2 plasmid into this bacterium, another PmG5 promoter will be inserted into the host chromosome, this time controlling the Psl operon. As there is already a XylS regulator integrated into the chromosome, pCSG2 is lacking XylS to avoid a too high production of it. Since pCSG2 proved to be very difficult to insert into the chromosome of other SBW25 strains, and we already had pCSG8 made, this new plasmid with the apramycin gene was to be inserted into SBW25*mucA*HE230.

4.7.1 Transferring pCSG8 into SBW25*mucA*HE230

pCSG8 contains the terminator rrnBT1T2, the promoter PmG5, and Apr, flanked by a putative segment and PslA as previously shown in Figure 31. The plasmid was to be integrated into SBW25*mucA*HE230 by homologous recombination.

The SBW25*mucA*HE230 strain was tested using the HE230 primer pair, yielding a 0.8 kb band for the HE230 mutant, and no bands for the SBW25*mucA* wild-type. As seen in Figure 41, the HE230 strain yielded the correct mutant band.

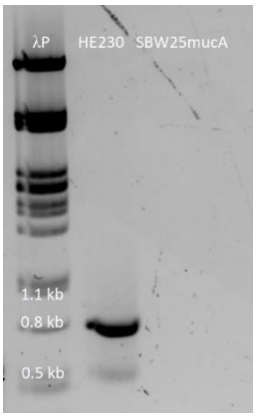

Figure 41: Verification of SBW25mucAHE230 strain, denoted HE230, using the HE230 primer pair. *The primer pair gave 0.8 kb for the correct mutant, and no band for the wild-type SBW25mucA.*

Before inoculating blue colonies in LB after conjugation, eight colonies were tested using the CSG2blåA primer pair to see what the rarest integration type would be, as for SBW25*mucA*-pCSG8 in section 4.4.2. CSG2blåA would yield 2.6 kb for integration type A, and no bands for integration type B. The results are shown in Figure 42A, showing samples 1, 2, and 3 having the expected bands for integration type A, while the remaining samples have an unexpected band of around 1.2 kb. However, samples 1, 2, and 4 seemed to be the rarest, and these were therefore inoculated in LB with apramycin.

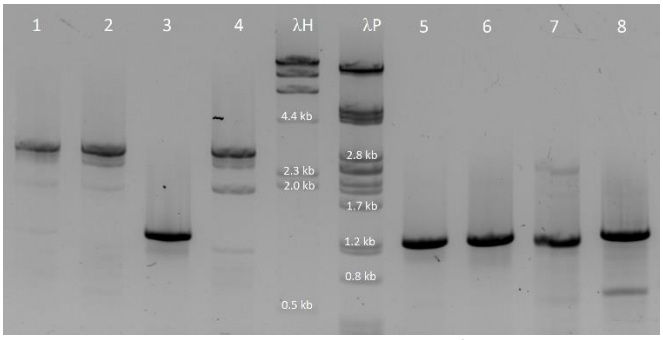

Figure 42: Testing blue colonies with CSG2blåA primer pair to determine the orientation of the pCSG8 plasmid. *Eight blue colonies from the initial recombination event were tested with CSG2blåA giving three samples with integration type A and a 2.6 kb band. All remaining samples had an unexpected 1.2 kb band.*

After transfer number seven of the colony into new LB media, when most colonies had turned white, mutants were plated out on LA with and without Tet, and tetracycline-sensitive colonies were tested with PCR using PslWT primer pair. As seen in Figure 43, none of the colonies had the desired mutant band of 3.6 kb, but several colonies had an unknown band of around 2.2 kb.

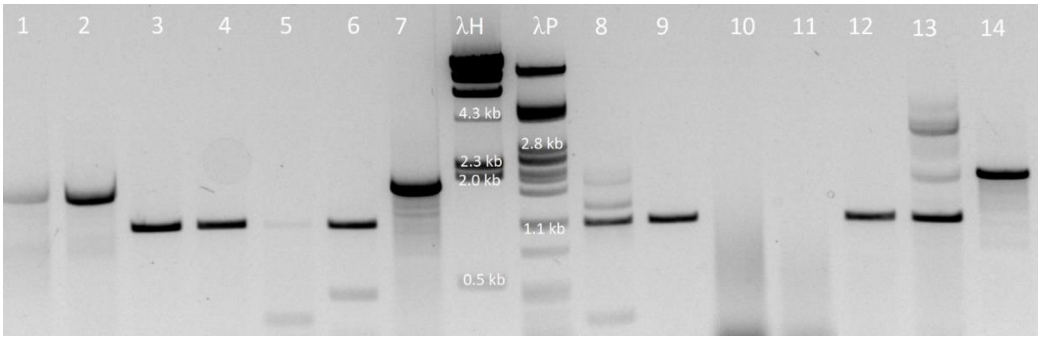

Figure 43: Separation of PCR products of SBW25mucAHE230-CSG8 mutant using PslWT primers*. No mutants have the desired band of 3.6 kb, but several samples have an unknown 2.2 kb band.*

To see what these mutants were, they were sent into sequencing using the PslSjekk primer pair, that would bind within the amplified fragment with PslWT primers. The results, shown in Appendix F indicated that the sequences before and after the apramycin gene were as expected for the mutant, but since the sequence did not span through the apramycin gene, a new sample from the same colony was to be sequenced using additional primers that bound within the DNA fragment to be sequenced. Mutants 2, 8, and 14 were therefore cultivated in LB containing apramycin and their DNA sequence were amplified again using the PslSjekk primer pair and put on a gel, as seen in Figure 44. Unexpectedly, sample 2 now gave the correct mutant band of 2.9 kb, while samples 16 and 17 had a smaller band than the mutant, but larger than the 0.5 kb wild-type band, with 2.0 kb and 1.2 kb respectively. Sample 2 was therefore concluded to be correct, denoted SBW25*mucA*HE230-CSG8, and stored at -80 ℃. Testing with the HE230 primer pair (not shown) also confirmed that the mutant was Pseudomonas.

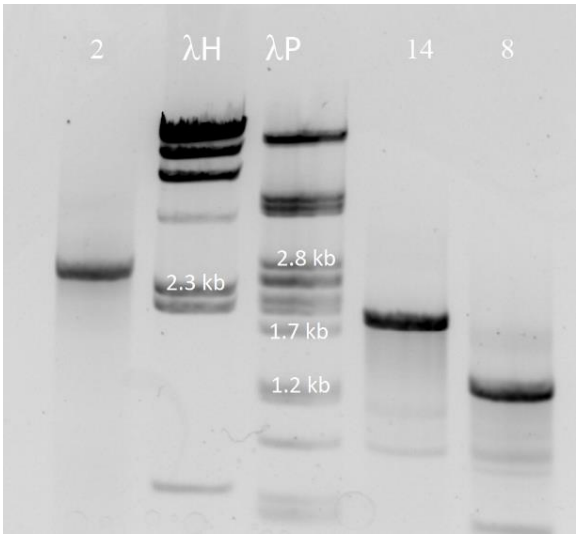

Figure 44: Verification of PCR product of SBW25mucAHE230-CSG8 mutant using the PslSjekk primer. *Sample 2 had the expected 2.9 kb mutant band using the PslSjekk primer pair, while samples 14 and 8 had neither the correct mutant band nor the wild-type band.*

4.8 Construction of SBW25*mucA*HE230-CSG8 derivative lacking genes within the Alg operon ($A^+C^+P^+$)

While AC^+P^+ is a mutant with the PmG5 promoter controlling the Psl operon as well as having a PmG5 promoter controlling the AlgC gene, it is still able to produce alginate. To be able to see the effect of AlgA when overexpressing AlgC and the Psl operon, the alginate operon was therefore deleted in the $A^+C^+P^+$ mutant, using pCSG1 to remove all alginate genes but the AlgA gene, which was put under the control of the PmG5 promoter as shown in Figure 45.

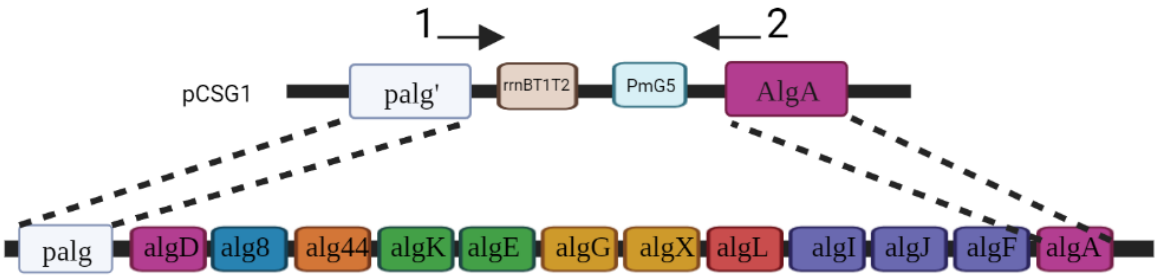

Figure 45: A schematic overview of the DNA fragment with rrnBT1T2 and PmG5 flanked by the alginate operon and the last gene in the operon, AlgA, from the pCSG1 plasmid integrated into the P. fluorescens SBW25mucAHE230-CSG8 chromosome*. The arrows denote the primer binding seats for CSG1SjekkR (1) and CSG1SjekkF (2).*

4.8.1 Transferring pCSG1 into SBW25*mucA*HE230-CSG8

The creation of pCSG1 is shown in Figure 17. pCSG1 was inserted into SBW25*mucA*HE230-CSG8 by homologous recombination, resulting in only four resulting colonies in total that had taken up the plasmid and turned blue. Three of these were further inoculated in fresh LB with m-toluate and apramycin. After being plated out on plates with m-toluate and apramycin, enough colonies became white after the sixth and seventh transfer of the culture into new LB. 50 colonies from these plates were replica plated on PIA plates with apramycin, and LA with tetracycline. From these, only a few were tetracycline resistant, meaning that they either had thrown out the whole plasmid or had become the desired mutant. 23 of the tetracycline-sensitive colonies were further tested with colony PCR using the CSG1sjekk primer pair. In addition, the pCSG1 plasmid was added as a positive control in the analysis. For the desired mutant, a band of 1.3 kb would emerge, while the colonies without the plasmid would give a 15 kb band that was not expected to show up on the gel. The result is shown in Figure 46A, where sample 14 seems to have a very weak correct mutant band. To further check this, the colony was grown in LB overnight, with the liquid culture used as a PCR substrate. As Figure 46B figure shows, this gave a clear correct mutant band of 1.3 kb, and the mutant strain was denoted SBW25mucAHE230-CSG8+1 and frozen at -80°C.

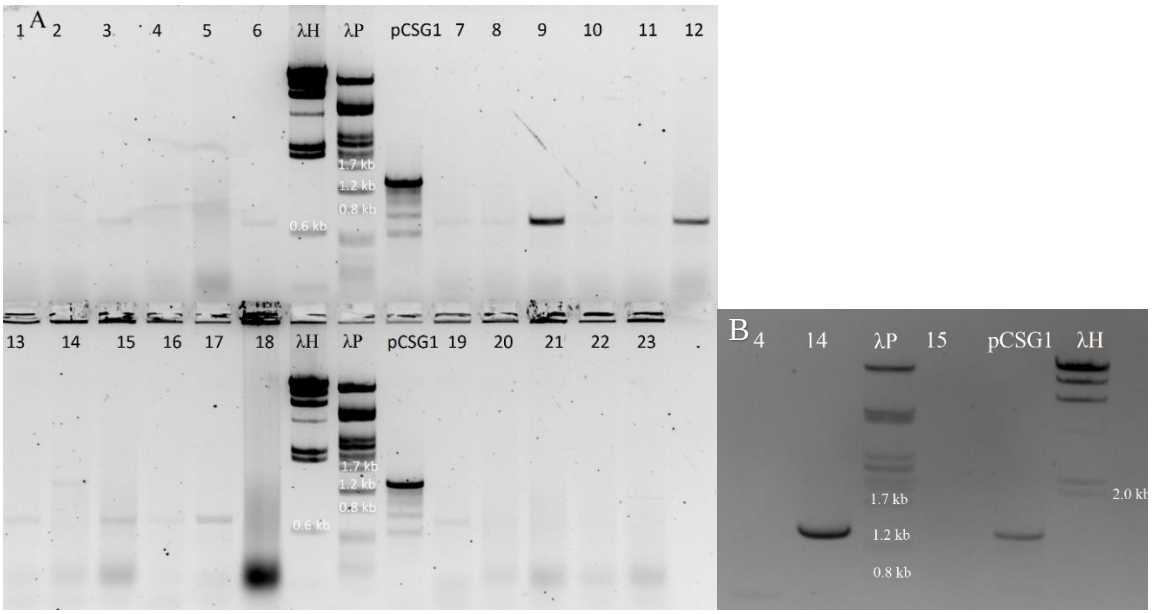

Figure 46: Verification of PCR product of SBW25mucAHE230-CSG8-1 mutant using CSG1Sjekk primers*. A) Sample 14 has a weak band with the same length as the pCSG1 plasmid, being 1.3 kb long. B) Samples 4, 14, and 15 were checked on a separate gel using double the amount of DNA.*

4.9 Construction of an SBW25*mucA* derivative lacking PslA (ACP$^-$)

The SBW25*mucA* strain was selected to be Psl negative, as this does not have the regulator XylS in its genome. In addition, both AlgA and AlgC are intact and not controlled by the PmG5 promoter, and the strain can thus be used for easy comparison with the ACP$^+$, A$^-$CP$^+$, and AC$^-$P$^+$ strains.

4.9.1 Creation of the pCSG5 and pCSG10 plasmids

Initially, the Psl-negative pCSG5 plasmid (creation not shown) was constructed using pCSG2 cut with MfeI, removing 226 base pairs of the start of PslA, as well as 981 base pairs of the 5' UTR. However, as it later proved to be too difficult to select for the correct mutant strains, a new plasmid containing the Apr gene was made. As pCSG8 was thought to replace pCSG2, both lacking the XylS fragment in front of the PmG5 promoter, this plasmid was used to remove the start of PslA in the Psl-negative strain, as shown in Figure 47. XbaI and StuI-cut pCSG8 is thus lacking the start of the PslA gene. Several studies have shown that disrupting the PslA gene will cause a deficiency in Psl production, meaning that the strain with pCSG10 should be Psl negative as well [3, 32].

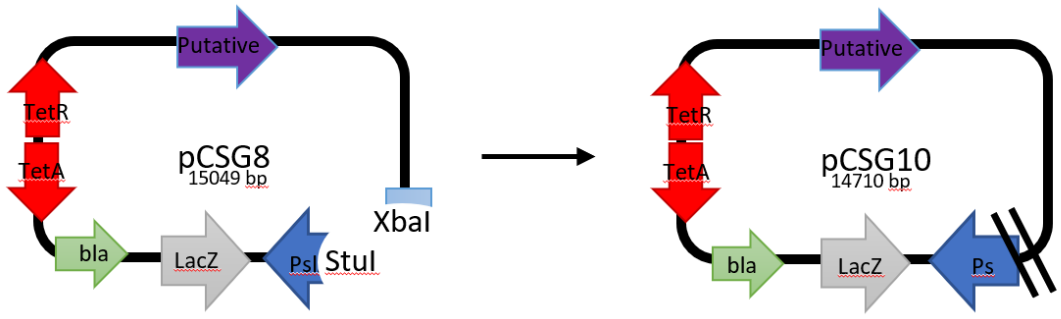

Figure 47: The creation of pCSG10. *pCSG8 was cut with XbaI and StuI to remove a fragment containing PslA and a 5'UTR region. The restriction enzymes and their sites are shown in the figure.* The black lines indicate the deletion of parts of the Psl gene cluster.

To make pCSG10, pCSG8 was cut using StuI and XbaI. The large 15kb fragment shown in Figure 48A was then cut from the gel, ligated together, and transformed into competent *E. coli* S17 cells. To test the plasmids, they were isolated and cut with NdeI, as shown in Figure 48A. As seen, pCSG8 gave three bands of 9.8, 3.5, and 1.7 kb, while sample number 2 gave the expected bands of 9.8 and 4.9 kb. Sample number 2 was then denoted pCSG10 and frozen.

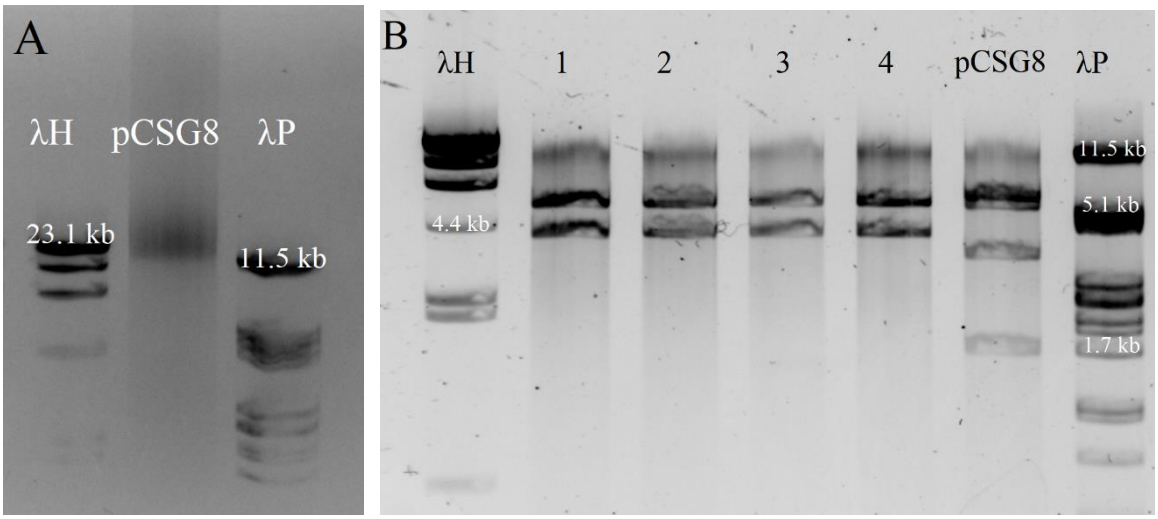

Figure 48: Digestion of pCGS8 and verification of pCSG10*. A) pCSG8 was cut using StuI and XbaI, yielding a 15kb fragment lacking the beginning of PslA. B) The ligated plasmids were checked using NdeI and as seen on the gel all samples were different from pCGS8 and had the expected bands of 9.8 kb and 4.9 kb.*

4.9.2 Transferring pCSG10 into SBW25*mucA*

As shown in Figure 49, a truncated version of PslA was to be inserted into the host chromosome, rendering the mutant unable to produce Psl.

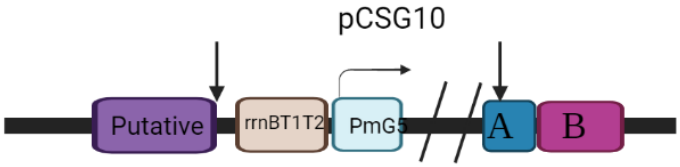

Figure 49: A schematic overview of the DNA fragment with XylS, rrnBT1T2, and PmG5 from the pCSG4 plasmid integrated into the P. fluorescens chromosome. *The arrows pointing down denotes the primer binding seats for PslSjekkR and PslSjekkF*

After inoculating three blue colonies after the initial recombinational event, they were transferred to new LB, and a sample was plated out on LA with Apr and Xgal after each new transfer. 50 colonies from the plate were replica plated on LA with Apr and on LA with Tet. Tetracycline-sensitive colonies were further tested using PCR and the PslWT-primer pair, yielding a band of 3.3 kb for the correct mutant, and 1.1 kb for the wild-type. As seen in Figure 50, samples 2-7 seem to have the correct mutant band, while sample 8 seems to have the wild-type band. As these samples were checked using colony-PCR, the first four colonies were grown in LB overnight and frozen. From the liquid cultures, a new PCR was run, using the same primer pair. From this verification, only sample number 4 gave a visible band on the gel. For further analysis of the mutants, colony number 4 was therefore used and is now denoted SBW25*mucA*-CSG10 (ACP$^-$).

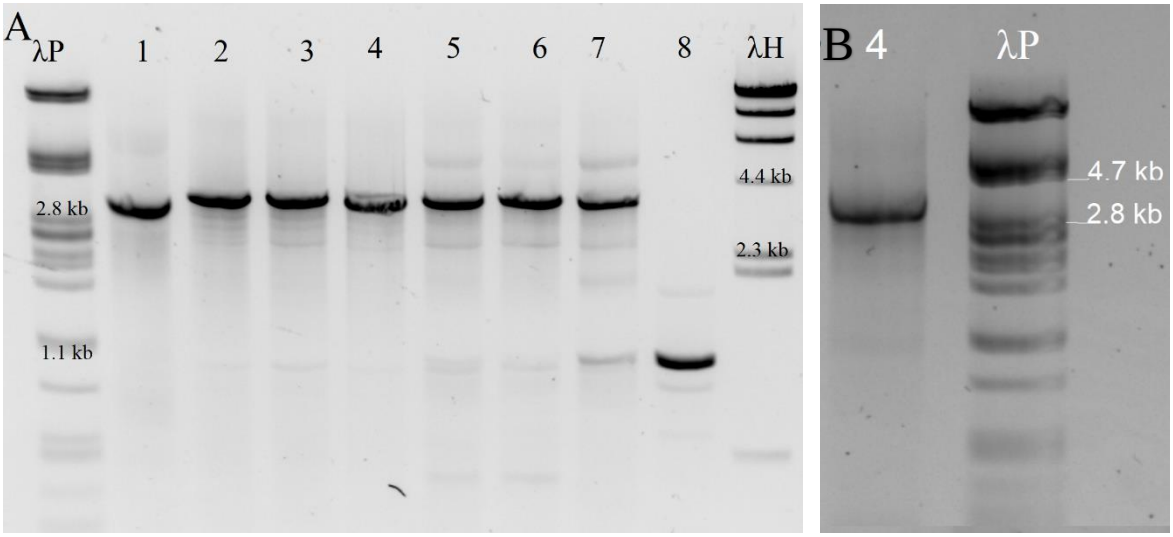

Figure 50: Verification of PCR product of SBWmucA-CSG10 mutant using PslWT primers. *A) The wild-type will give a band of 1.1, while the correct mutant band is 3.3 kb long. B) Sample 4 was checked twice, yielding the correct mutant band each time.*

4.10 Phenotype and morphology of the Psl operon overproducing strains

As Psl is an important compound of the *P. aeruginosa* biofilm and has been shown to affect the phenotype of the colonies for some *P. aeruginosa* mutant strains [34], this was also tested for *P. fluorescens* by plating mutant colonies out on LA. In addition, the motility of the Psl operon overproducing strains was tested, as well as the diameter of the colonies.

4.10.1 Phenotype of mutants grown on LA

During the attempts at reconstructing several of the mutants, dry and wrinkly colonies appeared on the plate (not shown), possibly being so-called Wrinkly Spreaders, characterised by having a distinct morphology due to the overproduction of an acetylated form of cellulose. As none of these colonies proved to have the Psl mutant PCR band when tested, they were discarded. None of the correct mutants were observed to mutate into these WS colonies.

To test the phenotype for the constructed strains, five parallels were replica plated on LA and grown for 30°C for 24 hours. The colony size is made up of both the cell mass and exopolysaccharides including alginate and Psl, and the result can be seen in Figure 51. The colonies were imaged at the approximate same distance, allowing for a direct comparison of size. Most notable is the Psl operon overproducing mutants A^-CP^+, and AC^-P^+ having larger colonies than the corresponding Psl wild-type strains, as well as the Psl-negative ACP^- strain having both smaller and more “loose” colonies.

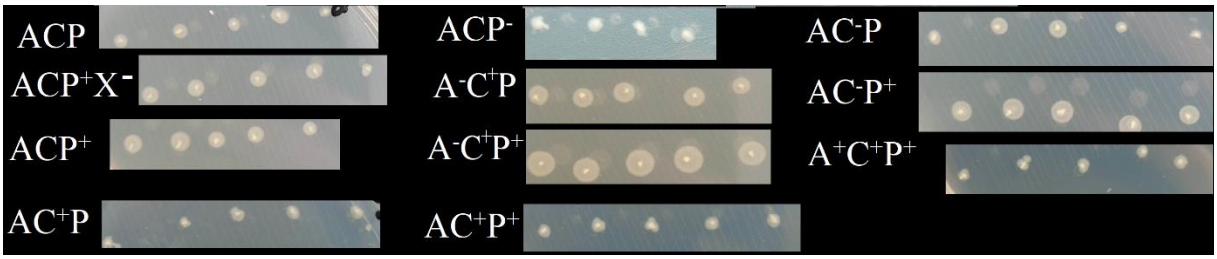

Figure 51: Phenotypic traits for the mutant strains overexpressing Psl genes and the wild-type strains. *Mutant strains grown on LA having PmG5 seems to yield larger colonies than their parental wild-type strains*

4.10.2 Growth in different temperatures yielded different phenotypes

The temperature effect on Psl production was also investigated for the Psl operon overproducing strains. For *P. syringae*, Psl production has been found to be stimulated by low temperatures [125]. To see if this was also the case for *P. fluorescens*, four parallels of ACP^-, $A^+C^+P^+$, AC^+P^+, $A^-C^+P^+$, and AC^-P^+ were thus replica plated on a LA plate with antibiotics and m-toluate. One plate was incubated at 30 ℃ for two days, while the other plate was incubated at 8 ℃ for six days, to allow for growth even in cold temperatures. The results are given in Figure 52 and show that the cold-incubated mutants (A) all have a larger volume than those incubated at 30 ℃ (B), which could also be due to the longer inoculation period. The shape of each mutant looks similar for both temperatures. However, the Psl-negative strain barely grew for the cold-incubated mutants, further indicating that Psl could be important for growth and biofilm formation in cold temperatures.

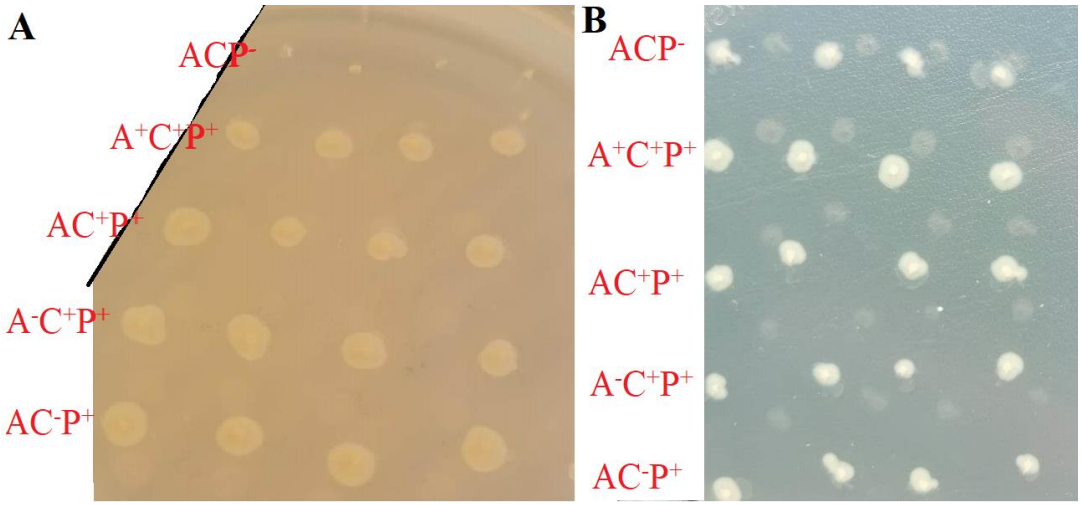

Figure 52: Growth at 8 and 30 ℃ for Psl mutants. *A) Colonies grown at 8 ℃ for six days. B) Colonies grown at 30 ℃ for two days.*

4.10.3 Motility assay

To test the motility of the Psl operon overexpressing strains, a swarming motility assay was conducted. For *P. aeruginosa*, mutations in flagellar genes leading to impaired motility seem to cause overproduction of Psl and Pel [126]. A study by Heredia-Ponce et al. [87] showed that for *P. syringae*, only Δ*pslE* mutants showed a decrease in motility. It was therefore interesting to see how Psl would affect the biofilm architecture and swarming motility in *P. fluorescens.* With different strains overexpressing Psl genes and overproducing or lacking AlgA, AlgC, or

alginate, the motility pattern could potentially be different. In the assay, the overproduction of Psl genes was investigated by seeing if the strains did wander on the plates, and if so, how the other sugar nucleotides would affect the motility.

The colonies were stab inoculated on 0.5% KB agar plates and cultivated for 48 hours at 30℃ before they were stored at 4 ℃. As cold temperatures were thought to positively affect Psl production [125], the diameter of the colonies was measured after two days of growth and again after five days in the refrigerator (shown in Figure 53). Three replicas per parallel were tested, yielding colonies with different sizes and shapes for each parallel. The average sizes of the triplicates are indicated in the figure along with the standard deviation. The colour can be a bit misleading due to light differences.

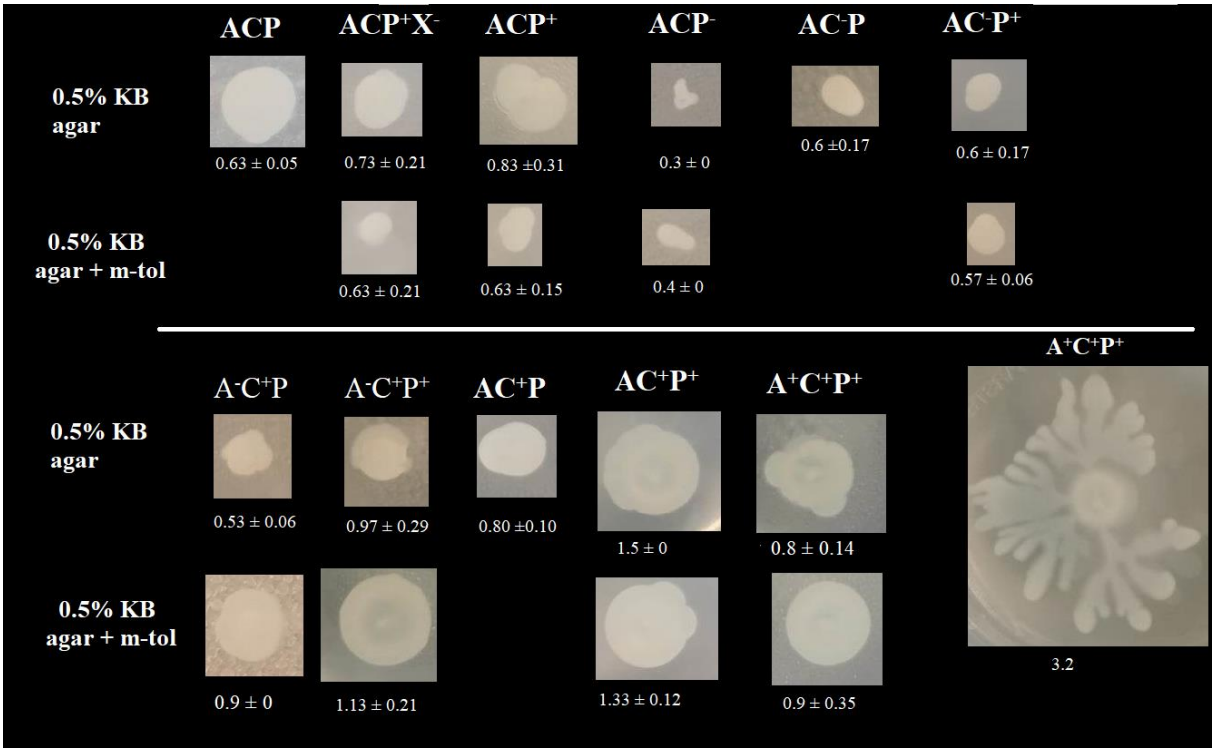

Figure 53: Colony morphology for the different strains and mutants grown on KB 0.5% agar plates with and without m-toluate. *The images show the difference in shape for the different mutants along with the average diameter (in cm) and the standard deviation. Three replicas were made for each experiment. In addition, a colony from the $A^+C^+P^+$ strain inoculated in 0.5% KB agar (lacking m-toluate) is shown, as it had an interesting swarming pattern.*

Strain ACP and $ACPX^-$ had quite a similar colony morphology, being white and round. ACP^+ had a slightly more oval-shaped form, also when being induced by m-toluate. ACP^- had a notably smaller phenotype. AC^-P and AC^-P^+ colonies looked similar both in shape and size.

A^-C^+P and $A^-C^+P^+$ had similar shapes, with the latter having a notably larger diameter. When growing A^-C^+P and $A^-C^+P^+$ in m-toluate, the colonies became rounder, and the diameter increased even more. This indicates that overexpression of AlgC causes larger colonies, even in the absence of AlgA. Strains lacking AlgA could have their phosphomannoisomerase activity substituted by the overexpressed PslB, which seems to cause large colony diameters. While AlgA/PslB/WbpW are isoenzymes coupled to the operon of the polysaccharide they are part of synthesising [3], AlgC is thought to be necessary for the biosynthesis of several

polysaccharides, possibly having a larger effect on polysaccharide biosynthesis than deletion of either AlgA or PslB.

Both AC^+P^+ and $A^+C^+P^+$ yielded large colonies. When grown in m-toluate, the colonies become rounder and whiter, and the diameter decreased. The $A^+C^+P^+$ strain had one replica showing increased motility, as shown in the figure above.

4.11 Monosaccharide analysis

The mutant strains ACP^+X^-, ACP^+, ACP^-, AC^-P^+, and $A^-C^+P^+$ had their exopolysaccharide composition analysed using HPAEC-PAD. At the point of analysis, the AC^+P^+ and $A^+C^+P^+$ mutants were not yet confirmed, which is why they were not included. The monomer composition for all tested strains and the alginate content for strains ACP^+ and ACP^+X^- were analysed simultaneously.

4.11.1 Analysis of the exopolysaccharide content in the mutant strain

To test the monosaccharide content of the exopolysaccharides produced by *P. fluorescens*, the mutants were grown in DEF3 for 24 and 48 hours, with m-toluate being added after 1.5 hours to allow for some growth before forcing the bacteria to overproduce Psl proteins. The first notable event was the excess foaming of strains ACP^+X^- and ACP^+, while ACP^- had no trace of foam for any of the time points. $A^-C^+P^+$ had no foam after 24 hours, but some foam after 48 hours. AC^-P^+ had foam for both time stamps. The exopolysaccharides were then extracted according to protocol, with the creation of a gel-like structure for mutant strains ACP^+X^- and ACP^+ when adding ethanol and $CaCl_2$, as seen in Figure 54. After removing the salt through dialysis, the samples were no longer gel-like.

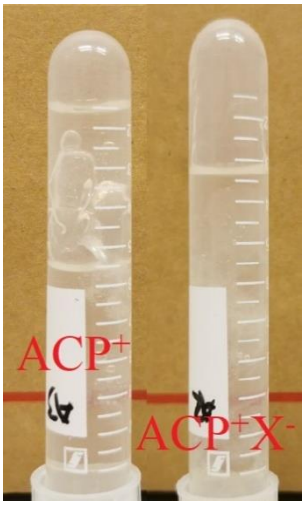

***Figure 54: Gelling during Psl extraction**. The samples ACP^+ and ACP^+X^- become very gel-like after the addition of ethanol and $CaCl_2$ to the samples.*

The samples were lyophilised and weighed prior to acid hydrolysis. Due to the low weight of samples ACP^+X^-, AC^+P^+, and AC^-P^+, the parallels were dissolved in MQ-water, combined, and re-lyophilised. The results for the two parallels of ACP^+ and ACP^- strains grown for 48 hours were therefore added together for easier comparison.

Evaluating the results by HPAEC-PAD analysis

The quantification of each sugar residue presented in Table 7, apart from fucose, is thought to be reliable. When looking at the resulting chromatograms for each mutant, however, some curves are clearly shifted, as seen in Appendix G. To test if this was due to a too high or low pH of the samples during analysis, the monosaccharide analysis was conducted twice, with a more thorough pH adjustment the second time ensuring that all samples had a pH between 4 and 7. The retention time did not differ as much between the two sets of analysis, meaning that the analysis was not sensitive to pH. It is therefore most likely the sulphate that causes the shift in the curves. Usually, the sulphate can be diluted away, however, for most of the samples, the exopolysaccharide mass and the resulting sample concentration were too small for this to work efficiently. This can be seen with the samples having the biggest dilutions being less affected than those who were diluted less, such as for ACP^+-1 vs AC^-P^+. In addition to the shifts, some samples had an unknown shoulder to the left of glucose, which could correspond to the presence of an unknown sugar.

The monomer content in the SBW25mucA mutant strains

The quantification is based on the analysis of the sugar mixture with known composition before and after the analysis of the sample, and the resulting monosaccharide composition is shown in Table 7. The percentage of the sugars in each sample is calculated based on dilution and the initial weight of the sample. In addition to the results shown in the table, samples ACP^+ and AC^-P^+ had traces of mannitol, and ACP^- 24h had traces of galactose. Most samples had some content of fucose, as shown in the table, but as the tops in the chromatogram were very much shifted for this monomer in all samples, the identity of that sugar cannot be concluded to be fucose. All samples grown for 48 hours were incubated in 2x50 mL DEF3, and while some parallels were combined prior to analysis, the content for the remaining samples were added together for easier comparison between the mutant strains.

Table 7: Monosaccharide components in each sample. Each mutant was grown for 24 hours and 48 hours. For the 48-hour mutants, two parallels for each sample were made, with the samples having a low weight being added together.

	Sample weight	Fucose[a]	Arabinose[a]	Rhamnose[a]	Glucose[a]	Xylose[a]	Mannose [a]
ACP^- 24h	0.1 mg	2.3	-	-	41.4	-	5.7
ACP^- 48h	0.2 mg		0.2	-	16.6	0.2	2.7
ACP^+ 24h	6.5 mg	0.5	0.2	0.6	1.3	0.0	0.4
ACP^+ 48h	6.1 mg	0.9	0.3	1.0	2.8	0.1	1.0
ACP^+X^- 24h	9.3 mg	0.3	0.1	0.4	0.8	-	0.4
ACP^+X^- 48h	5.6 mg	0.2	0.1	0.6	1.2	-	0.3
$A^-C^+P^+$ 24h	0.1 mg	2.4	-	-	12.0	1.0	7.4
$A^-C^+P^+$ 48h	0.6 mg	3.3	0.7	4.4	5.5	0.1	1.3
AC^-P^+ 24h	2.2 mg	0.8	0.2	0.8	46.8	0.7	0.9
AC^-P^+ 48h	0.7 mg	1.3	0.3	1.3	2.5	0.1	0.5

[a] Amounts are given as % dry weight

As seen in the table, the initial weighting of the sample showed that the isolated mass was very different for each of the mutants. The alginate-producing strains ACP^+ and ACP^+X^- had quite a lot more mass than those not producing alginate. This is most likely due to the alginate mass weight; however, it is also possible that more Psl is produced when alginate is present, increasing the weight of the sample mass.

The rhamnose content for each sample seems to correlate with the observed foaming, which could be due to the production of rhamnolipids. As seen in the table, the Psl-negative ACP^- strain contained no rhamnose. In addition, the ACP^- strain grown for 24 hours contained high amounts of what is thought to be fucose, while the mutant grown for 48 hours contained traces of arabinose and galactose. The amount of both glucose and mannose increased for the mutant grown for 48 hours.

The Psl overproducing operon ACP^+ sample contained rhamnose, glucose, and mannose, which all increased for the mutant grown for 48 hours. Traces of xylose was found in the ACP^+ sample with the highest glucose content, which also contained a higher amount of what is thought to be fucose. The traces of arabinose seemed to increase slightly when the mutant was grown for 48 hours. The XylS-negative ACP^+X^- strain was found to have slightly lower amounts of rhamnose, glucose, and mannose than ACP^+ when grown for 24 hours, with glucose and rhamnose increasing slightly after 48 hours of growth. The mutants for both time points had similar amounts of fucose and arabinose content.

The alginate-negative $A^-C^+P^+$ strain was found to produce high amounts of glucose and mannose after 24 hours, both decreasing after 48 hours. For the mutant grown for 48 hours, rhamnose was also present in high amounts, indicating that rhamnose was not produced in this mutant before at least 24 hours of growth. The AlgC-negative AC^-P^+ was found to have a large glucose content after 24 hours, along with some mannose and rhamnose present. As the mutant was grown for 48 hours, the glucose content decreased, along with a decrease in xylose and mannose content, and an increase in rhamnose and fucose content.

4.11.2 Alginate analysis

In addition to testing the monosaccharide composition, the alginate content relative to the other polysaccharide amounts present in the sample was measured for the two alginate-producing strains ACP^+ and ACP^+X^-. Both strains contained AlgA and AlgC, and with one strain overproducing Psl proteins, the other had a PmG5 promoter controlling the Psl operon but lacked the XylS activator in its genome. The alginate measurements could therefore be used as an indication of the alginate produced when the Psl operon is not induced (by the XylS-lacking strain) or when the Psl operon is overexpressed (by ACP^+).

As seen in Table 8, alginate is the polysaccharide found in the highest amounts of all exopolysaccharide monomers analysed in both samples. The F_G content is also similar in both strains, with only the ACP^+ mutant grown for 24 hours being different, having less of both uronic acids.

Table 8: Alginate composition of two alginate-producing strains grown in DEF3 for 24 and 48 hours.

Strain	% dry weight **guluronic acid**	% dry weight **mannuronic acid**	**F_G**
ACP^+ 24h	6.3	17.8	0.26
ACP^+ -1 48h	18.8	47.6	0.28
$ACPX^-$ 24h	18.6	48.4	0.28
$ACPX^-$ 48h	19.0	49.6	0.28

4.12 PMM/PMI assay

4.12.1 Optimal assay conditions

To try to see the effects of AlgA and AlgC on Psl production, a PMM/PMI assay was attempted being established for *P. fluorescens*. The total volume of the assay mixture was about seven times lower than in the original assay by Sá-Correia et al. [88]. The thought was therefore that a reduction in cell mass would give sufficient enzymes for detection. 1.5 mL cells were prepared using the B-PER method, and 100 mL cells by sonication. Results gave no detectable activity for either of the cells, causing the cell mass to be increased to 200 mL and prepared by sonication. As not all strains gave detectable differences in activity even when increasing the cell mass, higher volumes might be needed for optimal assay conditions. The activity (mU/mg protein) for the strains having activated their inducible PmG5 promoter were also significantly higher in the original assay [88], either due to increased cell mass used or the different promoter system. It is also easy to conduct mechanical errors due to the very small volumes, which should be taken into consideration when analysing the data, even when having multiple technical replicates. By looking at the initial plots of the raw data, the results also indicate that the reaction begins immediately, which could also negatively have affected the results. Sá-Correia et al. [88] also tested the growth period for the different mutants used, and found the early stationary phase to be better than during the exponential phase for capturing enzyme activity. The PMM/PMI levels for *P. aeruginosa* have in general also been noted to be low and barely detectable. Therefore, all colonies were grown for 16 hours to ensure that the enzymes were expressed in the cells before measuring protein concentrations for easy comparison.

4.12.2 PMM and PMI measurements

To ensure PMM and PMI activity was detectable, the strains were grown for 16 hours prior to harvesting. The amount of protein was measured using OD_{280} on the same day as the assay was conducted. The resulting enzymatic activities in mU/mg protein for the measured mutants are shown in Table 9. The standard derivation is the standard error for the increase in samples with substrate, calculated for all parallels included in the calculation of the enzymatic activity. Standard errors for parallels lacking substrate are given in table G1 in appendix G. U is defined as the enzyme required to reduce 1 µmol NADP per min under the specified assay conditions.

Table 9: Protein concentration for each sample and the specific activity of enzymes involved in alginate- and Psl production in different mutations of P. fluorescens SWB25mucA.

Strain	mg protein/ml	PMI*	Standard deviation (±)	PMM*	Standard deviation (±)
ACP	48.3	0.4	0.37	1.0	*0.17*
ACPX$^-$	82.2	ND[b]	*0.86*	ND[c]	*1.15*
ACP$^+$	94.9	0.6	*2.1*	0.3	*0.03*
ACP$^-$	33.7	ND[b]	*0.43*	1.5	*0[c]*
AC$^-$P	90.3	0.2	*1.29*	ND[b]	*0.11*
AC$^-$P$^+$	86.3	0.3	*0.72*	0.0	*0.06*
AC$^+$P$^+$	87.4	- [a]		0.6	*0.09*
A$^+$C$^+$P$^+$	108.7	0.5	0.46	- [a]	
A$^-$C$^+$P	70.0	0.1	*0.21*	- [a]	
A$^-$C$^+$P$^+$	198.6	0.4	*0.68*	- [a]	

* Specific activity in mU/mg protein/minute

[a] Not tested, as the combination of AlgA/AlgC/Psl expression is already covered by another mutant.

[b] Not Detected, the difference was negative, with the substrate-less cells having a higher increase in activity than the cells with substrate

[c] Only one parallel was used for the calculation, yielding no standard deviations

The calculated specific enzymatic PMI rates were not only very low for all mutants but with the high standard deviations found for all calculations, the conclusion was that the PMI activity in *P. fluorescens* SBW25*mucA* mutants were found not to be detectable.

The SBW25*mucA* (ACP) was found to have high phosphomannomutase activity, likely because of AlgC and its role in several biosynthetic pathways for production of precursor molecules in different exopolysaccharides. ACP^+X^- had no detectable activity for either PMI or PMM, but $ACPX^-$ was also very viscous after enzyme extract preparation which could have negatively affected the measurements. The PMM activity seems to decrease when the Psl operon and PslB are overexpressed, as seen by a higher PMM activity for ACP than for ACP^+. PMM results for ACP^- also strengthen this hypothesis with its high PMM activity, possibly indicating that loss of PslB could be causing a higher AlgC activity in the cells. However, the standard deviation for this mutant is zero due to the removal of several parallels due to air bubbles, which could influence the results.

Strain AC^-P had no detectable PMM activity, which was expected due to its deleted AlgC gene. AC^-P^+ had zero PMM activity as well, indicating that no PMM activity is present in the cell when the Psl operon is overexpressed either.

Overexpression of AlgC, as for AC^+P^+ gave a detectable PMM activity, however even when AlgC is overexpressed, the enzymatic activity was smaller than for ACP. A lower PMM activity could be due to the strain not being able to produce alginate, a process requiring AlgC, possibly causing less AlgC activity in the cell even when overexpressing the gene. Still, the PMM activity is bigger than for ACP^+, indicating that overexpression of AlgC and Psl proteins might cause a higher PMM activity than for overexpression of PslB alone as seen in ACP^+, as the cell would most likely need AlgC for the production of Psl precursor molecules, as in *P. aeruginosa* [3].

5 Discussion:

5.1 Creation of the mutants

A common challenge for the creation of all mutants was the high rate of conversion back to wild-type after the second cross-over event. The PCR itself had several challenges, where a proper boiling of the colonies prior to PCR proved to yield the highest rate of successful PCR samples. The high number of revertants highlighted the need for a more efficient way of finding the correct mutants. As LacZ and Tet^r could be used for positive selection, negative selection affecting the recombination cross-over events would have been more efficient but would require creating new vectors and plasmids and finding a functional and appropriate negative selection marker for *P. fluorescens*. By inserting an apramycin-resistant gene as a negative selection, the selection of mutants still having the plasmid integrated into its chromosome became easier, even if the PCR still revealed low frequencies of the correct Psl mutant band for tetracycline-sensitive colonies grown on agar containing Apr.

The high amounts of revertants could indicate that Psl is important for growth and that the cells do not want us to tamper with the Psl operon by adding a new promoter. The successful creation of the Psl-negative mutant indicates that Psl is not necessary for the cells, but by looking at both the reduced colony sizes of ACP^- when plated on agar, and by looking at the low cell density compared to other mutant strains after 16 hours of growth before the PMM/PMI assay (shown in Table G1 in Appendix G), its reduced growth indicate the importance of Psl on growth and biofilm formation. To try to force the mutants into producing Psl, m-toluate was added to the media and the agar plates. As the wild-type band came back when testing tetracycline-sensitive colonies, even when grown in apramycin, this could indicate that either the mutants acquired resistance against apramycin with the gene placed elsewhere in the chromosome, or the more probable hypothesis being that the mutant produced biofilm where the non-resistant cells were protected against the antibiotic. This is known for alginate-producing strains such as mucoid strains of *P. aeruginosa* [127]. Nonetheless, all mutants were successfully made in the end, laying the groundwork for analysing the effect of AlgA, AlgC, and alginate on Psl production.

5.2 Operon gene analysis

By analysing the genes PslABCDEFGHIJKL, results showed that they are located within the same operon and are therefore controlled by the same promoter. This allowed the use of an inducible promoter to overexpress the Psl genes and investigate the exopolysaccharide. Based on the similarities between *P. aeruginosa* and *P. fluorescens* Psl genes as shown in Table 4, it is also likely that the actual Psl polysaccharide consists of the same compounds, being D-mannose, D-glucose, and L-rhamnose [3, 32]. However, Psl is not thought to be identical in the two genera, as *P. aeruginosa* contains the non-essential PslMNO genes thought to be involved in Psl modification, which is not found in *P. fluorescens* [3].

5.3 Analysis of the exopolysaccharide components in *P. fluorescens* mutants overproducing the Psl operon

One of the main goals was to determine the composition of Psl produced by the Psl genes within the Psl operon found in *P. fluorescens*. To conduct a monosaccharide analysis, several suitable methods exist. All methods have strengths and weaknesses that must be considered when choosing the best-suited analysis method. In addition, different analytical tools have also been shown to give different results for the detection of Psl composition. While Byrd et al. [3] used both NMR and gas chromatography, Ma et al. [128] used gas-liquid chromatography. Byrd et al found no traces of galactose in the Psl compound, while Ma et al found galactose to be present in considerable amounts. In addition to the different methods used for the analysis, different environments, growth media, pH, and temperature could also be the source of these differences.

HPAEC-PAD as the chosen method for monosaccharide analysis

The chosen method based on HPAEC-PAD was a relatively easy, fast, and suitable method, requiring little sample preparation. The detector was quite specific, meaning that debris such as cell proteins did not have to be removed before the analysis, avoiding unnecessary losses. In addition, analysis of the uronic acid composition could be conducted simultaneously, using standards with known concentrations of mannuronic acid and guluronic acid. HPAEC-PAD was chosen over GS due to the minimal sample preparation and to avoid derivatisation steps to make the sample volatile [115]. HPAEC-PAD was also determined to be a better choice than HPLC due to having a higher capacity to separate and quantify the sugars [129]. NMR would have been suitable for finding detailed information about the structure and linkages of the compound [74], but this is not necessarily the best approach when determining the compounds making up a novel polysaccharide, as Psl produced by *P. fluorescens* has not been characterised yet.

5.3.1 Alginate production

To try to see the effect of Psl on alginate production, the alginate content of two alginate-producing strains was measured. The uronic acid analyses shown in Table 8 revealed that both ACP^+X^- and ACP^+ mutants grown for 48 hours had an F_G content of 0.28 and that the composition of the uronic acids make up over half of the total exopolysaccharide monomers in the samples. This indicates that quite a lot of the sample mass was alginate. By comparing the ACP^+X^- and ACP^+ mutants cultivated for 24 hours, we saw that the ACP^+X^- mutant produces roughly double the amount of alginate as ACP^+, which had a reduced amount of both mannuronic acid and guluronic acid. While growth for the two strains was not accurately measured, the alginate differences could be due to a slower growth of one of the mutants, or it could possibly indicate that increased Psl gene expression could cause a lower alginate production in the first 24 hours of growth, as the two polysaccharides are thought to compete for the same GDP-mannose precursor molecule [3].

In *P. aeruginosa*, AmrZ can repress Psl expression, while AmrZ deficient strains had observed increased Psl expression indicating the existence of transcriptional regulation of the Psl operon functioning as an inverse regulation of alginate and Psl [43]. It is therefore possible that increased Psl expression in *P. fluorescens* can affect AmrZ indirectly, and thereby also affect

alginate production. However, Psl and alginate are also competing for the same precursor molecule, GDP-D-mannose [11]. Increased production of one of the exopolysaccharides can therefore cause less production of the other, as fewer sugar nucleotides would be available.

It would thus have been interesting to include the SBW25*mucA* strain with wild-type Psl to properly assess the effect of Psl on alginate production, as well as to investigate the effect of the PmG5 promoter more thoroughly, as $ACP^{+}X^{-}$ is seen to have some background expression of PmG5-Psl, even if lacking XylS, as it has quite a substantial rhamnose production compared to the ACP^{-} strain as discussed more in section 5.3.2.

5.3.2 Psl is a polysaccharide most likely composed of glucose, mannose, and rhamnose

As the identity of the top laying close to the fucose top from the standard monosaccharide mixture is not certain, and as one of the Psl negative parallels contains the monomer, it is not thought to be part of the Psl polysaccharide even if it could be related to Psl. In addition, some of the samples had a shoulder left of glucose as seen for samples ACP^{+} in Appendix H, which could be an unknown sugar and part of Psl. When looking at the monomer percent in each sample, found in Table 7, it is also clear that Psl from *P. fluorescens* is highly unlikely to contain galactose, as found by Ma et al. [128] for *P. aeruginosa*, as the Psl-negative ACP^{-} is the only strain containing traces of this compound.

A high glucose content possibly corresponding to the production of a polyglucose component in P. fluorescens Psl mutant strains

Perhaps the most notable result in the analysis was the high glucose content found for some of the strains. Both strains ACP^{-} and $AC^{-}P^{+}$ produced large amounts of glucose after 24 hours of growth before the amount decreased for the mutant strains grown for 48 hours. The same trend was seen for $A^{-}C^{-}P^{+}$, even if the amount of glucose was significantly lower. The glucose could thus belong to a polyglucose component, being produced early before disappearing after a given amount of time. Interestingly, as this is seen for ACP^{-} and ACP^{+}, increased Psl operon expression could cause less production of such a compound.

P. fluorescens SBW25 genome was then investigated to see if it contained genes that were able to synthesise a storage polysaccharide that later would be converted into another molecule or disappear from the cell, possibly explaining the high glucose content. α-glucan is such a storage polysaccharide, consisting of thousands of D-glucose molecules that can be broken down into trehalose, consisting of two D-glucose residues [130]. *P. aeruginosa* is known to encode genes involved in the synthesis of trehalose, having genes involved in two of three different synthesis pathways known in bacteria, being the ability to degrade α-glycan into trehalose by *glgA, treZ, malQ, treY,* and *glgX,* and convert maltose into trehalose by *glgE, treS/pep2, glgB,* and *glgP* [130]. By searching for homologous genes in SBW25 using Pseudomonas Genomic Database, the glycogen synthase *glgA* (PFLU_3364) was found, in addition to a putative trehalose hydrolase (PLFU_3365, an ortholog to *treZ*), a putative glucanotransferase (PFLU_3366, ortholog to *malQ*), a maltooligosyltrehalose hydrolase (PFLU_3367, ortholog to *treY*), and a glycogen debranching enzyme (PFLU_3369, ortholog to *glgX*), likely involved in breaking down α-glycan [130]. In addition, genes for the maltose pathway were found, further indicating that *P. fluorescens* can produce trehalose. To confirm such a hypothesis, intracellular polymers could be measured, or the Psl extraction protocol could be modified to induce some cell lysis,

which the current protocol does not do. However, the mutants grown for 48 hours could have had traces of cell lysis, thus strengthening the hypothesis of a polyglucose component produced.

Such a polyglucose component could also have been cellulose. *P. fluorescens* SBW25 is known to be able to overexpress an acetylated form of cellulose, causing the wrinkly spreader phenotype [13]. No distinct wrinkly spreaders appeared for any of the mutant strains, however, the bacteria could still be producing cellulose. Cellulose is also involved in the formation of host-bacteria interactions, and the formation of pellicles in SBW25. In *P. aeruginosa*, pellicle formation is promoted by Pel, which SBW25 is lacking the genes for [2]. When Psl is upregulated, it is therefore not impossible that cellulose expression is upregulated as well to maintain biofilm integrity and function.

The rhamnose, mannose, and xylose content

When looking at the rhamnose content in the *P. fluorescens* mutant, the most notable besides the correlation between foaming and rhamnose content, was the lack of rhamnose in ACP^-. This is a clear indication that *P. fluorescens* can produce a Psl-like compound containing rhamnose, just as for *P. aeruginosa* [3]. For the rhamnose content of the other samples, it is not clear how much would belong to Psl, and how much would belong to a probable rhamnolipid production. In *P. aeruginosa*, decreased rhamnolipid production was found to be correlated with increased Psl production [46], but to conclude the same for *P. fluorescens*, the rhamnolipid content would have to be measured as well.

All strains were found to contain mannose but in higher amounts for the Psl-negative ACP^- strain. In addition, $A^-C^+P^+$ had a high content of mannose after 24 hours of growth followed by a large decrease after 48 hours. A smaller decrease was seen for the AC^-P^+ mutant. The ACP^+X^- mutant had a similar level of mannose after both 24 and 48 hours of growth. The differences between ACP^+ and ACP^- could indicate that mannose is produced as a part of Psl, and that mutants not producing Psl, such as ACP^-, have an excess amount of mannose which could be used to produce other compounds rich in mannose not seen in large degrees in Psl-producing mutants. Furthermore, the mannose content seen in the $A^-C^+P^+$ strain grown for 48 hours is similar to the ACP^+ 48 mannose content found in ACP^+ after 48 hours of growth, which could indicate that it takes longer to produce detectable amounts of Psl in strains lacking AlgA. As PslB is thought to have a similar function as AlgA [3], it would make sense that it would take time before the Psl production is high enough, as PslB would have to be created in high enough amounts to make enough precursor sugar nucleotides. Alternatively, even if the PmG5 promoter is rapidly activated when induced causing protein production, this does not mean that the cell begins synthesis of the polysaccharide immediately, as previously found for alginate [131]. Psl production in *P. fluorescens* could therefore also potentially be dependent on additional factors such as growth phase, even if all proteins are produced and assembled.

AC^-P^+ is lacking AlgC, a protein thought to be necessary to produce precursor nucleotides in Psl, and if Psl is produced by this strain it is thought to be in reduced amounts compared to strains having AlgC. Furthermore, as seen for this strain and for $A^-C^+P^+$ grown for 24 hours, the xylose content is high. This is not seen in ACP^+ and ACP^+X^-, possibly indicating that increased Psl production could correspond to low levels of xylose.

It is also interesting to look at the glucose amounts in the different strains. All samples contain glucose, where it for strains ACP^+X^-, $A^-C^-P^+$, and AC^-P^+ is high after 24 hours of growth before it decreases significantly after 48 hours. The opposite trend can be seen for ACP^-, where glucose content increases drastically after 48 hours of growth. This could also indicate that Psl production is correlated to a smaller amount of glucose, as seen for ACP^+ and $A^-C^+P^+$ after 48 hours of growth. However, to separate any possible glucose content in Psl from glucose content in other EPSs, other analytical methods such as mass spectrometry or NMR would be needed to confirm this.

Psl in *P. fluorescens* thus seems to be a polysaccharide composed of rhamnose, mannose, and possibly glucose, with traces of xylose and arabinose. For AlgC or AlgA deficient strains, the Psl production seems to be delayed, with the presence of a glucose-rich compound prior to the possible Psl production. Further work should include the use of analytical methods such as NMR to be able to separate the monomer components from the different exopolysaccharides, as well as investigate the potential delay in Psl production by taking samples at regular time intervals. By finding details about the components, Psl quantification could also be conducted by finding lectins or stains able to bind to the specific components. In addition, adding cell lysis in the samples could be conducted to further investigate the high glucose component.

5.4 Phenotypic analysis of the mutants along with a swarming motility assay

The effect of non-induced Psl on colony sizes and Psl overexpression in low temperatures.

When growing mutants on LB without m-toluate, the effect of low Psl production compared to the Psl wild-type strains can be observed. For the non-induced AC^-P^+ and A^-CP^+ mutant strains not producing alginate, the colonies were larger than for wild-type Psl strains when grown on LB, as seen in Figure 51. For ACP^+, the colony size was slightly lower than for ACP and ACP^+X^- as well. This indicates that lower Psl operon expression due to the inactivated PmG5 promoter seems to yield larger colonies when either AlgA or AlgC are overexpressed. The largest difference was seen for AC^-P^+ and A^-CP^+, indicating that lack of either AlgA or AlgC combined with little to no Psl expression causes the largest colonies, possibly due to an imbalance in exopolysaccharide production not seen for the other mutant strains.

Furthermore, Psl seems to be important for growth in cold temperatures, as seen for the small sizes of the ACP^- mutants in Figure 52. Krishna et al. [125] found an upregulation of Psl genes and reduced levels of alginate genes when incubated at 8 °C, indicating that cold suppressed alginate while promoting Psl production along with α-glucan and cellulose for *P. syringae*. As the $A^-C^+P^+$, AC^+P^+, and $A^+C^+P^+$ colonies were bigger than the alginate producing AC^+P^+ for cold-incubated mutants, and the opposite was seen for mutants incubated at 30 °C, cold seems to suppress alginate production for *P. fluorescens* to some degree. However, to be certain of the Psl effect, gene expression of Psl, Wss, and Alg genes, or analysis of biofilm components could be conducted and compared to the wild-type strain.

Psl and its role on motility and colony size in soft agar for P. fluorescens Psl mutants

The swarming motility assay showed a range of different shapes and sizes for the mutant strains. Both AlgA and AlgC are involved in the synthesis of precursor molecules for biofilm, and

deleting or overexpressing their genes would therefore be expected to affect the biofilm. Psl operon overexpressing mutants were compared to Psl wild-type colonies as shown in Figure 53, and in addition to the difference in shape, the diameter of each colony was measured. As only one colony showed a substantial swarming motility, being a non-induced colony overexpressing AlgA and AlgC, this $A^+C^+P^+$ colony was excluded when the diameter size was used to determine the role of Psl on the remaining colonies. The average size diameter for each triplicate is also shown in Figure 55.

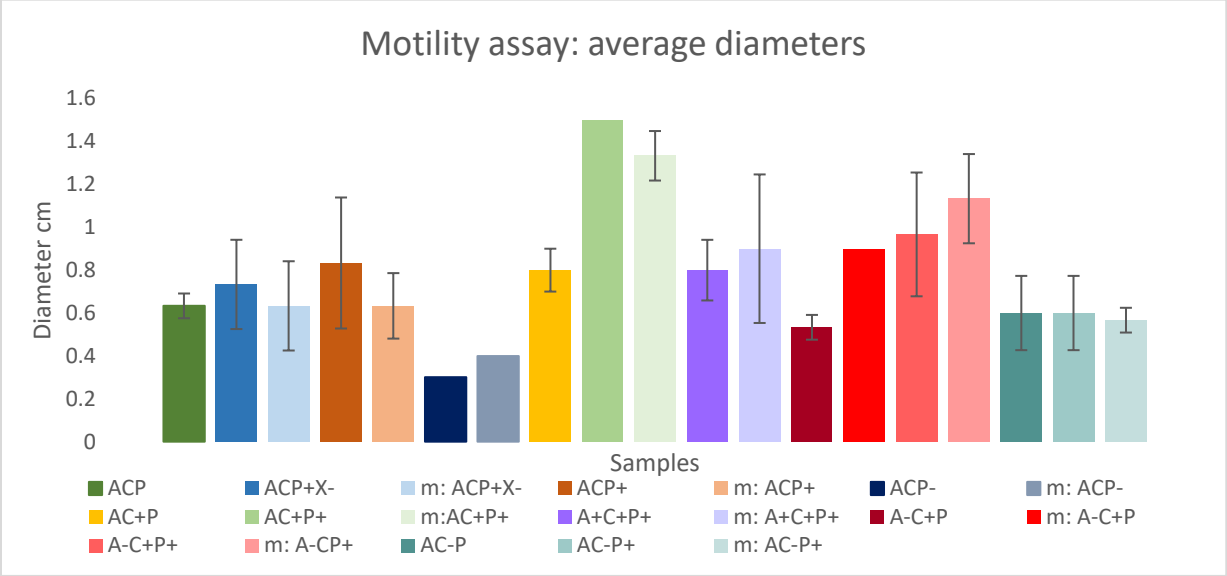

Figure 55: The average diameter of colonies stab inoculated in 0.5% KB agar. *All samples but $A^+C^+P^+$ have three replicas, with the standard deviation shown in the figure as bars. m: indicates that the mutant was stab inoculated on plates containing m-toluate.*

Increased Psl operon expression does seem to be positively correlated to an increase in motility and size diameter to some degree, as the Psl-negative ACP^- strain showed no increase in diameter after two days. It is also possible that there was a mechanical error when stab inoculating the colonies, as some motility and growth would have been expected even in the absence of Psl.

The Psl wild-type ACP strain had roughly the same colony size as the ACP^+ strain being both non-induced and induced by m-toluate, indicating that solely overexpressing the Psl operon does not cause higher motility and diameter size, but that it could be important for growth and biofilm formation as seen with the lower ACP^- diameter size. Furthermore, the induced AC^+P strain is seen to have the same diameter size as ACP, indicating that alginate production combined with increased Psl operon overexpression does not yield larger diameter sizes. In addition, overexpression of AlgA also seems to not yield large colonies, indicating that AlgA have little effect on colony diameter size.

For all mutants except $A^-C^+P^+$ and $A^+C^+P^+$, Psl operon overexpression seems to cause colonies to yield a slightly smaller diameter when Psl is non-induced, possibly indicating that Psl operon overexpression causes hindered motility and is restraining the diameter size to some degree. It could also indicate that overexpression of AlgC is necessary for increased Psl production. The role of AlgC can be further investigated by looking at the AlgC overexpressing strains. When

both AlgC and Psl are induced, the diameter size increases, as seen for AC^+P^+. This is also seen for the AlgA-negative overproducing AlgC and Psl $A^-C^+P^+$ strain, having slightly lower diameter than AC^+P^+ strains, but much higher than induced ACP and ACP^+ strains. Surprisingly, the colony diameter seems to increase drastically when the Psl operon is controlled by the PmG5 promoter as well as AlgC, even for the non-induced strains as seen for AC^+P^+ and $A^-C^+P^+$. The $A^+C^+P^+$ strain yielded similar colony size to ACP and ACP^+, both when uninduced and induced, indicating that when both AlgA, AlgC, and Psl are overexpressed, motility and diameter size are not affected. This could indicate that the cell needs AlgC in excess amounts to effectively produce Psl, and that AlgC might function as a limiting enzyme in Psl production in *P. fluorescens*, as AlgC is already needed in the production of several exopolysaccharides [3]. To further test this hypothesis, the $A^+C^+P^+$ and AC^+P^+ exopolysaccharide content should be analysed and compared with ACP^+.

Psl has been seen to decrease swarming motility for *P. aeruginosa* [67], and to increase motility for *P. syringae* [87]. In *P. fluorescens*, overexpressing the Psl operon thus seems to have similar effects as Psl production in *P. aeruginosa*, probably playing a role in attachment of the biofilm to the substrate and limiting motility. The one mutant strain showing increased motility, seen in Figure 53, could either have received a mutation causing the swarming phenotype, or due to less Psl being expressed causing the mutant to start wandering on the plate. Furthermore, the colony sizes indicate that overexpressing Psl alone have little effect on the diameter size, also when alginate is present. AlgA seems to have little or no effect on diameter size, which increases when AlgC is overexpressed. In addition, the diameter is big when both AlgC and the Psl proteins are overexpressed, possibly indicating that AlgC might be a limiting step in Psl production.

5.5 PMM and PMI activity

The PMM/PMI assay were conducted with the aims of establishing it for *P. fluorescens*, and then assess the enzymatic activity to try to assess the role of the enzymes thought to be involved in Psl biosynthesis.

PMM

The results were a bit unexpected for some of the tested mutants. The PMM activity is thought to be necessary for the production of precursor sugar nucleotides needed in alginate and Psl. The ACP^+ strain contains a PmG5 promoter in front of the Psl operon and were shown to have lower PMM activity than the Psl wild-type ACP strain. This could indicate that increased Psl expression causes lower PMM activity, possibly by reducing synthesis of other polysaccharides such as alginate. This hypothesis is further supported by the high PMM activity by ACP^-, indicating that loss of PslB increases the PMM activity.

Strain AC^-P and AC^-P^+ are lacking AlgC, and as expected, the PMM activity was found to be zero for both mutants. By overexpressing AlgC and Psl and containing wild-type AlgA, strain AC^+P^+ was found to have a PMM activity of 0.6 mU/mg protein. As AC^+P^+ is able to produce alginate, PMM activity was expected, but thought to be higher when forced to overproduce Psl as well. In comparison, both ACP and ACP^- had higher PMM activities, possibly indicating

that PMM activity could be affected negatively by Psl overproduction. This hypothesis is further strengthened by the low PMM activity seen for the Psl overproducing mutant ACP^{+}.

PMI

Not only were all calculated PMI activities very low, but the standard deviations were also high, rendering all measurements unreliable. While Sá-Correia et al. [88] also found reduced PMI activities for *P. aeruginosa* when non-induced, their enzymatic results yielded much higher activity when induced using a different promoter system. To change promoter could therefore be an option, however, optimalisation of the assay for *P. fluorescens* should be done prior to testing new promoters. In addition, the phenotypic analysis did also show that the PmG5 promoter is functional, as activation changed the colony diameters for several of the strains. It would thus be more reasonable to try to concentrate the enzymes through ultrafiltration [132], or by testing other parameters such as pH, temperature, and salt concentrations to optimise the assay as the first step. In addition, more accurate measurements of the protein content in each sample could be conducted instead of NanoDrop, such as trypsinization and mass spectrometry.

For both measurements of enzymatic activities, the low number of biological and technical replicates makes the results unreliable. The numbers were found by finding the linear increase for each parallel, which could range from almost zero to seven for some replicas. The resulting specific enzymes could therefore be used to find the tendencies in the mutant, but for both assays, further optimalisation would thus be preferred. This could be done by expressing the PMM and PMI proteins in *E. coli* using a HisTag for purification, and find the optimal the optimal temperature, pH, salt concentration, and other variable parameters for the proteins. This would be beneficial, especially for the PMI assay, which is essentially testing the activity of three genes located in three different operons simultaneously, being AlgA, PslB, and WbpW. By deleting one or several of the genes, the synthesis of the remaining PMI enzymes could be increased. As we do not know if all three enzymes have the same requirements for environmental parameters, it is hard to draw any solid conclusions from the observed measurements of the PMI activities.

6 Conclusion

In this study, analysis found that the genes within the Psl gene-cluster in *P. fluorescens* is part of the same operon, allowing for control of gene expression by inserting an inducible promoter. Analysis of the translated proteins also showed high similarity (73-81%) with orthologous genes in *P. aeruginosa*. Therefore, Psl synthesis is also likely to be similar in *P. fluorescens* and *P. aeruginosa.*

The following exopolysaccharide analysis of *P. fluorescens* mutant strains revealed the possible content of a Psl polysaccharide being rhamnose, mannose, and glucose. Furthermore, analysis indicated that Psl production might be delayed in mutants lacking either AlgA or AlgC. To investigate this further, and to separate monomer content in Psl from the monomer content in other EPSs, the exopolysaccharide fraction should be analysed using methods such as NMR or mass spectrometry.

When testing motility and phenotypes, increased Psl genes expression was shown to affect phenotypical traits, yielding more round-shaped colonies when overexpressed, and bigger colonies when non-induced. The diameter size was further affected by overexpression of both AlgA, AlgC and the Psl operon, indicating that similar expression levels of AlgC and Psl creates colonies with large diameters, together with lower AlgA expression.

Lastly, there was an attempt to measure the PMM and PMI activities for the mutant strains to determine the role of AlgA and AlgC in Psl production. While PMM activities indicated that overexpression of PslB might cause reduced PMM activity, both enzymatic assays should be optimised further to draw any conclusions of the effect of AlgA and AlgC enzymatic activity on Psl expression.

Bibliography

1. Silverio, M.P., G.B. Kraychete, A.S. Rosado, and R.R. Bonelli, *Pseudomonas fluorescens Complex and Its Intrinsic, Adaptive, and Acquired Antimicrobial Resistance Mechanisms in Pristine and Human-Impacted Sites.* Antibiotics (Basel), 2022. **11**(8).
2. Heredia-Ponce, Z., A. de Vicente, F.M. Cazorla, and J.A. Gutiérrez-Barranquero, *Beyond the Wall: Exopolysaccharides in the Biofilm Lifestyle of Pathogenic and Beneficial Plant-Associated Pseudomonas.* Microorganisms, 2021. **9**(2).
3. Byrd, M.S., I. Sadovskaya, E. Vinogradov, H. Lu, A.B. Sprinkle, et al., *Genetic and biochemical analyses of the Pseudomonas aeruginosa Psl exopolysaccharide reveal overlapping roles for polysaccharide synthesis enzymes in Psl and LPS production.* Mol Microbiol, 2009. **73**(4): p. 622-38.
4. Scales, B.S., R.P. Dickson, J.J. LiPuma, and G.B. Huffnagle, *Microbiology, genomics, and clinical significance of the Pseudomonas fluorescens species complex, an unappreciated colonizer of humans.* Clin Microbiol Rev, 2014. **27**(4): p. 927-48.
5. Timm, C.M., A.G. Campbell, S.M. Utturkar, S.R. Jun, R.E. Parales, et al., *Metabolic functions of Pseudomonas fluorescens strains from Populus deltoides depend on rhizosphere or endosphere isolation compartment.* Front Microbiol, 2015. **6**: p. 1118.
6. Garrido-Sanz, D., J.P. Meier-Kolthoff, M. Göker, M. Martín, R. Rivilla, et al., *Correction: Genomic and Genetic Diversity within the Pseudomonas fluorescens Complex.* PLoS One, 2016. **11**(4): p. e0153733.
7. Garrido-Sanz, D., J.P. Meier-Kolthoff, M. Göker, M. Martín, R. Rivilla, et al., *Genomic and Genetic Diversity within the Pseudomonas fluorescens Complex.* PLoS One, 2016. **11**(2): p. e0150183.
8. Meyer, J.M. and M.A. Abdallah, *The Fluorescent Pigment of Pseudomonas fluorescens: Biosynthesis, Purification and Physicochemical Properties.* Microbiology, 1978. **107**(2): p. 319-328.
9. Yoder, M.F. and W.S. Kisaalita, *Iron specificity of a biosensor based on fluorescent pyoverdin immobilized in sol-gel glass.* Journal of Biological Engineering, 2011. **5**(1): p. 4.
10. Borgos, S.E.F., S. Bordel, H. Sletta, H. Ertesvåg, Ø. Jakobsen, et al., *Mapping global effects of the anti-sigma factor MucA in Pseudomonas fluorescens SBW25 through genome-scale metabolic modeling.* BMC Systems Biology, 2013. **7**(1): p. 19.
11. Franklin, M.J., D.E. Nivens, J.T. Weadge, and P.L. Howell, *Biosynthesis of the Pseudomonas aeruginosa Extracellular Polysaccharides, Alginate, Pel, and Psl.* Front Microbiol, 2011. **2**: p. 167.
12. Spiers, A.J., J. Bohannon, S.M. Gehrig, and P.B. Rainey, *Biofilm formation at the air-liquid interface by the Pseudomonas fluorescens SBW25 wrinkly spreader requires an acetylated form of cellulose.* Mol Microbiol, 2003. **50**(1): p. 15-27.
13. Spiers, A.J. and P.B. Rainey, *The Pseudomonas fluorescens SBW25 wrinkly spreader biofilm requires attachment factor, cellulose fibre and LPS interactions to maintain strength and integrity.* Microbiology (Reading), 2005. **151**(Pt 9): p. 2829-2839.
14. Mann, E.E. and D.J. Wozniak, *Pseudomonas biofilm matrix composition and niche biology.* FEMS Microbiol Rev, 2012. **36**(4): p. 893-916.
15. Bonnichsen, L., N. Bygvraa Svenningsen, M. Rybtke, I. de Bruijn, J.M. Raaijmakers, et al., *Lipopeptide biosurfactant viscosin enhances dispersal of Pseudomonas fluorescens SBW25 biofilms.* Microbiology, 2015. **161**(12): p. 2289-2297.

16. Passos da Silva, D., M.L. Matwichuk, D.O. Townsend, C. Reichhardt, D. Lamba, et al., *The Pseudomonas aeruginosa lectin LecB binds to the exopolysaccharide Psl and stabilizes the biofilm matrix.* Nature Communications, 2019. **10**(1): p. 2183.
17. Maleki, S., M. Mærk, R. Hrudikova, S. Valla, and H. Ertesvåg, *New insights into Pseudomonas fluorescens alginate biosynthesis relevant for the establishment of an efficient production process for microbial alginates.* N Biotechnol, 2017. **37**(Pt A): p. 2-8.
18. Silby, M.W., A.M. Cerdeño-Tárraga, G.S. Vernikos, S.R. Giddens, R.W. Jackson, et al., *Genomic and genetic analyses of diversity and plant interactions of Pseudomonas fluorescens.* Genome Biology, 2009. **10**(5): p. R51.
19. Michael T. Madigan, K.S.B., Daniel H. Buckley, W. Matthew Sattley, David A. Stahl, *Brock Biology of Microorganisms, Global Edition*. 2018: Pearson Educated Limited.
20. Sauer, K., P. Stoodley, D.M. Goeres, L. Hall-Stoodley, M. Burmølle, et al., *The biofilm life cycle: expanding the conceptual model of biofilm formation.* Nature Reviews Microbiology, 2022. **20**(10): p. 608-620.
21. Wu, H., D. Wang, M. Tang, and L.Z. Ma, *The advance of assembly of exopolysaccharide Psl biosynthesis machinery in Pseudomonas aeruginosa.* MicrobiologyOpen, 2019. **8**(10): p. e857.
22. Ma, L., K.D. Jackson, R.M. Landry, M.R. Parsek, and D.J. Wozniak, *Analysis of Pseudomonas aeruginosa conditional psl variants reveals roles for the psl polysaccharide in adhesion and maintaining biofilm structure postattachment.* J Bacteriol, 2006. **188**(23): p. 8213-21.
23. Coenye, T., *Biofilms*, in *Brenner's Encyclopedia of Genetics (Second Edition)*, S. Maloy and K. Hughes, Editors. 2013, Academic Press: San Diego. p. 335-337.
24. Friedman, L. and R. Kolter, *Two genetic loci produce distinct carbohydrate-rich structural components of the Pseudomonas aeruginosa biofilm matrix.* J Bacteriol, 2004. **186**(14): p. 4457-65.
25. Koza, A., P.D. Hallett, C.D. Moon, and A.J. Spiers, *Characterization of a novel air-liquid interface biofilm of Pseudomonas fluorescens SBW25.* Microbiology (Reading), 2009. **155**(Pt 5): p. 1397-1406.
26. Andrew, J.S., Y.D. Yusuf, O.F. Ayorinde, K. Anna, M. Olena, et al., *Cellulose Expression in Pseudomonas fluorescens SBW25 and Other Environmental Pseudomonads*, in *Cellulose*, V. Theo van de and G. Louis, Editors. 2013, IntechOpen: Rijeka. p. Ch. 1.
27. Schmid, J., *Recent insights in microbial exopolysaccharide biosynthesis and engineering strategies.* Current Opinion in Biotechnology, 2018. **53**: p. 130-136.
28. Abidi, W., L. Torres-Sánchez, A. Siroy, and P.V. Krasteva, *Weaving of bacterial cellulose by the Bcs secretion systems.* FEMS Microbiology Reviews, 2021. **46**(2).
29. Islam, S.T. and J.S. Lam, *Synthesis of bacterial polysaccharides via the Wzx/Wzy-dependent pathway.* Canadian Journal of Microbiology, 2014. **60**(11): p. 697-716.
30. Whitfield, C., *Biosynthesis and Assembly of Capsular Polysaccharides in Escherichia coli.* Annual Review of Biochemistry, 2006. **75**(1): p. 39-68.
31. Rocchetta, H.L., J.C. Pacan, and J.S. Lam, *Synthesis of the A-band polysaccharide sugar D-rhamnose requires Rmd and WbpW: identification of multiple AlgA homologues, WbpW and ORF488, in Pseudomonas aeruginosa.* Molecular Microbiology, 1998. **29**(6): p. 1419-1434.
32. Jackson, K.D., M. Starkey, S. Kremer, M.R. Parsek, and D.J. Wozniak, *Identification of psl, a locus encoding a potential exopolysaccharide that is essential for Pseudomonas aeruginosa PAO1 biofilm formation.* J Bacteriol, 2004. **186**(14): p. 4466-75.

33. Matsukawa, M. and E.P. Greenberg, *Putative exopolysaccharide synthesis genes influence Pseudomonas aeruginosa biofilm development.* J Bacteriol, 2004. **186**(14): p. 4449-56.
34. Colvin, K.M., Y. Irie, C.S. Tart, R. Urbano, J.C. Whitney, et al., *The Pel and Psl polysaccharides provide Pseudomonas aeruginosa structural redundancy within the biofilm matrix.* Environ Microbiol, 2012. **14**(8): p. 1913-28.
35. Billings, N., M. Ramirez Millan, M. Caldara, R. Rusconi, Y. Tarasova, et al., *The Extracellular Matrix Component Psl Provides Fast-Acting Antibiotic Defense in Pseudomonas aeruginosa Biofilms.* PLOS Pathogens, 2013. **9**(8): p. e1003526.
36. Irie, Y., A.E.L. Roberts, K.N. Kragh, V.D. Gordon, J. Hutchison, et al., *The Pseudomonas aeruginosa PSL Polysaccharide Is a Social but Noncheatable Trait in Biofilms.* mBio, 2017. **8**(3): p. e00374-17.
37. Hay, I.D., Z. Ur Rehman, M.F. Moradali, Y. Wang, and B.H. Rehm, *Microbial alginate production, modification and its applications.* Microb Biotechnol, 2013. **6**(6): p. 637-50.
38. Overhage, J., M. Schemionek, J.S. Webb, and B.H. Rehm, *Expression of the psl operon in Pseudomonas aeruginosa PAO1 biofilms: PslA performs an essential function in biofilm formation.* Appl Environ Microbiol, 2005. **71**(8): p. 4407-13.
39. Baker, P., G.B. Whitfield, P.J. Hill, D.J. Little, M.J. Pestrak, et al., *Characterization of the Pseudomonas aeruginosa Glycoside Hydrolase PslG Reveals That Its Levels Are Critical for Psl Polysaccharide Biosynthesis and Biofilm Formation.* J Biol Chem, 2015. **290**(47): p. 28374-28387.
40. Campisano, A., C. Schroeder, M. Schemionek, J. Overhage, and B.H. Rehm, *PslD is a secreted protein required for biofilm formation by Pseudomonas aeruginosa.* Appl Environ Microbiol, 2006. **72**(4): p. 3066-8.
41. Irie, Y., M. Starkey, A.N. Edwards, D.J. Wozniak, T. Romeo, et al., *Pseudomonas aeruginosa biofilm matrix polysaccharide Psl is regulated transcriptionally by RpoS and post-transcriptionally by RsmA.* Mol Microbiol, 2010. **78**(1): p. 158-72.
42. Irie, Y., B.R. Borlee, J.R. O'Connor, P.J. Hill, C.S. Harwood, et al., *Self-produced exopolysaccharide is a signal that stimulates biofilm formation in Pseudomonas aeruginosa.* Proc Natl Acad Sci U S A, 2012. **109**(50): p. 20632-6.
43. Jones, C.J., C.R. Ryder, E.E. Mann, and D.J. Wozniak, *AmrZ modulates Pseudomonas aeruginosa biofilm architecture by directly repressing transcription of the psl operon.* J Bacteriol, 2013. **195**(8): p. 1637-44.
44. Yu, S., T. Su, H. Wu, S. Liu, D. Wang, et al., *PslG, a self-produced glycosyl hydrolase, triggers biofilm disassembly by disrupting exopolysaccharide matrix.* Cell Research, 2015. **25**(12): p. 1352-1367.
45. Muriel, C., E. Arrebola, M. Redondo-Nieto, F. Martínez-Granero, B. Jalvo, et al., *AmrZ is a major determinant of c-di-GMP levels in Pseudomonas fluorescens F113.* Scientific Reports, 2018. **8**(1): p. 1979.
46. Zhang, J., H. Wu, D. Wang, L. Wang, Y. Cui, et al., *Intracellular glycosyl hydrolase PslG shapes bacterial cell fate, signaling, and the biofilm development of Pseudomonas aeruginosa.* eLife, 2022. **11**: p. e72778.
47. Hirst, E. and D.A. Rees, *The Structure of Alginic Acid. Part V.l Isolation and Unambiguous Characterization of Some Hydrolysis Products of the Methylated Polysaccharide* . J. Chem. Soc, 1965.
48. Fischl, R., K. Bertelsen, F. Gaillard, S. Coelho, G. Michel, et al., *The cell-wall active mannuronan C5-epimerases in the model brown alga Ectocarpus: From gene context to recombinant protein.* Glycobiology, 2016. **26**(9): p. 973-983.

49. Draget, K.I., O. Smidsrød, and G. Skjåk-Bræk, *Alginates from Algae*, in *Biopolymers Online*.
50. Skjåk-Bræk, G., H. Grasdalen, and B. Larsen, *Monomer sequence and acetylation pattern in some bacterial alginates.* Carbohydr Res, 1986. **154**: p. 239-50.
51. Ertesvåg, H., *Alginate-modifying enzymes: biological roles and biotechnological uses.* Front Microbiol, 2015. **6**: p. 523.
52. Abasalizadeh, F., S.V. Moghaddam, E. Alizadeh, E. akbari, E. Kashani, et al., *Alginate-based hydrogels as drug delivery vehicles in cancer treatment and their applications in wound dressing and 3D bioprinting.* Journal of Biological Engineering, 2020. **14**(1): p. 8.
53. Draget, K.I. and C. Taylor, *Chemical, physical and biological properties of alginates and their biomedical implications.* Food Hydrocolloids, 2011. **25**(2): p. 251-256.
54. Aarstad, O., B.L. Strand, L.M. Klepp-Andersen, and G. Skjåk-Bræk, *Analysis of G-Block Distributions and Their Impact on Gel Properties of in Vitro Epimerized Mannuronan.* Biomacromolecules, 2013. **14**(10): p. 3409-3416.
55. Lee, K.Y. and D.J. Mooney, *Alginate: properties and biomedical applications.* Prog Polym Sci, 2012. **37**(1): p. 106-126.
56. Chanasit, W., Z.J.C. Gonzaga, and B.H.A. Rehm, *Analysis of the alginate O-acetylation machinery in Pseudomonas aeruginosa.* Applied Microbiology and Biotechnology, 2020. **104**(5): p. 2179-2191.
57. Maleki, S., M. Mærk, S. Valla, and H. Ertesvåg, *Mutational Analyses of Glucose Dehydrogenase and Glucose-6-Phosphate Dehydrogenase Genes in Pseudomonas fluorescens Reveal Their Effects on Growth and Alginate Production.* Applied and Environmental Microbiology, 2015. **81**(10): p. 3349-3356.
58. Lien, S.K., S. Niedenführ, H. Sletta, K. Nöh, and P. Bruheim, *Fluxome study of Pseudomonas fluorescens reveals major reorganisation of carbon flux through central metabolic pathways in response to inactivation of the anti-sigma factor MucA.* BMC Systems Biology, 2015. **9**(1): p. 6.
59. Maleki, S., R. Hrudikova, S.B. Zotchev, and H. Ertesvåg, *Identification of a New Phosphatase Enzyme Potentially Involved in the Sugar Phosphate Stress Response in Pseudomonas fluorescens.* Appl Environ Microbiol, 2017. **83**(2).
60. Bakkevig, K., H. Sletta, M. Gimmestad, R. Aune, H. Ertesvåg, et al., *Role of the Pseudomonas fluorescens alginate lyase (AlgL) in clearing the periplasm of alginates not exported to the extracellular environment.* J Bacteriol, 2005. **187**(24): p. 8375-84.
61. D'Andrea, L.D. and L. Regan, *TPR proteins: the versatile helix.* Trends in Biochemical Sciences, 2003. **28**(12): p. 655-662.
62. Martin, D.W., M.J. Schurr, H. Yu, and V. Deretic, *Analysis of promoters controlled by the putative sigma factor AlgU regulating conversion to mucoidy in Pseudomonas aeruginosa: relationship to sigma E and stress response.* Journal of Bacteriology, 1994. **176**(21): p. 6688-6696.
63. King, J.D., D. Kocíncová, E.L. Westman, and J.S. Lam, *Review: Lipopolysaccharide biosynthesis in Pseudomonas aeruginosa.* Innate Immunity, 2009. **15**(5): p. 261-312.
64. Olvera, C., J.B. Goldberg, R. Sánchez, and G. Soberón-Chávez, *The Pseudomonas aeruginosa algC gene product participates in rhamnolipid biosynthesis.* FEMS Microbiology Letters, 1999. **179**(1): p. 85-90.
65. Zegans, M.E., D. Wozniak, E. Griffin, C.M. Toutain-Kidd, J.H. Hammond, et al., *Pseudomonas aeruginosa exopolysaccharide Psl promotes resistance to the biofilm inhibitor polysorbate 80.* Antimicrob Agents Chemother, 2012. **56**(8): p. 4112-22.

66. Soberón-Chávez, G., A. González-Valdez, M.P. Soto-Aceves, and M. Cocotl-Yañez, *Rhamnolipids produced by Pseudomonas: from molecular genetics to the market.* Microb Biotechnol, 2021. **14**(1): p. 136-146.
67. Wang, S., S. Yu, Z. Zhang, Q. Wei, L. Yan, et al., *Coordination of swarming motility, biosurfactant synthesis, and biofilm matrix exopolysaccharide production in Pseudomonas aeruginosa.* Appl Environ Microbiol, 2014. **80**(21): p. 6724-32.
68. Becker, M., K. Ahn, M. Bacher, C. Xu, A. Sundberg, et al., *Comparative hydrolysis analysis of cellulose samples and aspects of its application in conservation science.* Cellulose (Lond), 2021. **28**(13): p. 8719-8734.
69. Menna, A., M. Fischer-Stettler, B. Pfister, G.S. Andrés, D. Holbrook-Smith, et al. *Single-run HPLC Quantification of Plant Cell Wall Monosaccharides*. Bio-protocol, 2020. **10**, e3546 DOI: 10.21769/bioprotoc.3546.
70. Zhang, Z., N.M. Khan, K.M. Nunez, E.K. Chess, and C.M. Szabo, *Complete Monosaccharide Analysis by High-Performance Anion-Exchange Chromatography with Pulsed Amperometric Detection.* Analytical Chemistry, 2012. **84**(9): p. 4104-4110.
71. JF, C.M.a.K., *Carbohydrate analysis. A practical approach*. 1994, USA: 2nd ed. IRL Press Ltd.
72. Meyer, V.R., *Practical High Performance Liquid Chromatography*. Vol. Fifth Edition. 2010, Swiss Federal Laboratories for Materials Testing and Research (EMPA), St. Gallen, Switzerland: John Wiley and Sons, Ltd.
73. Forgács, E. and T. Cserháti, *9 - Gas chromatography*, in *Food Authenticity and Traceability*, M. Lees, Editor. 2003, Woodhead Publishing. p. 197-217.
74. Singh, M.K. and A. Singh, *Chapter 14 - Nuclear magnetic resonance spectroscopy*, in *Characterization of Polymers and Fibres*, M.K. Singh and A. Singh, Editors. 2022, Woodhead Publishing. p. 321-339.
75. Corradini, C., *CARBOHYDRATES | Liquid Chromatography*, in *Encyclopedia of Separation Science*, I.D. Wilson, Editor. 2000, Academic Press: Oxford. p. 2224-2235.
76. Rohrer, J. *Analysis of Carbohydrates by HighPerformance Anion-Exchange Chromatography with Pulsed Amperometric Detection (HPAE-PAD). Technical Note 20*. [cited 2023 13. April]; Available from: https://archemica-international.com/wp-content/uploads/2021/06/File-No.-1-11.pdf.
77. Scientific, T.F., *High-Performance Anion-Exchange Chromatography with Pulsed Amperometric Detection*. 2013.
78. Reece, R.J., *Analysis of Genes and Genomes*. Vol. 469. 2004, Chichester: John Wiley & Sons Ltd.
79. Clark, D.P., Pazdernik, N. J, McGehee, M. R.,, *Molecular biology*. 2018: Academic Cell.
80. Gawin, A., S. Valla, and T. Brautaset, *The XylS/Pm regulator/promoter system and its use in fundamental studies of bacterial gene expression, recombinant protein production and metabolic engineering.* Microb Biotechnol, 2017. **10**(4): p. 702-718.
81. Winther-Larsen, H.C., K.D. Josefsen, T. Brautaset, and S. Valla, *Parameters Affecting Gene Expression from the Pm Promoter in Gram-Negative Bacteria.* Metabolic Engineering, 2000. **2**(2): p. 79-91.
82. Marqués, S., M. Manzanera, M.M. González-Pérez, M.T. Gallegos, and J.L. Ramos, *The XylS-dependent Pm promoter is transcribed in vivo by RNA polymerase with sigma 32 or sigma 38 depending on the growth phase.* Mol Microbiol, 1999. **31**(4): p. 1105-13.

83. Gimmestad, M., H. Sletta, H. Ertesvåg, K. Bakkevig, S. Jain, et al., *The Pseudomonas fluorescens AlgG protein, but not its mannuronan C-5-epimerase activity, is needed for alginate polymer formation.* J Bacteriol, 2003. **185**(12): p. 3515-23.
84. Court, D.L., J.A. Sawitzke, and L.C. Thomason, *Genetic engineering using homologous recombination.* Annu Rev Genet, 2002. **36**: p. 361-88.
85. David L. Cox, M.N., *Lehninger Principles of Biochemistry*. 2017, United States of America: W. H. Freeman and Company.
86. Prorocic, M.M. and W.M. Stark, *Site-specific Recombination*, in *Brenner's Encyclopedia of Genetics (Second Edition)*, S. Maloy and K. Hughes, Editors. 2013, Academic Press: San Diego. p. 459-462.
87. Heredia-Ponce, Z., J.A. Gutiérrez-Barranquero, G. Purtschert-Montenegro, L. Eberl, F.M. Cazorla, et al., *Biological role of EPS from Pseudomonas syringae pv. syringae UMAF0158 extracellular matrix, focusing on a Psl-like polysaccharide.* npj Biofilms and Microbiomes, 2020. **6**(1): p. 37.
88. Sá-Correia, I., A. Darzins, S.K. Wang, A. Berry, and A.M. Chakrabarty, *Alginate biosynthetic enzymes in mucoid and nonmucoid Pseudomonas aeruginosa: overproduction of phosphomannose isomerase, phosphomannomutase, and GDP-mannose pyrophosphorylase by overexpression of the phosphomannose isomerase (pmi) gene.* Journal of Bacteriology, 1987. **169**(7): p. 3224-3231.
89. Research, Z. *ZymoPURE™ Plasmid Miniprep Kit - INSTRUCTION MANUAL Ver.2.0.3*. 2022 [cited 2023 01. May].
90. Birnboim, H.C. and J. Doly, *A rapid alkaline extraction procedure for screening recombinant plasmid DNA.* Nucleic Acids Res, 1979. **7**(6): p. 1513-23.
91. Li, X., Y. Wu, L. Zhang, Y. Cao, Y. Li, et al., *Comparison of three common DNA concentration measurement methods.* Analytical Biochemistry, 2014. **451**: p. 18-24.
92. *NanoDrop Micro-UV/Vis Spectrophotometer. NanoDrop One. User Guide*, T.F.S. Inc, Editor. 2021 Thermo Fisher Scientific Inc.
93. Roberts, R.J., *How restriction enzymes became the workhorses of molecular biology.* Proceedings of the National Academy of Sciences, 2005. **102**(17): p. 5905-5908.
94. Loenen, W.A.M., D.T.F. Dryden, E.A. Raleigh, and G.G. Wilson, *Type I restriction enzymes and their relatives.* Nucleic Acids Research, 2013. **42**(1): p. 20-44.
95. Lee, P.Y., J. Costumbrado, C.Y. Hsu, and Y.H. Kim, *Agarose gel electrophoresis for the separation of DNA fragments.* J Vis Exp, 2012(62).
96. Stephenson, F.H., *Chapter 5 - Nucleic acid quantification*, in *Calculations for Molecular Biology and Biotechnology (Second Edition)*, F.H. Stephenson, Editor. 2010, Academic Press: Boston. p. 99-122.
97. Monarch®, N.A. Purification, and T. GUIDE. *Monarch® Nucleic Acid Purification. TECHNICAL GUIDE*. 2020 [cited 2023 10. May]; Available from: https://international.neb.com/-/media/nebus/files/brochures/monarch_brochure.pdf?rev=0e6c18a67c79463b9b4d1fb27adad72d&hash=04EB2734366192914F06C00EF4477014.
98. McCormick, R.M., *A solid-phase extraction procedure for DNA purification.* Analytical Biochemistry, 1989. **181**(1): p. 66-74.
99. Shaw, K.J., L. Thain, P.T. Docker, C.E. Dyer, J. Greenman, et al., *The use of carrier RNA to enhance DNA extraction from microfluidic-based silica monoliths.* Analytica Chimica Acta, 2009. **652**(1): p. 231-233.
100. LGC, *Manual. MasterPure Complete DNA and RNA Purification Kit*. 2021, Biosearch Technologies. Genomic analysis by LGC.

101. Ricardo, P.C., E. Françoso, and M.C. Arias, *Fidelity of DNA polymerases in the detection of intraindividual variation of mitochondrial DNA.* Mitochondrial DNA B Resour, 2019. **5**(1): p. 108-112.
102. *INSTRUCTION MANUAL Monarch® PCR & DNA Cleanup Kit (5 µg)*. 2021 [cited 2023 30. April]; Available from: https://international.neb.com/-/media/nebus/files/manuals/manualt1030.pdf?rev=3a38f156896540df9191eef0f51eed72&hash=9BE8B7A6FD3C7543BE01A29E7DE3CB1B.
103. Burmeister, A.R., *Horizontal Gene Transfer.* Evol Med Public Health, 2015. **2015**(1): p. 193-4.
104. Hall, R.J., F.J. Whelan, J.O. McInerney, Y. Ou, and M.R. Domingo-Sananes, *Horizontal Gene Transfer as a Source of Conflict and Cooperation in Prokaryotes.* Frontiers in Microbiology, 2020. **11**.
105. Baur, B., K. Hanselmann, W. Schlimme, and B. Jenni, *Genetic transformation in freshwater: Escherichia coli is able to develop natural competence.* Appl Environ Microbiol, 1996. **62**(10): p. 3673-8.
106. Li, M.Z. and S.J. Elledge, *Harnessing homologous recombination in vitro to generate recombinant DNA via SLIC.* Nature Methods, 2007. **4**(3): p. 251-256.
107. Jeong, J.Y., H.S. Yim, J.Y. Ryu, H.S. Lee, J.H. Lee, et al., *One-step sequence- and ligation-independent cloning as a rapid and versatile cloning method for functional genomics studies.* Appl Environ Microbiol, 2012. **78**(15): p. 5440-3.
108. Hanahan, D., *Studies on transformation of Escherichia coli with plasmids.* Journal of Molecular Biology, 1983. **166**(4): p. 557-580.
109. Asif, A., H. Mohsin, R. Tanvir, and Y. Rehman, *Revisiting the Mechanisms Involved in Calcium Chloride Induced Bacterial Transformation.* Front Microbiol, 2017. **8**: p. 2169.
110. Shen, C.-H., *Chapter 11 - Techniques in Sequencing*, in *Diagnostic Molecular Biology*, C.-H. Shen, Editor. 2019, Academic Press. p. 277-302.
111. *PubChem Bioassay Record for AID 1545, Source: Burnham Center for Chemical Genomics*. 2023 [cited 2023 28. April]; Available from: https://pubchem.ncbi.nlm.nih.gov/bioassay/1545.
112. Ye, R.W., N.A. Zielinski, and A.M. Chakrabarty, *Purification and characterization of phosphomannomutase/phosphoglucomutase from Pseudomonas aeruginosa involved in biosynthesis of both alginate and lipopolysaccharide.* J Bacteriol, 1994. **176**(16): p. 4851-7.
113. Naught, L.E. and P.A. Tipton, *Formation and reorientation of glucose 1,6-bisphosphate in the PMM/PGM reaction: transient-state kinetic studies.* Biochemistry, 2005. **44**(18): p. 6831-6.
114. Veskoukis, A.S., N.V. Margaritelis, A. Kyparos, V. Paschalis, and M.G. Nikolaidis, *Spectrophotometric assays for measuring redox biomarkers in blood and tissues: the NADPH network.* Redox Rep, 2018. **23**(1): p. 47-56.
115. Xu, G., M.J. Amicucci, Z. Cheng, A.G. Galermo, and C.B. Lebrilla, *Revisiting monosaccharide analysis - quantitation of a comprehensive set of monosaccharides using dynamic multiple reaction monitoring.* Analyst, 2017. **143**(1): p. 200-207.
116. Navazo, A., E. Barahona, M. Redondo-Nieto, F. Martínez-Granero, R. Rivilla, et al., *Three independent signalling pathways repress motility in Pseudomonas fluorescens F113.* Microb Biotechnol, 2009. **2**(4): p. 489-98.
117. Bateman, A., E. Birney, L. Cerruti, R. Durbin, L. Etwiller, et al., *The Pfam protein families database.* Nucleic Acids Res, 2002. **30**(1): p. 276-80.

118. Winsor, G.L., E.J. Griffiths, R. Lo, B.K. Dhillon, J.A. Shay, et al., *Enhanced annotations and features for comparing thousands of Pseudomonas genomes in the Pseudomonas genome database.* Nucleic Acids Res, 2016. **44**(D1): p. D646-53.
119. Kelley, L.A., S. Mezulis, C.M. Yates, M.N. Wass, and M.J.E. Sternberg, *The Phyre2 web portal for protein modeling, prediction and analysis.* Nature Protocols, 2015. **10**(6): p. 845-858.
120. Taboada, B., K. Estrada, R. Ciria, and E. Merino, *Operon-mapper: a web server for precise operon identification in bacterial and archaeal genomes.* Bioinformatics, 2018. **34**(23): p. 4118-4120.
121. Simon, R., U. Priefer, and A. Pühler, *A Broad Host Range Mobilization System for In Vivo Genetic Engineering: Transposon Mutagenesis in Gram Negative Bacteria.* Bio/Technology, 1983. **1**(9): p. 784-791.
122. Tauch, A., O. Kirchner, B. Löffler, S. Götker, A. Pühler, et al., *Efficient electrotransformation of corynebacterium diphtheriae with a mini-replicon derived from the Corynebacterium glutamicum plasmid pGA1.* Curr Microbiol, 2002. **45**(5): p. 362-7.
123. Ertesvåg, H., H. Sletta, M. Senneset, Y.-Q. Sun, G. Klinkenberg, et al., *Identification of genes affecting alginate biosynthesis in Pseudomonas fluorescens by screening a transposon insertion library.* BMC Genomics, 2017. **18**(1): p. 11.
124. Syson, K., C.E.M. Stevenson, D.M. Lawson, and S. Bornemann, *Structure of the Mycobacterium smegmatis α-maltose-1-phosphate synthase GlgM.* Acta Crystallogr F Struct Biol Commun, 2020. **76**(Pt 4): p. 175-181.
125. Krishna, P.S., S.D. Woodcock, S. Pfeilmeier, S. Bornemann, C. Zipfel, et al., *Pseudomonas syringae addresses distinct environmental challenges during plant infection through the coordinated deployment of polysaccharides.* J Exp Bot, 2022. **73**(7): p. 2206-2221.
126. Harrison, J.J., H. Almblad, Y. Irie, D.J. Wolter, H.C. Eggleston, et al., *Elevated exopolysaccharide levels in Pseudomonas aeruginosa flagellar mutants have implications for biofilm growth and chronic infections.* PLOS Genetics, 2020. **16**(6): p. e1008848.
127. Hentzer, M., G.M. Teitzel, G.J. Balzer, A. Heydorn, S. Molin, et al., *Alginate overproduction affects Pseudomonas aeruginosa biofilm structure and function.* J Bacteriol, 2001. **183**(18): p. 5395-401.
128. Ma, L., H. Lu, A. Sprinkle, M.R. Parsek, and D.J. Wozniak, *Pseudomonas aeruginosa Psl is a galactose- and mannose-rich exopolysaccharide.* J Bacteriol, 2007. **189**(22): p. 8353-6.
129. Carabetta, S., R. Di Sanzo, L. Campone, S. Fuda, L. Rastrelli, et al., *High-Performance Anion Exchange Chromatography with Pulsed Amperometric Detection (HPAEC-PAD) and Chemometrics for Geographical and Floral Authentication of Honeys from Southern Italy (Calabria region).* Foods, 2020. **9**(11).
130. Woodcock, S.D., K. Syson, R.H. Little, D. Ward, D. Sifouna, et al., *Trehalose and α-glucan mediate distinct abiotic stress responses in Pseudomonas aeruginosa.* PLoS Genet, 2021. **17**(4): p. e1009524.
131. Maleki, S., E. Almaas, S. Zotchev, S. Valla, and H. Ertesvåg, *Alginate Biosynthesis Factories in Pseudomonas fluorescens: Localization and Correlation with Alginate Production Level.* Appl Environ Microbiol, 2016. **82**(4): p. 1227-1236.
132. Vijayaraghavan, P., S.R.F. Raj, and S.G.P. Vincent, *Chapter 4 - Industrial Enzymes: Recovery and Purification Challenges*, in *Agro-Industrial Wastes as Feedstock for Enzyme Production*, G.S. Dhillon and S. Kaur, Editors. 2016, Academic Press: San Diego. p. 95-110.

Appendix A - Primers

Table A1 shows the primers and the relevant information about them used in this study. The annealing temperature refers to their melting temperature, and the used annealing temperature for PCR was 3℃ minus the lowest Tm for the primer pair used in the reaction.

Table A1: The primers used in this study. Their name, sequence, the Tm (℃), and the source of each primer is listed up in the table.

NAME	SEQUENCE	ANNEALING TEMPERASURE
AT75XYLSF	5'TGGAGTGCAATGAGCCTGCAGACAGCACGAACTTCTGG3'	60
AT75XYLSR	5'CATCGACTTGGCATCCTGCATCGCCTAGGTTCGTAATC3'	57
OPSLF	5' TCTTGAACACCAGCCACAAC 3'	62
PSLAR	5' CGAACCACCGGAAATGATGC 3'	64
PSLSJEKKF	5' AACCTATCTAGCACGCCACTCC 3'	65
PSLSJEKKR	5' GGCGGTTGCTGAACAATTCCTC 3'	66
ALGCSJEKKF	5' GCGCGGACTTTATCAGCGAG 3'	65
ALGCSJEKKR	5' GTCGTCAAAGCCGAACCAG 3'	63
230SJEKKF	5' TTTCGGCAGTCAGCGTCTTAGG 3'	66
230SJEKKR	5' AAACCGCCCAGTCTAGCTATCG 3'	66
DPALGDF	5' CACATACTGCGCCAACGTAAC 3'	64
DPALGDR	5' ATGCCTGTACGCGGTAAGTCG 3'	66
CSG2BLÅAF	5' AGAAACACCCGGCCCAAGG 3'	66
CSG2BLÅAR	5' GACCGCTTCTGCGTTCTG 3'	63
CSG2BLÅBF	5' TTCGCCCTTTGGCACACGG 3'	68
CSG2BLÅBR	5' GGCGTTCCACAGGTGCTTG 3'	66
PSLAM3F	5' GGCGAACTACTTACTCTAGC 3'	59
PSLAM3R	5' TCGACGGACGACTTATCTC 3'	60
PSLAM5F	5' GGGTTGAGCAGACTATTGAG 3'	59
PSLAM5R	5' TAAGCCCACTGCAAGCTAC 3'	61
PSLWTF	5' TGGACCGTGGCACTCAAC 3'	64
PSLWTR	5' CGGTGCGGTCGTCGATAAAC 3'	65

Appendix B – Restriction enzymes

The restriction enzymes used in this study are shown in Table B1, together with the recognition site, the optimal buffer, and the optimal temperature for the reaction.

ACTG stands for the four different bases, N stands for any of the four, R stands for either A or G (purines), while Y stands for C or T (any pyrimidine).

Table B1: Overview of the restriction enzymes used in this study, along with the necessary information for obtaining an optimal reaction.

NAME	RECOGNITION SITE (5' – 3')	OPTIMAL BUFFER	OPTIMAL TEMPERATURE [°C]
AvrII	CCTAGG	CutSmart	37
BaeI	ACNNNNGTAYC	CutSmart	37
BglII	AGATCT	NEB 3.1	37
BsaI	*GGTCTC*	CutSmart	37
DraII	RGGNCCY	CutSmart	37
DraIII-HF	CACNNNGTG	CutSmart	37
EcoRI-HF	GAATTC	CutSmart	37
EcoRV-HF	GATATC	CutSmart	37
HindIII-HF	AAGCTT	CutSmart	37
MfeI-HF	CAATTG	CutSmart	37
NcoI-HF	CCATGG	CutSmart	37
NdeI	CATATG	CutSmart	37
NotI-HF	GCGGCCGC	CutSmart	37
PspOMI	GGGCCC	CutSmart	37
PstI-HF	CTGCAG	CutSmart	37
SbfI-HF	CCTGCAGG	CutSmart	37
SpeI-HF	ACTAGT	CutSmart	37
SphI-HF	GCATGC	CutSmart	37
StuI	AGGCCT	NEB 2.1	37
XbaI	TCTAGA	CutSmart	37
XhoI	CTCGAG	CutSmart	37

Appendix C – Psl operon analysis

The predicted localization, domains, and functions of the genes within the Psl operon found in *P. fluorescens* SBW25. The predicted functions and localisation were found in Pseudomonas Genomic Database, while the predicted domains were found using PHMMER and Pfam databases. e-value describe the significance of the match and says something about how many hits to expect by chance when analysing data sets with the same size. e-values larger than 10^{-3} were therefore excluded from the results. The subcellular location was attempted analysed using pSORTb v.3.0, but only yielded inconclusive results for most of the proteins. The results are shown in table C1

Table C1: Predicted localisations, domains, and functions of the Psl proteins in P. fluorescens SBW25

Locus (PFLU….)	**Protein**	**Length**	**Localization**	**Predicted domains**			**Predicted protein function based on homology with orthologous groups**
				Domain	**Position**	**e-value**	
2082	PslA	1440	Cytoplasmic membrane	Bacterial sugar transferase	285 - 473	6.2 e-67	Capsular polysaccharide biosynthesis protein/undecaprenyl-phosphate glucose phosphotransferase (POG005117)
				CoA-binding	71 - 249	1.2e-26	
2081	PslB	1461	Cytoplasma	Mannose-G-phosphate isomerase	325-475	2.1e-65	phosphomannose isomerase/GDP-mannose (POG004998)
				Nucleotidyl transferase	9-295	1.2e-51	
				MobA-like NTP transferase domain	10-149	2.2e-9	
				Cupin domain	392-457	2.3e-8	
2080	PslC	912	Cytoplasma	Glycosyl transferase family 2	4-171	6.9e-15	Glycosyl transferase (POG005118)
				Glycosyl transferase like family 2	3-210	1.9e-13	
				Glycosyl transferase family group 2	154-219	4.7e-6	
2079	PslD	777	Unknown	Polysaccharide biosynthesis/export protein	47-129	1.7e-15	Exopolysaccharide exporter/ sugar ABC transporter substrate-binding protein (POG005119)
				SLBB domain	139-183	0.00023	
2078	PslE	1992	Unknown	G-rich domain on putative tyrosine kinase	402-478	0.00022	lipopolysaccharide biosynthesis protein/exopolysaccharide export (POG003251)
				Chain length determinant protein	9-89	0.00076	
2077	PslF	1191	Cytoplasma	Glycosyl transferases group 1	192-365	3.1e-12	Glycosyl transferase (POG003250)
				Glycosyltransferase family 4	47-173	0.00064	
2076	PslG	1329	Unknown	Glycosyl hydrolases family 39	59-360	1.3e-9	Glycosyl hydrolase/beta-xylosidase (POG003249)

				Cellulase (glycosyl hydrolase family 5)	46-289	7.2e-7	
2075	PslH	1218	Unknown	Glycosyl transferases group 1	222-358	3.8e-21	Glycosyl transferase (POG003248)
				Glycosyl transferase 4-like domain	16-206	2.3e-21	
				Glcosyl transferase family 4	17-210	3.9e-17	
				Glycosyl transferase group 1	298-387	2.8e-6	
2074	PslI	1104	Cytoplasma	Glycosyl transferases group 1	199-303	1.2e-12	Glycosyl transferase (POG001311)
				Glycosyl transferases group 1	203-307	1.1e-10	
				Glycosyl transferases Family 4	17-183	7.5e-9	
				Glycosyl transferase 4-like domain	16-183	1.2e-6	
2073	PslJ	1434	Cytoplasmic membrane	O-antigen ligase	257-384	2e-6	Membrane protein (POG003247)
2072	PslK	1410	Cytoplasmic membrane	Lipid II flippase MurJ	28-412	5.9e-42	Membrane protein/glycosyl transferase (POG003246)
				Polysaccharide biosynthesis protein	70-324	4.3e-10	
				Polysaccharide biosynthesis C-terminal domain	333-464	8.4e-7	
2071	PslL	1050	Cytoplasmic membrane	Acyltransferase family	7-320	3.1-19	Acyltransferase/membrane protein (POG003245)

To see how similar the genes were and if they indeed were part of the same operon, the whole Psl sequence was tested using the Operon Mapper, a tool for predicting operons within the bacterial genome. The sequence was sent in, and one operon containing 12 genes stood out. A closer look revealed that these genes predicted to be part of the operon was identical to the Psl genes in the sequence. The tool also gave the predicted function for the genes in the operon, which also can be seen in Table C2.

Table C2:Testing of the genes to determine if they are part of the same operon using Operon Mapper

Protein name	IdGene	Position left	Position right	Strand	Function
PslA	LGALHFHO_00003	1749	3188	+	[M] Sugar transferases involved in lipopolysaccharide synthesis
PslB	LGALHFHO_00004	3188	4648	+	[M] Mannose-1-phosphate guanylyltransferase
PslC	LGALHFHO_00005	4650	5561	+	[R] Predicted glycosyltransferases
PslD	LGALHFHO_00006	5567	6367	+	[M] Periplasmic protein involved in polysaccharide export
PslE	LGALHFHO_00007	6383	8374	+	[M] Uncharacterized protein involved in exopolysaccharide biosynthesis
PslF	LGALHFHO_00008	8374	9564	+	[M] Glycosyltransferase
PslG	LGALHFHO_00009	9554	10882	+	[G] Beta-xylosidase
PslH	LGALHFHO_00010	10891	12108	+	[M] Glycosyltransferase
PslI	LGALHFHO_00011	12099	13202	+	[M] Glycosyltransferase
PslJ	LGALHFHO_00012	13199	14632	+	[M] Lipid A core - O-antigen ligase
PslK	LGALHFHO_00013	14632	16041	+	[R] Uncharacterized membrane protein, putative virulence factor
PslL	LGALHFHO_00014	16085	17113	+	[G] Fucose 4-O-acetylase and related acetyltransferases

Appendix D – Plasmids constructed in this study

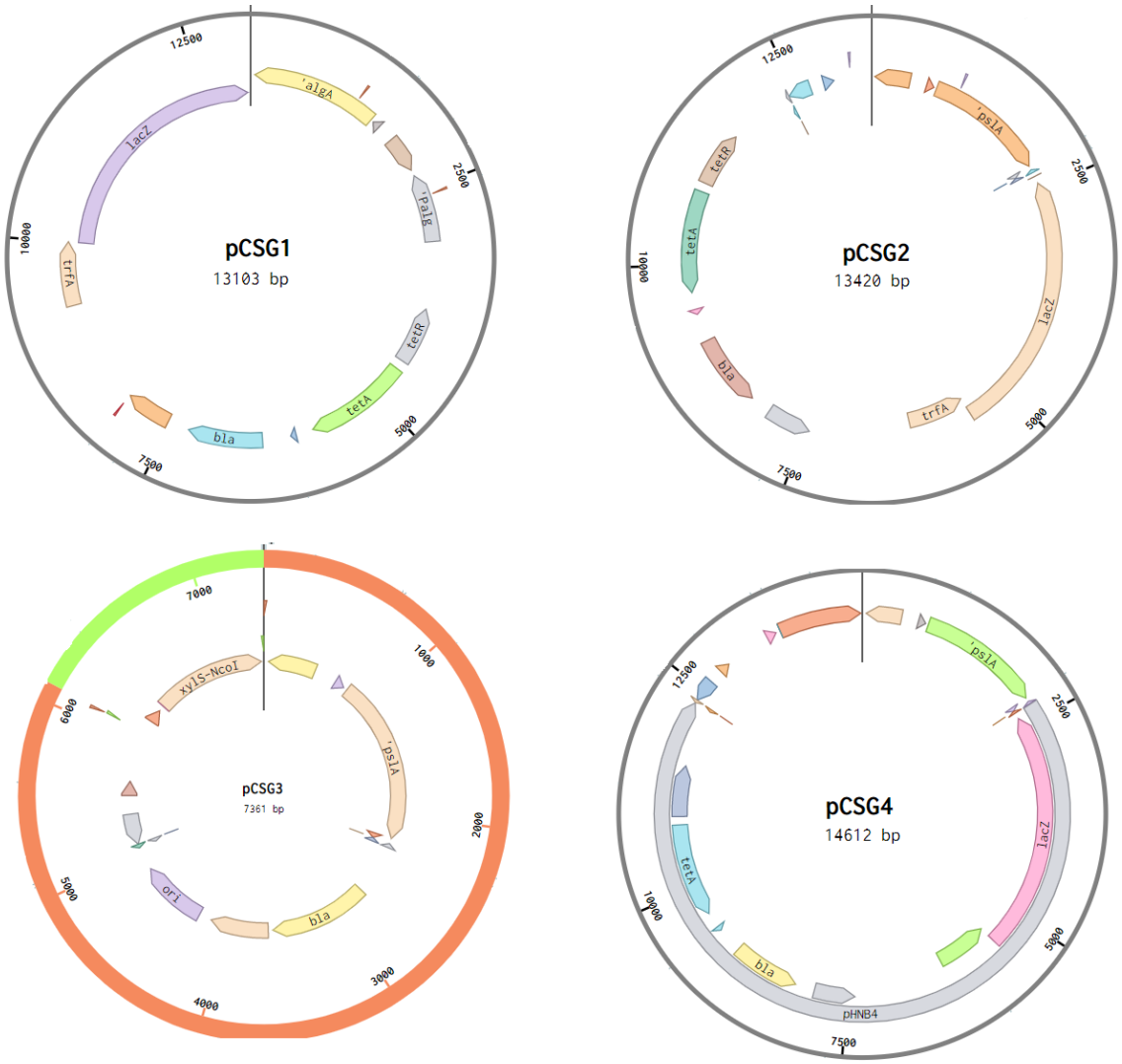

Figure D1: pCSG1, pCSG2, pCSG2, and pCSG4 shown using the Benchling display version

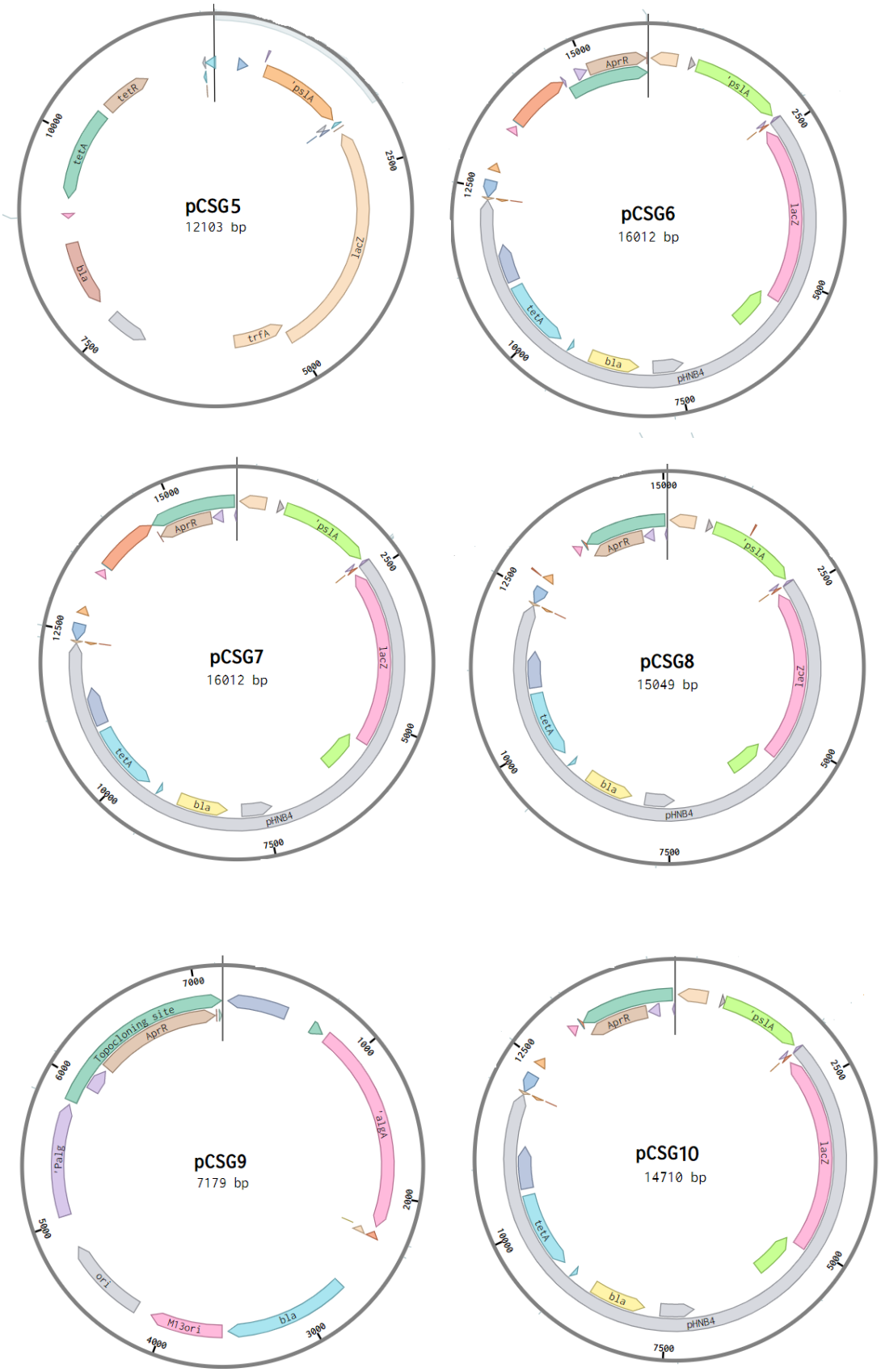

Figure D2: pCSG5, pCSG6, pCSG7, pCSG8, pCSG9, and pCS10 shown using the Benchling display version

Appendix E – DNA ladders

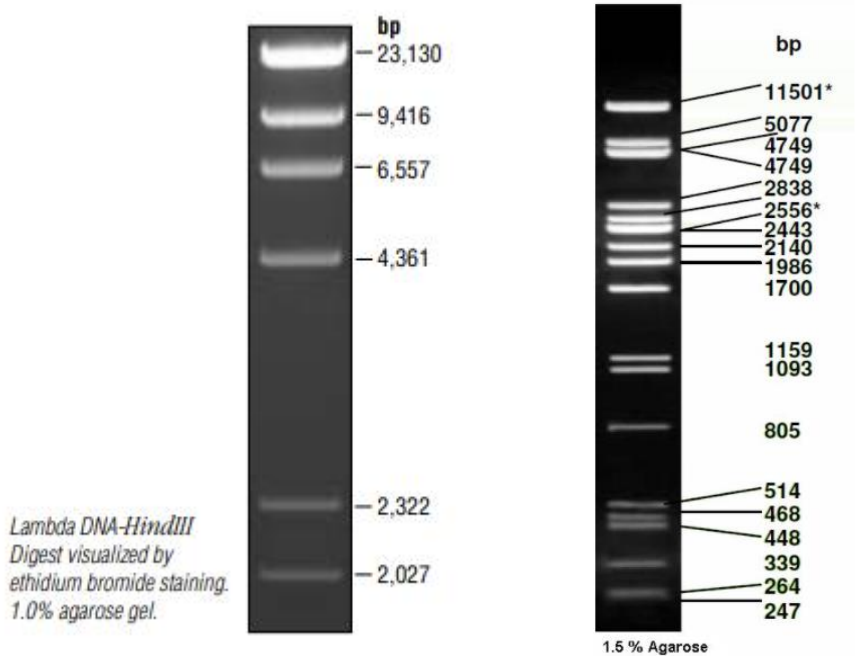

Figure E1: DNA ladders along with the bands when cutting λDNA with HindIII (λH) and PstI (λP)

Appendix F – Sequences

The SWB25*mucA*HE230pAlgD^{-} mutant strain had its AlgD operon sequenced, using the DPAlgD primer pair. The resulting sequence show the resulting sequence from Eurofins Genomic, with the DPAlgDF primer notated "del" and the DPAlgDR primer notated "delAlgC"

```
del         TTTGCGCCAACGTAACCGAGACCAAATATGCTGATGCGCATATGTTCATGACTCCATTAT      60
delAlgC     ------------------------------------------------------------      0


del         TATTGTACATGTACCGCCGTTGGATAGCTCCGCTACCGGCCTCGACCGGATCTACGCAAA      120
delAlgC     ----------------------------------------------TCTACGCATA      10
                                                          ******** *

del         AAGGCCATCCGTCAGGATGGCCTTCTGCTTAATTTGATGCCTGGCAGTTTATGGCGGGCG      180
delAlgC     AAGGCCGTCGGTCAGGATGGCCTTCTGCTTAATTTGATGCCTGGCAGTTTATGGCGGGCG      70
            ****** ** **************************************************

del         TCCTGCCCGCCACCCCTCGGGCCGTTGCTTCGCAACGTTCAAATCCGCTCCCGGCGGATT      240
delAlgC     TCCTGCCCGCCACCCTCCGGGCCGTTGCTTCGCAACGTTCAAATCCGCTCCCGGCGGATT      130
            ***************  ******************************************

del         TGTCCTACTCAGGAGAGCGTTCACCGACAAACAACAGATAAAACGAAAGGCCCAGTCTTT      300
delAlgC     TGTCCTACTCAGGAGAGCGTTCACCGACAAACAACAGATAAAACGAAAGGCCCAGTCTTT      190
            ************************************************************

del         CGACTGAGCCTTTCGTTTTATTTGATGCCTGGCAGTTCCCTACTCTCGCATGGGGAGACC      360
delAlgC     CGACTGAGCCTTTCGTTTTATTTGATGCCTGGCAGTTCCCTACTCTCGCATGGGGAGACC      250
            ************************************************************

del         CCACACTACCATCGGCGCTACGGCGTTTCACTTCTGAGTTCGGCATGGGGTCAGGTGGGA      420
delAlgC     CCACACTACCATCGGCGCTACGGCGTTTCACTTCTGAGTTCGGCATGGGGTCAGGTGGGA      310
            ************************************************************

del         CCACCGCGCTACTGCCGCCAGGCAAATTCTGTTTTATCAGACCGCTTCTGCGTTCTGATT      480
delAlgC     CCACCGCGCTACTGCCGCCAGGCAAATTCTGTTTTATCAGACCGCTTCTGCGTTCTGATT      370
            ************************************************************

del         TAATCTGTATCAGGCTGAAAATCTTCTCTCATCCGCCAGGGGGGGATCTCGAATTAATTC      540
delAlgC     TAATCTGTATCAGGCTGAAAATCTTCTCTCATCCGCCAGGGGGGGATCTCGAATTAATTC      430
            ************************************************************

del         CTGCATTTTCATCGACTTGGCATCCTGCAGGAATTCCTCGAGGCCTCGAGGCATGGCATT      600
delAlgC     CTGCATTTTCATCGACTTGGCATCCTGCAGGAATTCCTCGAGGCCTCGAGGCATGGCATT      490
            ************************************************************

del         TACCTCTTCGTCATTCAAGACTGTGTTAATCGTGCCTATAAGGCCCCGGAGTTTCATGTT      660
delAlgC     TACCTCTTCGTCATTCAAGACTGTGTTAATCGTGCCTATTAAGGCCGGAGTTC-ATGTTT      549
            ****************************************** * * ** *   *      **

del         GCAAGCGTCACTGATGCCGGAAAT-----------------------------------      684
delAlgC     GCAAGCGTCACTGATGCCGCGAAAGTTGGGCGAATAGACGCCGACTTACCGCGTACAGGC      609
            ******************  **

del         ----        684
delAlgC     ATAA        613
```

Figure F1: Sequencing of the AlgD deletion in SBW25mucAHE230pAlgD^{-}

The sequencing results for the SBW25HE230*mucA* pAlgD¯CSG8 mutant, using Pslsjekk primer pair is shown below, with the forward and reverse PslSjekk primer pair annotated in the figure, and the desired Psl mutation sequence in the middle. The part in the middle, not covered by any of the primers is part of the upstream Apr gene sequence.

```
forward     ------------------------------------------------------------      0
Psl         AACCTATCTAGCACGCCACTCCCGCAGCATCGTCAATCAATTGACTAACCATACAAGGAA      60
revers      -----------------------------------TATTGGACTAACCATACAAGGAA      23

forward     ------------------------------------------------------------      0
Psl         CACTCCTTTAGTCACTACCCCCGCAAGATCAATTCAAATGGTTAGTTGTTTTTGTATCGT      120
revers      CACTCCTTTAGTCACTACCCCCGCAAGATCAATTCAAATGGTTAGTTGTTTTTGTATCGT      83

forward     ------------------------------------------------------------      0
Psl         GCATTTGAATTGGAAAGTTGCGTATTACCCAGAGTAGTCGTTCGGCCTACGTTCTAAAGC      180
revers      GCATTTGAATTGGAAAGTTGCGTATTACCCAGAGTAGTCGTTCGGCCTACGTTCTAAAGC      143

forward     ------------------------------------------------------------      0
Psl         GGCTCGCCGCCTTATTGAGCCAATAGCCGAACAGTGGAATCTGGAGTGCAATGAGCCTGC      240
revers      GGCTCGCCGCCTTATTGAGCCAATAGCCGAACAGTGGAATCTGGAGTGCAATGAGCCTGC      203

forward     ------------------------------------------------------------      0
Psl         AGACAGCACGAACTTCTGGTGTTCTCGCTTCTTAAAAAGAACGGGAATTCGTAGCTTGCA      300
revers      AGACAGCACGAACTTCTGGTGTTCTCGCTTCTTAAAAAGAACGGGAATTCGTAGCTTGCA      263

forward     ------------------------------------------------------------      0
Psl         GTGGGCTTACATGGCGATAGCTAGACTGGGCGGTTTTATGGACAGCAAGCGAACCGGAAT      360
revers      GTGGGCTTACATGGCGATAGCTAGACTGGGCGGTTTTATGGACAGCAAGCGAACCGGAAT      323

forward     ------------------------------------------------------------      0
Psl         TGCCAGCTGGGGCGCCCTCTGGTAAGGTTGGGAAGCCCTGCAAAGTAAACTGGATGGCTT      420
revers      TGCCAGCTGGGGCGCCCTCTGGTAAGGTTGGGAAGCCCTGCAAAGTAAACTGGATGGCTT      383

forward     ------------------------------------------------------------      0
Psl         TCTTGCCGCCAAGGATCTGATGGCGCAGGGGATCAAGATCGACGGATCGATCCGGGGAAT      480
revers      TCTTGCCGCCAAGGATCTGATGGCGCAGGGGATCAAGATCGACGGATCGATCCGGGGAAT      443

forward     ------------------------------------------------------------      0
Psl         TAATTCCGGGGCAATCCCGCAAGGAGGGTCCATGGATTTTTGCTTATTGAACGAGAAAAG      540
revers      TAATTCCGGGGCAATCCCGCAAGGAGGGTCCATGGATTTTTGCTTATTGAACGAGAAAAG      503

forward     ------------------------------------------------------------      0
Psl         TC----ACTAGGTCAGGCTGCGCAACTGTTGGGAAGGGCGATCGGTGCGGGCCTCTTCGC      596
revers      TCAGATCCTAGGTCAGGCTGCGCAACTGTTGGGAAGGGCGATCGGTGCGGGCCTCTTCGC      563

forward     ------------------------------------------------------------      0
Psl         TATTACGCCAGCTGGCGAAAGGGGGATGTGCTGCAAGGCGATTAAGTTGGGTAACGCCAG      656
revers      TATTACGCCAGCTGGCGAAAGGGGGATGTGCTGCAAGGCGATTAAGTTGGGTAACGCCAG      623

forward     ------------------------------------------------------------      0
Psl         GGTTTTCCCAGTCACGACGTTGTAAAACGACGGCCAGTGAATTAATTCGAGCTCAGCCAA      716
revers      GGTTTTCCCAGTCACGACGTTGTAAAACGACGGCCAGTGAATTAATTCGAGCTCAGCCAA      683

forward     ------------------------------------------------------------      0
Psl         TCGACTGGCGAGCGGCATCGCATTCTTCGCATCCCGCCTTCTGGCGGATGCAGGAAGATC      776
revers      TCGACTGGCGAGCGGCATCGCATTCTTCGCATCCCGCC-TCTGGCGGATGCAGGAAGATC      742
```

```
forward     ------------------------------------------------------------      0
Psl         AACGGATCTCGGCCCAGTTGACCCAGGGCTGTCGCCACAATGTCGCGGGAGCGGATCAAC      836
revers      AACGGATCTCGGCCCAGTTGACCCAGGGCTGTCGCCACAATGTCGCGGGAGCGGATCAAC      802

forward     ------------------------------------------------------------      0
Psl         CGAGCAAAGGCATGACCGACTGGACCTTCCTTCTGAAGGCTCTTCTCCTTGAGCCACCTG      896
revers      CGAGCAAAGGCATGACCGACTGGACCTTCCTTCTGAAGGCTCTTCTCCTTGAGCCACCTG      862

forward     ------------------------------------------------------------      0
Psl         TCCGCCAAGGCAAAGCGCTCACAGCAGTGGTCATTCTCGAGATAATCGACGCGTACCAAC      956
revers      TCCGCCAAGGCAAAGCGCTCACAGCAGTGGTCATTCTCGAGATAATCGACGCGTACCAAC      922

forward     ------------------------------------------------------------      0
Psl         TTGCCATCCTGAAGAATGGTGCAGTGTCTCGGCACCCCATAGGGAACCTTTGCCATCAAC      1016
revers      TTGCCATCCTGAAGAATGGTGCAGTGTCTCGGCACCCCATAGGGAACCTTTGCCATCAAC      982

forward     ------------------------------------------------------------      0
Psl         TCGGCAAGATGCAGCGTCGTGTTGGCATCGTGTCCCACGCCGAGGAGAAGTACCTGCCCA      1076
revers      TCGGCAAGATGCAGCGTCGTGTTGGCATCGTGTCCCACGCCGAGGAGAAGTACCTGCCCA      1042

forward     ------------------------------------------------------------      0
Psl         TCGAGTTCATGGACACGGGCGACCGGGCTTGCAGGCGAGTGAGGTGGCAGGGGCAATGGA      1136
revers      TCGAGTTCATGGACACGGGCGACCGGGCTTGCAGGCGAATGAGGTGGCAGGGGCAATGGA      1102

forward     ------------------------------------------------------------      0
Psl         TCAGAGATGATCTGCTCTGCCTGTGGCCCCGCTGCCGCAAAGGCAAATGGATGGGCGCTG      1196
revers      TCAGAGATGATCTGCTCTGCCTGTGGCCCCGCTGCCGCAAAGGCAAATGGATGGGCGCTG      1162

forward     ------------------------------------------------------------      0
Psl         CGCTTTACATTTGGCAGGCGCCAGAATGTGTCAGAGACAACTCCAAGGTCCGGTGTAACG      1256
revers      CCCTTTA-ATTTGGCAGGGGCCAGAATGTGTCAAAGACA--------------------      1200

forward     ------------------------------------------------------------      0
Psl         GGCGACGTGGCAGGATCGAACGGCTCGTCGTCCAGACCTGACCACGAGGGCATGACGAGC      1316
revers      ------------------------------------------------------------      1200

forward     ------------------------------------------------------------      0
Psl         GTCCCTCCCGGACCCAGCGCAGCACGCAGGGCCTCGATCAGTCCAAGTGGCCCATCTTCG      1376
revers      ------------------------------------------------------------      1200

forward     ------------------------------------------------------------      0
Psl         AGGGGCCGGACGCTACGGAAGGAGCTGTGGACCAGCAGCACACCGCCGGGGGTAACCCCA      1436
revers      ------------------------------------------------------------      1200

forward     ------------------------------------------------------------      0
Psl         AGGTTGAGAAGCTGACCGATGAGCTCGGCTTTTCGCCATTCGTATTGCACGACATTGCAC      1496
revers      ------------------------------------------------------------      1200

forward     ------------------------------------------------------------      0
Psl         TCCACCGCTGATGACATCAGTCGATCATAGCACGATCAACGGCACTGTTGCAAATAGTCG      1556
revers      ------------------------------------------------------------      1200
```

```
forward  ------------------------------------------------------------  0
Psl      GTGGTGATAAACTTATCATCCCCTTTTGCTGATGGAGCTGCACATGAACCCATTCAAAGG  1616
revers   ------------------------------------------------------------  1200

forward  ------------------------------------------------------------  0
Psl      CCGGCATTTTCAGCGTGACATCATTCTGTGGGCCGTACGCTGGTACTGCAAATACGGCAT  1676
revers   ------------------------------------------------------------  1200

forward  ------------------------------------------------------------  0
Psl      CAGTTACCGTGAGCTCACATTAATTGCGTTGCGCTCACTGCCCGCTTTCCAGTCGGGAAA  1736
revers   ------------------------------------------------------------  1200

forward  ------------------------------------------------------------  0
Psl      CCTGTCGTGCCAGCTGCATTAATGAATCGGCCAACGCGCGGGGAGAGGCGGTTTGCGTAT  1796
revers   ------------------------------------------------------------  1200

forward  ------------------------------------------------------------  0
Psl      TGGGCGCTCTTCCGCTTCCTCGCTCACTGCAGGTCGACGGATCGCAAACTATTAACTGGC  1856
revers   ------------------------------------------------------------  1200

forward  ------------------------------------------------------------  0
Psl      GAACTACTTACTCTAGCTTCCCGGCACCTGCAGGAAGGGCGAATTCCAGCACACTGGCGG  1916
revers   ------------------------------------------------------------  1200

forward  ------------------------------------------------------------  0
Psl      CCGTTACTAGCTAGGCGATGCAGGATGCCAAGTCGATGAAAATGCAGGAATTAATTCGAG  1976
revers   ------------------------------------------------------------  1200

forward  -----------GATGAAGAGAAAGATTTTCCAGCCCTGATACCAGATTTAAATCAGAAAC  49
Psl      ATCCCCCCCTGGCGGATGAGAGAAGATTTTCAGCC-TGATACA-GAT-TAAATCA-GAAC  2032
revers   ------------------------------------------------------------  1200

forward  GCAGAAGGCGGTTCTGATAAAACAGAAATTTGCCTGGCGGCAGTAGCGCGGTGGTCCCAC  109
Psl      GCAGAAG-C-GGTCTGATAAAACAG-AATTTGCCTGGCGGCAGTAGCGCGGTGGTCCCAC  2089
revers   ------------------------------------------------------------  1200

forward  CTGACCCCATGCCGAACTCAGAAGTGAAACGCCGTAGCGCCGATGGTAGTGTGGGGTCTC  169
Psl      CTGACCCCATGCCGAACTCAGAAGTGAAACGCCGTAGCGCCGATGGTAGTGTGGGGTCTC  2149
revers   ------------------------------------------------------------  1200

forward  CCCATGCGAGAGTAGGGAACTGCCAGGCATCAAATAAAACGAAAGGCTCAGTCGAAAGAC  229
Psl      CCCATGCGAGAGTAGGGAACTGCCAGGCATCAAATAAAACGAAAGGCTCAGTCGAAAGAC  2209
revers   ------------------------------------------------------------  1200

forward  TGGGCCTTTCGTTTTATCTGTTGTTTGTCGGTGAACGCTCTCCTGAGTAGGACAAATCCG  289
Psl      TGGGCCTTTCGTTTTATCTGTTGTTTGTCGGTGAACGCTCTCCTGAGTAGGACAAATCCG  2269
revers   ------------------------------------------------------------  1200

forward  CCGGGAGCGGATTTGAACGTTGCGAAGCAACGGCCCGGAGGGTGGCGGGCAGGACGCCCG  349
Psl      CCGGGAGCGGATTTGAACGTTGCGAAGCAACGGCCCGGAGGGTGGCGGGCAGGACGCCCG  2329
revers   ------------------------------------------------------------  1200
```

```
forward     CCATAAACTGCCAGGCATCAAATTAAGCAGAAGGCCATCCTGACGGATGGCCTTTTTGCG      409
Psl         CCATAAACTGCCAGGCATCAAATTAAGCAGAAGGCCATCCTGACGGATGGCCTTTTTGCG      2389
revers      ------------------------------------------------------------      1200

forward     TAGATCCGGTCGAGGCCGGTAGCGGAGCTATCCAACGGCGGTATACCAGGAAAACACACA      469
Psl         TAGATCCGGTCGAGGCCGGTAGCGGAGCTATCCAACGGCGGTATACCAGGAAAACACACA      2449
revers      ------------------------------------------------------------      1200

forward     GCAGGTACATCAGAACAGTACCATGACTGAAGAACAAATAGTTTTTTCCTGATCCATAAA      529
Psl         GCAGGTACATCAGAACAGTACCATGACTGAAGAACAAATAGTTTTTTCCTGATCCATAAA      2509
revers      ------------------------------------------------------------      1200

forward     GCAGAACGGCCTGCTCCATGACAAATCTGGCTCCCCAACTAATGCCCCATGCAGCCAGCA      589
Psl         GCAGAACGGCCTGCTCCATGACAAATCTGGCTCCCCAACTAATGCCCCATGCAGCCAGCA      2569
revers      ------------------------------------------------------------      1200

forward     TAACCAGCATAAACGTGTCCGGTTTGATAGGGATAAGTCCAGCCTTGCAAGAAGCGGATA      649
Psl         TAACCAGCATAAACGTGTCCGGTTTGATAGGGATAAGTCCAGCCTTGCAAGAAGCGGATA      2629
revers      ------------------------------------------------------------      1200

forward     CAGGAGTGCAAAAAATGGCTATCTCTAGAAAGACCTACCCCTGAGGCTTTATGCAACATG      709
Psl         CAGGAGTGCAAAAAATGGCTATCTCTAGAAAGACCTACCCCTGAGGCTCTATGCAACATG      2689
revers      ------------------------------------------------------------      1200

forward     TACAATAATAATGGAGTCATGAACATATGCGAGATAAGTCGTCCGTCGACAGCCTGTTTT      769
Psl         TACAATAATAATGAAGTCATGAACATATGCGAGATAAGTCGTCCGTCGACAGCCTGTTTT      2749
revers      ------------------------------------------------------------      1200

forward     TAACGCGCGCCGGTTTTGTTGAGTTCTTTGTTGTATTCGTCAAGTTGATCCACGGCCTGA      829
Psl         TAACGCGCGCCGGTTTTGTTGAGTTCTTTGTTGTATTCGTCAAGTTGATCCACGGCCTGA      2809
revers      ------------------------------------------------------------      1200

forward     GTGCCATTTTACCCCCACTGGTCCTGGTGTTCGTCCTGGACCCGTTGGACCCCGAGCTGC      889
Psl         GTGCCATTTTACCCCCACTGGTCCTGGTGTTCGTCCTGGACCCGTTGGACCCCGAGCTGC      2869
revers      ------------------------------------------------------------      1200

forward     GCGCCCACTTCCTGGGCCTGCTGGTTTTTTTCG--------------------------      922
Psl         GCGCCCACTTCCTGGGCCTGCTGGTTTTTTTCGCGGTCCTGACCATTATTCTGTTCCAGG      2929
revers      ------------------------------------------------------------      1200

forward     ---------------------------------------    922
Psl         CCCTGGGCATCTATTCCGAGGAATTGTTCAGCAACCGCC    2968
revers      ---------------------------------------    1200
```

Figure F2: Sequencing results of the SBW25HE230mucA pAlgD⁻ CSG8 mutant with the PslSjekk primer pair

Appendix G – PMM/PMI assay

The graphs used to get the increase in NADP reduction is shown for all samples below. The graph from the raw data with all tested parallels are displayed first, followed by the parallels included in the calculation for the enzyme activity with cells with and without substrate. Only the linear increase is used, as most parallels flattened out after around 30 minutes. First, the parallels used for the cells with substrate is attached, then cells lacking substrate, followed by all six parallels for the mutants. For the increase, the numbers are corrected for the first measurement, causing the graphs to start at 0.

Two rounds of the assay were conducted, using more strains in the second round. The measuring time was then shortened to one hour instead of two, and for the strains run twice, the results were similar enough for the different strain samples to be compared to one another.

Strain B8 refers to SBW25*mucA*HE230CSG8

Strain B8 refers to SBW25*mucA*HE230CSG8+1

Strain C refers to SBW25*mucA*HE230pAlgD^{-}

Strain C8 refers to SBW25*mucA*HE230pAlgD^{-}CSG8

P1 refers to parallel 1

P1-s refers to parallel 1 lacking substrate

PMM: ACP (SBW25*mucA)***:* One parallel from strain ACP was excluded due to flattening out faster than the two other parallels, while one "ACP minus substrate"-parallel was excluded due to having an unrealistically high jump in the beginning of the assay.

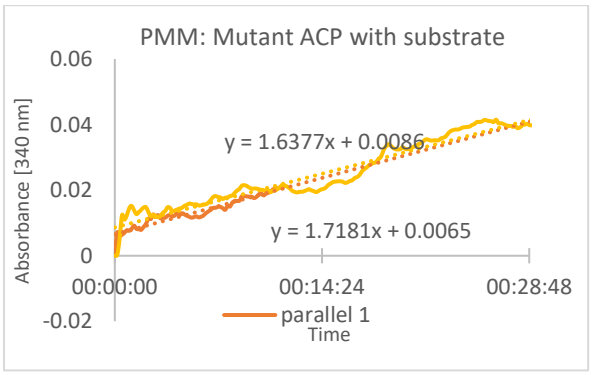

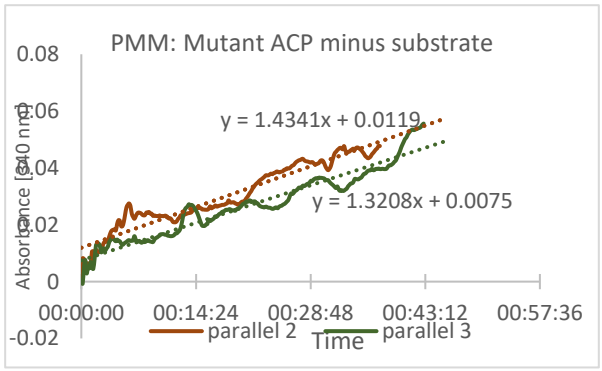

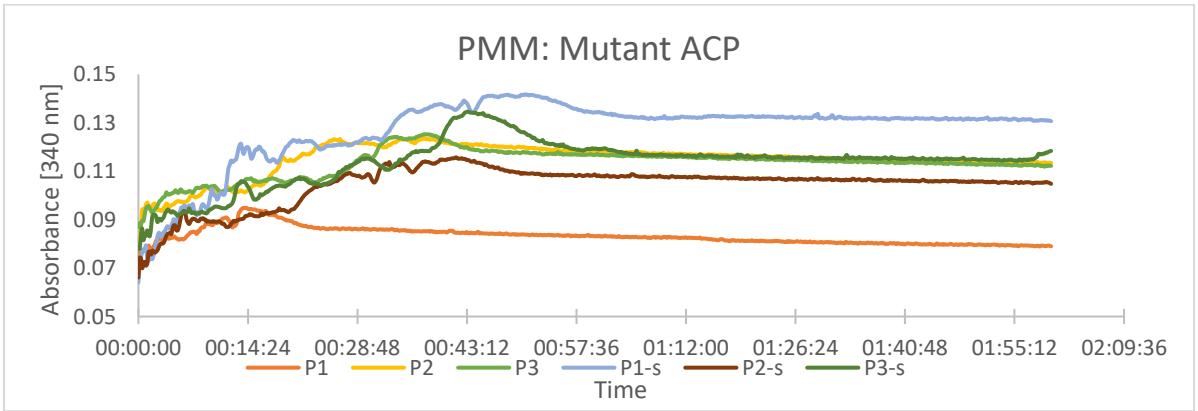

PMM: ACP$^+$X$^-$(SBW25*mucA*-CSG2)**:** The ACP$^+$X$^-$ mutants had a thick viscous layer after the last centrifugation step, causing the protein samples to be more viscous and have a strong white-yellow colour, giving higher absorbance values than for the other strains. The sample is still included, as both the substrate-less parallels and the cell + substrate parallels gave curves with expected increases for the mutant.

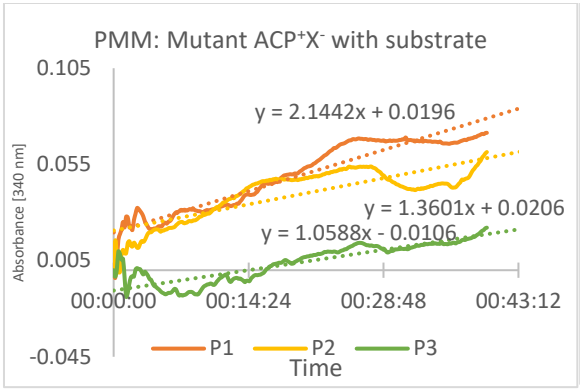

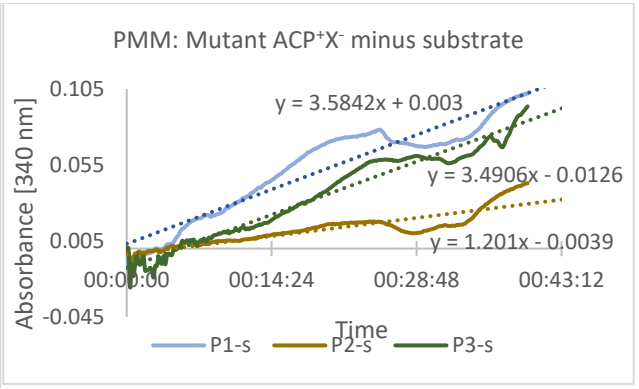

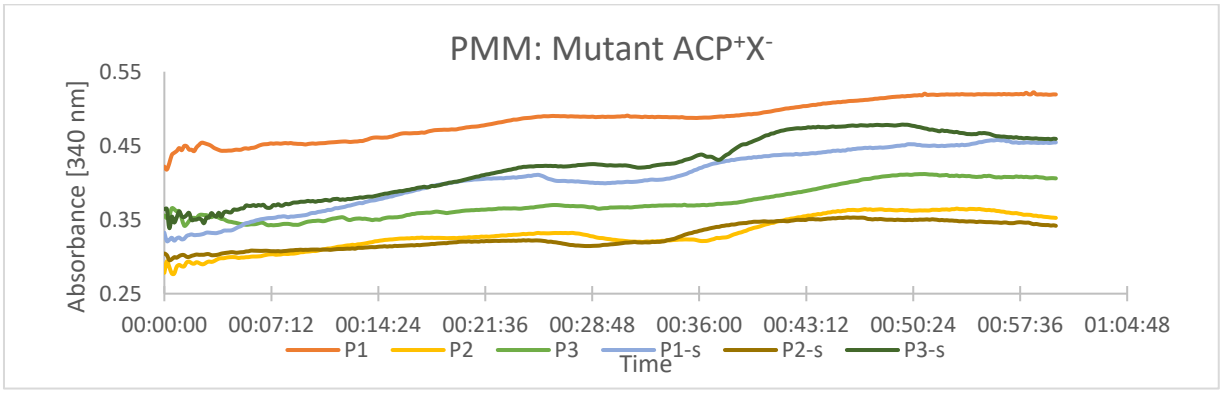

PMM: ACP$^+$ (SBW25*mucA*-CSG4**):** The highest non-substrate parallel was excluded, as well as the lowest cells with substrate-parallels, as these had high jumps in the beginning, possibly due to air bubbles.

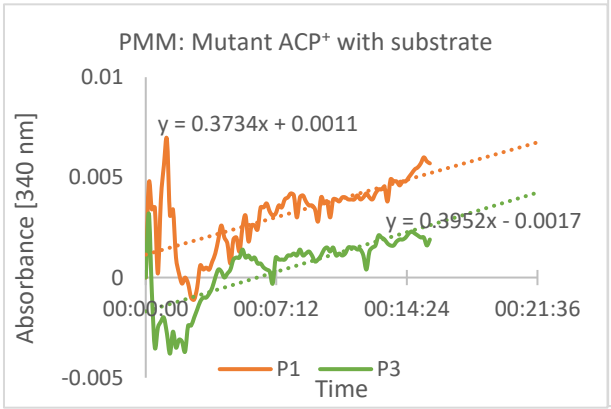

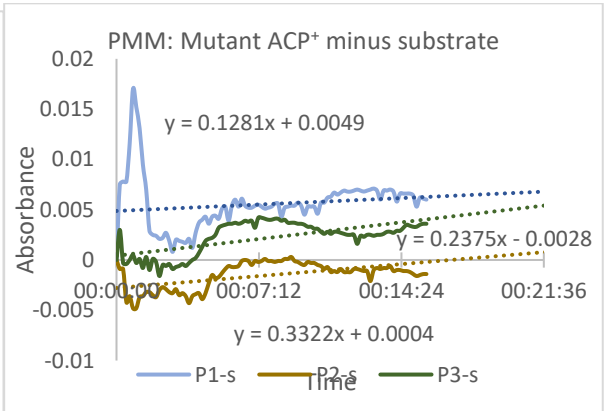

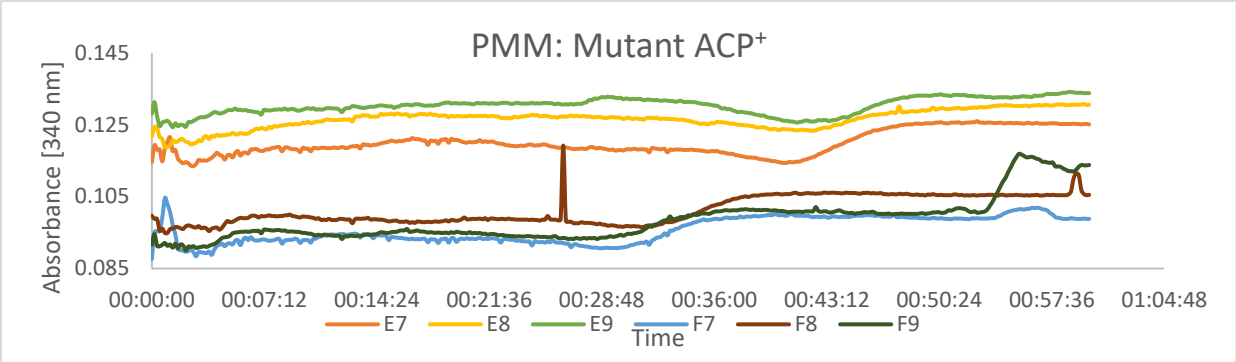

PMM: ACP$^-$ (SBW25*muc*A-CSG10)**:** Both the third parallel for A10 with substrate and the third parallel lacking substrate were jumping a lot up and down, possibly due to air bubbles in the sample, and the second parallel with substrate having no increase at all were excluded.

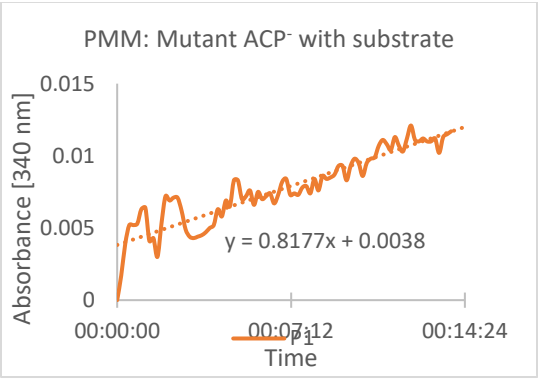

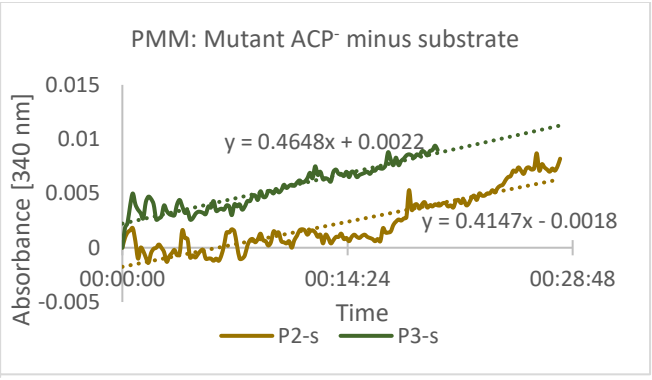

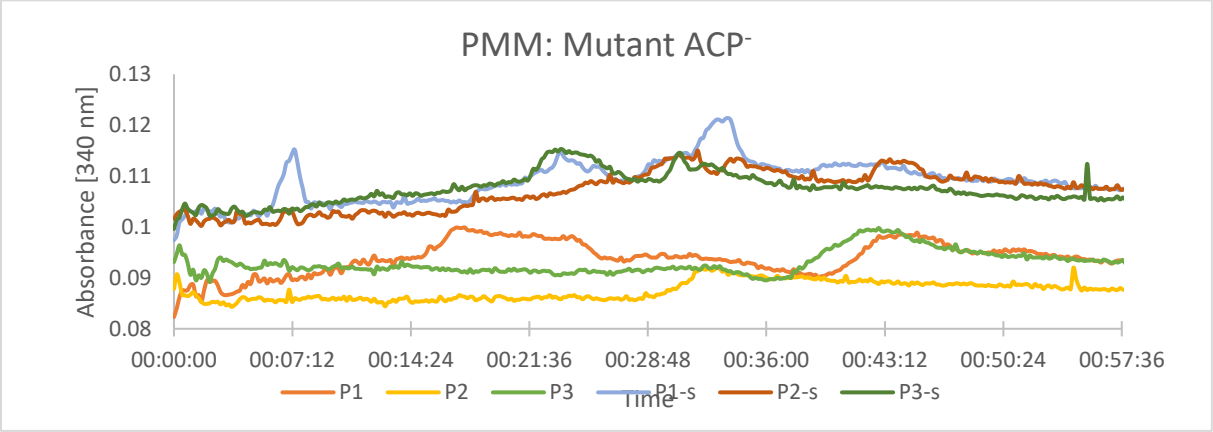

PMM: AC⁻P (SBW25*muc*AΔ*algC*): The third parallel minus substrate was excluded because the absorbance values was expectedly high throughout all measurements

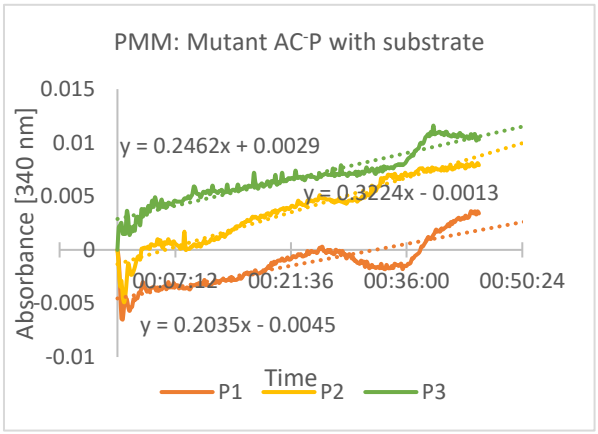

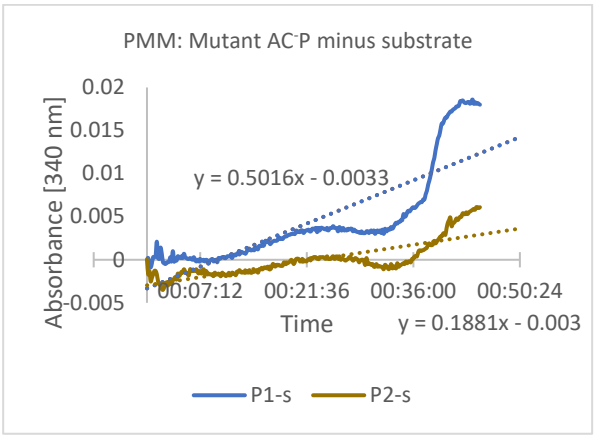

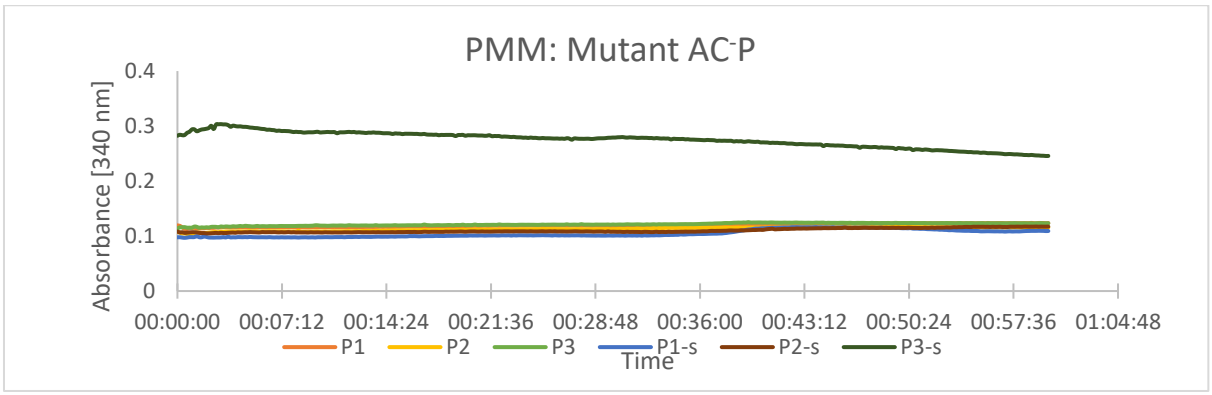

PMM: AC⁻P⁺ (SBW25*muc*AΔ*algC*-CSG6)**:** One parallel for the substrate-lacking samples was excluded due to the big jump in the start most likely coming from bubbles in the sample.

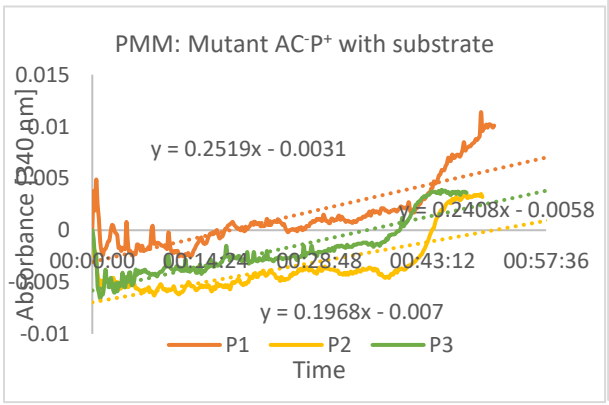

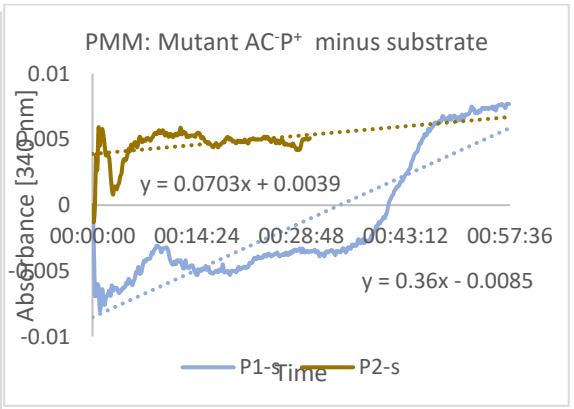

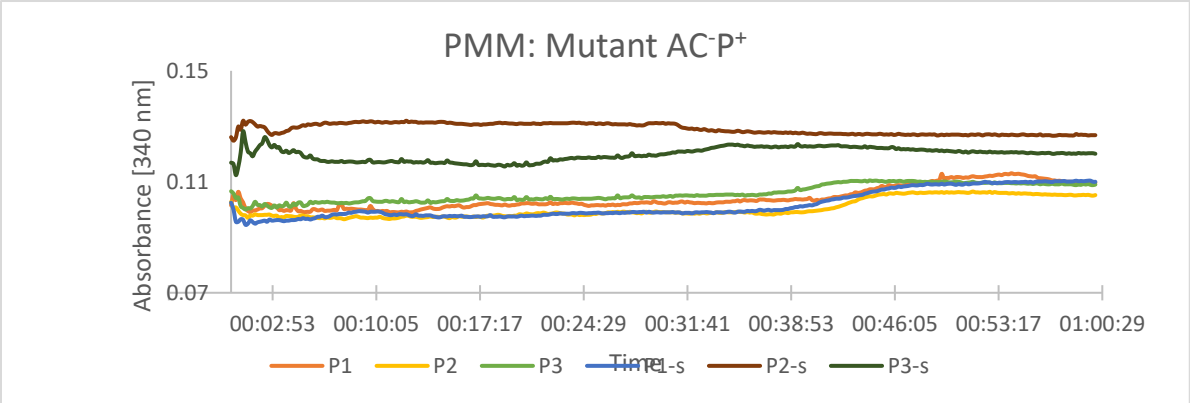

PMM: AC⁺P⁺ (SBW25*muc*AHE230-CSG8**):** One of the parallels lacking the substrate had a very brief increase before it flattened out after less than 3 minutes and is therefore excluded.

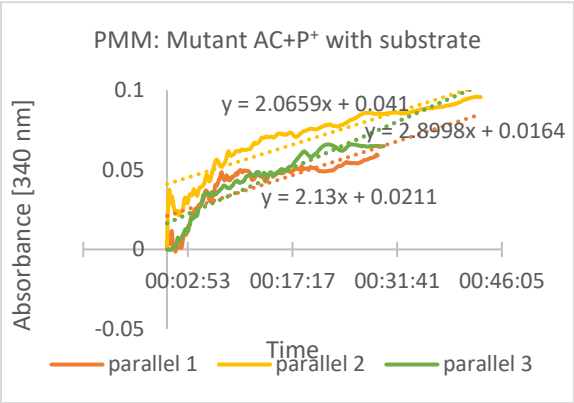

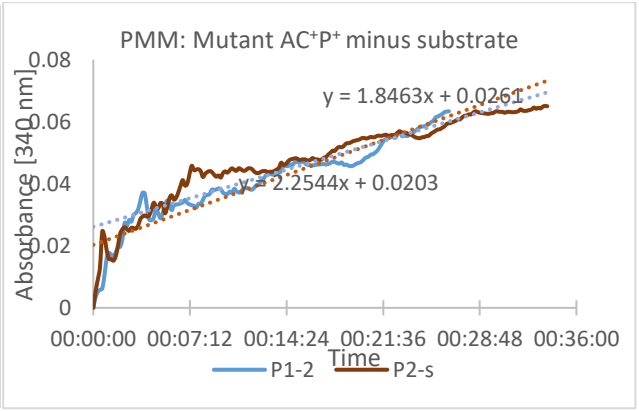

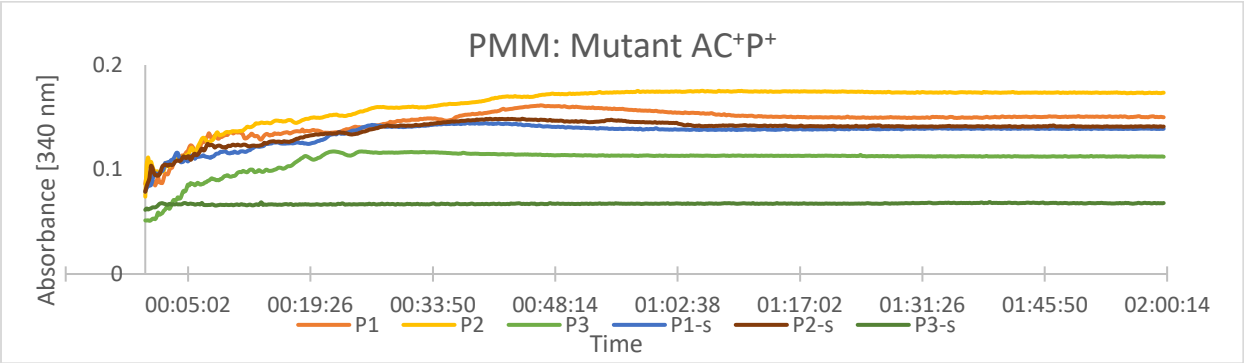

PMI: ACP (SBW25*mucA)*

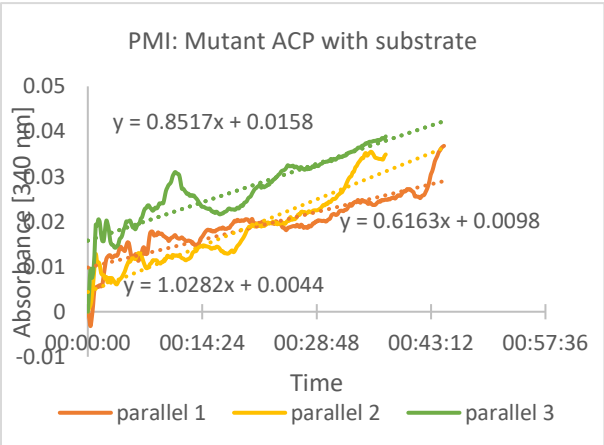

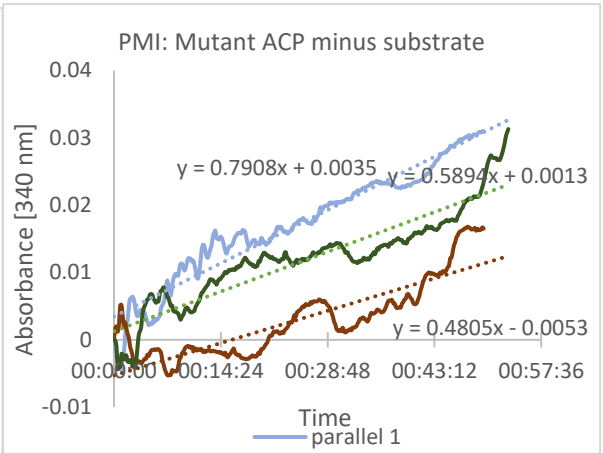

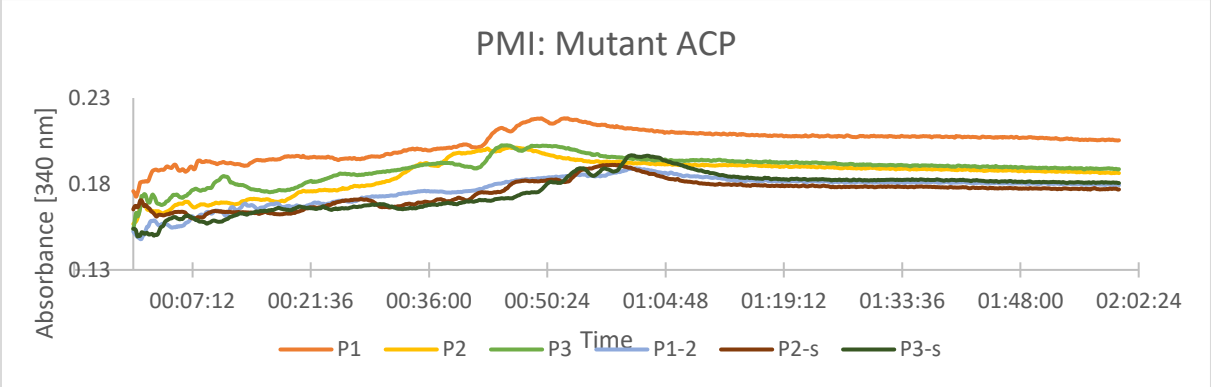

PMI: ACP^{+}X^{-} (SBW25*mucA*-CSG2):

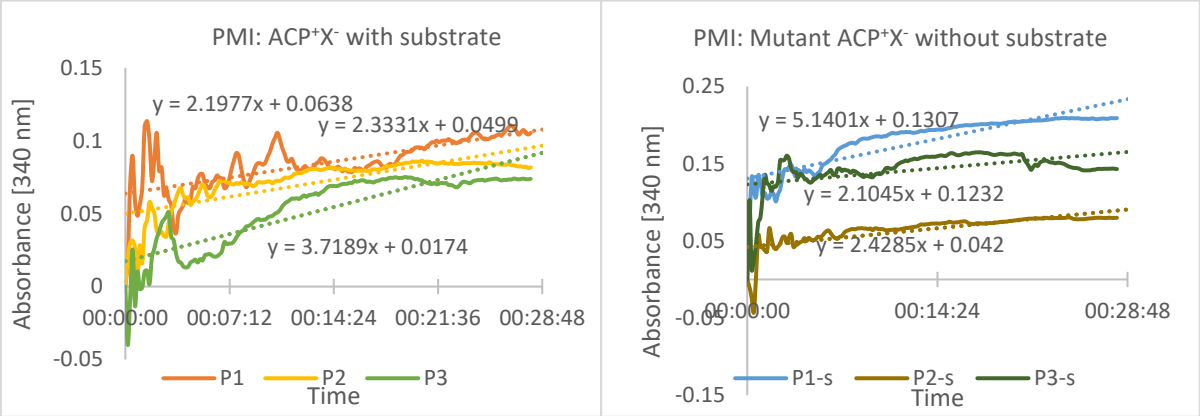

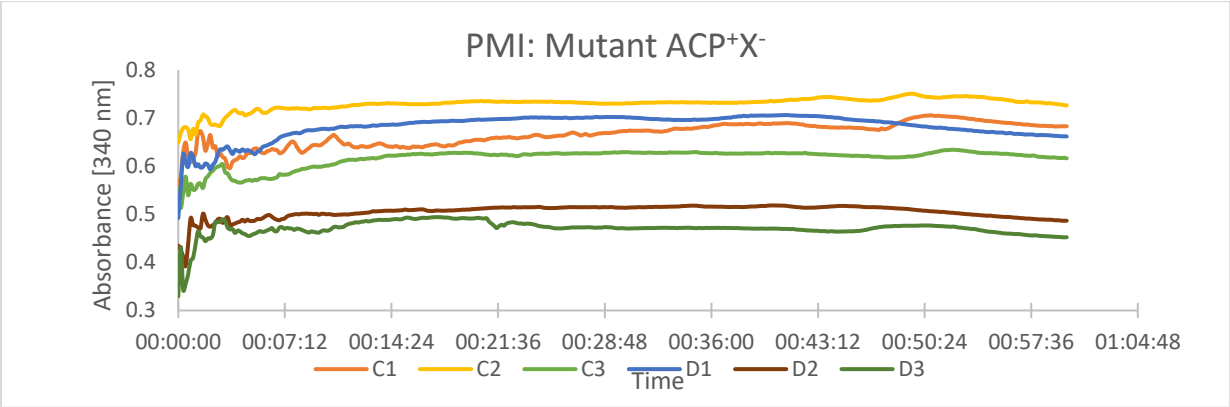

PMI: ACP$^+$ (SBW25*muc*A-CSG4)

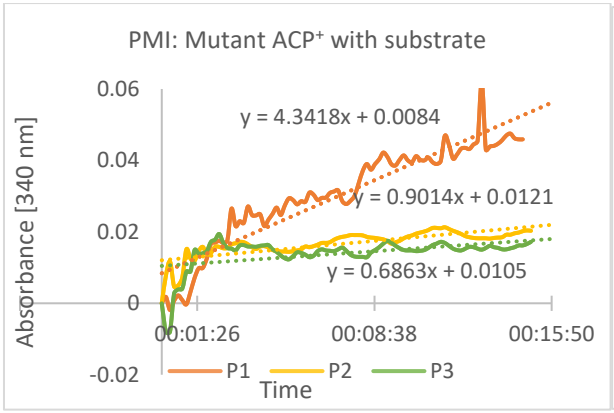

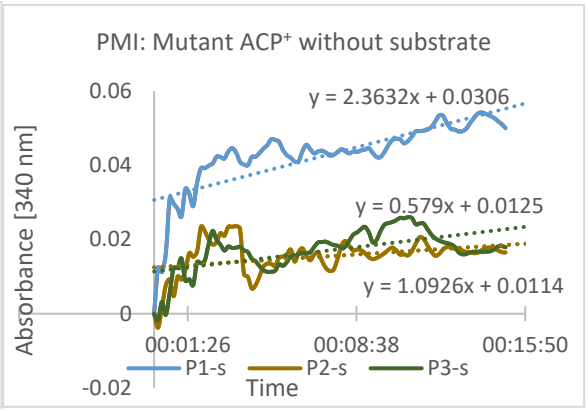

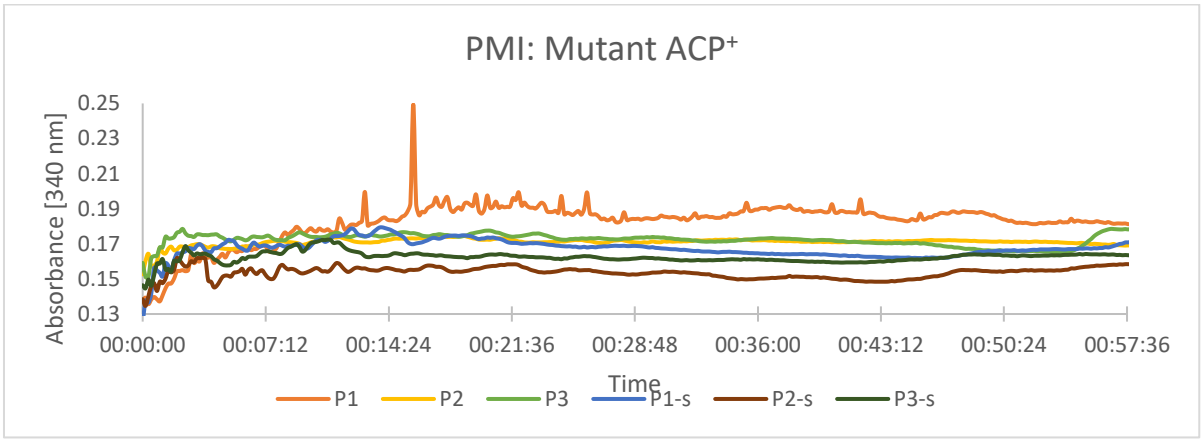

PMI: ACP$^-$ (SBW25*muc*A-CSG10)

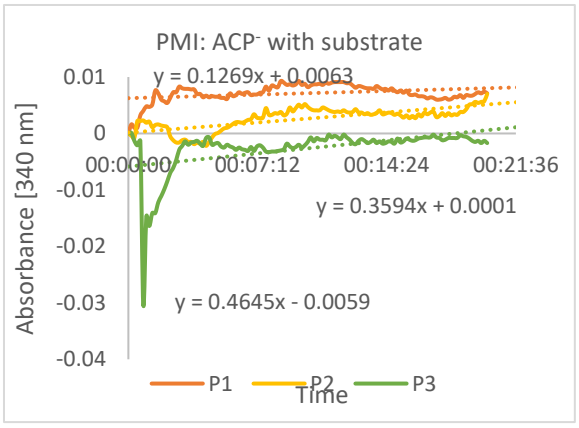

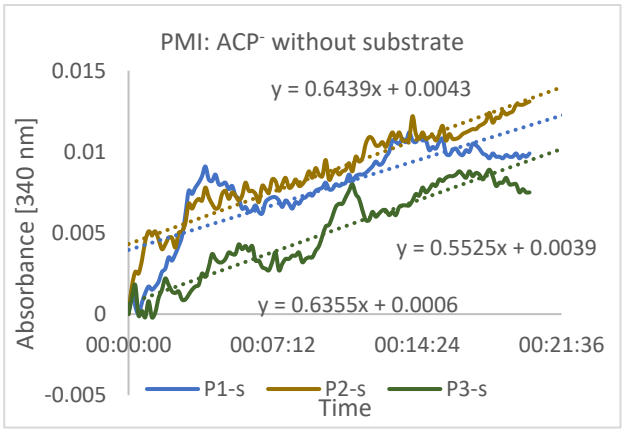

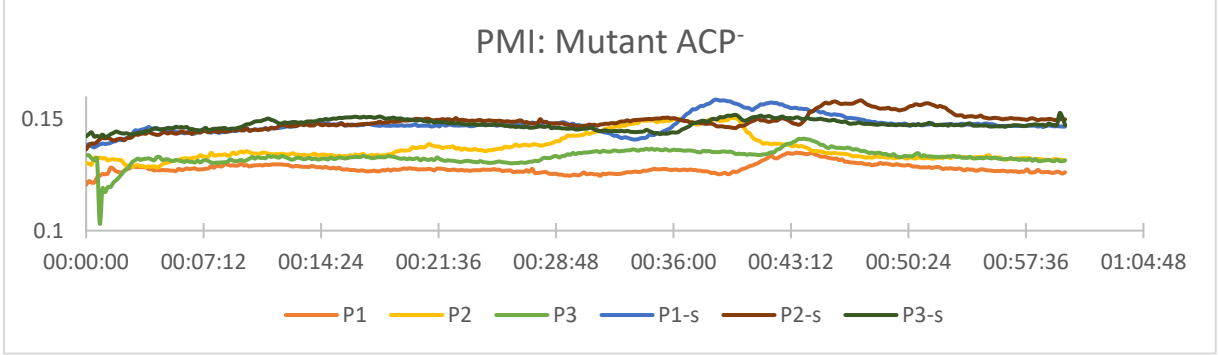

PMI: AC$^-$P (SBW25*muc*AΔ*algC*): A parallel lacking substrate had a negative value and was therefore excluded

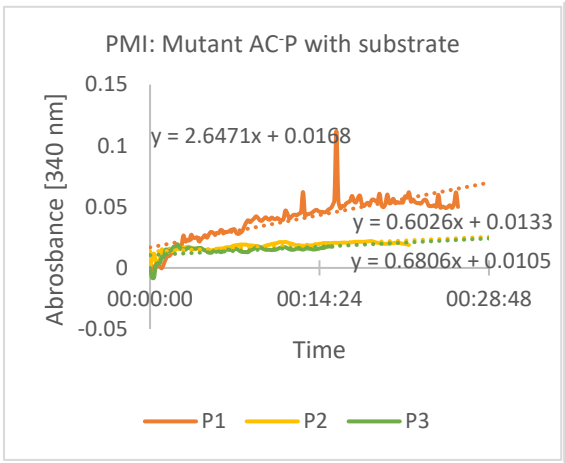

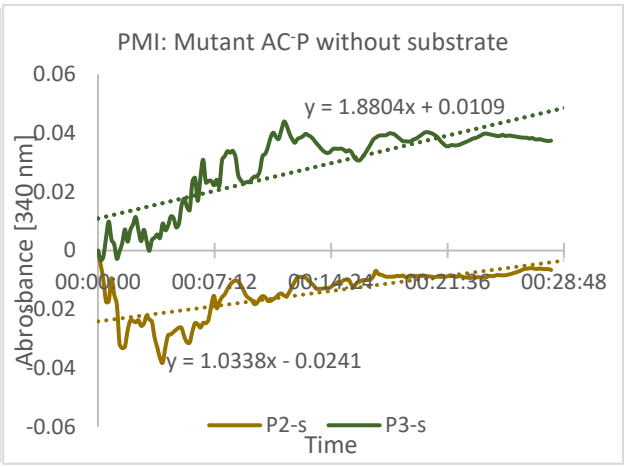

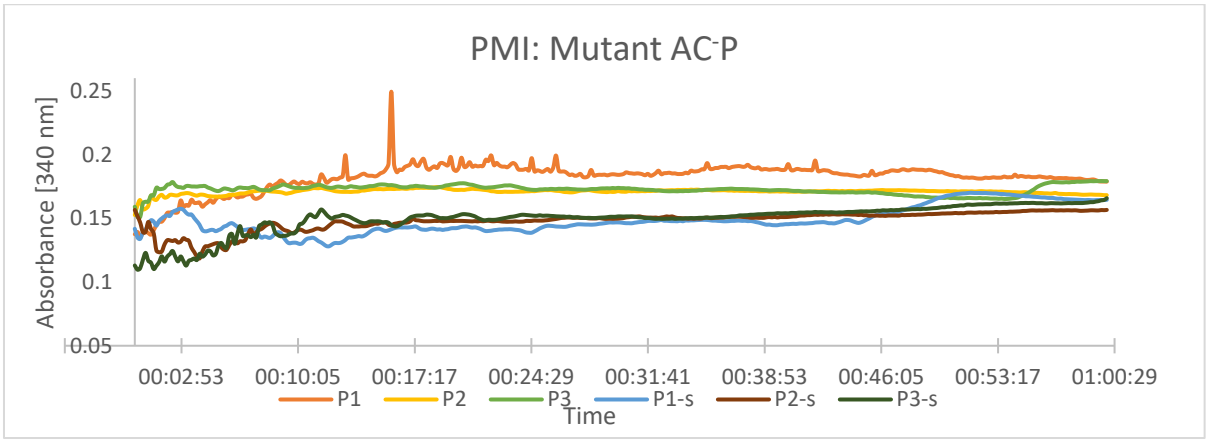

PMI: AC$^-$P$^+$ (SBW25*muc*AΔ*algC*-CSG6): The third parallel with substrate was excluded due to a lot of jumping in the start, possibly caused by air bubbles. Likewise, the third parallel lacking substrate had a huge jump before it rapidly declined and was not included.

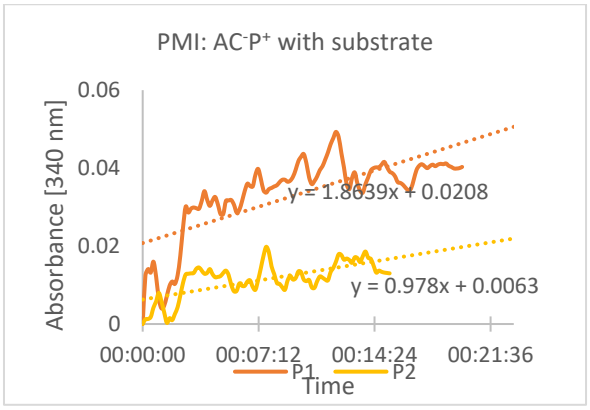

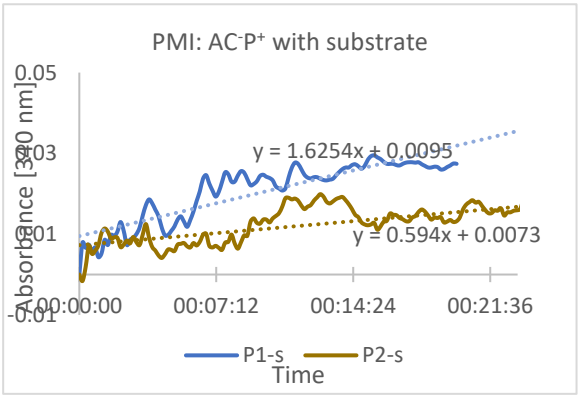

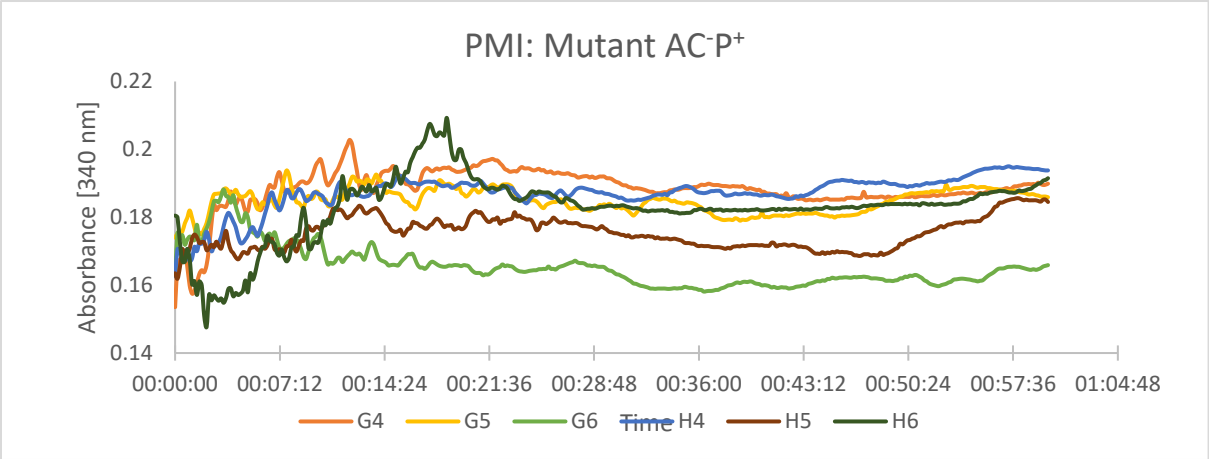

PMI: A⁺C⁺P⁺ (SBW25*mucA*HE230CSG8+1)

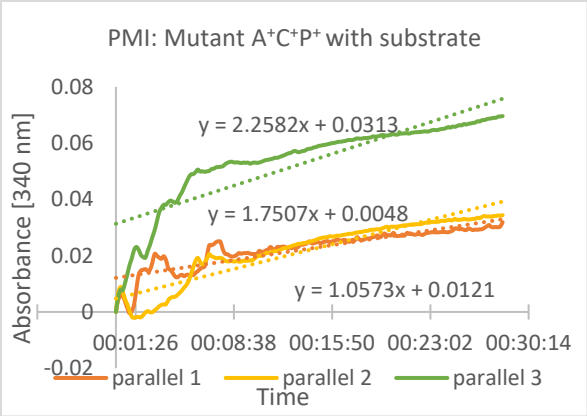

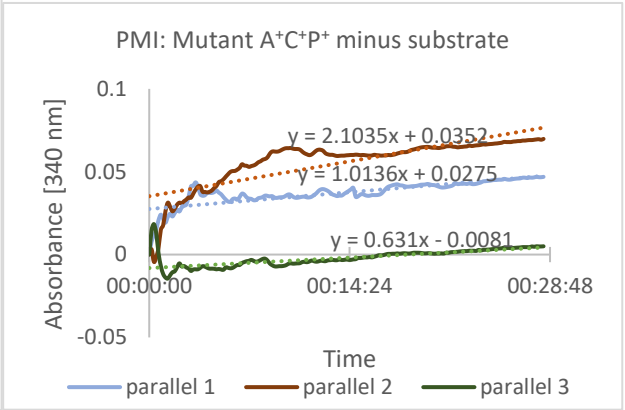

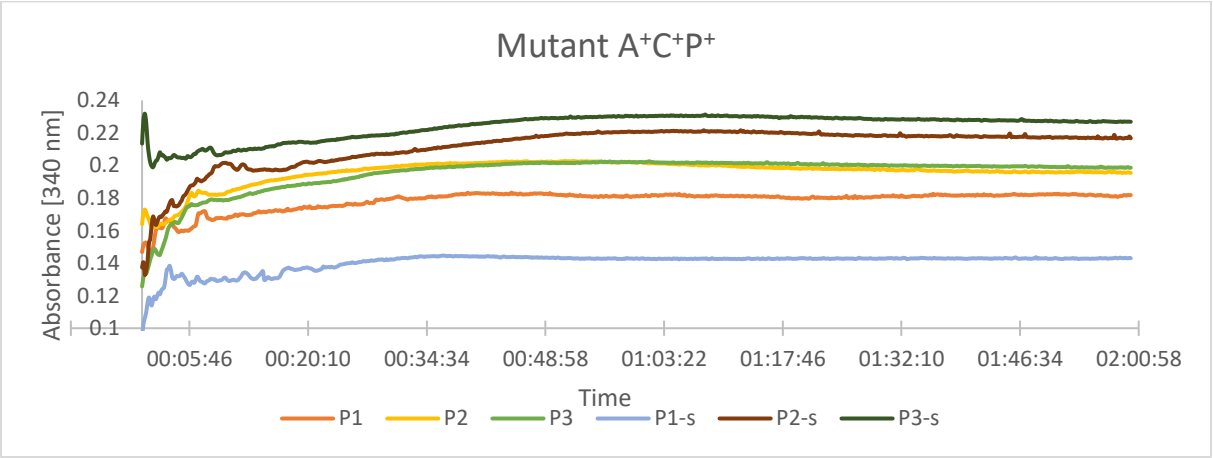

PMI: A⁻C⁺P (SBW25*mucA*pAlgD⁻**):** Parallel 3 with substrate had a lot of jumping in the beginning, probably due to bubbles in the sample, causing the linear decrease instead of an increase, and was therefore excluded.

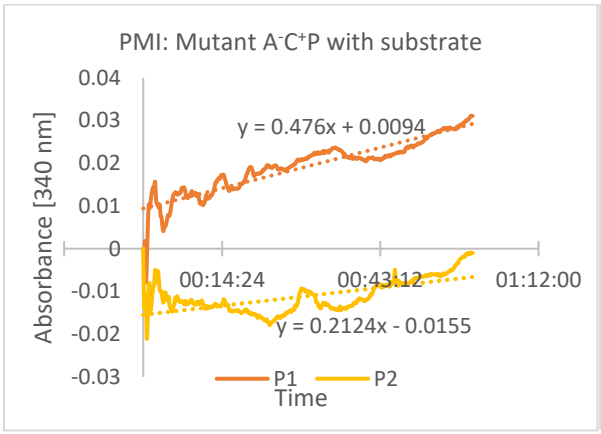

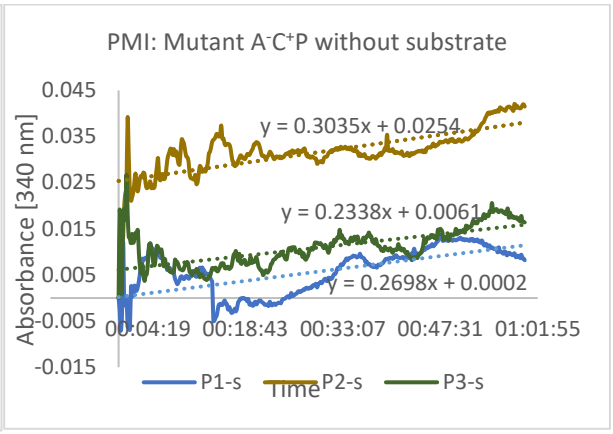

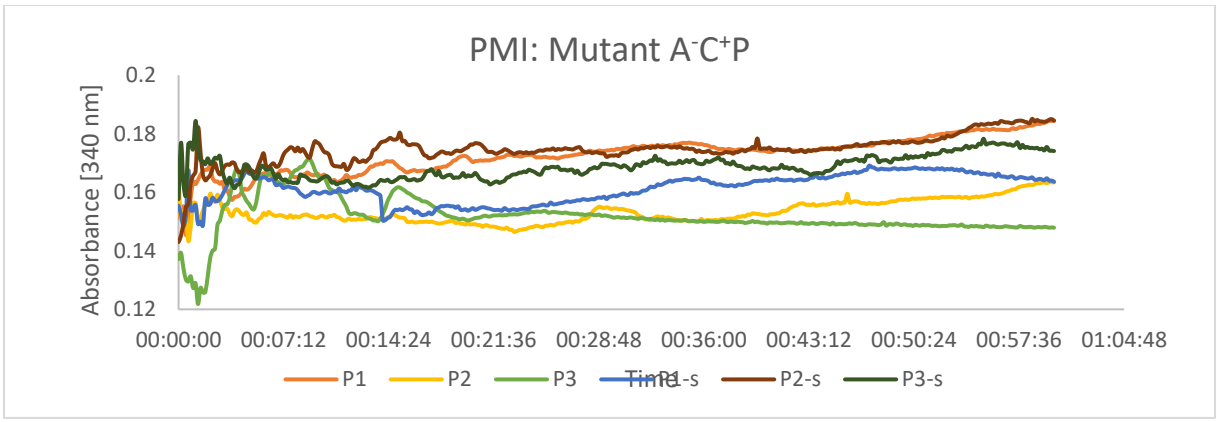

PMI: A⁻C⁺P⁺(SBW25*mucA*pAlgD⁻⁻CSG6**):** As seen in the graph with all six parallels, they go up, down, and it is hard to find a linear increase in any of the parallels. Therefore, the average increase for the whole measuring time was used.

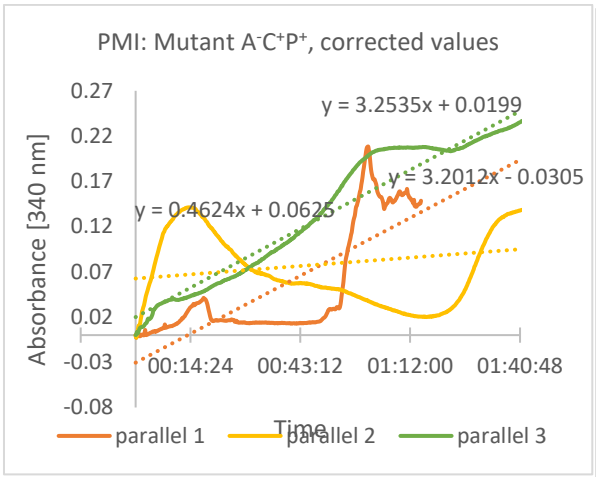

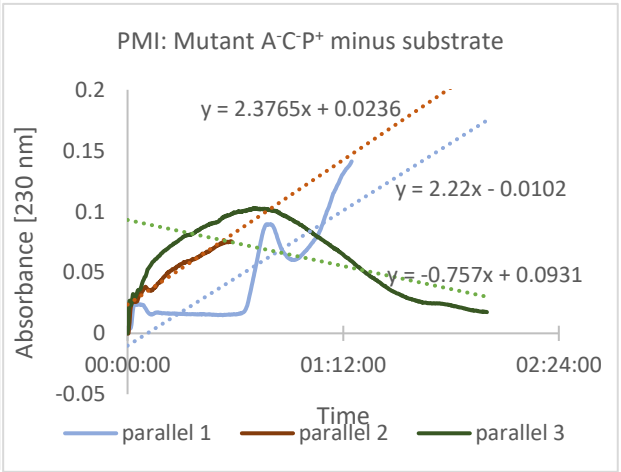

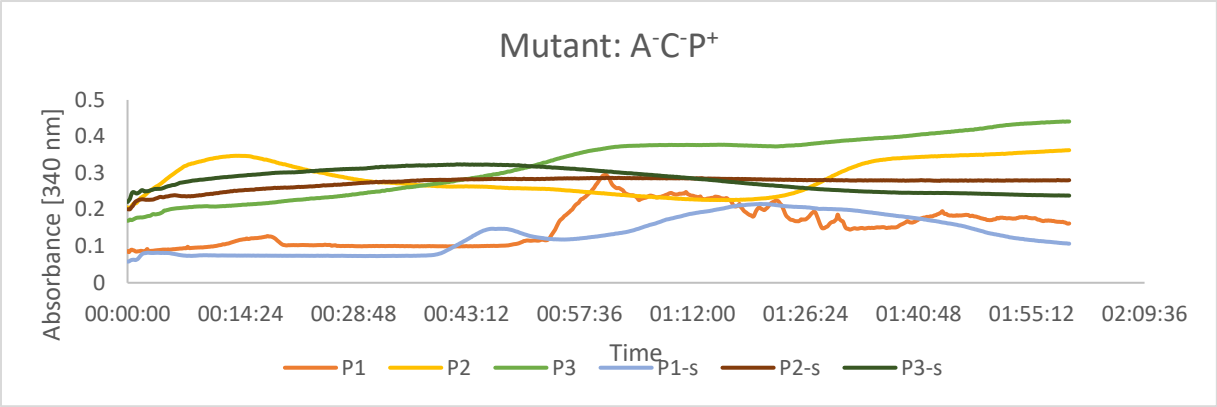

Strain	OD_{600}	Values	PMI[a] (±)	PMI[b] (±)	Values	PMM[a] (±)	PMM[b] (±)
ACP	5.59	0.4	0.37	0.28	1.0	0.17	0.25
ACPX$^-$	5.46	0	0.86	1.71	0	1.15	2.78
ACP$^+$	5.87	0.6	2.1	0.95	0.3	0.03	0.21
ACP$^-$	3.35	0	0.43	0.13	1.5	0	0.75
AC$^-$P	5.45	0.2	1.29	0.10	0	0.11	0.41
AC$^-$P$^+$	4.04	0.3	0.72	0.56	0.0	0.06	0.39
AC$^+$P$^+$	5.83	-			0.6	0.09	0.56
A$^+$C$^+$P$^+$	5.69	0.5	0.46	0.52	-		
A$^-$C$^+$P	5.32	0.1	0.21	0.04	-		
A$^-$C$^+$P$^+$	4.56	0.4	0.68	0.40	-		

[a] Standard deviations for parallels with substrate calculated from three parallels

[b] Standard deviations for parallels minus substrate calculated from three parallels

OD_{600} measurements were done after 16 hours of growth with a 10-fold dilution.

The activities were calculated by finding a linear increase for each of the parallels in the assay, adding the three parallels, and subtracting the obtained value for cells lacking substrate from cells with substrate. Parallels jumping a lot up and down, probably due to air bubbles, or parallels with negative or no increase were discarded. The standard deviation is calculated for each of the linear increases found, using the following formula in excel:

$$SD = \sqrt{\frac{\sum |x - \bar{x}|^1}{n - 1}}$$

The values for each enzymatic activity were measured as the average increase converted from 10 seconds to one minute, and Beer Lambert's law and the absorbance coefficient for NADPH was used to find the concentration, which was then divided by the protein content in each sample. One U is defined as the enzyme required to reduce 1 µmol NADP per min under the specified assay conditions.

Appendix H – Monosaccharide analysis

Monosaccharide analysis chromatogram are attached below. The name of the strains is added over each chromatogram

ACP^{+} 24 hours

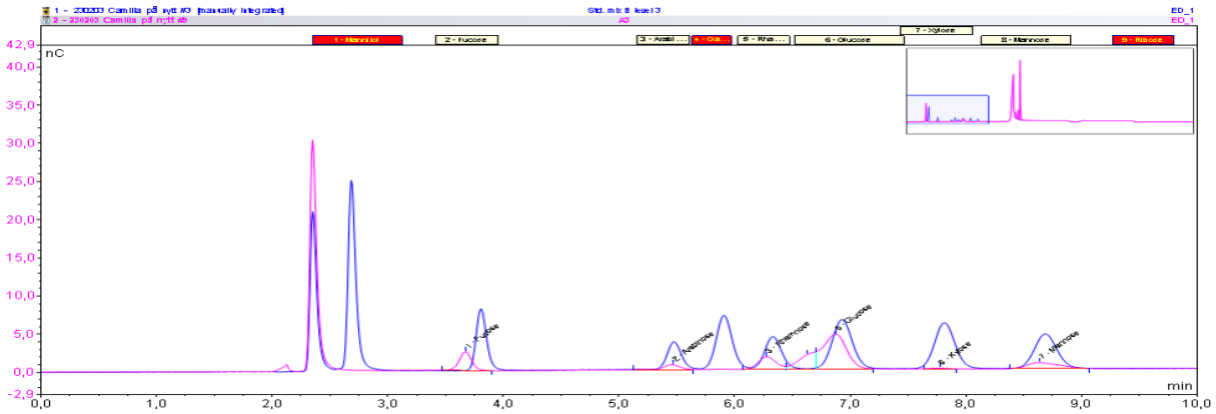

ACP^{+}-1 48 hours

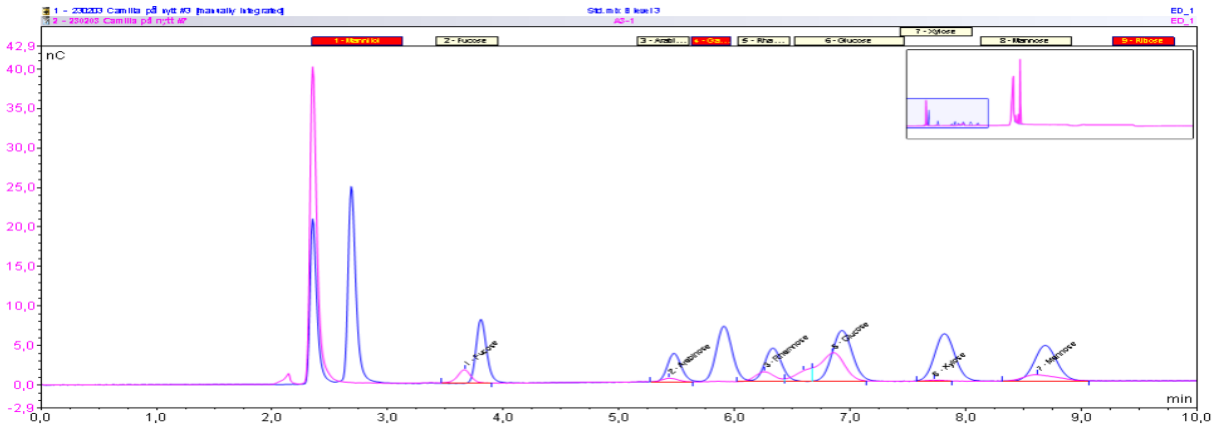

ACP^{+}-2 48 hours

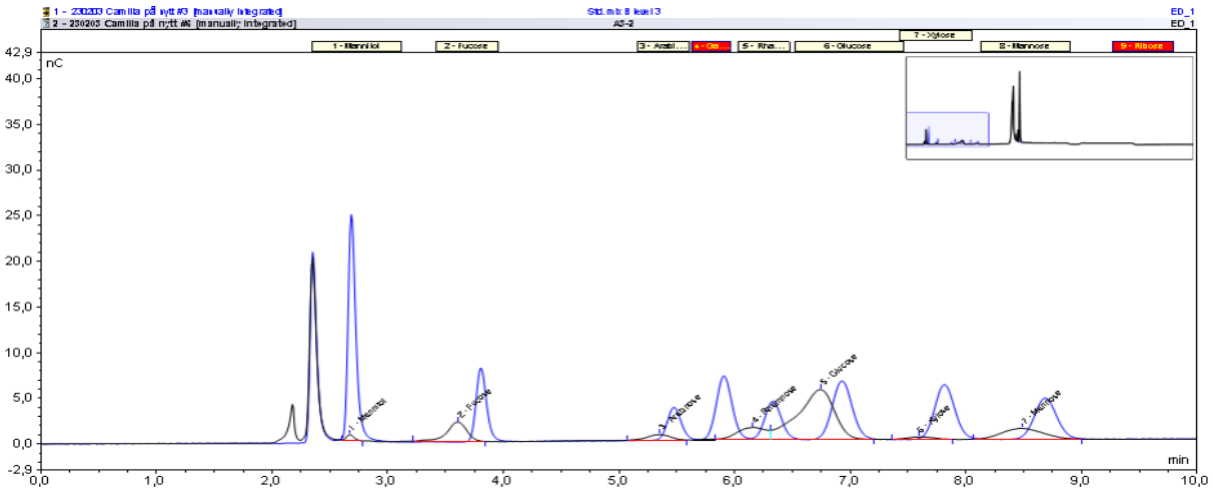

ACP^{+}X^{-} 24 hours

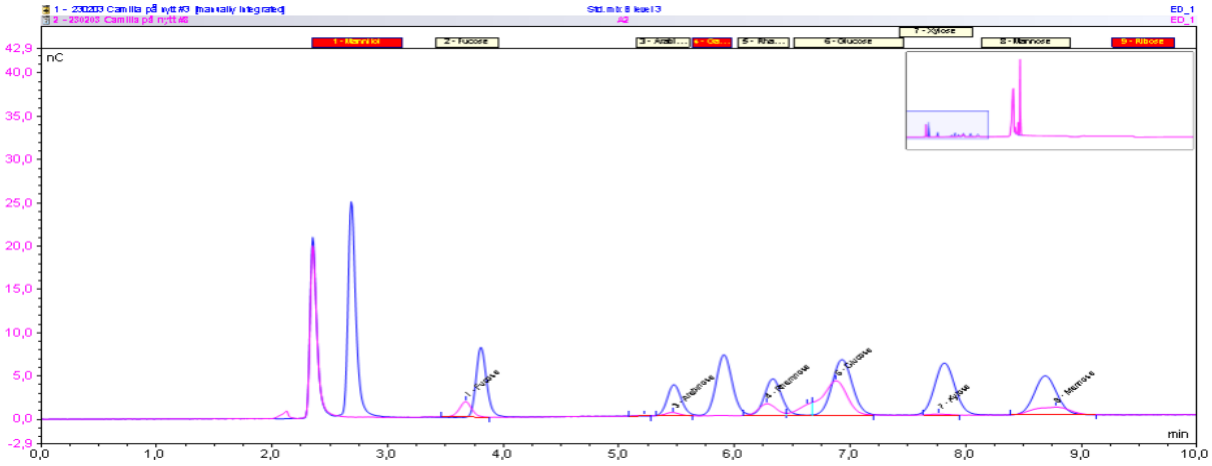

ACP^{+}X^{-}-1 48 hours

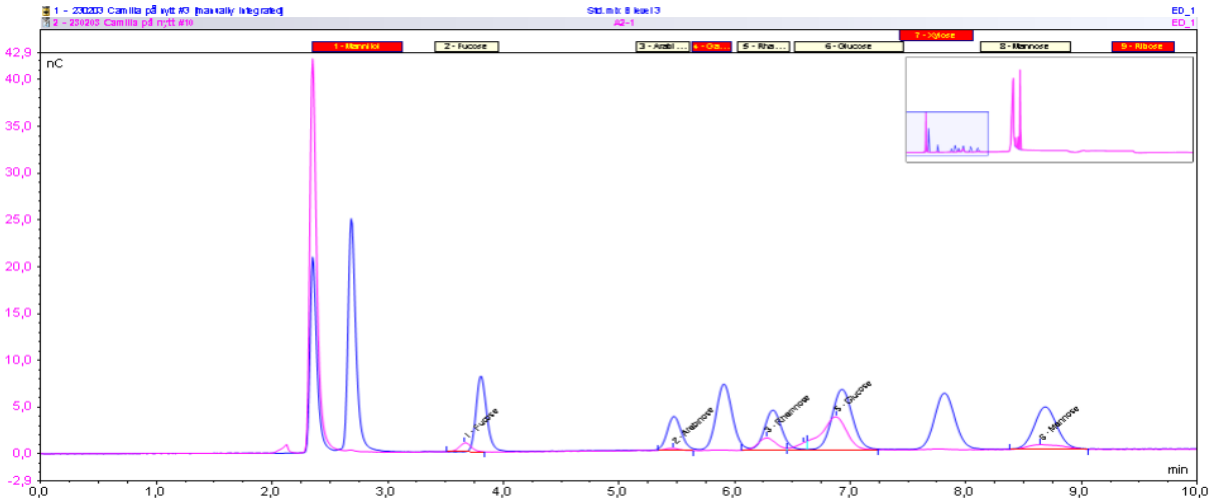

ACP^{-} 24 hours

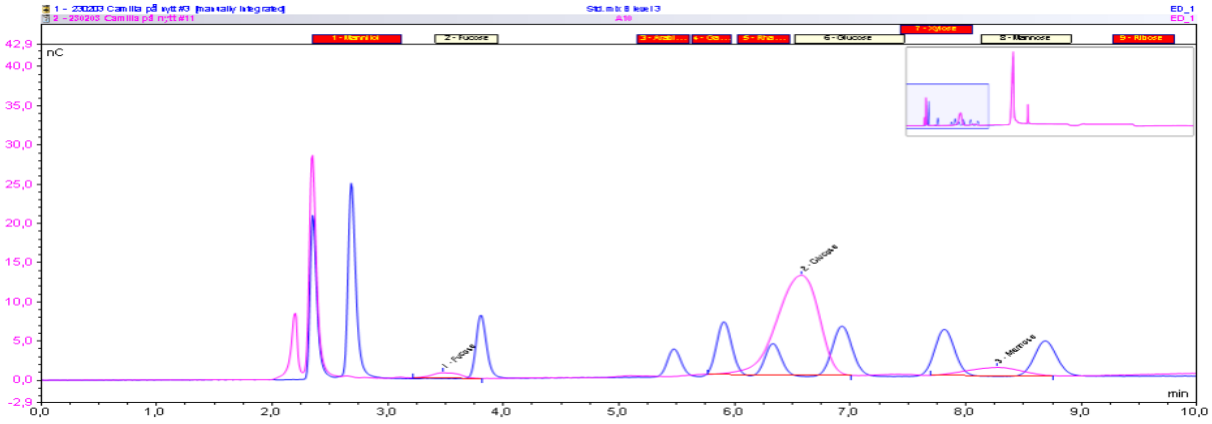

ACP^{-}-1 48 hours

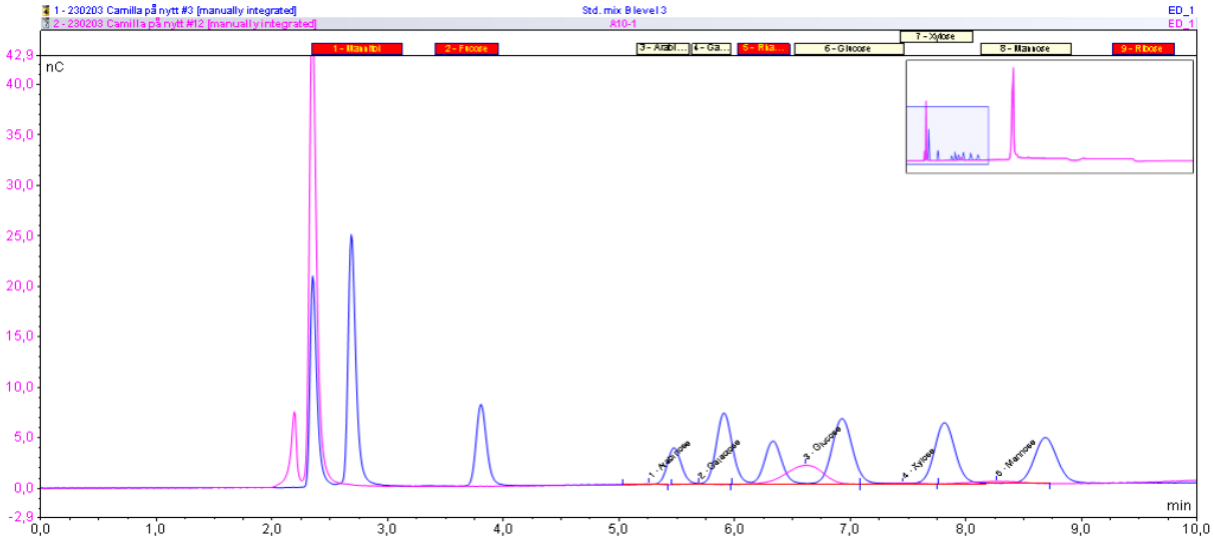

ACP^{-}-1 48 hours

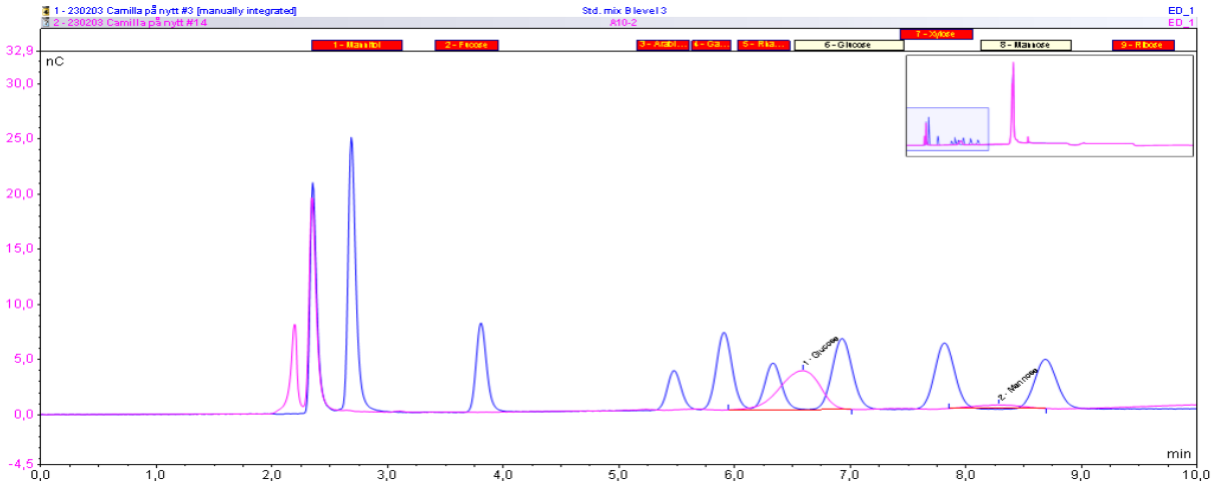

A^{-}CP^{+} 24 hours

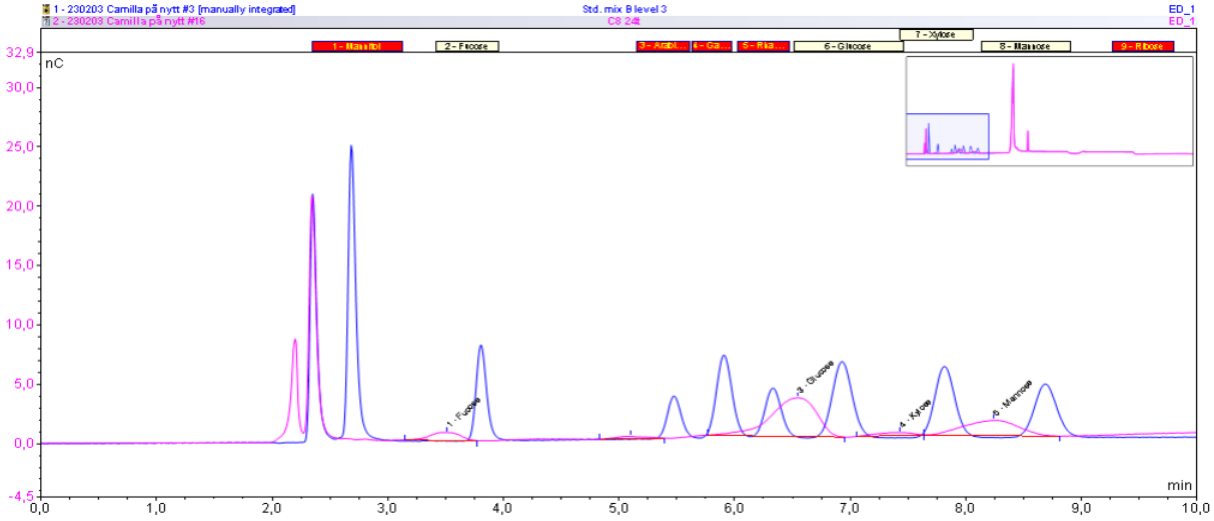

A^{-}CP^{+} 48 hours

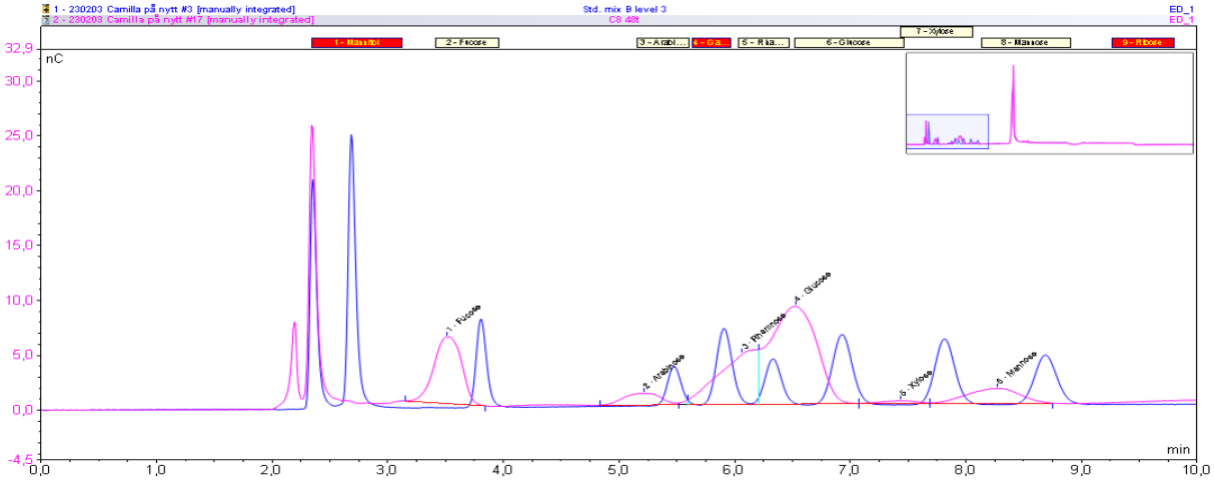

AC^{-}P^{+} 24 hours

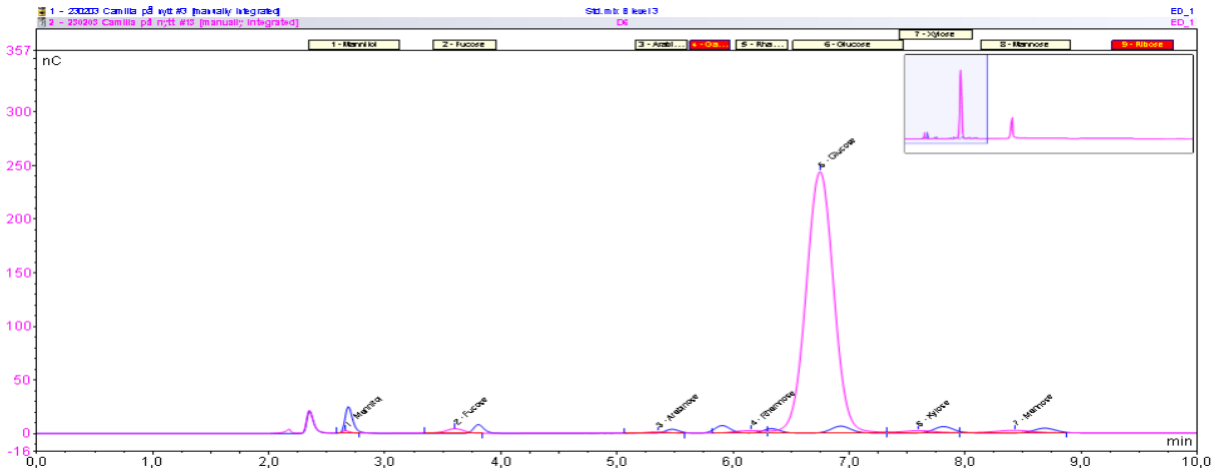

AC^{-}P^{+} 48 hours

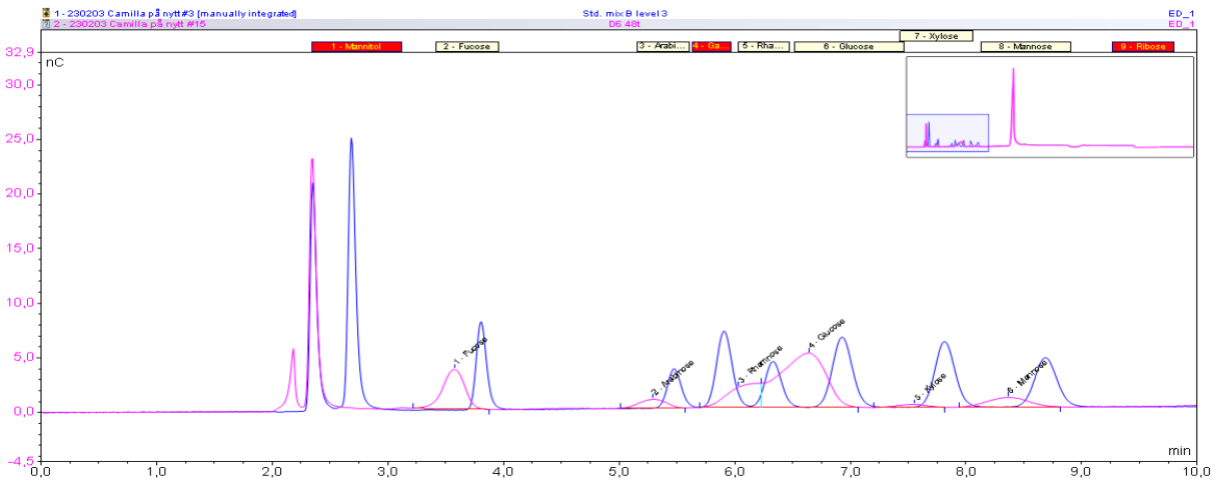

Monosaccharide composition

The raw data obtained for the monomer content in the samples are shown in figure H1-

Inj.	Injection Name	Type	% Dry wei	% Dry wei	% Dry wei	% Dry wei	% Dry wei	% Dry wei	% Dry wei	% Dry weight
No.	Selected Peak:		%	%	%	%	%	%	%	%
			ED_1	ED_1	ED_1	ED_1	ED_1	ED_1	ED_1	ED_1
			Mannitol	Fucose	Arabinose	Galactose	Rhamnose	Glucose	Xylose	Mannose
1	MQ	Unknown	n.a.	n.a.	n.a.	n.a.	n.a.	n.a.	n.a.	n.a.
2	Std. mix B level 1	Calibration Standard	n.a.	n.a.	n.a.	n.a.	n.a.	n.a.	n.a.	n.a.
3	Std. mix B level 3	Calibration Standard	n.a.	n.a.	n.a.	n.a.	n.a.	n.a.	n.a.	n.a.
4	Std. mix B level 5	Calibration Standard	n.a.	n.a.	n.a.	n.a.	n.a.	n.a.	n.a.	n.a.
5	Std. mix B level 7	Calibration Standard	n.a.	n.a.	n.a.	n.a.	n.a.	n.a.	n.a.	n.a.
6	ACP+ 48h2	Unknown	0.055	0.655	0.193	n.a.	0.748	2.087	0.097	0.68
7	ACP+ 48h1	Unknown	n.a.	0.283	0.085	n.a.	0.377	0.764	0.027	0.306
8	ACP+X- 24h	Unknown	n.a.	0.274	0.062	n.a.	0.366	0.809	0.024	0.368
9	ACP+ 24h	Unknown	n.a.	0.535	0.163	n.a.	0.633	1.292	0.026	0.403
10	ACP+X- 48h	Unknown	n.a.	0.239	0.066	n.a.	0.598	1.251	n.a.	0.342
11	ACP- 24h	Unknown	n.a.	2.291	n.a.	n.a.	n.a.	41.448	n.a.	5.737
12	ACP- 48h-1	Unknown	n.a.	n.a.	0.154	0.117	n.a.	5.506	0.221	1.216
13	AC-P+ 24h	Unknown	0.121	0.759	0.21	n.a.	0.796	46.835	0.719	0.897
14	ACP- 48h-2	Unknown	n.a.	n.a.	n.a.	n.a.	n.a.	10.926	n.a.	1.533
15	AC-P+ 48h	Unknown	n.a.	1.262	0.308	n.a.	1.313	2.503	0.126	0.52
16	A-C+P+ 24h	Unknown	n.a.	2.423	n.a.	n.a.	n.a.	11.973	0.961	7.445
17	A-C+P+ 48h	Unknown	n.a.	3.287	0.701	n.a.	4.431	5.463	0.14	1.25

Figure H1: Monomer content in the different samples calculated based on the content of the known concentrations in the standard polysaccharide mixture

Uronic acid analysis

The values for the content of mannuronan and guluronan are shown in table H1.

Table H1: The values for the uronic acid analysis

Inj.	**Injection Name**	**Type**	**Amount**	**% Dry weight**	**Amount**	**% Dry weight**	
No.	Selected Peak:		mg/l	%	mg/l	%	
			ED_1	ED_1	ED_1	ED_1	
			GulA	GulA	ManA	ManA	**FG**
22	F(G) = 0.504 - nr. 1	Std 1	1,4442	0,00	1,38		**0,51**
23	F(G) = 0.504 - nr. 2	Std 2	5,9661	0,00	5,89	0,00	**0,50**
24	F(G) = 0.504 - nr. 3	Std 3	12,1185	0,00	11,94	0,00	**0,50**
25	ACP^{+} 48 hours	Unknown	0,9648	6,3	2,71	17,8	**0,26**
26	$ACP^{+}X^{-}$ 24 hours	Unknown	2,9479	18,8	7,49	47,6	**0,28**
27	ACP^{+} 24 hours	Unknown	2,0545	18,6	5,36	48,4	**0,28**
28	$ACP^{+}X^{-}$ 48 hours	Unknown	1,7721	19,0	4,63	49,6	**0,28**

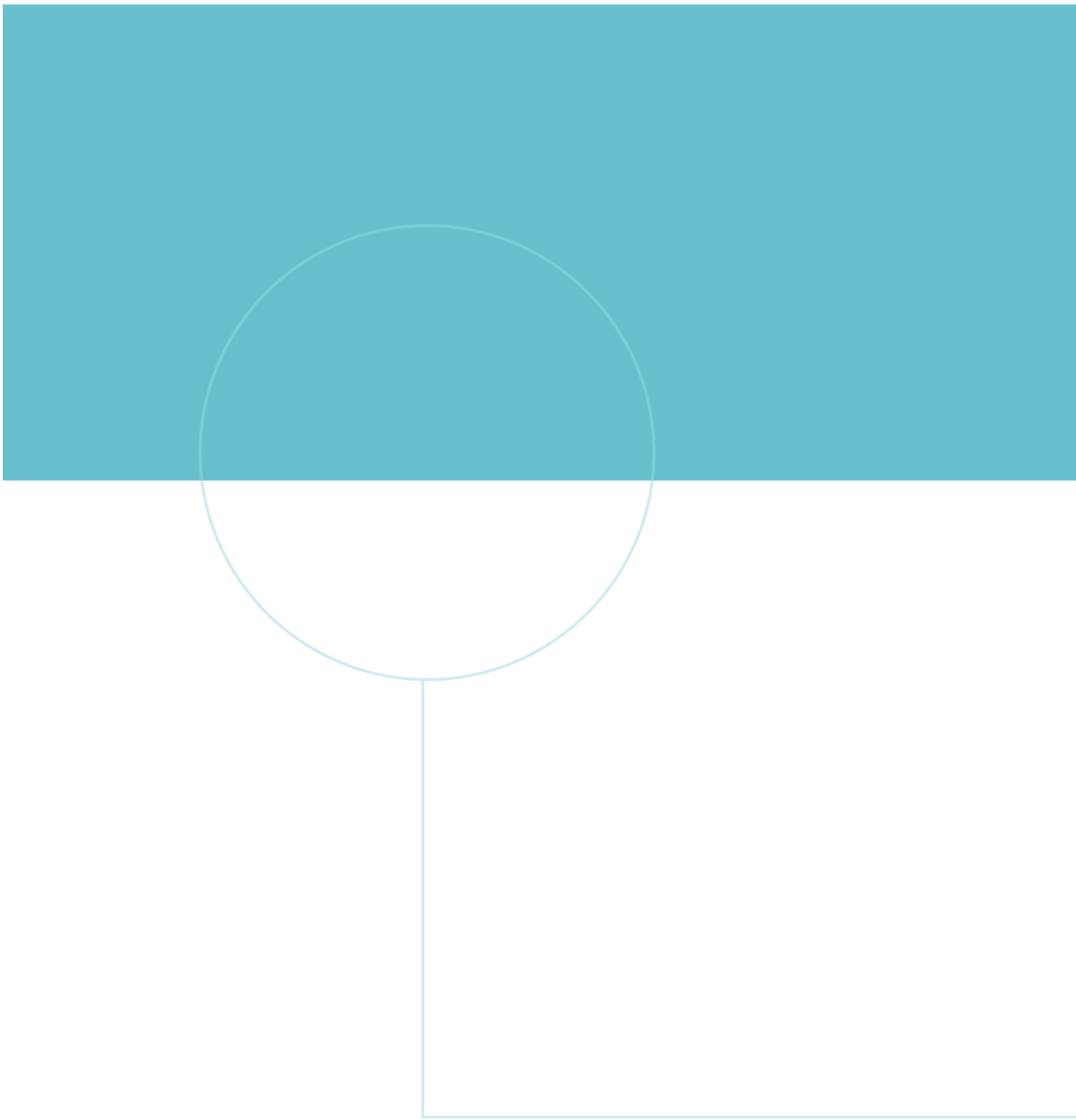

NTNU

Norwegian University of
Science and Technology